AN INTEGRATED APPROACH TO STUDY THE DIVERSITY IN MOLECULAR MECHANISMS OF SALT TOLERANCE IN TROPICAL MAIZE

Ana SOARES

Supervisors:
Prof. Wannes Keulemans
Dr. Sebastien Carpentier

Chairman:
Prof. dr. ir. Jan Michiels

Members of the Examination Committee:

Prof. Dr. Tassos Economou
Prof. Dr. Maurice De Proft
Prof. Dr. Christoph-Martin Geilfus
Prof. Dr. Filip Rolland
Dr. Santiago Signorelli

Dissertation presented in partial fulfilment of the requirements for the degree of Doctor of Bioscience Engineering

November 2019

© 2019 Faculty of Bioscience Engineering
Uitgegeven in eigen beheer, Ana Luísa Corrêa Soares, Willem de Croylaan 42
3001 Leuven

Alle rechten voorbehouden. Niets uit deze uitgave mag worden vermenigvuldigd en/of openbaar gemaakt worden door middel van druk, fotokopie, microfilm, elektronisch of op welke andere wijze ook zonder voorafgaandelijke schriftelijke toestemming van de uitgever.

All rights reserved. No part of the publication may be reproduced in any form by print, photoprint, microfilm, electronic or any other means without written permission from the publisher.

Acknowledgments

The Coordenação de Aperfeiçoamento de Pessoal de Nível Superior (CAPES), from the Brazilian Ministry of Education is acknowledged for granting me a scholarship for the conduction of this work.

I would like to thank Sebastien Carpentier, for giving me the opportunity to join his lab, for sharing your knowledge, time and friendship with me. During all these years you were not only a brilliant guide to my research, but an inspiration and the source of challenging and fascinating discussions. Thank you so much for opening the doors for a new and exciting journey that was only possible to conclude because of your leadership.

I would also like to declare my profound gratitude to Prof. Wannes Keulemans, for trusting in me and in our work. Thank you for sharing your time, for the good advices and for standing with us at a rough period. I really appreciate your availability and your understanding at all moments.

I am very grateful to all the members of my examination committee for taking the time to read my work, for the very constructive comments and feedback.

Thank you very much for all TPL team, for helping me so much not only with my research, but to go through all this knowing that I could sincerely count on you. I will always remember the good talks, the laughs, the advices, the parties and how you embraced me so kindly. It was a pleasure to have you around every day.

To the friends that Leuven brought me, I have no words to express my gratitude. Gabi, Nadinha, Lisa, Duda, Amanda, Jassmine, Fê, Rosália, Kusay, Geert and family, all Viva Leuven, you have been my strength, my happiness and the

support to keep me going and make this journey possible. Thank you for being by my side.

Aos meus amigos no Brasil, Claudinha, Lu, Mi, Araújo, Albatrozes, Dé, Carol, Stela, Mari, Bebela, eu só tenho a agradecer pelo amor incondicional e por sempre me receberem de braços abertos nos meus retornos. Sem vocês isso não seria possível.

Aos meus pais, Glaucia e José Maria, ao meu querido irmão Ivan, à minha madrinha Laetitia, meu muito obrigada. Vocês são minha força e minha inspiração. Eu não saberia continuar sem vocês. Agradeço por tudo, sempre.

Table of Contents

Acknowledgments i

Table of Contents iii

List of Abbreviation vii

Summary ix

Samenvatting xi

Chapter 1 Introduction 1

1.1 Soil salinization and impact on crops 4

1.1.1 The two effects of salt stress 6

1.2 Maize relevance and morpho-physiological aspects 19

1.2.1 The physiological basis of salt stress response in maize 23

1.2.2 The molecular basis of salt stress response in maize 26

1.3 Plant phenotyping 35

1.3.1 Methods on physiological phenotyping 37

1.3.2 Proteome analysis 40

1.3.3 Label-free shotgun proteomics 47

1.4 Research approach and objectives 54

Chapter 2 Material and methods 56

2.1.1 Plant material and experimental conditions 59

2.1.2 Phenotyping optimization and growth traits selection 60

2.1.3 Genotype-specific early detection of salt stress 61

2.1.4 Screening of genetic diversity towards salt stress 61

2.2 Growth analysis traits, ion content and proteomics methodologies 62

2.2.1 Shoot area – image-based phenotyping 62

2.2.2 Plant height 63

2.2.3 Fresh weight.....63

2.2.4 Dry weight 63

2.2.5 Ion content 64

2.2.6 Gel-free proteomics approach 64

2.3 Statistics.....66

Chapter 3 Phenotyping optimization, growth traits selection and establishment of the stress level 68

3.1 Introduction.....68

3.2 Results and discussion.....69

3.2.1 Phenotyping optimization and growth traits selection 69

3.2.2 Establishment of the stress level 73

3.3 Conclusions.....86

Chapter 4 Genotype-specific growth and proteomic responses of maize towards salt stress.....88

4.1 Introduction.....88

4.2 Results 91

4.2.1 Physiological phenotyping toward NaCl effects 91

4.2.2 Ion Content Determination 95

4.2.3 Protein identification and responsiveness to salt stress 96

4.2.4 Proteins differently abundant in response to salt stress, according to genotype 101

4.3 Discussion 111

4.3.1 Growth impact caused by salt stress 111

4.3.2 LEA proteins as markers of salt stress 112

4.3.3 Antioxidant responses 112

4.3.4 Class III plants peroxidase 113

4.3.5 Genotype-specific reactions 114

4.4 Conclusions 117

Chapter 5 Growth analysis and tissue phenotyping of additional maize genotypes differing in salt stress responses 118

5.1 Introduction 118

5.2 Results and discussion 119

5.2.1 Physiological phenotyping 119

5.2.2 Tissue phenotyping toward salt stress 126

5.3 Conclusions 162

Chapter 6 General conclusions, discussion and future research 165

6.1 General conclusions and discussion 165

6.1.1 Salt stress related proteome responses - parallel between experimental chapters 171

6.2 Future research 177

Reference List 183

Supplementary Table S4.1 List of proteins found in roots of four maize genotypes at the fourth week after sowing (Chapter 4). 221

Supplementary Table S5.1 List of proteins found in leaves of five maize genotypes at the seventh week after sowing (Chapter 5)..... 363

Supplementary Table S5.2 List of proteins found in roots of five maize genotypes at the seventh week after sowing (Chapter 5)..... 463

List of Abbreviation

2-DE: two-dimensional gel electrophoresis
ABA: abscisic acid
ATP: adenosine triphosphate
BLAST: basic local alignment tool
BP: biological process
Chr: chromosome
CLC: chloride channel
CIMMYT: International Maize and Wheat Improvement Center
Da: Dalton or unified atomic mass unit
DNA: desoxyribonucleic acid
dS m^{-1}: deciSiemens per meter
DTT: dithiothreitol
DW: dry weight
EC: electrical conductivity
$EC_{1:5}$: 1:5 soil to water ratio electrical conductivity
ECe: electrical conductivity of a saturated soil extract
EC_i: initial EC
EC_f: final EC
ECsw: electrical conductivity of soil water suspensions
EDTA: ethylenediaminetetraacetic acid
ESI: electrospray ionization
ETC: electron transport chain
FDR: false discovery rate
FW: fresh weight
GO: gene ontology
H^+-ATPase: proton-pumping ATP phosphohydrolase
H^+-PPase: proton-pumping inorganic pyrophosphatase
HKT: high-affinity Na^+/K^{+-} permeable transporter
LC: liquid chromatography
LN: liquid nitrogen
LSD: least significant difference
MALDI: matrix assisted laser desorption ionization
Mb: millions of base pairs
mRNA: messenger RNA
MS: mass spectrometry
MS/MS: tandem mass spectrometry
mM: millimolar
mV: millivolts
m/z: mass-to-charge ratio
NaCl: sodium chloride
NADP: nicotinamide adenine dinucleotide phosphate
NADPH: reduced form of NADP
NSC: non-selective ion channels
OT: orbitrap
PSI: photosystem I
PSII: photosystem II
RNA: ribonucleic acid
ROS: reactive oxygen species
Rpm: revolutions per minute
SEA: Singular Enrichment Analysis
SPS: saturated extract paste method
SS1: salt stress 1
SS2: salt stress 2
TOF-MS: time-of-flight mass spectrometers
Tris: tris(hydroxymethyl)-methyl glycine
TSS: total soluble salts
UPLC: ultra high performance liquid chromatography
USDA: United States Department of Agriculture
v / v: volume / volume

Summary

Maize is one of the most produced crops in the world, ranking second in 2017. However, despite having higher genetic diversity than temperate germplasm, tropical maize production and research has been clearly neglected, especially by the private sector. Furthermore, production of maize is constantly confronted by the presence of biotic and abiotic stresses, including salinity, which already affects 19.5% of irrigated lands. Salinity in maize impacts all developmental stages with different strength. Tolerance is dependent on multiple biochemical and physiological pathways. Thus, it is important to understand and quantify the disorders and responses, which allows in a later stage the detection of salt tolerant plants. Results obtained over time can point out critical moments for molecular analysis, such as proteomics. In this context, our general aim was to develop a simple phenotyping protocol to characterize tropical genotypes. For that, we characterized the stress in different tropical maize genotypes to understand the reactions at different levels.

To establish our phenotyping protocol, we focused in chapter 3 on the selection of appropriate traits that are transferrable to countries where research is less intensive ("cheap and easy phenotyping technology"). We monitored the growth of three maize genotypes in control conditions: the temperate B73, and the tropical genotypes Across8023 and Across8024. Secondly, for the establishment of an appropriate stress level, the growth of those three maize genotypes was monitored in three conditions: control, 0.6% NaCl and 1.2% NaCl. A picture from the top area allows a reliable monitoring of the same individuals through all the experimental time. It is a powerful variable and together with plant height it is a low-cost non-destructive resource for growth determination. We determined 0.6% NaCl as the most appropriate level of stress to rank our genotypes.

In chapter 4 we applied the methodology determined in chapter 3 to screen more genotypes and to get an insight into the responses at the cellular level at an early stage. In addition to the sequenced genotype B73, three tropical maize genotypes were evaluated during four weeks after sowing: CML421, CML448 and CML451. Experimental chapter 4 proved that growth monitoring in terms of top area, fresh weight and ion content during salt stress is a successful strategy to guide roots proteomics analyses and study the early reactions. Proteomics responses indicated an increase in the abundance of proteins related to cellular respiration, response to oxidative and water stress, and cell redox homeostasis in roots of salt-stressed plants.

In chapter 5 we focused on the growth and molecular characterization of the roots and the leaves of more three new genotypes (CML465, CML488 and CML491) and we investigated the molecular responses at a later stage. As molecular responses, leaf proteomics pointed to a general decrease in photosynthesis, regulation of biological quality and light harvesting ATP synthase activity for all the salt-treated plants. Roots proteomics showed that salt stress affected the protein abundance more than three times fold than leaves, being related to energy synthesis, antioxidant response and protein synthesis.

In conclusion, we used a systems-level approach uniting plant responses at different scales to classify and characterize different tropical maize genotypes towards salt stress. An overall ranking of all genotypes groups Across8023, Across8024 and CML465 as the most tolerant in salt stress, followed by CML488, B73, CML 448, CML451, CML491 and, finally, CML421 as the most sensitive. A low-budget research approach was established for maize phenotyping and molecular mechanisms of salt tolerance and stress markers were identified through the applied methodology.

Samenvatting

Mais is een van ’s werelds meest geteelde gewas en wordt gebruikt voor voeder, biobrandstof en als voedsel. Het biedt voor vele ontwikkelingslanden een belangrijke voedselbron en onderzoek naar gewasverbetering is van cruciaal belang. Helaas gebeurt er nog veel te weinig onderzoek naar tropische maissoorten omdat de private sector voornamelijk investeert in de maissoorten die groeien in gematigde contreien. De maisproductie staat voortdurend onder druk van zowel biotische als abiotisch factoren. De kwaliteit van het irrigatiewater heeft een grote invloed op de gronden en reeds 19.5% van het geïrrigeerde land heeft een te hoog zoutgehalte. Een te hoog zoutgehalte heeft een negatieve invloed op zowel ieder ontwikkelingsstadium van de maisplant maar sommige stadia zijn gevoeliger dan andere. Tolerantie is complex en is het resultaat van zowel fysiologische aanpassingen op weefselniveau als van biochemische aanpassing op cellulair niveau. Het is dus van cruciaal belang om inzicht te krijgen in deze mechanismen. Wanneer mais onderzocht wordt tijdens de blootstelling aan zout doorheen de tijd kunnen cruciale momenten in kaart gebracht worden om de cellulaire biochemische reacties te karakteriseren. Het algemeen doel van ons onderzoek was om de kostbare tropische biodiversiteit te onderzoeken en zo zaadbanken vooruit te helpen om de juiste variëteit bij e juiste boer te brengen. Hiervoor hebben wij een onderzoeksmethode ontwikkeld om de tolerantie naar zoutstress te onderzoeken, tolerante variëteiten te identificeren en beter te begrijpen. We hebben een protocol op punt gesteld dat simpel en goedkoop is om de groei en de zout gerelateerde groeivertraging van de verschillende variëteiten objectief in kaart te brengen en ze te rangschikken.

Om ons fenotyperingsprotocol te realiseren, hebben we in hoofdstuk 3 toegespitst op het vinden van een methode die de meest geschikte

eigenschappen van een plant in kaart brengen. Dit op een manier die efficiënt, objectief maar toch goedkoop is, zodat die overgeleverd kan worden naar landen die minder middelen ter beschikking hebben voor onderzoek. Om deze methode op punt te stellen, hebben we de groei van 3 genotypes bestudeerd in een serre (de referentie varieteit B73 en 2 tropische variëteiten Across8023 en Across8024). Vervolgens hebben we ervoor gezocht dat we de planten blootgesteld hebben aan een relevant zoutgehalte. Twee concentraties werden hiervoor uitgetest: 0.6% NaCl en 1.2%. Wanneer de plant vanuit de hoogte gefotografeerd wordt, krijgen we een betrouwbaar beeld van de plant. Deze geprojecteerde plantoppervlakte is samen met de planthoogte een zeer krachtige niet-destructieve variabele en kan de groei en dus de groeivertraging van iedere individuele plant opvolgen in de tijd. We hebben vastgesteld dat 0.6% NaCl het meest geschikt was om de diversiteit aan reacties goed in kaart te brengen en deze 3 verschillende variëteiten te rangschikken.

In hoofdstuk 4 hebben we deze fenotyperingsmethode toegepast op meerdere variëteiten. We hebben samen met de gematigde B73 referentie 3 tropische variëteiten succesvol bestudeerd gedurende 4 weken: CML421, CML448 en CML451. De combinatie van het geprojecteerde plantoppervlak, het versgewicht en de zoutopstapeling in de bladeren stelden ons in staat om de interessante tijdstippen aan te duiden om de biochemische cellulaire reacties te bestuderen in de wortels (proteomics). De veranderingen in het proteoom wezen op een verschuiving van eiwitten betrokken in celrespiratie, en het neutraliseren van oxidatieve stress.

In hoofdstuk 5 hebben we ons toegespitst op de analyse van zowel de wortels als van de bladeren van 3 extra variëteiten: CML465, CML488 and CML491. Opnieuw heeft fenotyperen ons geleid naar interessante tijdstippen om de cellulaire reacties te bestuderen. De veranderingen in het proteoom waren 3

keer meer intensief in de wortels als in het blad. De accumulatie van zoutionen in het blad hebben een negatieve invloed op de fotosynthese terwijl in de wortels veranderingen in energie- en eiwitsynthese plaatsvinden alsook verdedigingsmechanismen tegen oxidatie.

Wij besluiten dat onze aanpak om eerst planten te observeren hoe hun groei beïnvloed wordt tijdens de blootstelling aan zoutstress en dan op cruciale tijdstippen de biochemische reacties in kaart te brengen geschikt is om de verschillende genotypes te rangschikken en een inzicht te verkrijgen in de verschillende tolerantiemechanismen. Van alle genotypes die we onderzocht hebben kunnen we de volgende rangschikking opstellen: Across8023 > Across8024 > CML465 > CML488 >B73 >CML 448> CML451 CML491 > CML421. De genotypes Across8023, Across8024, CML465 en CML488 beschouwen we als tolerant. De fenotypering is een efficiënte objectieve en goedkope manier om de maisbiodiversiteit in kaart te brengen.

Chapter 1 INTRODUCTION

The basis of human nutrition is 52% composed of cereals, with maize included as one of the most important (FAO, 2015). This crop reached in 2014 a global production of more than 1 billion tons, being ranked as the second most produced crop in the world (http://faostat.fao.org/). Maize is an important source of food and animal feed, as well as feedstock for biofuel production (Gong et al., 2014).

As a worldwide planted crop, maize is potentially susceptible to several abiotic and biotic stresses, such as pathogens, drought and soil salinity. It is estimated that by the year of 2050, soil salinity and drought will negatively affect more than 50% of arable lands in the world (Gong et al., 2014), while the population will increase from 7.3 billion to 9.7 billion people (Melorose et al., 2015). Thus, considering the current dietary framework, it is calculated that cereal demand will raise from approximately 2.1 billion tons to 3 billion tons to satisfy the demand for food and animal feed by 2050 (FAO, 2009).

Since the 1960s, a considerable rise of 138% was achieved for crop production until 2007 (Langridge and Fleury, 2011). However, factors that led to this accomplishment face serious struggles, including the amplification of the use of irrigation and large fertilizers application, which can be both non-sustainable procedures when no proper draining system is applied, proved to lead to the accumulation of salts on the soil, a process referred as salinization (Langridge and Fleury, 2011; Munns, 2005).

Salinity stress has a two-phase effect on plants: the first one is the osmotic stress, which has a rapid onset, followed by a slower second phase, the ionic stress (Munns, 1993). Thus, tolerance mechanisms are, in literature, artificially divided according to these two phases. The use of different mechanisms and its

effectiveness are the distinguishing factors between salt-sensitive and salt-tolerant plant species (Munns and Tester, 2008). In addition, since lands affected by salinity are commonly at arid and semiarid areas, plants are generally also adapted with mechanisms of tolerance to osmotic stress, independent of ionic tolerance level (Munns and Tester, 2008). With that, the selection of tolerance traits should be based on specific aims, to specific species. Maize is considered moderately sensitive to salt (Maas and Hoffman, 1977) and due to the world significance of this crop, it is of paramount importance to study the effects on it when subjected to the salt stress.

Salinity effects in plants manifests on the whole plant level and impacts all developmental stages, becoming gradually more severe. Thus, the tolerance of plants is dependent on multiple pathways (Ahmad et al., 2016). Due to the multiple and dynamic nature of salt stress, it is important that the responses are divided in different traits to understand and quantify the disorders and reactions. Such division of traits should enable the distinction of levels of tolerance between crops or genotypes (Cattivelli et al., 2008). Phenotyping at different developmental stages aggregates valuable information to stress studies (Cattivelli et al., 2008) and linking this analysis to molecular analysis (cellular phenotyping) is a powerful approach. Plant responses are continuous and dynamic, while the molecular analysis is a static time point. Moreover, molecular analysis is very expensive. Results obtained from non-destructive phenotyping over time can point out critical moments for sample collection for further molecular analysis.

Adjacent to the physiological phenotyping, cellular phenotyping also contributes to understand the perception and reaction of plants towards stress. In fact, cell morphology and function are the result of multiple processes involving gene and protein expression, which in conjunct, form the cellular

phenotype (Sul et al., 2009). Since both phenotyping spheres can be complemental, a workflow integrating them are ideal to provide useful information about stress responses. One needs to be able to look beyond the cell and tissue and integrate this information towards plant behavior.

It is relevant to mention that gene banks are crucial in the process of characterizing and understanding stress responses of crops. Having the responsibility of conserving the genetic diversity of cultivated and wild plants, it is also a valuable source of information.(McCouch et al., 2012a). For maize, for example, more than 135,000 accessions are conserved worldwide (IPCC, 2007). However, gene banks struggle with the systematization of their conserved material, mainly caused by improper genetic characterization, and an even worse picture when it comes to phenotypic characterization (Prasanna, 2012). Not only characterization based on DNA across the whole genome for an entire collection is still a non-achieved aim for gene bank management, but phenotypic evaluation have often not been held as their responsibility (Prasanna, 2012). In developing countries this frame is even worse, due to a lack of resources and strategies for germplasm systematic characterization (Prasanna, 2012). With the advance of genetic and phenotypic characterization technologies, it is expected and highly necessary that these issues are overcome, and that an increased amount of genetic and phenotypic information become available for use in other research programs, such as stress-related ones.

In this context, the general objective of this work was to generate useful information, focused on tropical genotypes, to farmers and germplasm banks, assisting in food security. For that, we aimed specifically in the characterization of the stress in different tropical maize genotypes, to understand the signaling and defense at different levels. We assumed that a systems-level approach has the potential to unite the plant responses at different scales and enhances the

understanding of a plant's reaction towards stress. Linking physiological measurements to phenotyping at the cellular level helps to understand small physiological changes by guiding the cellular analyses to the right physiological moment. Consequently, we will be able to interpret phenotypical changes of salt stress.

1.1 Soil salinization and impact on crops

Salinity is one of the major factors of soil damage (Gong et al., 2014). It is characterized by the presence of soluble salts in waters or soils, such as sodium bicarbonate ($NaHCO_3$), sodium carbonate (Na_2CO_3) and the most common, sodium chloride (NaCl) (Munns and Tester, 2008; Rengasamy et al., 2003).

Levels of salt concentration are used to classify the soils according to the electrical conductivity of the saturated paste extract (EC_e). Thus, soil classification ranges from non-saline ($EC_e < 2$ dS m^{-1}) to extremely-saline ($EC_e > 16$ dS m^{-1}) (Table 1.1) (USDA).

Table 1.1 Classification of soil salinization according to electrical conductivity of the saturated paste extract (EC_e) (USDA)

Soil classification	**EC_e Range**
Non-Saline	< 2 dS m^{-1}
Slightly Saline	2 – 4 dS m^{-1}
Moderately Saline	4 – 8 dS m^{-1}
Highly Saline	8 – 16 dS m^{-1}
Extremely Saline	> 16 dS m^{-1}

Field analysis shows a wide range of EC_e values for saline soils in different regions. In Iraq, for example, for superficial portions of the soil (0-15 cm), the EC_e varied from 12 to 75 dS m^{-1} (FAO, 1988). However, there is no quantitative inventory available for soil salinity reliably mapping affected areas worldwide (Scudiero et al., 2015).

Saline soils can be divided in two types: natural or primary and secondary or human-induced. The primary saline soil results from the accumulation over long periods of time of salts originated from natural sources. The release of soluble salts from rocks by weathering processes and the oceanic salt brought with rain and wind to the inland constitutes the processes driven by nature contributing to the soil salinization (Munns, 2005).

Secondary saline soil emerges from anthropogenic activities, with a special weight from deforestation for annual crop cultivation, irrigation using low quality water or without proper draining system, and overuse of fertilization products (Munns, 2005). The first two processes together, land clearing and irrigation, causes the mobilization of deep soil stored salts closer to the soil

surface. This occurs due to the inability of the crops to absorb all the available irrigation plus rainwater, which will run to below the roots, encountering the lower water tables. Thus, this will cause the rising of water tables and subsoil salts to the root zone, resulting in the salt accumulation through time (Rengasamy et al., 2003).

In the year of 2016, it was estimated that 19.5% of irrigated lands were salt-affected (FAO, 2016). Despite representing only 20% of the total cultivated land, irrigated land produces the double of rain fed land, accounting for 40% of world's food production (FAO, 2015). With the prediction of more than half of arable lands being affected by salinity and drought in 30 years from now (Gong et al., 2014), the rise in population to 9.7 billion people (Melorose et al., 2015) and the aggravation of the environmental situation by climate change (IPCC, 2007), the challenge now is to produce more effectively but in a sustainable system.

1.1.1 The two effects of salt stress

Definition of stress can be based in terms of energy production versus energy costs. A plant is in a stress state when the total acquired energy is reduced by a decrease in photosynthesis rate/leaf area and/or by redirecting energy originally aimed to growth into self-defense. Thus, overcoming a stress in maize means to guarantee sufficient energy to be directed to grain production and yield improvement (Munns and Gilliham, 2015).

1.1.1.1 Osmotic stress phase of salinity

Salinity stress has a double effect on plants: osmotic stress and ionic specific stress (Munns, 1993). In the first phase, the ions surrounding the roots lower the osmotic potential hindering the uptake of water (Munns and Tester, 2008).

An immediate effect is the reduction on shoot and root elongation (Passioura and Munns, 2000; Rodriguez et al., 1997). In case of mild stress, the growth can be rapidly recovered or stabilized at a certain level that is usually lower than normal conditions. However, this lack of water can escalate in time if the salt concentration is high and sustained during long periods, leading also to a slower emergence of new leaves and lateral buds (Munns and Tester, 2008).

1.1.1.2 Ionic stress phase of salinity

Since the ions are water soluble, they enter the apoplastic root space and might enter into the symplast. Also, the strength of the Caspari strips controls the rate in which the ions can penetrate towards other tissues. Later, when the plant absorbed sufficient saline water, the soluble ions are accumulated in the shoot and may reach toxic concentrations (Munns and Tester, 2008). The dynamics of ion transportation are further discussed later in this chapter.

The intoxication occurs especially in older leaves, when vacuoles can no longer compartmentalize incoming ions (Flowers and Yeo, 1986). Therefore, a visible effect of specific ionic stress is the senescence of older leaves and reduced shoot growth (Munns and Tester, 2008). Toxicity of accumulated ions can have a variety of causes, such as dehydration of the cell, when there is apoplast concentration of sodium (Na^+) or chloride (Cl^-) (Tester and Davenport, 2003; White and Broadley, 2001).

A major intoxication effect caused by Na^+ accumulation in the cytoplasm is the inhibition of enzymes. Being a competitor of binding sites with potassium (K^+), sodium disrupts the activation of K^+-dependent enzymes, leading to the disturbance of important metabolic processes (Tester and Davenport, 2003). For chloride, despite being considered a matter of great relevance, the study of

its accumulation effects over enzymes activity have been neglected (Geilfus, 2018).

Toxic accumulation of Na^+ and Cl^- also leads to a reduction of photosynthetic activity, being the action mode different for each ion. For sodium intoxication, its interference with K^+ uptake results in a disruption of stomatal regulation, causing the stomata to reduce their conductivity and stomatal closure, leading to photosynthesis decrease (Slabu et al., 2009). In the case of chloride, photosynthesis reduction is linked to the chlorophyll degradation promoted by the concentration of this ion probably on PSII (Tavakkoli et al., 2010).

Growth reduction caused by specific ion-toxicity can also be explained by a competition of chloride with phosphate and nitrogen. The transport antagonism of these anions with Cl^- can result in a reduction of uptake and storage of the nutrients, leading to the growth retardation observed in plants subjected to this stress (Cubero-Font et al., 2016; Hu and Schmidhalter, 1997).

1.1.1.3 Salt-tolerance classification and mechanisms

Different species will present distinct reactions to salinity, being classified as halophytes and non-halophytes (glycophytes) (Jennings, 1976). Halophytes are nearly or not affected or even stimulated by salt. Glycophytes have their growth negatively affected by salinity and have responses varying from tolerant to intermediate until very salt-sensitive glycophytes (Greenway and Munns, 1980).

The tolerance mechanisms to salt are correlated to osmotic tolerance and ionic stress tolerance, which includes ion exclusion and tissue tolerance (Munns and Tester, 2008). A plant that features osmotic tolerance during salt stress should present maintenance of photosynthesis and growth, and high ability of osmotic

adjustment. For that, perception and signaling starts from the roots and, despite the whole process is still not known, valuable insights were cleared.

It is broadly known that the osmotic stress effect of salinity, causes an immediate reduction of leaf growth (Munns, 2002a), but the mechanisms behind this effect are not totally clear. Phytohormones and their interaction with signaling polypeptides have an important role in the regulation of growth and plant acclimation to detrimental environment (Munns and Tester, 2008; Ryan et al., 2001). The modulation of the distribution of abscisic acid (ABA), for example, induces the closure of guard cells, in a sequence of events involving pH change (Felle, 2001; Geilfus et al., 2015). The encounter of water stress by the roots triggers a systematic apoplast alkalinization, which is carried through the stem, reaching the leaves (Geilfus and Mühling, 2012; Wilkinson and Davies, 1997). Xylem sap alkalinization causes the dissociation of ABA (from ABAH to ABA^-), that loses the ability to readily cross membranes and, consequently, is not sequestrated by mesophyll cells as normally (Taiz and Zeiger, 2010a; Wilkinson and Davies, 1997). Thus, ABA is accumulated in the surroundings of guard cells, leading to stomatal closure (Wilkinson and Davies, 1997).

In the roots, ABA also inhibits its growth and a crosstalk with the signaling peptide RALF (*Rapid Alkalinization Factor*) in this process is proposed by Chen et al. (2016). RALF was first described by Pearce et al. (2001) and its activity was also related to roots growth and development regulation, as well as alkalinization of cell suspensions.

Halophytes largely rely on the balancing of inorganic ions (Na^+, Cl^- and K^+) to keep osmotic and turgor pressure (Flowers et al., 1977), while glycophytes plants count mainly on *de novo* synthesis of compatible organic solutes, such

as proline, betaine, polyols, sugar alcohols and soluble sugars (Shabala et al., 2016). However, while inorganic ion accumulation implies a low energy cost (3.5 ATP molecules requirement for Na^+) the synthesis of organic solutes comes with a high cost for the plant (Raven, 1985). Requirements of 34 ATP molecules for mannitol, 41 for proline and 52 for sucrose, for example, translates in loss of energy for plant growth, but can be its survival and recovery best shot in a saline environment (Munns and Tester, 2008; Raven, 1985).

Specifically to ionic stress, the complex pathway based on the SOS (*Salt Overly Sensitive*) genes is related to an increase in cytosolic free Ca^{2+} (Zhu, 2002). This increase is a direct response of the Na^+ present around the salt stressed roots and triggers the expression and activity modulation of ion transporters (Zhu, 2002). The increased concentration of cytosolic Ca^{2+} may be sensed by a calcineurin B-like protein (CBL4), originally SOS3, which will interact with a CBL-interacting protein kinase (CIPK24, previously named SOS2) (Halfter et al., 2000; Munns and Tester, 2008). This SOS3/SOS2 complex is then directed to the plasma membrane (Ishitani et al., 2000), leading to the activation of the Na^+/H^+ antiporter (SOS1) (Qiu et al., 2002; Shi et al., 2002).

Hardening of the leaves and roots cell wall as a response to salt stress is also a contributing factor for growth retardation (Geilfus et al., 2017; Neumann et al., 1994). Geilfus et al. (2017) proposes the alkalinization of the leaf apoplast during a chloride-salt stress as a relevant factor in the mechanism of cell wall stiffening, by the detected increase of enzymes that synthesizes cell wall compounds, like lignin and hemicellulose. Stiffening of the cell wall would benefit water stressed plants by diminishing water loss and wilting (Kutschera and Schopfer, 1986).

Oxidative stress is another consequence a plant can face when exposed to a saline environment. ROS are a group of free radicals, reactive molecules and ions (Sharma et al., 2012) formed through conversion of molecular oxygen (O_2) by transfer of energy (singlet oxygen - $^1O_2$) or electron transfer reactions (superoxide anion - $O_2^{\bullet-}$; hydrogen peroxide - H_2O_2; and hydroxyl radical - $^{\bullet}OH$) (Apel and Hirt, 2004). They are constantly produced and removed in steady physiological conditions, being a secondary product of metabolic pathways of plants (Apel and Hirt, 2004). ROS have a role in cellular processes, including stress signaling (Munns and Gilliham, 2015), but in a disequilibrium of the system, they can be highly damaging to the cells (Sharma et al., 2012). In this case, their overproduction can disturb enzymatic activity, as well as the functions of cell wall and plasma membrane (Munns and Gilliham, 2015).

ROS are formed in several locations of different plant cell compartments: chloroplasts, mitochondria, endoplasmic reticulum, peroxisomes, plasma membranes and cell walls (Sharma et al., 2012). In chloroplasts and mitochondria, besides other spots, the main sources of ROS production are the electron transport chains (ETCs). When in certain stress conditions, such as salt stress, the ETCs in PSI and PSII are overloaded due to a reduction of nicotinamide adenine dinucleotide phosphate (NADP) supply, leading to a leakage of e^- and ROS production (Hippeli and Elstner, 1996). In mitochondria, several sites of the ETC are ROS producers, with an increase during stress caused by the over-reduction of electron carriers (Blokhina and Fagerstedt, 2010).

In endoplasmic reticulum, superoxide anion ($O_2^{\bullet-}$) is formed because of the NAD(P)H-dependent electron transport (Mittler, 2002), while peroxisomes are possibly the main H_2O_2 production site (del Río et al., 2006). Plasma membranes have electron transporting oxidoreductases responsible for ROS

production (Sharma et al., 2012) and cell walls possess associated peroxidases, generating cell wall H_2O_2 and other enzymes which produce apoplastic ROS (Apel and Hirt, 2004; Heyno et al., 2011).

Plant respiratory burst oxidase homologs (Rbohs), also known as NADPH oxidases, are a unique and extensively studied production site of ROS (Wang et al., 2018). Rbohs are a plasma membrane-bound protein complex that catalyzes the production of $O_2^{\bullet -}$ by transferring electrons from cytosolic NAD(P)H to apoplastic molecular oxygen in an electron transport chain (Torres and Dangl, 2005; Wang et al., 2018). In plants, Rbohs have an N-terminal extension region which contains elongation factor hand motifs that, binding with Ca^{2+}, regulates its activity (Liu and He, 2016)

Antioxidant defense systems in plants count with both non-enzymatic and enzymatic components to detoxification of ROS. Ascorbate (AsA), glutathione (GSH), tocopherols, carotenoids and phenolic compounds work as non-enzymatic antioxidants acting in different subcellular compartments. Enzymatic elements include superoxide dismutase (SOD), catalase (CAT), guaiacol peroxidase (GPX) (class III peroxidase), and enzymes of ascorbate-glutathione cycle, as ascorbate peroxidase (APX) and glutathione reductase (GR) (Sharma et al., 2012). These enzymes work in sequence, in different cell compartments (Munns and Tester, 2008). Plants naturally have ROS detoxifying mechanisms and, therefore, it is not really a factor of genetic adaptation to one specific stress, like ionic stress (Abogadallah, 2010; Apel and Hirt, 2004). However, the improvement of this already present system was shown to enhance the tolerance of plants towards specific stress, like salinity (Csiszár et al., 2014; Negi et al., 2015; Surender Reddy et al., 2015; Wang et al., 2016; Xu et al., 2015).

It is stated that the main ionic toxicity is generated by the accumulation of Na^+, rather than Cl^-, in the plants shoot (Maathuis et al., 2014). In fact, although NaCl is the dominant salt in the soil, studies to reveal Cl^- effects and tolerance mechanisms on plants have been significantly lower than for Na^+ (Teakle and Tyerman, 2010). However, studies demonstrated that, despite having different effects, Cl^- impacts the plants growth at the same degree as Na^+ (Tavakkoli et al., 2010) and that Cl^- is actually an important factor for signaling of the salt stress (Geilfus et al., 2015). The specificity for Na^+ and/or Cl^- intoxication is different among plants species, but it is basically dependent of the ability of exclusion from the leaves (Li et al., 2017a). For that, the control of sodium and chloride transportation from the roots during salt stress is an important mechanism for damage avoidance.

The movement of sodium and chloride ions from the roots to the shoot counts mainly with ion transport proteins, which can occur both active- and passively (Tester and Davenport, 2003; White and Broadley, 2001).

When in ordinary condition, chloride enters the roots cells via passive uptake through Cl^- channels, a process that occurs actively when at high salinity, by a plasma membrane $Cl^-/2H^+$ symporter of root-hair cells (Felle, 1994), (Figure 1.1) (White and Broadley, 2001). Efflux of chloride across plasma membrane can also be mediated by Cl^- channels (White and Broadley, 2001) and can have a role in its concentration reduction during salinity (Li et al., 2017a). Already inside the roots, the way to the xylem will be mostly crossed via selective symplastic pathway, through plasmodesmata and involving Cl^- transporters, or via apoplast, a non-selective pathway, in which the ion movement is restricted by Casparian bands (White and Broadley, 2001). Chloride movement from roots cells symplast into xylem apoplast is entirely passive and the activity and

expression of the responsible Cl^- transporters may be downregulated during salt stress (Gilliham and Tester, 2005).

Leaf mesophyll cells and guard cells are possessors of chloride channels (CLCs) and transporters, which have roles in shoot chloride accumulation and can inflict tolerance towards salt stress (Cubero-Font et al., 2016; Li et al., 2017a; Qiu et al., 2017; Ramesh et al., 2015). In vacuoles, influx of chloride is mediated by Cl^-/nH^+ antiports and by the presence of CLCs to either direction (Li et al., 2017a; White and Broadley, 2001). In soybean, the overexpression of a CLC (*GmCLC1*) gene resulted in a larger Cl^- sequestration by the vacuoles during salinity, decreasing cell death and mitochondrial damage (Li et al., 2006).

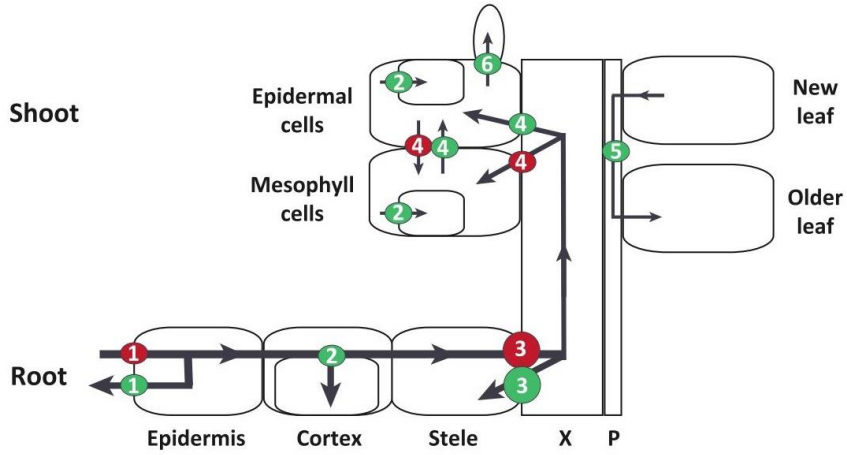

Figure 1.1 Chloride route from root cells to shoot. Red circles: process inhibition lowers Cl^- leaves concentration. Green circles: processes that regulates positively Cl^- tolerance. X, xylem. P, phloem. (1) Uptake and efflux of Cl^- into and out of root cells. (2) Vacuole sequestration of Cl^-. (3) Xylem loading and retrieval of Cl^-. (4) Compartmentalization of Cl^- in different cell types. (5) Compartmentalization of Cl^- in different plant organs. (6) Excretion of Cl^- through specialized salt glands and bladders (Li et. al., 2017).

Figure 1.1 describes the chloride pathways from root to leaves, but it can also be extrapolated to sodium transportation, with some particularities. The interior

of a cell is negatively charged (-150 to 200 mV), thus Na^+ is compelled to enter it in nearly all circumstances, while sodium efflux will not occur without energy consumption (Maathuis et al., 2014). Carrier type transporters and ion channels are responsible for the uptake of Na^+ into the roots cells from the exterior (Davenport, 2002; Horie et al., 2001; Mian et al., 2011; Newton and Smith, 2004; Tester and Davenport, 2003), while extrusion from the cytosol to apoplast is mediated by Na^+/H^+ antiporters, which were already related with tolerance to salinity (Evans et al., 2012; Maathuis et al., 2014).

As well as chloride, passage of sodium through the roots until the xylem occurs via symplast or apoplast, with Casparian strips presenting a barrier for the ion apoplastic route (Maathuis et al., 2014). However, the exact influx site into the xylem is not totally clear, despite transporters and channels have been suggested to mediate Na^+ loading, such as Shaker-like outward channel (SKOR) (Zhu et al., 2017), chloride cation co-transporter (CCC) (Colmenero-Flores et al., 2007), high-affinity $Na^+/K+^-$permeable transporter (HKT) (Moller et al., 2009; Sunarpi et al., 2005) and a Na^+/H^+ antiporter (Feki et al., 2011a; Shi et al., 2002).

The loading into the xylem apoplast is mediated by plasma membrane transporters, actively via Na^+/H^+ exchanges or passively through Na^+ channels (Lacan and Durand, 1996). Non-selective ion channels (NSCs) are also responsible for the release of Na^+ to xylem apoplast (Demidchik and Maathuis, 2007). The HKT transporter has a rule in the retrieval mechanism of sodium from the xylem, preventing its transportation to the leaves and consequent intoxication, and its absence confers a lower tolerance to salinity (Davenport et al., 2007; Moller et al., 2009; Ren et al., 2005).Vacuolar sequestration of Na^+ is catalyzed by a Na^+/H^+ antiporter in a system which inner and outer H^+

difference is produced by H^+-ATPase and proton-pumping inorganic pyrophosphatase (H^+-PPases) (Apse et al., 1999; Blumwald et al., 2000).

Another mechanism to avoid ion accumulation within the leaves is possibly the retranslocation through the phloem, a movement not completely understood and still in judgment about its relevance for salt stress tolerance (Maathuis et al., 2014). However, Lohaus et al. (2000) showed that in salt stressed maize 13 % of Na^+ and 36 % of Cl^- transported into the leaves via xylem was recirculated via phloem, representing an important mechanism of NaCl control.

Halophytes can have additional adaptive resources to prevent high ion concentration in the leaves, such as salt glands, bladders and succulence (Flowers et al., 1977) and, as well as for the glycophytes, the level of tolerance will be determined by the combination of different mechanisms of salt tolerance (Greenway and Munns, 1980).

Tissue tolerance is defined as the capacity of tissues to keep functioning despite the high concentration of sodium and chloride (Li et al., 2017a). Normal tissue function means no chlorophyll damage, growth maintenance and no dehydration (Munns et al., 2016; Yeo and Flowers, 1983). This is usually achieved with an efficient ion compartmentalization within cells and the accumulation of compatible solutes (Greenway and Munns, 1980; Munns and Tester, 2008).

An indicator of high sequestration of Na^+ and Cl^- is the detection of a large concentration of these ions within tissues that keep normal operation (Munns et al., 2016). This mechanism was proposed when Flowers (1972) found that halophytic and glycophytic enzymes are equally affected by the presence of salt in the solution. Thus, it was clear that rather than a difference among enzymes, a physical barrier was preventing the malfunctioning of halophytic enzymes.

Therefore, chloride and sodium are sequestrated by vacuoles to diminish their availability in the cytosol (Flowers et al., 1977).

As previously mentioned, the tolerance of plant species towards salinity is in direct correlation with vacuolar salt sequestration and the overexpression of each specific transporter can lead to increased tolerance (Apse et al., 1999; Blumwald et al., 2000; Fukuda et al., 1998; Li et al., 2017a; Staal et al., 1991). Moreover, ion partitioning among different cell types is also a tolerance factor to guarantee normal function of cells. Epidermal cells for example, can be the preferable accumulation site of ions, instead of mesophyll cells, which largely contains the photosynthesis apparatus (Conn and Gilliham, 2010).

Compatible solutes accumulation, as well as increased K^+ concentration, becomes then an osmotic pressure requirement imposed by the vacuolar sequestration of ions (Munns and Tester, 2008). They have the function of mounting up within the cell, to guarantee not only a balance of the osmotic difference (Singh et al., 2015), but also having a role in stabilizing proteins and membranes, as well as preventing cell dehydration driven by the high membranes osmotic potential (Hussain Wani et al., 2013). Overexpression of osmoprotectants induced salt tolerance in several transgenic plant species, generated mainly with focus on genes involved in the biosynthesis pathways of such organic solutes (Hmida-Sayari et al., 2005; Kasukabe et al., 2004; Sawahel and Hassan, 2002; Shirasawa et al., 2006; Surekha et al., 2014; Yang et al., 2008; Zhou et al., 2008).

Several genetic manipulations, either to prevent ion accumulation in leaves or to enhance tissue tolerance, were successful in improving the salt tolerance of plants (Apse et al., 1999; Blumwald et al., 2000; Fukuda et al., 1998; Li et al., 2017a; Staal et al., 1991; Hmida-Sayari et al., 2005; Kasukabe et al., 2004;

Sawahel and Hassan, 2002; Shirasawa et al., 2006; Surekha et al., 2014; Yang et al., 2008; Zhou et al., 2008). However, there is still a lack of field trials to determine if manipulation of one pathway is enough to guarantee not only survival and reproduction, but also yield maintenance and improvement. In the case of interference in the expression and activity of an ion transporter, for example a tonoplast Na^+/H^+ antiporter, indeed more salt can be sequestered into vacuoles. But due to the dependence relationship with H^+-ATPases or H^+-PPases, these should also be overexpressed in order to keep the activity (Shabala, 2013). Since vacuolar accumulation of ions is commonly followed by *de novo* synthesis of compatible solutes or K^+ concentration, the competition for ATP usage will be high and can deplete H^+-ATPase activity (Shabala, 2013). Regarding H^+-PPases, in saline conditions their activity may be disturbed by the lack of disponible K^+, once it is dependent on it and which will be acting as an osmoprotectant, (Rea and Poole, 1993). Thus, a single improvement of vacuolar Na^+/H^+ antiporter should not be the only focus and all the involved factors should be considered as a whole.

Furthermore, the set of acclimatization or tolerance traits should be investigated and considered for each plant species separately. For a species that possess higher tolerance to ion accumulation, the search for improvement of osmotic stress tolerance mechanisms sounds more positive than manipulation of vacuolar ion transporters (Roy et al., 2014). The same reasoning applies to a plant species that does not tolerate high levels of ion accumulation in the H+-ATPases or H^+-PPases leave cytoplasm, but with levels of osmotic tolerance. In this case, it can be beneficial to invest in ion compartmentalization mechanisms as a whole and improve tissue tolerance (Roy et al., 2014).

In any case, it is primarily important to screen and rank plant species, especially crops, and deeply investigate traits of tolerance and potential markers. Due to

the multiple and dynamic nature of salt stress, the plant responses must be divided in different traits to better understand and quantify the disorders and reactions. Such division should enable the distinction of levels of tolerance between crops or genotypes to allow the detection of salt tolerant plants (Cattivelli et al., 2008).

1.2 Maize relevance and morpho-physiological aspects

Maize is one of the most produced crops in the world, with 169 countries producing it in 2017 and ranking second in terms of world production (http://faostat.fao.org/). In Brazil, maize production was of 98.5 million tons for the years of 2016/17, with a harvested area of 17.6 million hectares (USDA 2015). It is an important source of food and animal feed, as well as feedstock for biofuel production (Gong et al. 2014).

There is, however, a relevant discrepancy between tropical and temperate maize production, research and germplasm. Despite the occupation of almost 50% of global maize-planted area, its production in tropical countries corresponds to only 30% of the total (Edmeades et al., 2017). This difference is caused not only by biotic and abiotic stresses, as well as a high impact of climate change, but it is also accentuated by a lower interest of research investment towards tropical maize, especially by the private sector (Edmeades et al., 2017). In spite of being described as having higher genetic diversity than temperate germplasm, tropical maize studies are neglected probably due to the poverty of the majority of the inhabitants of tropical areas (Hainey et al., 2015; Laborda et al., 2005; Matsuoka et al., 2002).

Moreover, it is a fact that in the developing countries, 75% of maize production is situated in tropical environments, against 90% production in temperate climate in the industrialized world. Putting together the fact that the private

sector mostly invests in maize for animal feed, while developing countries are bounded to a maize food diet, the pressure for increasing the productivity of food-maize is constantly rising, but prospects are uncertain (Pingali and Pandey, 2000). International agricultural research centers, such as CIMMYT, have been targeting the needs of countries located on the tropics, which are mostly poor and counting with low-tech subsistence maize farming. However, more efforts must be done to meet the increasing demands of maize production, and this especially implies a much higher tropical maize research investment, once good performance temperate germplasm cannot be directly introduced into tropical regions (Pingali and Pandey, 2000).

The progenitor of maize is one of a group commonly named teosinte, native to Mexico (Gaut and Doebley, 1997). Before being domesticated around 10,000 years ago, its ancestor went through allotetraploidization and diploidization, as it is presently (Gaut and Doebley, 1997). Maize has 10 haploid chromosomes and the sequenced reference maize B73 RefGen_v4 has a genome size of 2106 Mb (Jian et al., 2017).

Maize has a high genetic diversity, arising from single-nucleotide polymorphisms (SNPs) (Wang et al., 1998), insertions/deletions (indels) mutations (Chia et al., 2012), copy-number variation (CNV) (Swanson-wagner et al., 2010) and movement of transposable elements (TEs) (Morgante et al., 2007). This is encouraging for biotechnology applications, which can build on the provision of several alleles bonded to desirable traits. However, the high dispersion of these alleles through populations or landraces (Barros et al., 2010) presents a challenge in its discovery and gathering of genetic information. Thus, systematic actions aiming the broadening of our knowledge of the genetic base of maize linked with favorable traits, are of extreme importance for improvement of this crop towards climate-resilience.

During growth and development, maize leaves are initiated one by one, in opposite directions, being settled in an alternate and distichous phyllotaxy (Jackson and Hake, 1999).Their leaves are amphistomatous, i.e., stomata are present in both abaxial and adaxial surfaces (Driscoll et al., 2006) and leaves are built to perform C4 photosynthesis (Jackson and Hake, 1999).

The root system of maize plants is formed by an embryonic set of primary and seminal roots, and post-embryonic lateral, crown and brace roots (Feldman, 1994). Embryonic roots functionality due to developmental phase is maize line-dependent, becoming obsolete in some lines after the emergence of post-embryonic roots, and remaining functional during the whole life cycle (Hochholdinger, 2009). Post-embryonic crown roots forms a dense root system, essential for the ground support of the adult maize plant, while lateral roots will be the main responsible for water and nutrient uptake (McCully and Canny, 1988). Brace roots are grown aboveground, presenting functional differences of developed whorls: lower brace roots, typically the first two whorls, penetrates the soil and develops lateral roots, and higher whorls will function as an aboveground support, preventing bended plants to touch the soil (Feldman, 1994).

Maize is an annual crop and completes its cycle in around 120 days, producing 20 leaves and silking about 60 days after plant emergence. Timing and number differences occur among varieties and environmental conditions (Hanway, 1966). Maize is a monoecious plant, forming two separated and morphologically distinct male and female inflorescences during reproductive stage. The male inflorescence, called tassel, is borne at the apex of the mature plant and includes a central spike with several long branches at its base. The ears are female flowers, arising in the axils of one or more leaves, not forming the typical male long branches (Vollbrecht and Schmidt, 2003). Grass

inflorescence architecture has a basic unit called spikelet characterized by two bracts or glumes enclosing one to several florets. Maize spikelet owns two florets, each including a floral shoot, initially similar and bisexual, but differentiating during floral development: tassels florets have their pistils aborted and the developing stamens are aborted in ear florets (Dellaporta and Calderon-urrea, 1994). In addition, in upper ear florets, two carpels will fuse forming a long structure called silk, which is part stigma, part style (Vollbrecht and Schmidt, 2003).

As previously mentioned, development timing can greatly vary between maize varieties and climate conditions. This is true also for flowering time, which has an immense diversity and varies according to the latitudinal area to which the variety was selected for (Kuleshov, 1933). Teosinte, the ancestor of modern maize, is an obligate short-day plant (Colasanti and Muszynski, 2009). This changed over time, with cultivation of maize being spread throughout higher latitudes, which are characterized for having longer summer days. Thus, sensitivity towards photoperiod became extremely variated among maize lines, that can be from totally insensitive, to moderate and highly sensitive. According to Stephenson et al. (2019), maize can be considered a facultative short-day (SD) plant, due to the fact that SDs is flowering accelerating, while long days (LDs) will retard but not stop the process.

Maize is pollinated by wind and cross-pollination is generally favored over self-pollination, because silks become receptive after most of the pollen of the same plant are shed, although overlap in their development can occur (Henry et al., 2003). However, cross-pollination can be depleted in large monocultures (Potts et al., 2016). After landing on the silk, pollen grains produce a pollen tube that will grow throughout the silk, double fertilizing the egg and the central cell, producing the embryo (*2n*) and the aleurone plus the starchy endosperm (*3n*),

respectively (Nannas and Dawe, 2015). Fertilization will give rise to the kernels, which are single-seeded fruits, summing the production of 600 to 1000 seeds per plant (Magalhães and Souza, 2011).

1.2.1 The physiological basis of salt stress response in maize

Maize is generally considered moderately sensitive to salt (Maas and Hoffman, 1977). However, this relative concept is strongly influenced by several factors: the variety and stage of development, soil fertility, soil water and aeration, and climate (Maas and Hoffman, 1977). Maas et al. (1983) studied different maize cultivars responses to saline environment from germination to plant maturity. According to their results, the majority of the cultivars were salt-tolerant during germination, but seedling growth was considerable more sensitive (Maas et al., 1983). Seedlings started to be negatively affected from an electric conductivity (EC_{sw}) of 1 dS/m of soil water salinity. On the other hand, ear and grain yield presented more tolerance to salt stress than vegetative growth stage, and decrease was registered from 5.8 and 5.5 dS/m, respectively (Maas et al., 1983).

Due to the maize sensitiveness towards salinity, it is important to evaluate and identify potential salt tolerant genotypes. Despite screening data are available in the literature for maize, the high genetic variability of this crop, plus the complex nature of the salt stress and the several interfering factors cited previously, makes the tolerance screening a continuously necessary work. However, valuable information can be extracted from each published work.

Effects of salinity towards maize genotypes were studied by Hajibagheri et al. (1987). In a first experiment, there was a screening of 26 maize cultivars against 50, 100 and 200 mM NaCl, with plants growing in solution in a greenhouse. The first lowest NaCl treatments, 50 and 100 mM, did not induce significant differences on the survival rate among varieties and all plants were alive

(keeping some green leaves) for at least 65 days of treatment. For the 200 mM NaCl treatment, after 20 or 25 days, maize varieties showed significant differences on the survival percentage, ranging from 0 to 66% of plants alive. Thus, they were ranked from most sensitive to most salt tolerant according to the survival rate (Hajibagheri et al., 1987). From these results, the most salt-sensitive (LG_{11}) and the two most salt-tolerant (Across8024 and Protador) were selected for a deeper investigation over the NaCl effects. For 15 days, every 5 days, plants of all genotypes submitted to 100 mM NaCl were analyzed for dry weight (DW) of roots and shoot, as well as ion concentration of roots and shoot. In salt-tolerant varieties (Across8024 and Protador), root growth was more negatively affected than shoot growth, while in the salt-sensitive maize (LG_{11}), salt had the opposite effect. Sodium and chloride accumulated in a similar pattern, with Cl^- slightly higher in concentration than Na^+. There was a significant increase of Na^+ and Cl^- concentration on salt-treated plants of all genotypes, in both roots and shoot, but LG_{11} accumulated more Na^+ and Cl^- and less potassium (K^+) than the others. Thus, Hajibagheri et al. (1987) demonstrated a direct correlation of ion accumulation, detrimental effects of NaCl treatment and difference of tolerance towards salt stress.

In a genotype screening for salt tolerance of maize, De Azevedo Neto et al. (2004) categorized eight maize genotypes (BR3123, BR5004, BR5011, BR5026, BR5033, CMS50, D766 and ICI8447),which are used on the northeast of Brazil, according to its growth response (dry matter , shoot to root dry mass ratio, leaf area, relative growth rate, and net assimilation rate), as well as “leaf temperature, stomatal conductance, transpiration, predawn water potential, sodium, potassium, soluble amino acids and soluble carbohydrate contents” (Neto et al., 2004). Plants were grown for 15 days in nutrient solution-trays with gradual addition or not of 100 mM NaCl. After this period, all genotypes

showed changes for the previously cited parameters for both conditions. Growth responses in terms of dry matter, shoot to root dry mass ratio, leaf area, relative growth rate and net assimilation rate were considered responsive for salt stress and, with exception of net assimilation rate, could be used as salt stress markers for maize. Additionally, other two parameters were considered as appropriate morpho-physiological markers for salt stress, the sodium and soluble organic solutes concentration in roots. In conclusion to their work, in 100 mM NaCl, from the eight genotypes, BR5011 was determined as salt sensitive, with a reduction of 66.5% of shoot dry matter of salt stressed plants when compared to control and a decrease of 61.4% on roots dry matter. The tolerant genotype BR5033 had 33.8% shoot dry matter reduction and the roots were not affected (Neto et al., 2004). This work gives us a good overview of traits that can be used as salt stress markers at a physiological level. In addition, it also points out the importance of a primary test of the selected parameters for each research project analyzing salt stress of different genotypes.

Akram and colleagues (2010), working with seedlings of ten maize hybrids in solution and NaCl concentrations of 0, 40, 80 and 120 mM, screened the genotypes for salt tolerance (maize hybrids: Pioneer 3062, Pioneer 32B33, Pioneer 30Y87, Pioneer 31R88, Dekalb 919, Dekalb 979, Dekalb 922, Hycorn 984, Hycorn 11 plus and Hycorn 993). After 17 days of treatment, roots and shoot length, plant biomass and inorganic osmolytes were measured for all plants in every treatment. Salt treated plants had all the measured factors negatively affected, with higher impact according to the increasing concentration of salt. In terms of DW, the most sensitive genotype (Dekalb979) presented the highest reduction on shoot of treated plants and the highest sodium content at 120 mM NaCl. On the other hand, the tolerant genotype

(Pioneer32B33) had the lowest shoot DW reduction and the lowest Na^+ shoot concentration (Akram et al., 2010).

Several other studies are available regarding the screening of various maize genotypes for salt tolerance. Analyses were conducted with several different approaches and observations, including developmental stages of maize plants, morphological and physiological traits, salt concentrations and experimental periods. Thus, it is important that each researcher selects and test the feasibility of experimental conditions and traits according to the available infrastructure, objectives and chosen genotypes.

1.2.2 The molecular basis of salt stress response in maize

With the concrete knowledge that the salt stress response is genotype specific for maize, the next step is to identify the factors leading to each response. One way to achieve valuable answers is through proteomics investigation of the physiologically screened maize genotypes. In this matter, Geilfus and colleagues (2010) studied molecular aspects of salinity-related growth inhibition in two maize hybrids, a salt-sensitive (Lector) and a salt-resistant (SR03). As cell division and elongation are the main processes involved in growth retardation during salt stress, analysis of the mRNA expression of six maize β-expansin isoforms was combined with investigation of relative abundances of β-expansin proteins in plants treated for 8 days with 100 mM NaCl. It was found that salt-sensitive Lector had a significant reduction of shoot growth, with treated plants 65% smaller than non-treated ones. In accordance with this result, real-time quantitative RT-PCR showed the down-regulation of four β-expansin isoforms (ZmExpB2, ZmExpB6, ZmExpB7 and ZmExpB8) and up-regulation of only two (ZmExpB3 and ZmExpB5), while β-expansin protein abundance was 50% significantly reduced for this genotype in salt

condition. Meanwhile, salt-resistant SR03 did not present significant reduction of shoot growth for treated plants, as well as for β-expansin protein abundance. In addition, five from the six β-expansin isoforms was up-regulated (ZmExpB2, ZmExpB3, ZmExpB5, ZmExpB6 and ZmExpB8) and one was down-regulated (ZmExpB7) as a salt stress effect. Thus, the researchers assumed the correlation between growth inhibition caused by NaCl treatment and regulation of the expansin protein expression. Also, they have evidenced variations on the effects and mechanisms of different maize genotypes according to its salt-tolerance (Geilfus et al., 2010).

In a short-term salinity study, 14 root proteins of salt-resistant maize hybrid (SR12) plants treated with 25 mM NaCl for one hour were abundantly different from the control plants (Zörb et al., 2010). Among the nine proteins detected highly abundant in response to the stress, a sucrose synthase was found. Sucrose synthase works as a sugar sensor and stress sensor, and is involved in signal transduction cascades that stimulate several types of responses (Gupta and Kaur, 2005). Also highly abundant, Zörb and colleagues (2010) found a voltage-dependent Anion Channel Protein 1a, which has a role in energy metabolism and metabolite transport. As this protein can be salinity-affected, it is assumed to have a role in the stress response of the salt-treated plants. In addition, from the five low-abundant proteins responsive to salt, a 14-3-3 like protein was negatively affected in salt stress. This protein functions in the regulation of channels activity, such as K^+ channels, and in the activation of H^+-ATPase activity (Fuglsang et al., 1999; Van Den Wijngaard et al., 2005), Zörb et al. (2010) link the negative effect of salinity on elongation growth with changes on plasma membrane ATPase activity, due to disturbances on 14-3-3 like protein abundance. These changes affect the apoplastic pH, which, in turn, will change cell wall growth regulators, as XTH (Zörb et al., 2010).

Cheng et al. (2014) revealed that root proteomics response of maize seedlings (three-leaf stage) were different between a salt-sensitive (D340) and a salt-tolerant (N1145) inbred line. Growing in nutrient solution supplemented with 150 mM NaCl or not (control), roots proteomics using two- dimensional gel electrophoresis (2-DGE) was performed after 3 days of treatment and fresh weight (FW) and DW were analyzed at the 7th day after salt addition. The salt-sensitive genotype (D340) showed significantly reduced FW and DW of treated seedlings, while this reduction was irrelevant for the salt-tolerant ones (N1145). Proteomics analysis showed that acceleration of protein translation and proteolysis, manifested by higher abundance of proteins such as Elongation factor 1-delta (gi|226503896) and Proteasome subunit alpha type 5 (gi|226530826) in roots of the salt-tolerant genotype (N1145), are suggestively one of the processes ensuring the better performance of the tolerant line (Cheng et al., 2014). Other processes involved in the enhancement of genotype N1145 performance in NaCl are the improvement of energy production, represented by higher abundance of proteins as 6-phosphogluconate dehydrogenase (gi|3342800), which is a NADPH producer, and the antioxidant defense system.

Working with chloride-specific stress in maize, Geilfus et al. (2017) investigated the influence of this ion on the stress-related transient alkalinization of leaf apoplast and its effect on cell wall properties and proteins involved in cell wall changes. Using 50 mM chloride containing salts (NaCl and glucosamine hydro-chloride) in nutrient solution, they demonstrated the specific chloride response on the transient alkalinization of the leaf apoplast, as well as the impact of this process on the leaf proteome. Leaf proteome revealed 44 proteins highly abundant as a response to chloride-stress and transient alkalinization, as well as that these proteins were mainly linked with growth control. In addition, stress-related abundant proteins included enzymes

involved on synthesis of cell wall building blocks precursors, such as 2 phenylalanine ammonia-lyase (PAL) members, and enzymes from lignin and hemicellulose synthesis. Thus, they evidenced that chloride-stress induces transient alkalinization, leading to hardening of the cell wall (Geilfus et al., 2017).

Salinity tolerance is a complex polygenic trait (Flowers and Flowers, 2005) and interactions between plant and environment, as well as physiological, genetic and developmental plant interactions affects its expression (Bernstein and Hayward, 1958). The genetic basis of salinity effects was studied by Rao and McNeilly (1999) using 17 maize accessions previously categorized as highly tolerant, moderately tolerant or mostly susceptible to salt stress. Applying the North Carolina Model 2 (NCM 2) crossing design and analyzing seedlings grown in solution containing 0, 60 or 80 mM NaCl from F1 progenies, the estimation of components of variation and heritability was calculated based on root growth. The results indicates the presence of both additive and non-additive effects, with tolerance genes presenting some degree of dominance properties (Rao and Mcneilly, 1999).

Several genes which respond to salt stress were already detected in different plant species and are mostly grouped in four functional categories: (1) ion transport or homeostasis, (2) senescence-associated genes, (3) molecular chaperones and (4) dehydration-related transcription factors (Rao et al., 2016). Genes like *Salt Overly Sensitive* 1 (*SOS1*), *SOS2*, *SOS3* and *AtNHX1* were salt stress-responsive in *Brassica juncea* and *Brassica campestris* (Chakraborty et al., 2012). In rice, *PRP*, *SAG*, *HSPC025* (Roshandel and Flowers, 2009), *SNAC1* (Liu et al., 2014a), *OsRab7* (Peng et al., 2014) and *glyoxalase II* (Saxena et al., 2011) are examples of responsive genes in salinity conditions. In *Arabidopsis*, several salt-responsive genes were observed, including *atSKIP*

(Lim et al., 2010), *JcDREB* (Tang et al., 2011), *H3K4me3* (Han et al., 2013) and *AtSTO1* (Lawson and Michler, 2014).

Studies related to the investigation of genetic basics of salt tolerance have also identified several genes in maize. Differentially expressed genes in response to salinity in maize are exemplified in the table 1.2 below.

Table 1.2 Salt responsive genes detected in different maize genotypes.

Gene Name	[NaCl]	Functional Role	Gene Response	Genotype	Reference
ZmACA1	150 mM	Involved in Ca^{2+} signaling	Up-regulated	ETH-DH7	(Nguyen et al., 2009)
ZmDREB2A		Transcription factor			
ZmERF3		Transcription factor			
ZmCOI6.1		Unknown			
ZmMPK3	250 mM	Transduction of extracellular signaling	Up-regulated	Nongda 108	(Wang et al., 2010)
ZmPP2C	100 mM	Negative regulator of ABA signaling	Downregulated	Nongda 108	(Tan, 2010)
ZmGST		Involved in detoxification responses	Up-regulated		
ZmMKK4	250 mM	Transduction of extracellular signaling	Up-regulated	Zhengdan 958	(Kong et al., 2011)

Gene Name	[NaCl]	Functional Role	Gene Response	Genotype	Reference
ZmFKBP53a *ZmFKBP62a*	150 mM	Probably involved in development and signaling	Up-regulated	B73	(Yu et al., 2012)
ZmPMP3	200 mM	Ion homeostasis maintenance	Up-regulated	CN165	(Fu et al., 2012)
ZmNHX	200 mM	Tonoplast Na^+/H^+ antiporters	Up-regulated	SR03 SR05	(Pitann et al., 2013)
ZmMKK1	250 mM	Transduction of extracellular signaling	Up-regulated	Zhengdan 958	(Cai et al., 2014)
ZmFKBP20-1	150 mM	Possible roles in stress signal transduction pathways	Up-regulated	B73	(Yu et al., 2017)
ZmWRKY17	200 mM	Transcription factor	Up-regulated	B73	(Cai et al., 2017)

Gene Name	[NaCl]	Functional Role	Gene Response	Genotype	Reference
ZmMYB	200 mM	Transcription factor	14 genes responded	B73	(Chen et al., 2018)
ZmHKT1	100 mM	Encodes a class I Na^+-preferential HKT-type transporter	Up-regulated	Zheng58 Chang7-2	(Zhang et al., 2018)
ZmDGK2-4	200 mM	Formation of signaling molecule phosphatidic acid	Up-regulated	He344	(Gu et al., 2018)

Regarding the genetic engineering of maize, studies have been successful for salt tolerance improvement using transgenic approaches. Chen and colleagues (2007), after transferring an *Oryza sativa* Na^+/H^+ antiporter gene (*OsNHX1*) into four maize inbred lines (Zong3 (Z3), Zong31 (Z31), P9-10 and Qi31 (Q31)) and one hybrid line (F - first filial generation of Z3 crossed with Z31), detected significant higher tolerance of transgenic plants grown in 200 mM NaCl in greenhouse when compared to the wild types. *OsNHX1*-expressing maize plants presented considerably less affected biomasses, as well as lower proline content, indicating less salt stress than wild-type plants (Chen et al., 2007).

Ying et al. (2018) transformed a vacuolar membrane $Na^{+/}H^+$ antiporter gene of *Suaeda salsa* (*SsNHX1*) into a maize inbred line (18-599). *SsNHX1*-overexpressing transgenic maize growing in 1% NaCl solution in greenhouse showed enhanced tolerance to salt stress, being less impacted by salinity in terms of germination rate and roots length, as well as chlorophyll and relative water content. The wild-plants showed a significant negative impact on these parameters when under salt stress and a lower Na^+ content in their leaves and roots when compared to transgenic salt-treated plants. These results can be attributed to an enhancement of SsNHX1 activity in transgenic plants, increasing vacuolar sequestration of the Na^+ ion (Ying et al., 2018)

Despite the efforts and the urgent need of solutions to overcome the loss of crop lands to salinity, no salt-tolerant maize cultivars have been released for commercialization (Fita et al., 2015; Flowers and Flowers, 2005). The reason for this is a combination of factors, including the genetic and physiologic complexity of the salt tolerance, which shows characteristics of a multigenic trait, with salt-sensitivity being variable throughout the life cycle of a plant and a large range of morphological and biochemical adaptations (Flowers, 2004).

In addition, the low number of field trials and yield-based tolerance determination, as well as environmental risk assessment of transgenic plants, are also retardants of the commercial releasing of transformed salt-tolerant maize genotypes (Khan et al., 2016).

1.3 Plant phenotyping

The terms ‘genotype’ and ‘phenotype’ have long being introduced by Wilhelm Johannsen (1909) and since then multiple interpretations for these terms arose (Griffiths et al., 2005; Klug et al., 2015; Lewontin, 1992; Mahner and Kary, 1997; Rieger et al., 1991). According to Mahner and Kary (1997), the use of each concept varies according to the author and the specific context. In this work, the definition for genotype given by Mahner and Kary (Mahner and Kary, 1997) will be applied: “a set of allele-pair types of a diploid cell or organism” and it is going to be used to refer to a genotypic organism. In this work, the definition for phenotype given by (Mahner and Kary, 1997) will be applied: “the set of traits of an organism or one of its subsystems”, like an organ or a cell. Basically, the phenotype is a result of the genotype in combination with the dynamic environment and (agricultural) management and compiles several dimensions, processes, functions and structures in constant transformation throughout individual growth and development (Figure 1.2) (Mahner and Kary, 1997).

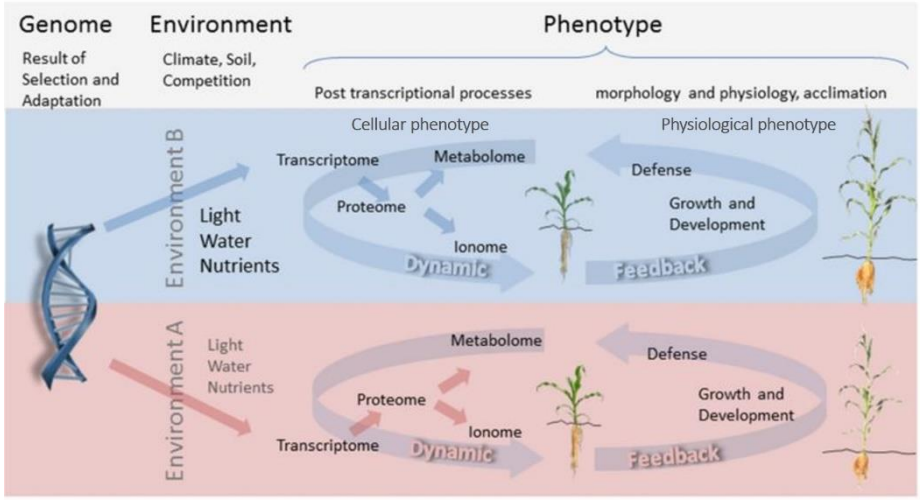

Figure 1.2 Relation among genotype, phenotype and environment influence. Adapted from Mahner and Kary (1997).

The term ‘phenotyping’ was introduced around the 1950s and its use has grown exponentially in the last 20 years (Costa et al., 2019; Passioura, 2012). As for ‘genotype’ and ‘phenotype’, the ‘phenotyping’ definition is subjected to different interpretations (Ghanem et al., 2015). Fiorani and Schurr (2013) define ‘phenotyping’ as the set of methodologies and protocols applied to measure specific traits associated with function or morphophysiological structure of an organism, at different scales ranging from cellular to whole individual level. Thereby, the phenotyping can be virtually divided in ‘cell phenotyping’, covering the post-transcriptional processes (Figure 1.2) and ‘physiological phenotyping’, including growth, development and defense responses (Figure 1.2).

As described, phenotyping involves several dimensions and levels, which leads to diverse possibilities of traits to track. Phenotyping based in component traits aggregates valuable information to stress studies, guiding and validating

posterior genetic expression studies. Results obtained over time can point out critical moments for sample collection for further analysis, reflecting in more relevant results to approaches such as DNA-based molecular marker. This technique of phenotyping the whole plant through time represents then an important way to reduce the distance between plant physiology and genetics (Finkel, 2009).

1.3.1 Methods on physiological phenotyping

Bioengineering solutions for crop improvement towards salinity rely on the identification of tolerant genotypes. For that, accurate physiological phenotyping becomes essential for screening plants and specific traits must be selected for specific aims and species. During salt stress, effects on growth are due to reduction on water uptake caused by the osmotic stress and cell injuries caused by ion transportation to the shoot via transpiration mainstream. With that, plants can face growth reduction and slower photosynthetic leaf area formation driven by inhibition of cell division and cell elongation (Tester and Davenport, 2003). These effects can be monitored by different methods, such as image techniques, plant biomass and height measurements.

Image-based phenotyping as we know today evolved from other non-destructive approaches, like thermography point sensors and satellite-based calculation of spectral indices (Walter et al., 2015). As evolution went on, some plant imaging techniques became available and among them, RGB (red, green, blue) imaging has the most common and simple methodology (Fiorani and Schurr, 2013). By using digital cameras and a single-specific color background, shoot growth profile is constructed by a series of pictures taken through time (Hartmann et al., 2011; Leister et al., 1999; Tackenberg, 2007). Thus, plants-derived pixels are identified by processing algorithms, and morphological,

geometric and color attributes are measured for individual plants (Fahlgren et al., 2015).

Non-destructive imaging techniques are ideal to track each individual response dynamically in time (Berger et al., 2010) and have the potential to calculate plant leaf area or volume, which can translate to shoot biomass (Chen et al., 2014a; Tessmer et al., 2013). Moreover, leaves wilting caused by stress factors can be detected even at an early phase (Berger et al., 2010).

Among other quantitative methods for plant growth analysis, FW and DW have potential to describe a plant system performance (Nogueira et al., 1994). Photosynthetic energy acquired and fixed into carbon compounds is used in different proportions by the plant, with around 10 to 40% directly used for biomass accumulation (Munns and Gilliham, 2015). This is calculated taking into account the metabolic processes that respiration support, more specifically growth of new biomass (adding to the total, for example cellulose production), maintenance of existing biomass (e.g., proteins turnover) and wastage, including heat and CO_2 release. Thus, the percentage of energy used for biomass accumulation will depend of variants as plant species and development stage (Amthor, 2000). When the plant is subjected to a stress situation, this part for biomass accumulation can decrease. This decrease is a result of slower growth of photosynthetic area, which can consequently lead to less mass accumulation, and also as a redistribution of acquired energy into stress defense (Munns and Gilliham, 2015). For example, one of the processes that can be triggered by stress, the protein turnover, will cause varied costs for a plant depending of the protein. The cost of a protein breakdown ranges from 0.13 to 2 ATPs per amino acid, while for protein synthesis, from 4.5 to 5.9 ATPs per amino acid (Amthor, 2000).

FW represents the complete system of the living plant, at a functional state. Wide distortions from a normal pattern due to stress, confirm the susceptibility of the plant to the abnormal condition (Nogueira et al., 1994). DW represents the daily gain of four main factors: the quantity of reduced-carbon units used to build the vegetal structure, mineral uptake, net gain by light assimilation and net loss by respiration (Evans, 1972). Therefore, FW and DW measurements can be valuable growth and stress descriptors.

Complementing the other physiological phenotyping techniques, plant height appears as an important yield-predictor variable for maize, presenting a positive correlation with final yield, leaf biomass and leaf area index (Liebisch et al., 2015; Yin et al., 2011). Thus, its track can be an indicator of genotype performance and developmental disturbances in saline environments, besides being a simple and non-destructive method.

In a context of soil salinity, tracking the leaf ion concentration can lead to an indication of salt tolerant species. Transportation of sodium and chloride from the roots into the leaves may induce disorders on the electroneutrality of cells, affecting also their normal turgor. Furthermore, ion accumulation can achieve levels in which they become toxic to most of cytosolic enzymes (Volkov, 2015). However, tolerant species have mechanisms that help to avoid the osmotic imbalance and/or leaf toxicity and generally show higher concentrations of ions in their leaves, while maintaining growth standards equivalent to non-stressed plants (Munns and Gilliham, 2015). Thus, the investigation of ion content within plants in saline conditions is an interesting and important trait to be observed.

Several other methods are available for plant physiological phenotyping. High throughput platforms have been developed for greenhouse and field

phenotyping (Granier et al., 2006; Hartmann et al., 2011), which can combine different remote sensors for a more complete scanning of the physiological conditions (Liebisch et al., 2015). The implementation of one or various approaches is dependent of financial resources and limitations in time and physical space.

1.3.2 Proteome analysis

As previously mentioned, the cellular phenotype is the set of multiple processes involving gene and protein expression (Sul et al., 2009). Therefore, phenotyping at cellular level runs from the transcription of the DNA into RNA (transcriptomics), to protein (proteomics), metabolites (metabolomics) and elemental composition (ionomics) (Walter et al., 2015). Gene expression at the transcriptome level is the main determinant of cellular phenotyping (Lockhart and Winzeler, 2000). Methods from the next-generation DNA sequencing can track millions of small fragments of DNA simultaneously (Shendure and Ji, 2008). However, a relevant issue is the possibility of discrepancy between transcripts, the carriers of genetic information, and the respective proteins, which are de facto the effector molecules (Oliver, 2000) . The correlation between protein and transcripts is not consistent (Baerenfaller et al., 2012; Ponnala et al., 2014; Walley et al., 2013b) including in abiotic stress conditions. Post-transcriptional and post-translational control mechanisms may decrease the correlation between these two levels of gene expression (Oliver, 2000) and so it is appropriate the investigation of other cellular phenotyping levels to complement and validate RNA-based measurements (Zivy et al., 2015b).

Proteome, i.e., proteins expressed by a genome (Wilkins and Hochstrasser, 1997), analysis is a great complementation method for RNA-based measurements. The profiling of the proteome in determined biological context,

in individual, tissue or cell level, is called ‘proteomics’ (Liska and Shevchenko, 2003). Proteomics is a more complex technique than transcriptomics approaches, due to the greater number of possible combinations of 20 amino acids for protein synthesis versus four nucleotides for RNA (Mann and Jensen, 2003). The complexity of protein technology is also strengthened by post-translational modifications, which comprises proteolytic cleavages, chemical modification of amino acid residues or addition of modifying non-amino acid groups (Lodish, 1981).

As previously mentioned, proteins are effector molecules, mediating complex biochemical pathways. Physiological disturbances caused by external stresses, will also affect proteins expression or activity (Oliver, 2000). Thus, studying the proteome of plants under unfavorable conditions would provide direct answers about its physiological state, as well as their perception and responses modes.

Historically, proteins were firstly recognized as a distinct class of biological molecules by Antoine Fourcroy in 1789, giving birth to the protein purification narrative (Walls and Loughran, 2017). After a series of important discoveries, the name “protein” was suggested by Jacob Berzelius, in 1838, from Greek “standing in front” or “in the lead” (Henryk Eisenberg, 2002). Jumping to 1956, the first time serum proteins were separated by a junction of two electrophoresis processes was performed by Smithies and Poulik (1956), using paper and starch gels. Later, O’Farrell (1975) developed the pioneer concept of two-dimensional (2-D) gel electrophoresis, in which proteins were separated according to their charge by isoelectric focusing in the first dimension, followed by molecular weight separation via sodium dodecyl sulfate (SDS) electrophoresis in the second dimension.

Mass spectrometry has been used for small molecule analysis long before the development of two-dimensional gel electrophoresis (2-DE) techniques (Patterson and Aebersold, 2003). The measurement of the mass-to-charge ratio (*m/z*) in a mass spectrometer require the ionization of the molecule, prior to sending it to the instrumental high vacuum system. However, peptides and proteins proved to be difficult to ionize without compromising these large molecules. Thus, with the incoming of new soft ionization methods at the end of the 1980's, the electrospray ionization (ESI) and matrix-assisted laser desorption ionization (MALDI), peptides and proteins could be shifted into the gas phase and efficiently ionized, avoiding excessive fragmentation (Fenn et al., 1989; Karas and Hillenkamp, 1988; Patterson and Aebersold, 2003). From there, mass spectrometers were manufactured with this type of ionization instruments, quickly spreading through scientific community (Patterson and Aebersold, 2003).

In the early 1990s, large-scale protein studies became possible by the computational advances, in which sequence databases and search tools were made available for protein expression examination (Henzel et al., 1993; James et al., 1993; Pappin et al., 1993). Database search algorithms, together with genomic and mass spectrometry advances, were the boosters of the new field called 'proteomics' (Figure 1.3) (Patterson and Aebersold, 2003).

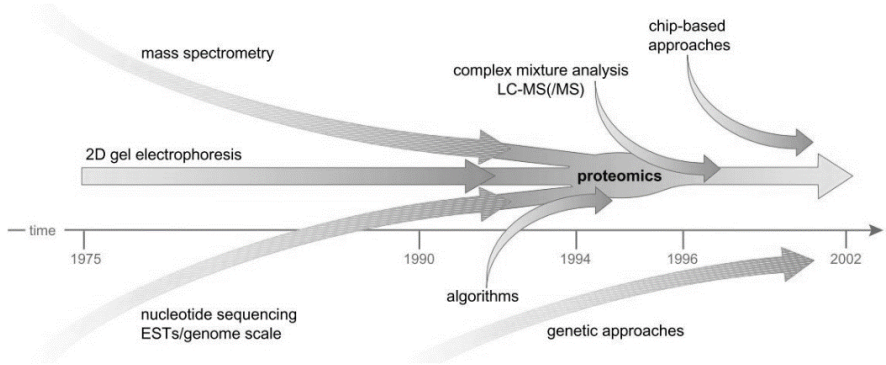

Figure 1.33 Technology advances leading to the proteomics field generation (Patterson and Aebersold, 2003).

The two main proteomics approaches are known as ‘gel-based’ and ‘gel-free’ or shotgun approaches, which differ in isolation, separation and detection of the (poly)peptides (Carpentier et al., 2008). Undoubtedly, the gel-based approach is a powerful technique and the two dimensional gel electrophoresis (2-DE) methodology delivers images in high resolution of intact proteins, allowing the detection of isoforms and post-translational modifications (Carpentier et al., 2008; Vanhove et al., 2015). However, 2-DE is a technically complex method, which makes it labor-intensive and difficult to automate (Patterson and Aebersold, 2003).

The development of a two-dimensional difference gel electrophoresis method (2D-DIGE) reduced the variation from one gel to the other, increasing accuracy and reliability of 2-DE approach. In this technique, multiple protein samples are migrated in a single gel and, by using differential fluorescent dyes to each sample, they are detected concomitantly (Ünlü et al., 1997). Still, a 2-DE gel frequently contain spots gathering more than one protein, which makes the quantification challenging (Vanhove et al., 2015; Zhu et al., 2010).

A faster proteomics technique was developed by McCormack et al. (1997), which became the gel-free approach pioneer. In this method, after digesting a mixture of proteins with a proteolytic enzyme, peptides are separated by coupling reversed-phase liquid chromatography (LC) and ESI tandem mass spectrometry (MS/MS).

LC is employed following digestion because different peptides can have similar or even equal masses, which will produce similar intensity peaks in an initial MS spectrum. The overlapped peptides are then difficult to distinguish and identify and this separation step have the power to reduce the issue, besides increasing the global dynamic range (Karpievitch et al., 2011).

The chromatographic separation is a technique comprising stationary and mobile phases, the last one containing and carrying samples to be separated. Samples run with and behind the mobile phase through the stationary phase, that retards differently each sample compound, according to its polarity and interaction levels. Thus, the basics of separation by chromatography is the difference on mobility and speed of the present components (Jandera and Henze, 2012).

Chromatography mobile phase can be composed of an inert gas (gas chromatography – GC) or a liquid (LC). While GC is faster and more efficient than LC, it demands volatilization of samples below 300 ºC, limiting the use of high boiling or non-volatile compounds. LC is not only universally applicable, but enhances the selectivity potential of the method, by allowing the selection of the mobile phase as well. Chromatography stationary phase can be built based on two states: solid, also called ‘adsorption chromatography’ or liquid, that when combined with a liquid mobile phase, is known as ‘partition chromatography’ (Jandera and Henze, 2012).

ESI is one of the most used ionization sources in proteomics (Karpievitch et al., 2011). In a mass spectrometer, an ionized molecule is measured according to the *m/z*. Thus, peptides are assigned with charges by ion sources, which exist in a wide variety and must be selected according to the physico-chemical properties of the sample under analysis (Hoffmann and Stroobant, 2007a).

In ESI, the sample is infused in the equipment in a solvated form (El-Aneed et al., 2009). This characteristics make ESI easily adaptable with LC instruments, as well as tandem mass analyzers (El-Aneed et al., 2009). Furthermore, another characteristic of ESI is the tendency of multiple charging biomolecules, (Fenn et al., 1989), allowing the analysis of high mass ions with a low *m/z* range instrument, which increases the sensitivity, while MALDI tends to produce singly charged ions.

The ESI procedure consists of a strong electric field application to the sample solution under atmospheric pressure. This solution passes in a slow flux through a capillary and the electric field induces a charge accumulation at the liquid surface at the end of the capillary, resulting in highly charged droplets (Hoffmann and Stroobant, 2007a). Large number of tandem mass spectra are then used to search protein databases, linking peptides to the respective proteins (McCormack et al., 1997).

A subsequent approach tackled the resolution problem of McComarck's methodology, in which the proteins identification is possible just in simple mixtures. Link et al. (1999) developed the Direct Analysis of Large Protein Complexes (DALPC) process, wherein peptides are separated through a two-dimensional chromatographic system, using its charge and hydrophobicity properties. Optimization of the DALCP process gave rise to the Multidimensional Protein Identification Technology (MudPIT) method

(Washburn et al., 2001), an ingenious approach that allowed the detection and identification of proteins not commonly seen in standard gel-based proteome analyses, as low-abundance proteins. However, the complexity of the peptides mixture is still very high with MudPIT.

Regarding gel-free methodologies, the different approaches can be branched according to their quantification procedure: labeled MS-based relative quantification and label-free quantification (Ashwin et al., 2017).

Labeled methods consist in differently labeling proteins prior to mixing, digesting and analyzing them at once (Figure 1.4) (Zhu et al., 2010). The general principle is to enable mass spectrometers to distinguish identical proteins from different samples, once the isotope labeled molecules differ solely by mass properties from the non-labeled ones. It was developed as a strategy to overcome difficulties on quantitative use of gel-free techniques. These difficulties are related to the ion suppress effect, in which molecules present during ionization process negatively influences the compound ionization (Wilm, 2011). This phenomenon is observed either under MALDI or ESI conditions. In the ESI method, a matrix effect, i.e., an ion suppression originated by a competition for charge acquisition between co-eluting, also occurs in-solution (Leroy et al., 2012). Thus, the labelled approaches are applied to minimize this matrix effect, by analyzing mixed samples simultaneously, guaranteeing that the peptides are quantified under the same effect (Leroy et al., 2012).

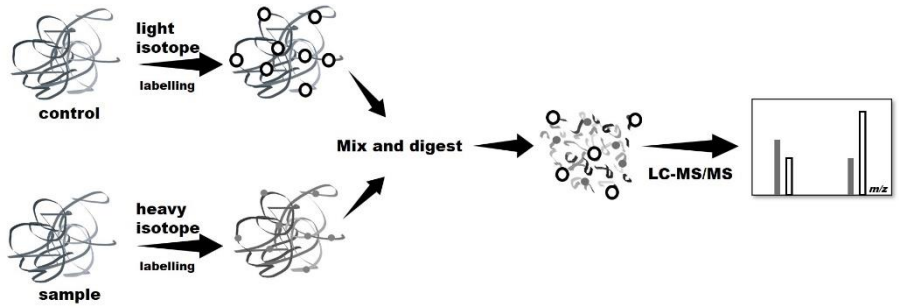

Figure 1.4 General approach of shotgun isotope labelling method. Adapted from Zhu et al. (2009).

1.3.3 Label-free shotgun proteomics

Label-free approaches, contrary to the labeled procedures, have the samples individually prepared and their analysis are performed separately (Figure 1.5). Fundamentally, label-free proteomics follows the steps of sample preparation, peptides separation and analysis by MS/MS and data analysis (Zhu et al., 2010). Methods for proteins quantification are roughly categorized in two: (i) measurement of chromatographic peak areas of the same peptides, known as area under the curve (AUC) or peak/signal intensity; and (ii) spectral count of a protein (Figure 1.5) (Neilson et al., 2011; Zhu et al., 2010).

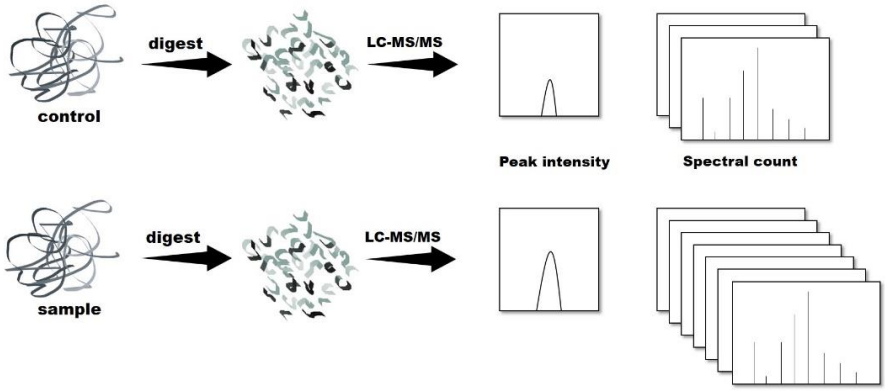

Figure 1.5 General approach of shotgun isotope label-free method. Adapted from Zhu et al. (2009).

1.3.3.1 Sample preparation

Preparation of the samples involves a few steps and the protocol can vary according to the objective of the proteomics study, as well as with available facilities. Typically, proteins disulfide bridges are reduced using dithiothreitol (DTT) and alkylation of thiol groups of the cysteines is accomplished using iodoacetamide or iodoacetic acid (Dickens, 1933), preventing its oxidation and formation of new disulfide bridges. Chaotropic agents, such as urea, are used to denature the proteins, by disruption of hydrogen bonds. An important step for further analysis is the proteins digestion. Several digestion techniques are available and the application of one or the other will be determined by the chosen proteomics strategy, middle-down or bottom-up (Switzar et al., 2013).

Bottom-up is the most used strategy by far, in which proteins are digested into peptides ranging from approximately 500 to 3000 Da. The digestion step significantly enhances the performance of LC separation, also improving sensitivity by decreasing charge state and molecular mass, when compared with top-down proteomics (Switzar et al., 2013). Intact proteins are detected in top-

down strategies, allowing preserved protein information. However, it costs sensitivity and mass range, limited to about 50 kDa, and requires high-end mass spectrometers (Calligaris et al., 2011).

Middle-down proteomics also makes use of protein digestion but producing fewer and larger peptides (Switzar et al., 2013). This approach is a combination of bottom-up and top-down strategies, using improved LC separation of peptides (ranging from ~3000 to 20000 Da) (Cannon et al., 2010) and subsequent efficient electron-based fragmentation (Boyne et al., 2009). It keeps sensitivity and refines protein sequence coverage (Wu et al., 2005, 2007).

The quality of protein identification is highly dependent on the protein digestion and approaches are divided in non-enzymatic and enzymatic. Non-enzymatic techniques make use of chemical reagents, such as formic acid (FA), hydrochloric acid (HCl) and acetic acid (HAc), which are highly specific for a single cleavage site. For that, high mass peptides may be produced, being ideal for middle-down proteomics (Wu et al., 2012). Electrochemical oxidation is also a non-enzymatic approach, relatively new, specific to tyrosine (Tyr) and tryptophan (Trp) cleavage sites. Many LC-MS instruments are appropriate for digested peptides by electrochemical oxidation, which is also a high-speed strategy (Permentier et al., 2003; Permentier and Bruins, 2004).

Of the enzymatic digestion approaches, trypsin is the most applied proteolytic enzyme. It has a defined specificity, cleaving C-terminal to arginine (Arg) and lysine (Lys) residues, except when these residues are followed by N-terminal proline peptides (Olsen et al., 2004). Trypsin digestion is able to generate a fragmentation mass spectra that is rich in information and easy to interpret, promote identification of peptides with high confidence level, leading to great protein identification accuracy (Hustoft et al., 2012). Due to its high specificity

to cleavage sites, it is possible to predict the produced peptide fragments, allowing the creation of theoretical databases (Karpievitch et al., 2011). Alternatively, endoproteinases (Arg-C, Asp-N, Glu-C and Lys-C) are used for a highly efficient enzymatic cleavage approach. They are very selective for an unique residue, becoming a great option to apply in middle-down proteomics (Switzar et al., 2013).

Peptides can be non- or wrongly identified in case of missed cleavages, compromising the protein identification and quantification. To overcome this issue, the adjustment of database searches can be done to include one or more missed cleavages, however increasing the search time (Karpievitch et al., 2011).

1.3.3.2 MS/MS analysis

After digestion of the samples, followed by LC separation and ESI, the produced ions will be separated according to their masses in a mass analyzer. As previously mentioned, this measurement is realized by the *m/z* of the ions and can be based in different principles of separation (Hoffmann and Stroobant, 2007b). Some examples of mass analyzers are the 'time-of-flight' (TOF), which separates ions based on their velocity crossing the instrument, the 'orbitrap' (OT), which is based on resonance frequency and the 'quadrupole' (Q), which trajectory stability is the separation principle. Mass analyzers use static or dynamic electricity and magnetic fields, combined or not, and the way they are used defines the type of instrument. They can also be placed in tandem, in different combinations, allowing the performance of multiple experiments and increasing results versatility. The most common form of MS in sequence involves the mass analysis in two stages: in the first one, the precursor ion is

isolated, which will be fragmented, and the product of the fragmentation is analyzed in the second mass analyzer (Hoffmann and Stroobant, 2007b).

The Orbitrap mass analyzer, relative to other ion trap instruments, such as ion cyclotron resonance (ICR) and quadrupole ion trap, is a small equipment, able to obtain high mass resolution and accuracy, as well as large dynamic and *m/z* ranges (Makarov, 1999).

1.3.3.3 Data processing and protein quantification

In label-free peptide quantification, the analysis of each sample is separately performed. Thus, this approach is more prone to technical error if the reproducibility of the analytical platform is not guaranteed (Nahnsen et al., 2013). It also generates a large amount of highly complex data when derived from LC-MS/MS experiments, which must be processed in order to be analyzed.

The process of *peak peaking* or *centroiding* of the raw signal data corrects inaccurate distribution of *m/z* values around the true one. This distribution occurs due to the random process of ionization and limitation on mass analyzer resolution. Thus, the measurement of identical ions may not occur at the same time, generating the so called (raw) peak. Peak peaking will provide a unique *m/z* value by selecting the maximal intensity position or determining the *m/z* average (weighted average of raw data points and intensity) (Nahnsen et al., 2013). Besides that, *noise filtering*, caused by electronic noise from the detectors and chemical noise of solvents, buffers and possible contaminants, as well as *baseline filtering* (average noise level) must be performed. For that, it is possible to find several algorithms in the literature (Christin et al., 2011).

Several *map alignment algorithms* available to correct variability of retention times. The variability can be caused by different factors, such as temperature shift of column or mobile phase and pressure variation and is not an uncommon phenomenon. Retention time change is called *warp*, and the alignment process which corrects the displacements is known as *dewarping* (Lange et al., 2008). A great number of algorithms were also developed for *intensity normalization*, correcting peptide ion intensity recording failures. They are mainly consequences of injection mistakes of sample amounts, differences in ionization efficiency, as well as in ion transmission and detection, and carryover between runs (Christin et al., 2011).

Label-free quantitative proteomics approach generally falls in two measurements categories: (i) signal intensity, also known as ion or peak intensity, area under the curve or feature-based; or (ii) spectral counting (Zhu et al., 2010) (Figure 1.6).

Relative signal intensity quantification involves the measurement of ion intensities of ionized peptides eluting from the ion source into the mass analyzer (Podwojski et al., 2010). It was observed that signal intensity from ESI of a determined ion and its concentration are correlated (Voyksner and Lee, 1999), i. e., increasing the concentration of injected peptides leads to an increase of the peak areas (Chelius and Bondarenko, 2002). Thus, peptide quantification can be determined by comparing maximum abundance or volume of ion count for each peak intensity in multiple LC-MS/MS datasets (Podwojski et al., 2010). Signal intensity approaches require a rigid processing of the raw data, specially normalization and map alignment (Figure 1.6) (Zhu et al., 2010).

Relative spectral count quantification is based on the knowledge that increased protein abundance is followed by increased number of its proteolytic peptides.

This will then result in a higher abundance of MS/MS spectra (Washburn et al., 2001). There is a tendency towards abundant peptides during the automated selection of precursor masses for MS/MS analysis. Despite attempts to avoid multiple measurements of the same peptides by the use of exclusion lists, highly abundant ones are still repeatedly sampled. Thus the counts-protein abundance relation (Podwojski et al., 2010). Therefore, differences can be quantified by the use of sampling statistics, as peptide or spectral count and sequence coverage (Figure 1.6) (Choi et al., 2008; Liu et al., 2004).

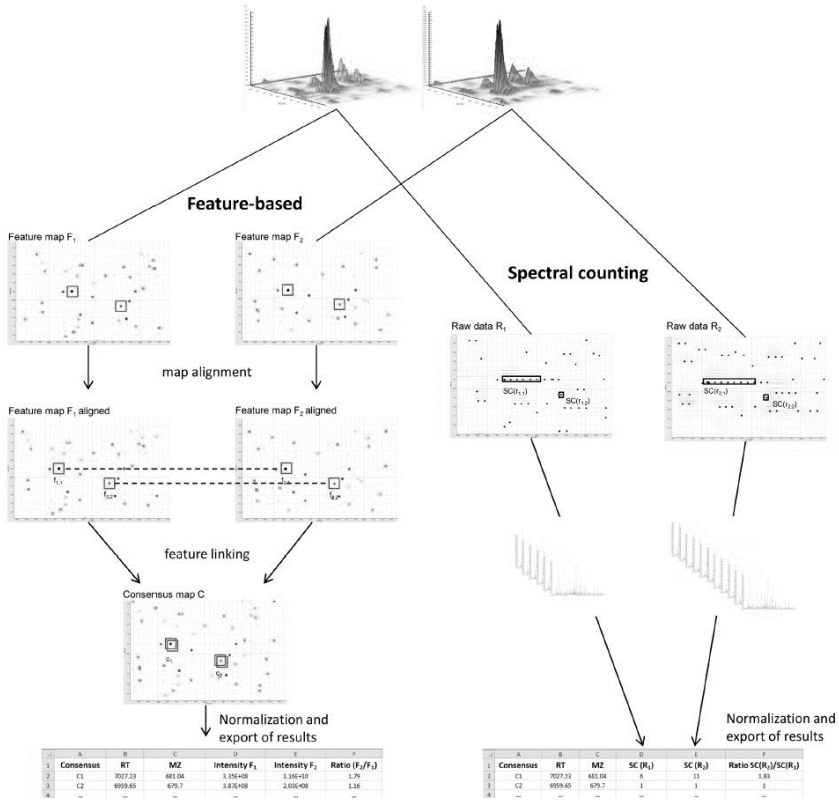

Figure 1.6 Computational label-free quantification workflow of feature-based and spectral counting methods, in which samples are separately processed and the data from different runs are combined for data analysis. Feature-based method relies on the counting of ion intensities of ionized peptides, while spectral counting relates spectral counts and protein abundance (Nahnsen et al., 2013).

1.4 Research approach and objectives

Most of the fundamental plant research is focused on the model plant Arabidopsis. However, several features and processes are unique to a particular plant species or family and cannot simply be extrapolated. Moreover, in many crops, a rigorous analysis at the molecular and physiological level has not yet been performed and stress and stress perception are usually approached from one side (e.g. plant physiology, genetics or molecular biology). Besides that, many studies in the field of remote sensing and phenomics are mainly linked solely to the genotype, seldomly phenotyping the plants at the cellular level.

Thus, to bridge the gap between genotype and phenotype, high resolution tools should be combined to cover plant performance during stress, as well as mechanisms of response and impact level. Our research approach is based on the assumption that salt stress associated growth parameters can lead to the detection of specific molecular effects and responses, targeting to specific time points of molecular stress responses. Investigating nine different genotypes of maize, an economically important crop worldwide, these stress responses can be associated with genotype-specific levels of tolerance.

Generally, we hypothesize that a systems-level approach has the potential to unite the plant responses at different scales (organism and cells) and will enhance the understanding of a plant's response towards stress. Specifically, we hypothesize that this approach is able to uncover proteins and their interlaced networks that are playing an important role in abiotic stress tolerance.

Through the dynamics of the plant responses towards salinity, our general aim was to enhance food security by providing useful information to farmers and germplasm banks, focusing on tropical genotypes and thus, less developed areas. To achieve this objective, it is necessary to unveil interesting cultivars

within a crop, which in our research maize was selected by its relevance. Our specific aim was to understand the diversity in molecular mechanisms behind salt stress in maize and the signaling and defense responses. To meet these goals, we worked with the following research approach:

1) Determine key growth traits and apply optimized plant phenotyping to get an insight into the stress dynamics (Chapter 3).
2) Classify different maize genotypes to get an insight on the genetic diversity towards salinity and provide valuable information for maize gene banks regarding the characterization of potential accessions (Chapters 4 and 5).
3) Identify proteins and molecular networks important for growth maintenance and tolerance (Chapters 4 and 5).

Chapter 2 MATERIAL AND METHODS

The plant growth phenotyping experiments were held in a greenhouse of the Faculty of Bioscience Engineering K.U. Leuven, Belgium, and consisted of three stages: phenotyping optimization, growth traits selection and establishment of the stress level (Chapter 3); genotype-specific growth and proteomic responses of maize towards salt stress (Chapter 4); growth analysis and tissue phenotyping of additional maize genotypes (Chapter 5).

The diagram below summarizes the experimental plans and performed analyzes of this work.

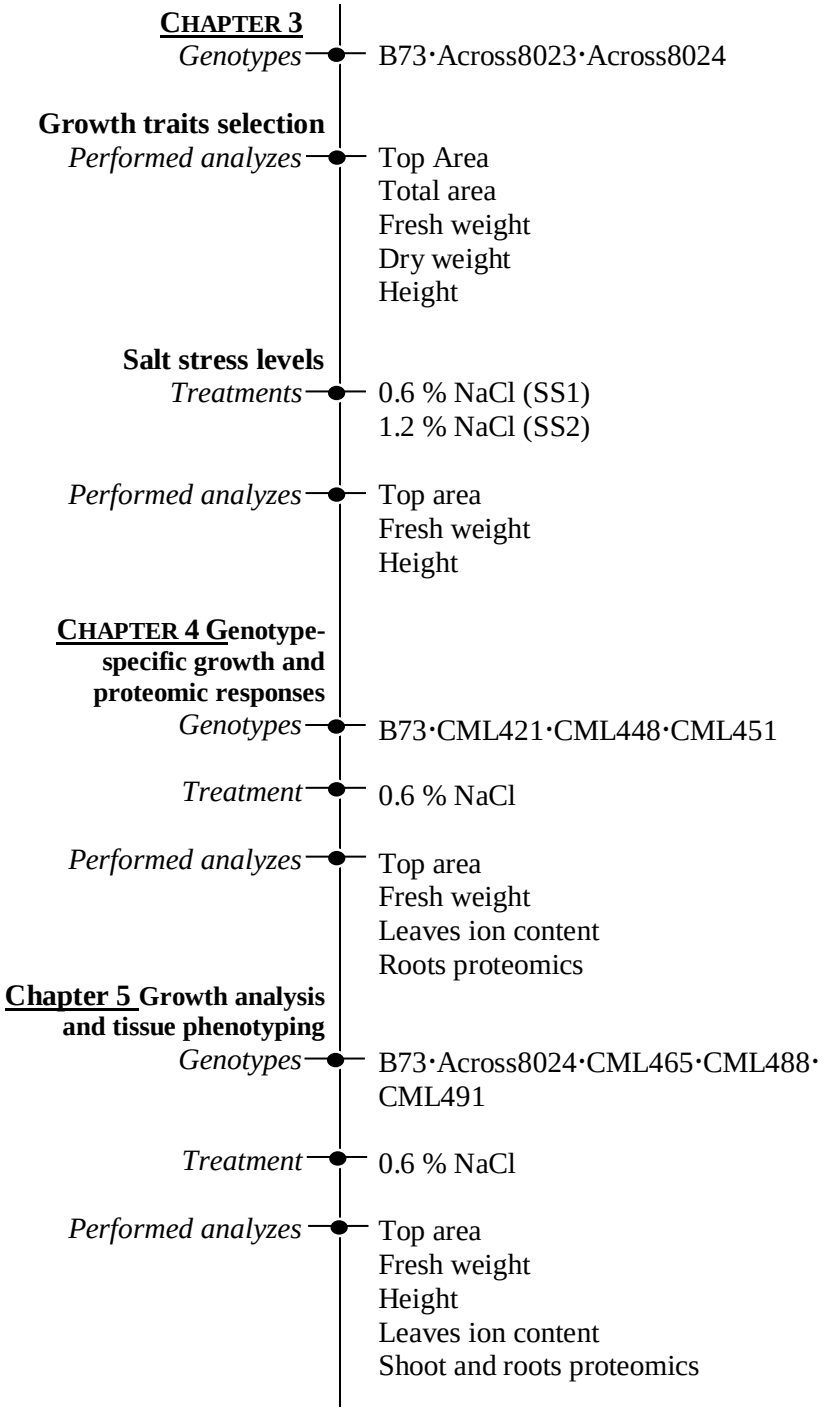
CHAPTER 3
Genotypes
B73·Across8023·Across8024
Growth traits selection
Performed analyzes
Top Area
Total area
Fresh weight
Dry weight
Height
Salt stress levels
Treatments
0.6 % NaCl (SS1)
1.2 % NaCl (SS2)
Performed analyzes
Top area
Fresh weight
Height
CHAPTER 4 Genotype-specific growth and proteomic responses
Genotypes
B73·CML421·CML448·CML451
Treatment
0.6 % NaCl
Performed analyzes
Top area
Fresh weight
Leaves ion content
Roots proteomics
Chapter 5 Growth analysis and tissue phenotyping
Genotypes
B73·Across8024·CML465·CML488·CML491
Treatment
0.6 % NaCl
Performed analyzes
Top area
Fresh weight
Height
Leaves ion content
Shoot and roots proteomics

For each stage, a certain number of maize genotypes was analyzed. In total, nine maize genotypes were studied: B73, Across8024, Across8023, CML465, CML488, CML491, CML421, CML448 and CML451 (Table 2.1). Genotype B73 was used in all experiments as a sequenced reference and was provided by North Central Regional Plant Introduction Station (NCRPIS, USA). Genotypes Across8024 and Across8023, acquired from the International Maize and Wheat Improvement Center (CIMMYT, Mexico), were chosen due to its response to salt stress in previous experiments, in which they were characterized as tolerant and sensitive, respectively (Hajibagheri et al., 1987; Pitann et al., 2013). CML491 is considered as drought tolerant genotype (Beyene et al., 2011).The other maize genotypes (CML465, CML488, CML421, CML448 and CML451) were also obtained from CIMMYT and, despite no information concerning salt tolerance was available, they are all adapted to tropical climate (CIMMYT, 2005; Lu et al., 2011).

Table 2.1 Maize genotypes information and chapters in which they were studied.

Genotype	Source	Adaptation Zone	Experimental Chapters
B73	NCRPIS	Temperate	Chapters 3, 4 and 5
Across8023	CIMMYT	Tropical	Chapter 3
Across8024	CIMMYT	Tropical	Chapters 3 and 4
CML465	CIMMYT	Tropical	Chapter 4
CML488	CIMMYT	Tropical	Chapter 4
CML491	CIMMYT	Tropical	Chapter 4
CML421	CIMMYT	Tropical	Chapter 5
CML448	CIMMYT	Tropical	Chapter 5
CML451	CIMMYT	Tropical	Chapter 5

In the first section of chapter 2, the experimental condition approaches are addressed. Each experiment was composed by a set of analysis traits, which are presented in the second section of this chapter, as well as the proteomics methodology.

2.1.1 Plant material and experimental conditions

Maize seeds from all experimental chapters were sown in 4 liters pots containing Brill potting soil Type 3 (Table 2.2), mixed (2:1; v/v) with sand. The plants grew in a 12 hours photoperiod and temperatures of 25° C/15° C, day and night, respectively. All experiments were conducted during the winter of 2014, 2015 or 2016, which provided a better control of photoperiod and temperatures. Water leakage from pots was avoided during irrigation by calculating the exact water volume necessary for each pot. Soil water evaporation was prevented using foil, also avoiding extreme salt concentration in salinity experiments.

Saline conditions were created by mixing sodium chloride (NaCl) directly with the soil mix, never added in the nutrient solution. We assessed salinity of treated soil through soil water suspensions (SWS) approach, with 1:5 soil to water ratio ($EC_{1:5}$). The conversion of SWS results to saturated extract paste method (SP) form is dependent of the type of soil used. In this study, the appropriate regression equation for conversion from $EC_{1:5}$ to ECe was: SP=7.98 SWS, with the EC in dS m^{-1} at 25 °C (Sonmez et al., 2008).

The nutrient solution used for irrigation had the following concentration: 2 mM KH_2PO_4, 1 mM K_2SO_4, 1.33 mM $Ca(NO_3)_2$, 0.67 mM NH_4NO_3, 2 mM $CaCl_2$, 0.5 mM $MgSO_4$, 0.1 g L^{-1} Fe-sequestrene, 5 µM H_3BO_3, 2 µM $MnSO_4$, 0.5 µM $ZnSO_4$, 0.3 µM $CuSO_4$, 0.01 µM $(NH_4)_6Mo_7O_{24}$.

Table 2.2 Drill Type 3 potting soil composition and chemical values

Composition	
65 % white peat	
35 % black peat	
500 g NPK- fertilizer m^{-3}	
Chemical values	
pH-value	5,7
Salt content:	0,5 mg L^{-1}
Nitrogen, N	70 mg L^{-1}
Phosphorus, P_2O_5	50 mg L^{-1}
Potassium, K_2O	90 mg L^{-1}

2.1.2 Phenotyping optimization and growth traits selection

Chapter 3 experiments occurred in two steps. Firstly, we optimized conditions for phenotyping and investigated different traits for growth monitoring in non-stressed conditions. The genotypes investigated were B73, Across8024 and Across8023. The experiment was carried out for eight weeks after sowing. We used eight repetitions for each genotype and each week. From the third week, top pictures for shoot area calculation were taken weekly, as well as the height measurement. Every week, eight plants of each genotype was sacrificed and we calculated total leaf area and biomass accumulation by means of shoot and root FW and DW.

Secondly, we established appropriate levels of salt stress, with the same maize genotypes (B73, Across8024 and Across8023) as the first step by using two NaCl concentrations into the soil mix, except for the control group: 0.6% NaCl (salt stress 1 – SS1) and 1.2% NaCl (salt stress 2 – SS2). For each treatment

and each genotype, eight repetitions were monitored from the sowing until the ninth week of growth. From the third week after sowing, plants top area and height were calculated weekly. Plant biomass was determined by FW and the destructive measurement took place at the ninth week after sowing.

2.1.3 Genotype-specific early detection of salt stress

Four maize genotypes were analyzed in chapter 4 experiments, with six repetitions each: B73, CML421, CML448 and CML451. Two experimental conditions were set up in a completely randomized design, in which the treatment consisted of sodium chloride (0.6% NaCl) addition and the control, without salt addition. The projected leaf area was measured for each of the six replicates per genotype from the second week after sowing. Pictures of individual plants were taken weekly from the top of the plants. The investigation of root growth was estimated by determining the FW of six samples per treatment and genotype at the fourth week after sowing. The analysis of leaf ions was performed on four replicates of each genotype per treatment, which were collected at the end of the experiment.

Roots from the plants sacrificed at the fourth week were cleaned with distilled water and immediately plunged in liquid nitrogen (LN). With that, root proteomics was performed with six replicates per genotype and for each treatment.

2.1.4 Screening of genetic diversity towards salt stress

In experiments of chapter 5, five maize genotypes were screened according to their reaction to salinity: B73, Across8024, CML465, CML488 and CML491. Apart from the control group, one salt treatment was evaluated (0.6% NaCl) and the plants were monitored from the sowing of the seeds until the seventh

week after sowing. The experiment was performed on six replicates of each genotype per treatment. Top area and height were determined weekly, while FW was analyzed at the seventh week after sowing.

After the sacrifice, the first transversal half of the last completely formed leaf of each plant was used for ion content determination (N = 8). The other half was plunged into LN and used for proteomics (N = 6). Roots of the sacrificed plants were immediately cleaned in distilled water and stored in LN until employed for proteomics analysis (N = 6).

2.2 Growth analysis traits, ion content and proteomics methodologies

2.2.1 Shoot area – image-based phenotyping

Digital images of maize plants were performed with a Canon EOS 350D camera and processed off-line using an in-house script (R core Team 2013). The green area of leaves was calculated with a red, green and blue channel (RGB), separating the green plant parts from the non-green background, and excluding the surroundings, such as the stand, the pot and shadows.

Pictures which were taken from the top position of the plant (Figure 2.1A), generated the *top area* data of individual plants. Images acquired from the detachment of the leaves (Figure 2.1B), configured the total leaf area of the plants, by the sum of each individual leaf area.

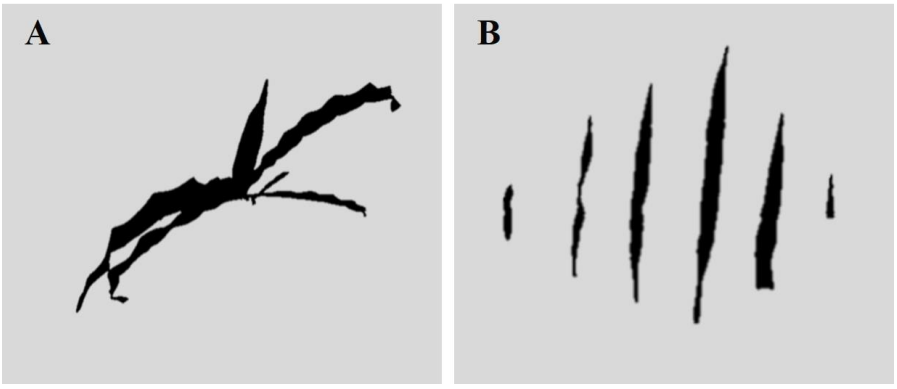

Figure 2.1 (A) Converted pictures taken at the top of a maize plant and (B) converted pictures taken from detached leaves of a maize plant.

2.2.2 Plant height

The height of each plant was measured from the base of the first completely formed leaf to the top of the last formed leaf, using a rigid ruler.

2.2.3 Fresh weight

Roots with soil remnants were washed out with water and weighted in an electronic scale coupled with a computer device. Shoots are also immediately weighted after sacrificing and the whole plant weight is calculated with the sum of the root and the shoot values.

2.2.4 Dry weight

Plant roots and shoot are separately packaged in paper bags and placed in an oven at 70 ºC until achieving constant weight. After being weighted in an electronic scale, roots and shoot values were summed for each plant.

2.2.5 Ion content

Ion content was performed in the Institute of Plant Nutrition and Soil Science, Christian Albrechts University, Kiel, Germany. For that, 20 mg of dried leaf material was dissolved and boiled in 1.6 mL of deionized water for 5 min. After cooling, samples were centrifuged and the supernatant was collected. Proteins were then precipitated by washes in chloroform and cleaned with C-18 columns (Thermo Fisher Scientific, Darmstadt, Germany). Na^+, K^+ and Cl^- concentrations were analyzed using ion chromatography (Dionex ICS-5000+ Capillary HPIC System, Thermo Fisher Scientific).

2.2.6 Gel-free proteomics approach

2.2.6.1 Protein extraction, digestion and peptides cleaning

Leaves of sacrificed plants, as well as distilled water cleaned roots, were immediately plunged in LN. The protein extraction was performed according to the phenol method described by Carpentier et al. (2005) at the Proteomics Lab of the Faculty of Bioscience Engineering and at SyBioMa of the Biomedical Sciences Group, KU Leuven. Each tissue was triturated in a mortar, with assistance of LN, and 300 mg of the homogenate was solubilized in 750 µL of ice cold extraction buffer (100 mM Tris-HCL pH 8.3; 5 mM EDTA; 100 mM KCL; 1% p/v DTT; 30% sucrose; 1 complete Mini EDTA-free protease inhibitor cocktail tablet -Roche Applied Science- per 10 mL buffer) and briefly vortexed. After, 750 µL of ice-cold Tris buffered phenol solution (pH 8.0) was added and the mixture was vortexed for ten minutes, at 4 ºC and then centrifuged at 12,000 rpm. The phenolic phase was collected and 750 µL buffered phenol was added into it, followed by the vortexing and centrifuging for five minutes. Once more, the phenolic phase was collected and 100 mM ammonium acetate in methanol was added. The mixture was kept in -20 ºC

overnight to precipitate. Afterwards, the samples were centrifuged for 60 minutes (4 ºC, 13,000 rpm) and the resulted supernatant was discarded. The formed pellet was kept in cold acetone and 0.2 % DTT solution twice for 60 minutes at -20 ºC to be rinsed. In between the two rinsing processes, there was a centrifugation (4 ºC, 13,000 rpm) and a discard of the supernatant. After being gently dried under a hood at room temperature, the pellet was resuspended with 150-200 µL lysis buffer (8 M urea; 5 mM DTT; 30 mM Tris). Protein concentration was quantified with the 2-D Quant Kit assay (GE Healthcare).

Sample aliquots containing 20 µg of proteins underwent digestion, in a process of successive addition of the following compounds, to the following final concentrations: DTT to 20 mM and incubated for 15 minutes; iodoacetamide to 50 mM, incubation in the dark for 30 minutes; three times dilution with 150 mM ammonium bicarbonate; addition of trypsin in a ratio of 0.2 µg trypsin per 20 µg protein and overnight incubation in 37 ºC; and acidification with trifluoracetic acid to 0.1 % final concentration. Desalting of samples was performed using Pierce™ C18 Spin Columns (Thermo Fisher Scientific), according to manufacturer instructions.

2.2.6.2 Peptides separation, identification and quantification

Separation of digested samples (1 µg / 5 µL) occurred via UPLC-MS/MS system, with the Ultimate 3000 UPLC system (Dionex, ThermoScientific) and Q Exactive Orbitrap mass spectrometer (Thermo Scientific, USA) used according Vanhove et al., (2015). Data were obtained with Xcalibur 3.0.63 software (ThermoScientific). Protein identification was performed with raw data conversion by Proteome Discover version 1.4 (Thermo Scientific) into mgf files and processing with MASCOT version 2.2.06 (Matrix Science) against the Uniprot *Zea mays* database (99 371 proteins). A minimum of one peptide was

used to identify proteins, to avoid the loss of interesting results the exclusion of such proteins would inherently cause. To enhance the identification confidence, Scaffold (Version: Scaffold 3.6.3; Proteome Software Inc., Portland, OR, USA) was used to calculate false discovery rate (FDR), which estimates the quantity of possible false positives in the processed data based on a decoy database simulation. Quantification of proteins was performed using Progenesis LC–MS version 4.1 (Nonlinear Dynamics), with automatic alignment from a selected reference run and based on ion intensity, summing the peptides relative abundance.

Singular Enrichment Analysis (SEA) were performed using the AgriGO SEA tool (http://bioinfo.cau.edu.cn/agriGO/analysis.php), with *Zea mays* background and significance level of 0.01 or 0.05. Biological networks were generated with the open source software platform Cytoscape (Shannon et al., 2003). Promoter analysis was realized using plantCARE (Lescot et al., 2002), up to 1500 bp with genotype B73 as sequenced reference.

2.3 Statistics

Statistics were performed with the software STATISTICA (version 13, Tulsa, OK, USA). Datasets were tested for normality with Kolmogorov-Smirnov (K-S) test. Not normal distribution data groups were compared by Mann-Whitney U test and were significant at $p<0.05$. Normal distributed data groups were tested with ANOVA analysis. The means were compared with Fisher's LSD test ($p<0.05$).

Box plots are composed by the median; the box is defined by the first and third quartiles. Whiskers are positioned 1.5 times the interquartile range from the median. Outliers are the individual points distancing more from the median than the extremes. Other plots were made using Microsoft Excel (Office 2016).

Correlation between variables were calculated by the Pearson's correlation coefficient (r). The Sample Correlation Coefficient Table was used to test the significance. Critical value for significance was always 95% ($\alpha = 0,05$).

Quadrant plots ranks the genotypes by the area of each individual genotype normalized to the median area of all genotypes. They were constructed in Microsoft Excel (Office 2016), according to Kissel et al. (2015). Thus, the division in four quadrants indicates the best and worst potential growers, according to the environmental conditions.

Chapter 3 PHENOTYPING OPTIMIZATION, GROWTH TRAITS SELECTION AND ESTABLISHMENT OF THE STRESS LEVEL

3.1 Introduction

Salinity stress has a two-phase effect on plants: the first one is the osmotic stress, followed by a later second phase, the ionic stress (Munns, 2005). Effects on plants growth are due to reduction on water uptake caused by the osmotic imbalance and cell injuries when the ions enter the transpiration mainstream. With that, plants can face growth reduction and slower photosynthetic leaf area formation driven by inhibition of cell division and cell elongation (Tester and Davenport, 2003).

As well as leaves, roots can also respond and be affected by salinity (Moya et al., 1999; Valdez-aguilar et al., 2011), despite the consensus that the effects are weaker and less prolonged than in the shoot (Munns, 2002a; Munns and Tester, 2008). In any case, the roots are the plant's venue with saline stress and analyzing its growth is an important factor to understand the reaction and effects of different genotypes toward this condition.

Accurate physiological phenotyping is an essential step for salt tolerance screening of different genotypes. The process involves a priori selection of appropriate traits to be monitored and this choice is dependent of available facilities, financial requirements and feasibility for each analyzed species. Furthermore, the whole experimental design will influence the traits feasibility, as well as the projected duration and the specific aims of the particular investigation (Fiorani and Schurr, 2013). Thus, to select appropriate traits and determine limitations of feasibility for future saline experiments, we monitored the growth of three maize genotypes in controlled conditions. The monitoring was based on projected shoot area, height, FW and DW.

3.2 Results and discussion

3.2.1 Phenotyping optimization and growth traits selection

Image-based top area calculations taken weekly, for six weeks, showed genotype B73 as the slowest grower (Figure 3.1A). Genotypes Across8024 and Across8023 presented similar growth performance during this time and were not statistically different at the eighth week of measurement (Table 3.1). Genotype B73 had, in the last week, 58% and 59% less green leaf area than Across8024 and Across8023, respectively (Table 3.1).

Height measurements of the maize genotypes also resulted in B73 as a slow grower in comparison to Across8024 and Across8023 (Figure 3.1B) from the third to eighth week after sowing. Across8024 and Across8023 genotypes once more exhibited similar growth trends in this period of time (Figure 3.1B), both presenting 30% statistically significant bigger height than genotype B73 at the last experimental week (Table 3.1).

Top area and height are advantageous growth parameters for being non-destructive parameters. This allows the monitoring and the analysis of the same plants through time. However, in one hand, top area is a fast and totally computerized process, which is not the case for height. On the other hand, taking top area pictures becomes challenging from a certain point, for the size of plants and weight of pots, different facilities are required.

As well as for the top area and height, FW and DW of genotype B73 were significantly lower than Across8024 and Across8023 at the eighth week after sowing (Table 3.1). However, the distinct division of the trend lines of the last two genotypes is not so clear as for top area and height. Through time, the biomass values of the three genotypes, especially Across8024 and B73,

intersect with each other, until the last time point of the experiment (Figure 3.1B). At the eighth week, FW of B73 was 38% and 42% lower than Across8024 and Across8023, respectively, and DW was 38% lower than both genotypes (Table 3.1).

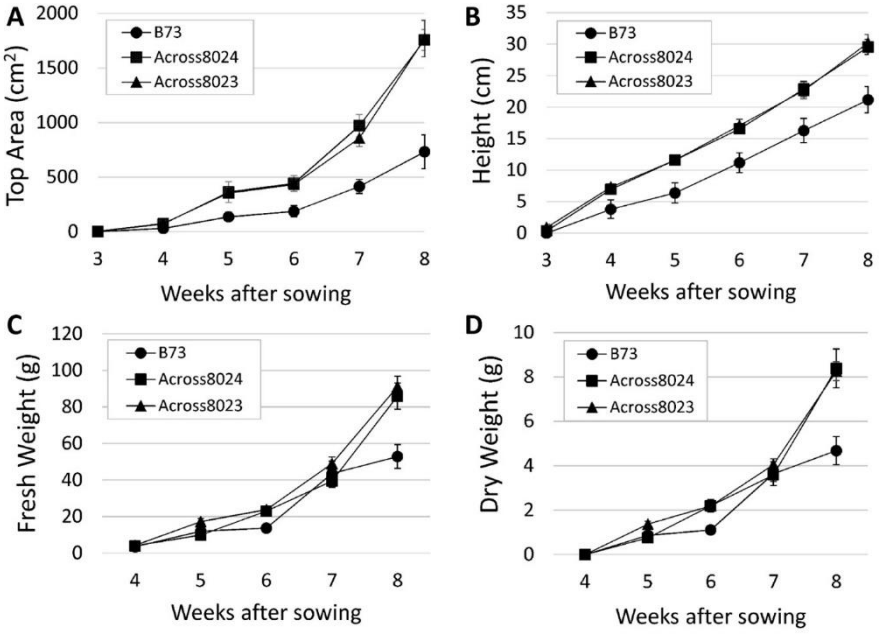

Figure 3.1 Trend lines of (A) top area; (B) height; (C) fresh weight; and (D) dry weight of three maize genotypes from the fourth to the eighth week after sowing. Bars stand to Standard Error. N = 8.

Table 3.1 Physiological traits measurements of three maize genotypes eight weeks after sowing.

Physiological traits	**GENOTYPES**		
	B73	**Across8024**	**Across8023**
Top area (cm^2)	732 a	1756 b	1769 b
Height (cm)	21 a	30 b	30 b
Fresh weight (g)	53 a	86 b	91 b
Dry weight (g)	5 a	8 b	8 b

Means followed by the same letter did not differ according to the LSD test ($p < 0.05$), which compares genotypes. N = 8.

Because maize has an alternate distichous phyllotaxy (Arber, 1925), pictures taken from the top of the plant could generate inexact area values, as a younger leaf may cover a previously formed one. Thus, the total area of the shoot was assessed by the sum of individual leaves, through pictures taken weekly after sacrificing the plants. We calculated then how strong was the relationship between top area and total area during the eight weeks of experiment (Figure 3.2A). Overall, there was a positive and significant correlation between top area and total area for the three genotypes. The greater correlation of genotype B73 (R^2 = 0,973) when comparing to Across8024 (R^2 = 0,893) and Across8023 (R^2 = 0,932) can be a result of the slower growth of B73 (Table 3.3). Therefore, not only the size of the plants challenges the obtaining of top pictures, it can also influence the reliability of shoot area values, possible by the physical covering of older leaves by young leaves. Thus, this must be considered when defining the experimental duration.

DW can be considered a better indicator of growth than FW, since the last one may oscillate according to changes in water status (Evans, 1972). However, the plant drying process to assess DW limits the tissue use for other analysis. Thus,

we verified whether the FW is a reliable measurement when DW is not advisable. By testing the relationship between them (Figure 3.2B), we found a positive and strong correlation between FW and DW for the three genotypes (Table 3.2) for the eight experimental weeks in control conditions.

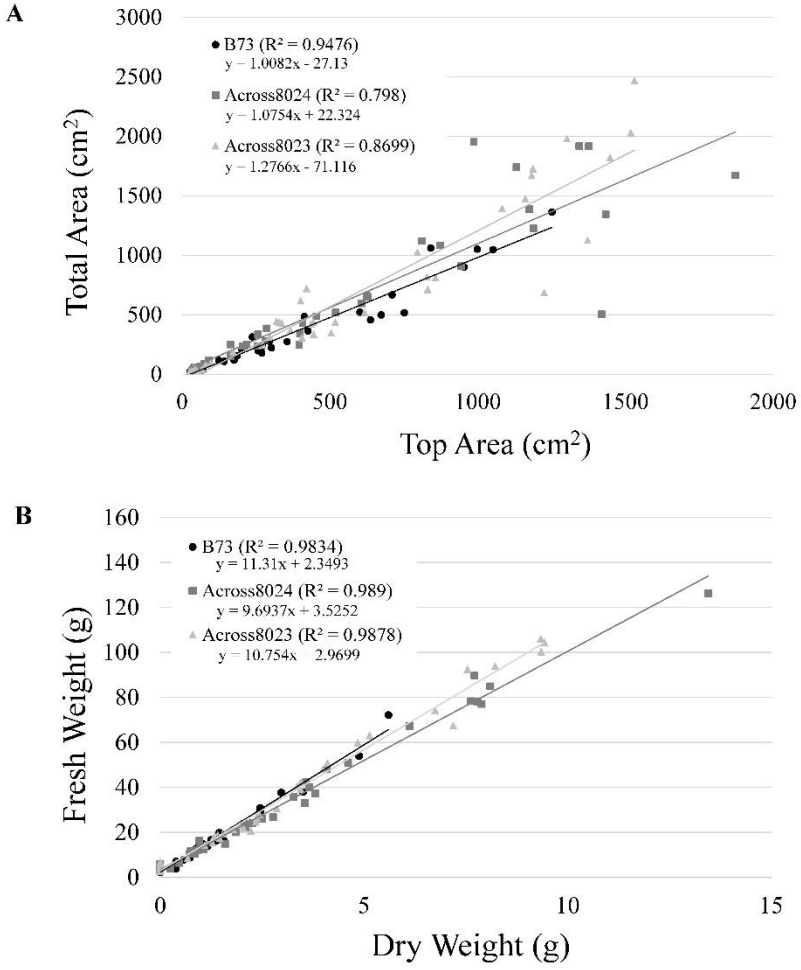

Figure 3.2 Correlation between (A) total area (cm^2) and top area (cm^2); and (B) fresh weight (g) and dry weight (g).

Table 3.2 Pearson's correlation coefficient significance between (A) top area and total area; and (B) fresh weight and dry weight, for three maize genotypes.

Pearson correlation	**GENOTYPES**		
Physiological traits	**B73**	**Across8024**	**Across8023**
A *Top area (cm^2) vs. total area (cm^2)*	0.973*	0.893*	0.932*
B *Fresh weight (g) vs. dry weight (g)*	0.991*	0.994*	0.993*

* Correlation is significant at the 0.05 level.

3.2.2 Establishment of the stress level

To establish the levels of stress in terms of salt concentration, in this study we made the first observations of the stress dynamics for three maize genotypes. The selection of salt stress level was based on its ability to divide the genotypes according to its growth reaction towards the salinity. For that, we monitored the top area, FW and height of maize growing in soil mixed with 0.6% NaCl or 1.2% NaCl, or in soil free of the salt for eight or nine weeks after sowing. The calculated EC_e for the control ($EC_{control}$) condition and for the treatments ($EC_{0.6\%}$ and $EC_{1.2\%}$) were: $EC_{control}$ = 0.8 dS m^{-1}; $EC_{0.6\%}$ = 7 dS m^{-1}; and $EC_{1.2\%}$ = 12 dS m^{-1}. Thus, we were able not only to test for salinity levels, but to confirm the feasibility of physiological traits for stress detection.

We observed that 1.2% NaCl was a very severe salt treatment for all three genotypes. It extremely reduced the growth rate of the plants, making it impossible to distinguish stress reaction patterns and to divide genotypes according to the tolerance. Claeys and colleagues (2014) concluded in a meta-analysis that the majority of published studies about salinity in *in vitro* conditions employ extreme levels of NaCl, resulting in too severe responses.

Those responses are possibly not related with the field reality and are leading to the detection of marker genes of severe stress, while mild stress markers are still missing (Claeys et al., 2014). In greenhouse experiments, many different conditions and analysis criteria can also be encountered for salt stress investigation. From different time of stress imposition, to the various growth media or substrate, which can be a soil mix, vermiculite, hydroponics, among others, to the kind of salt and levels of stress, that can reach 300 mM NaCl (Aguilar-Rangel et al., 2017; Aharon et al., 2003; Brini et al., 2007; Feki et al., 2011b; Forestan et al., 2016a; Murillo-Amador et al., 2006; Neto et al., 2004; Nohzadeh Malakshah et al., 2007; Saneoka et al., 1995). Often, there is not enough information to guarantee repeatability and reproducibility of the results, such as information about soil composition, which is necessary for the conversion of salinity units of the measurements. Thus, it is important that the choice of the stress level is made according to the specific settings of each experiment.

In case of 0.6 % NaCl, the genotypes presented different growth trends for top area (Figure 3.3) and for height (Figure 3.4). Until the eighth week, both treated and non-treated plants of genotypes Across8024 and Across8023 showed a similar top area through time, while genotype B73 was significantly the slowest grower during this period (Figure 3.3). However, at the ninth experimental week, salt treated plants of Across8024 and Across8023 faced a drop on growth rate, with Across8023 becoming significantly different from its own control (Table 3.3). Plants of genotype B73 growing in NaCl soil were the worse growers during the whole period, reaching an area 58% and 53% smaller than treated plants of Across8024 and Across8023 respectively at the ninth week (Table 3.3).

Leaf area is expected to be affected by salinity accordingly with the sensitivity of a genotype (Munns and Tester, 2008). Salt sensitive plants have their leaf area significantly reduced when growing in a saline environment (Poorter et al., 2009), which is also true for maize sensitive genotypes (Alberico and Cramer, 1993; Cha-um and Kirdmanee, 2009; Giaveno et al., 2007; Neto et al., 2004; Zo et al., 2009). This reduction in growth rate occurs rapidly due the osmotic effect of salt surrounding the roots, but it is also an ion effect later on, when ion-specific stress is reached (Munns and Tester, 2008). In our study, seeds germinated and grew in saline soil, thus their reactions are not a reflection of a shock stress. Since the osmotic factor was always present, we can infer that sudden alterations in the growth pattern of salt stressed plants is related to an ionic specific effect. Translocated ions possibly accumulated overtime, reaching toxic concentrations. This may be the cause of the growth reduction of genotypes Across8024 and Across8023 in 0.6 % NaCl treatment from the eighth to the ninth week (Figure 3.3). However, both genotypes achieved greater relative shoot area than B73 in both conditions and we can speculate the presence of adaptive mechanisms against osmotic stress and to avoid salt toxicity, such as vacuole accumulation or lower xylem translocation of ions.

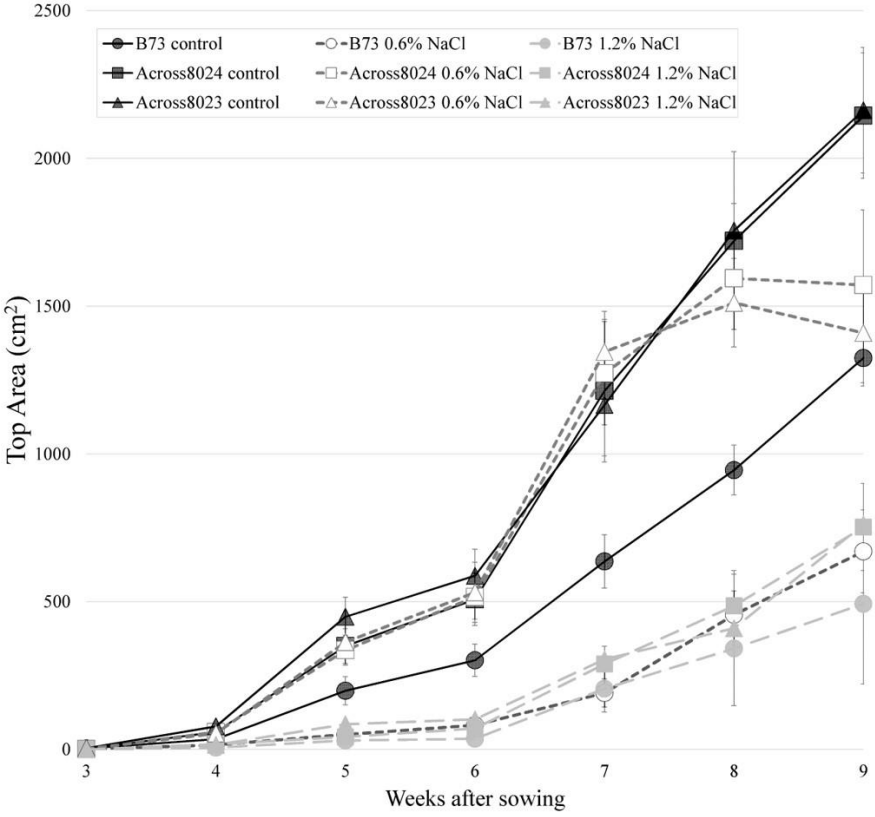

Figure 3.3 Trend lines of top area of three maize genotypes in control, 0.6¨% NaCl or 1.2% NaCl condition, from third to ninth week after sowing. Bars stand to Standard Error. N = 8.

Regarding the height measurements (Figure 3.4), until the eighth week salt treated plants of genotype B73 presented the slowest growth. This genotype had treated plants 32% and 34% smaller than Across8024 and Across8023, respectively, and control plants were significantly higher than treated ones (Table 3.3). Genotypes Across8024 and Across8023, otherwise, showed analogous trend growth between treated and non-treated plants until the eighth experimental week (Figure 3.4). Despite the ninth week was not recorded for height measurements due to practical incompatibilities, we can observe that the

patterns are similar with the top area trend lines until the week eight (Figure 3.3).

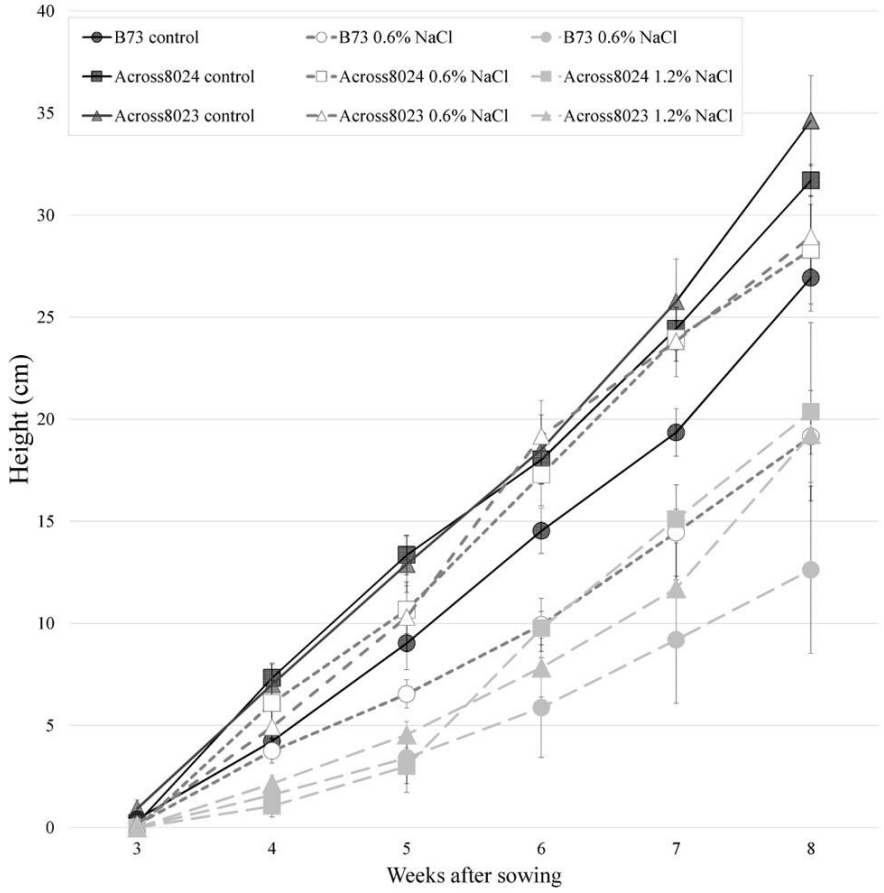

Figure 3.4 Trend lines of height of three maize genotypes in control, 0.6¨% NaCl or 1.2% NaCl condition, from third to eighth week after sowing. Bars stand to Standard Error. N = 8.

Plant height is an important agronomic trait, which affects several agronomical factors, such as density, yield, photosynthesis and harvest index (Beavis et al., 1991; Cai et al., 2012; Troyer and Larkins, 1985; Yan et al., 2003). Furthermore, height is a physiological trait that can be disturbed in case of

salinity and it was observed that maize genotypes are negatively affected by this stress (Forieri et al., 2016; Saneoka et al., 1995). Plants of the maize genotypes PUB3 and PUB1 had their height negatively affected by increase addition of a salt mix in the Saneoka and colleagues (1995) study. The betaine containing genotype PUB3 presented a significantly greater height than the non-betaine containing PUB1 in saline condition, reinforcing the betaine protective function towards salt stress (Saneoka et al., 1995). In the Forieri et al. (2016) work, maize plants treated with 50 mM and 100 mM NaCl had their height significantly lower than non-treated plants, and plant were more affected when growing in the higher stress. In our work, salt specially disturbed the height of genotype B73 (Figure 3.4) and the trait was an effective genotype-discriminator, which can be used as an alternative in case of absence of imaging technologies.

Table 3.3 Physiological traits measurements of three maize genotypes at the last experimental week (week 9 for top area and week 8 for height), in control or saline condition.

Physiological traits	**GENOTYPES**								
	B73			**Across8024**			**Across8023**		
	Control	0.6% NaCl	1.2% NaCl	Control	0.6% NaCl	1.2% NaCl	Control	0.6% NaCl	1.2% NaCl
Top area (cm^2)	1325 a	656 b	493 c	2145 a	1572 a	753 c	2163 a	1409 b	762 c
Height (cm)	27 a	19 b	13 c	32 a	28 a	20 b	35 a	29 a	19 b

Means followed by the same letter did not differ according to the LSD test ($p \leq 0.05$), which compares treatments within each genotype. N = 8.

Total FW of genotype B73 was significantly lower for treated plants when compared to non-treated ones (Figure 3.5) at the ninth week after sowing, at 0;6% NaCl. For genotypes Across8024 and Across8023, this difference was not statistically significant (Figure 3.5). As previously mentioned, 1.2% NaCl was a too extreme stress, resulting in low FW for all genotypes (Figure 3.5). The same was showed for shoot FW, with only genotype B73 presenting a significant decrease in salt-treated plants compared to control (Table 3.4). However, the root FW of genotype Across8023 was significantly smaller in saline condition, as well as for B73 at this experimental time (Table 3.4).

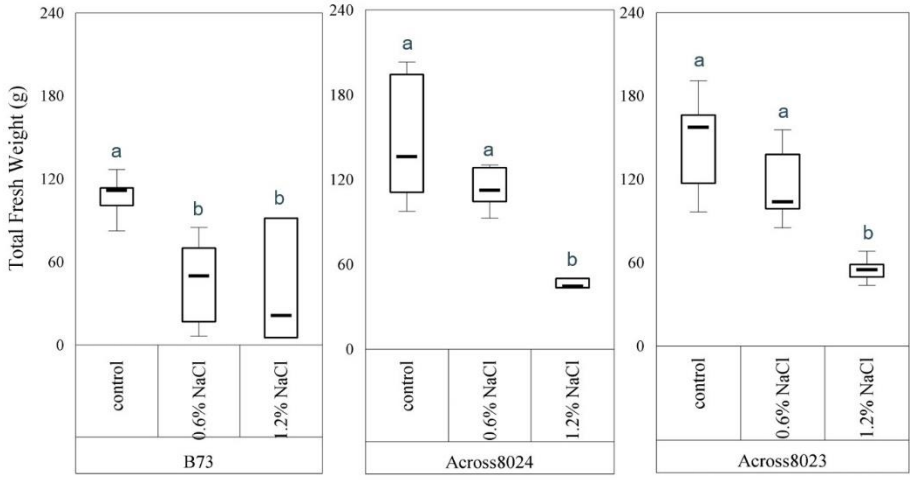

Figure 3.5 Total fresh weight (g) of three maize genotypes treated with NaCl or not (control), at the ninth week after sowing. Means followed by the same letter did not differ according to the LSD test ($p < 0.05$). N = 8.

Table 3.4 Roots and shoot fresh weight (g) of three maize genotypes nine weeks after sowing, in different soil conditions.

Fresh Weight (g)	**GENOTYPES**		
	B73	**Across8024**	**Across8023**
Shoot Control	76 A	86 A	94 A
Shoot 0.6% NaCl	39 B	78 A	79 A
Shoot 1.2% NaCl	28 B	34 B	42 B
Roots Control	32 a	58 a	52 a
Roots 0.6% NaCl	11 b	36 a	36 b
Roots 1.2% NaCl	11 b	12 b	13 c

Means followed by the same letter did not differ according to the LSD test ($p \leq 0.05$) which compares treatments within each genotype. N=8.

As previously mentioned, plant biomass measurements have the potential to describe a plant system performance and to indicate disturbances in growth (Nogueira et al., 1994). Different studies demonstrated that salinity can decrease the biomass of maize genotypes. For instance, Cheng et al. (2014) detected significantly lower shoot FW of a salt-sensitive maize genotype (D340) in comparison to the salt-tolerant (N11145), when seedlings were exposed to 150 mM NaCl for seven days. The total FW of *Zea mays* L. var. Hibiscus plants were significantly decreased when treated with 50 mM and 100 mM NaCl (Forieri et al., 2016). In our study, NaCl induced a significantly lower total biomass in genotype B73 and this trait could discriminate the genotypes Across8024 and Across8023 regarding the stress effect (Figure 3.4).

Increased root biomass as a water stress related response may indicate rooting depth in search of available water in the soil during drought (Sharp et al., 2018). However, in salt stress the root response may not have a direct explanation and can vary according to the plant strategy and tolerance. In citrus seedlings for

example, Moya et al. (1999) described a correlation between chloride uptake and shoot to root ratio in salt-sensitive (Carrizo) and salt-tolerant (Cleopatra) plants treated with NaCl. In Carrizo, the growth of this ratio lead to an increase Cl^- uptake, while in Cleopatra, increase of shoot to root ratio decreased Cl^- uptake with time, with shoot growth rates being higher in both species than root growth rates. Thus, for the salt-tolerant species, having a slower roots growth, was a beneficial response against Cl^- accumulation in leaves (Moya et al., 1999). On the other hand, for juniper plants treated with crescent salt accumulation up to 8 dS m^{-1}, the high root to shoot ratio was coincident with a higher tolerance of the stress (Valdez-aguilar et al., 2011). The tolerance increased because bigger roots accumulated more absorbed salt, preventing its translocation to the shoot (Valdez-aguilar et al., 2011). In our work, we observed that the root biomass was significantly smaller for salt treated plants (0.6% NaCl) of genotypes B73 and Across8023, while Across8024 did not record a significant reduction (Table 3.4).

Shoot FW of treated plants of genotype Across8023, unlike what occurred with roots, did not reduced statistically compared to control plants (Table 3.4). However, at the last week, the growth of treated plants in terms of top area for this genotype undergone a reduction trend (Figure 3.3). These results may indicate a strategy to prevent water loss, in which leaves would become thicker in response to the stress, by the stiffening of the cell wall (Kutschera and Schopfer, 1986). In fact, Geilfus et al. (2017) recently demonstrated stiffening of maize leaves cell wall induced by chloride-salinity stress in a process involving apoplast alkalinization. Thus, for genotype Across8023 the investment of treated plants in cell wall thickening would justify the loss in top area, but a relative growth maintenance in saline condition.

In the ranking quadrant, genotypes Across8024 and Across8023 were situated in the first quadrant, the latter having a better position regarding both the control and the (stress) treatment axis (Figure 3.6). On the other hand, genotype B73 was located at the third quadrant, meaning that for each treatment, each individual of this genotype showed a smaller leaf area than the median of all genotypes (B73, Across8024 and Across8023) in the respective treatment. Thus, genotype B73 is classified as the slowest grower in both conditions, while Across8023 stood out as the best grower in terms of shoot area, followed not by far by Across8024 (Figure 3.6).

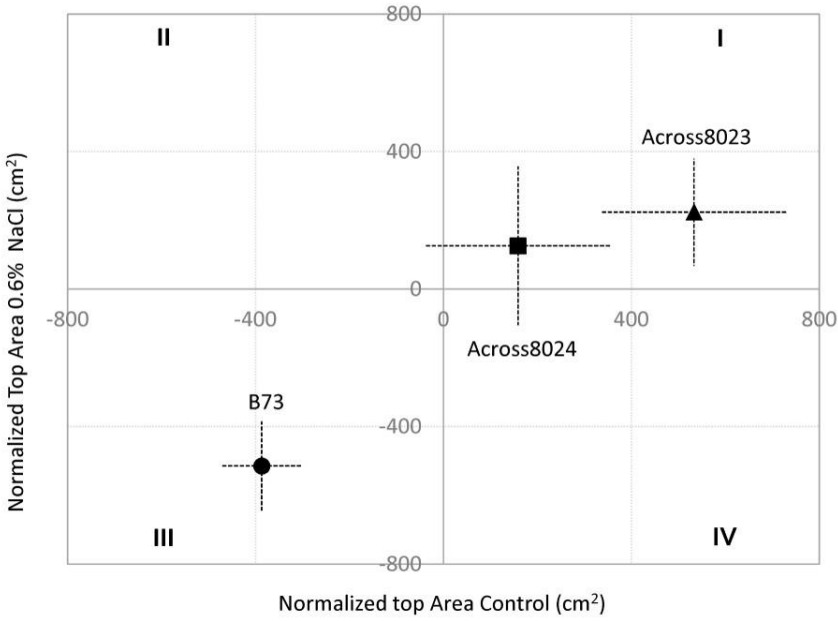

Figure 3.6 Quadrant rank of maize genotypes on the ninth week after sowing, according to the total median top area (cm^2) for each soil condition, control or 0.6% NaCl. Vertical and horizontal lines discriminate the growth potential of the plants in soil with or without salt, respectively. Dotted lines represent standard error. N = 8.

Maize genotype B73 showed to be negatively affected by salinity in both vegetative and reproductive stages in previous studies (Henry et al., 2015;

Morari et al., 2015; Niu et al., 2012). Henry et al. (2015) described a significant delay in growth and kernel set of B73 plants treated with 75 mM NaCl. The saline irrigation started from the initiation of floral development caused a growth reduction of approximately 21% in treated plants when compared to the control, based on plants height (Henry et al., 2015). In a work conducted by Niu and colleagues (2012), 55 days old B73 plants treated with 8 dS m^{-1} saline solution for 40 days, presented 65% of reduction in shoots DW from the non-treated plants. In an experimental farm study, treated plants from two different genotypes, watered with a saline solution of electrical conductivity equal to 20 dS m^{-1}, were differently affected (Morari et al., 2015). With the salt mix application from the V6 developmental stage, the maize hybrid P26 showed a better growth in stress condition than B73, which also did not recover after stress removal, differently from P26 (Morari et al., 2015). Genotype B73 in this experiment also presented negative growth effects in saline conditions and can be classified as the most salt sensitive in our study.

Genotypes Across8023 and Across8024 were studied by Hajibagheri et al. (1987), among other 24 maize genotypes, regarding the salt stress tolerance. In a first screening trial, Across8024 was classified as the most resistant genotype, having 66% survival in hydroponic solution containing 200 mM NaCl, while Across8023 was one of the most sensitive genotypes, with 15% survival after 25 days of salinization (Hajibagheri et al., 1987). However, at 50 mM and 100 mM NaCl concentrations, such varietal differences were not apparent. Afterwards, Across8024 was selected for a study of growth in 100 mM NaCl, showing a small reduction on shoots growth of treated plants, but a bigger roots reduction (Hajibagheri et al., 1987). Another work also classified Across8023 as a salt sensitive genotype, due to a high significant reduction of shoot DW (approximately 80%) of plants treated with 200 mM NaCl, relatively to the non-

treated ones (Pitann et al., 2013). Nevertheless, when in 30 mM NaCl, this reduction was not significantly different to the other analyzed genotypes (SR20, SR03 and SR05) (Pitann et al., 2013). Genotypes Across8024 and Across8023 were both classified as salt tolerant in our experiment, according to the ranking quadrant (Figure 3.5). Oppositely to the above cited studies, Across8023 had a better performance in salt stress than the other genotypes, despite having a small but significant drop in top area at the ninth week after sowing (Figure 3.3).

Despite the use of different units of measurements to express salt concentration, as molarity and electrical conductance, it is possible to calculate the conversion of one unit to the other, for approximate values, for example

$$TSS\ (mmol\ L^{-1}) = 10\ EC\ (dS\ m^{-1})$$

which is a widely used formula from the U.S. Salinity Laboratory Staff (1954) (TSS – total soluble salts). This is a recommended approximation to EC_e values up to 5 - 7 dS m^{-1} (US Salinity Laboratory, 1954). Above these EC_e values, the conversion formula

$$\log TSS = 0.990 + 1.055 \log EC_e$$

(Marion and Babcock, 1976) can be used. Thus, we can make a comparative analysis of the previously cited studies involving the genotypes Across8023 and Across8024, from Hajibagheri et al. (1987) and Pittan et al. (2013). In these experiments, we notice that the salt concentrations in which a growth retardation or an extremely low survival was reported for Across8023 (200mM NaCl) extremely exceeds the $ECss_1$ (6 dS m^{-1}) of our experiment. This may explain the different obtained results found for this genotype and reinforce the discussion about the use of extreme levels of NaCl in salinity studies.

3.3 Conclusions

From the experiments of phenotyping optimization, we selected and confirmed different growth traits that can be used for maize phenotyping. Plant top area (Figure 3.1A) is a valuable imaging technique, allowing a reliable monitoring of the same individuals through all the experimental time. Top area has advantages over the total area measurement, because being a faster and non-destructive method, while it keeps its reliability in projecting the shoot area (Figure 3.2A). However, it presents limitations regarding the plants age and the available facilities. We noticed that the correlation of top area and total area was greater for genotype B73 ($r = 0.973$), which we assume that it was due to the slower growth rate of this genotype (Table 3.2A). Furthermore, with time, the methodological dynamics for obtaining the top area pictures becomes increasingly laborious, what could be overcome with an automated platform.

Plant height (Figure 3.1B) showed to be a useful non-destructive approach for growth determination, with the restriction that it is not a computerized method, unlike the imaging techniques. We demonstrated that both top area and height distinguish growth rate of the genotypes from the fourth to the eighth week of measurements (Figure 3.1A; B). This was not the case for FW and DW, which overlapped genotypes through time, differentiating them only at the eighth week after sowing (Figure 3.1 C; D). However, the latter are important growth traits and may provide important root information that cannot be extracted from top area or height. We also concluded that, to preserve plant tissue for further analysis, FW can be used for these genotypes instead of DW, due to their strong positive correlation in control condition (Table 3.2B).

Regarding salt stress levels, we established 0.6% NaCl as the most appropriate level of both stress treatments. With this salt concentration, monitoring the top

area through time was a powerful method to get an insight into stress dynamics and to differentiate the three genotypes according to the stress effects (Figure 3.3). With top area images, we determined the moment in which genotypes Across8024 and Across8023 possibly faced ion specific stress. This moment is showed by the sudden growth brake from the eight to the ninth week after sowing (Figure 3.3). Height measurements also separated the differential genotypes growth (Figure 3.4), as well as the total FW at the ninth week (Figure 3.4).

Considering the root and shoot FW, we concluded that these are also important traits for stress quantification. The cross-results of top area and shoot FW for genotype Across8023 may indicate thickening of leaves cell wall as a salt acclimatation strategy (Table 3.4), but further research is needed. Regarding Across8024, the maintenance of FW of roots and shoot, as well as top area, suggests another salt stress acclimatization strategy.

Finally, we established a methodology for maize phenotyping and endorsed different traits for growth monitoring during salt stress. We classified the genotypes according to the salt tolerance and effects in top area projection as: Across8024 = Across8023 > B73. Despite Across8023 had a better position in the quadrant ranking (Figure 3.6), the genotype Across8024 did not show significant difference in top area at the eighth week (Table 3.3), nor in roots FW (Table 3.4) from treated to control plants.

Chapter 4 GENOTYPE-SPECIFIC GROWTH AND PROTEOMIC RESPONSES OF MAIZE TOWARDS SALT STRESS

This chapter is based on the manuscript:

"Genotype-specific growth and proteomic responses of maize towards salt stress"

Frontiers in Plant Science 2018, 9, 1- 15.

Ana Luísa Corrêa Soares, Christoph–Martin Geilfus and Sebastien Christian Carpentier

(These results are reported with the permission of all authors)

4.1 Introduction

Salinity is a key cause of arable land loss (Gong et al., 2014). It is estimated that 19.5% of irrigated lands, which provide 40% of the food production worldwide (FAO, 2015), are salt-affected (FAO, 2016). Considering the exponential growth of the population (Melorose et al., 2015), plus the aggravation of the environmental situation by climate change (IPCC, 2007), the challenge is set: increase food production per unit area of cultivated land from more sustainable production systems.

Globally, 52% of human nutrition relies on cereals including maize (FAO, 2015). In general, maize (*Zea mays*) is considered moderately sensitive to salt (Zörb et al., 2004), a category which comprises plants that maintain growth in saline soils with an ECe between 3 and 6 dS m^{-1} (Hasanuzzaman et al., 2013). However, few salt-tolerant cultivars have been commercialized (Flowers and Flowers, 2005).

Increased access to maize genetic diversity can provide several alleles linked to desirable tolerance traits. Yet, these alleles are highly dispersed and joint efforts must be made to make the information available (Barros et al., 2010).

Dynamic phenotyping should precede and guide genomic (Zhu, 2002; Zivy et al., 2015a) and will be critical in cases where the effects and responses have a dynamic nature, such as salt stress (Cattivelli et al., 2008). Phenotyping at different levels can help validate results from gene expression studies (Zhu, 2002).

Saline effects in plants occur with the combination of two stress phases: first, the osmotic, and second the ionic specific phase (Munns, 1993). For this, tolerance mechanisms are also virtually segmented according to those two phases. Lowering tissue water potential using proline and other compatible solutes contributes is a way to establish osmotic-stress tolerance (Meloni et al., 2001). Stress tolerance mechanisms during the ionic phase can include: ion exclusion, tissue tolerance (Munns and Tester, 2008) and directing sodium ions from the shoot back to the root via the phloem (Tester and Davenport, 2003). The use of each mechanism, aggregated or not, and its effectiveness, are the distinguishing factors between salt-sensitive and salt-tolerant plants (Munns and Tester, 2008).

Salt-tolerant species generally compartmentalize the accumulated ions away from the sites of primary photosynthesis and expanding tissues. The ions are stored in vacuoles and compatible solutes counterbalance the osmotic disequilibrium (Munns, 2002b; Munns and Gilliham, 2015). However, is this the most efficient stress-management strategy for crop plants, when aiming at high yield? Will the benefits of the compartmentalization overcome the energy

costs for these plants? The necessary investigations of salt-stress signaling and pathways of response will help answer these questions.

Researchers have been active in addressing these questions. A root proteomics study of maize seedlings exposed to 150 mM NaCl stress showed that the responses were quanti- and qualitatively different between a sensitive and a tolerant inbred line (Cheng et al., 2014). The authors suggested that an enhanced antioxidant defense system, allied to other processes, are the fighting arms of tolerant lines. Zörb et al. (2010) identified proteins related to cell wall growth regulation in an early salt stress response of a maize salt-tolerant hybrid. We showed recently that chloride-salinity stress induced in maize leaves stiffened the cell wall, via an apoplast alkalization process (Geilfus et al., 2017). Stiffening of the cell wall would benefit water stressed plants by diminishing water loss and wilting (Kutschera and Schopfer, 1986). Geng et al. (2013) found that the presence of abscisic acid (ABA) and the root endodermis act as a guard to prevent the plant from growing into salinized environments. With proteins having so many significant functions which help confer salt-tolerance to plants, proteomics and the role of proteins in overcoming salinity effects are an important topic of study (Kosová et al., 2013).

Despite many efforts, there are gaps in our understanding of salt stress response pathways, especially for responses by different specific genotypes. We hypothesize that (i) each genotype is capable to respond to the stress and (ii) that phenotyping at whole plant level guides the cellular analyses in identifying specific physiological events. In combining these hypotheses, we therefore used a system-levels approach to characterize salt stress in four different genotypes. We are using the dynamics of the plant responses to get an insight into the reactions at the cellular level. We bring up the challenging definition

of tolerance in agriculture and we open a discussion about energy costs and possible introduction of salt-tolerance mechanisms.

4.2 Results

4.2.1 Physiological phenotyping toward NaCl effects

The initial and final EC (EC_i and EC_f) for the control soil were 1 dS cm^{-1} and 1.3 dS cm^{-1}, respectively (Figure 4.1). For saline soil, the values were EC_i = 9.8 dS cm^{-1} and EC_f = 7.4 dS cm^{-1}. The EC of saline soil showed a significant difference in the median, with a slight decrease from the initial to the final EC.

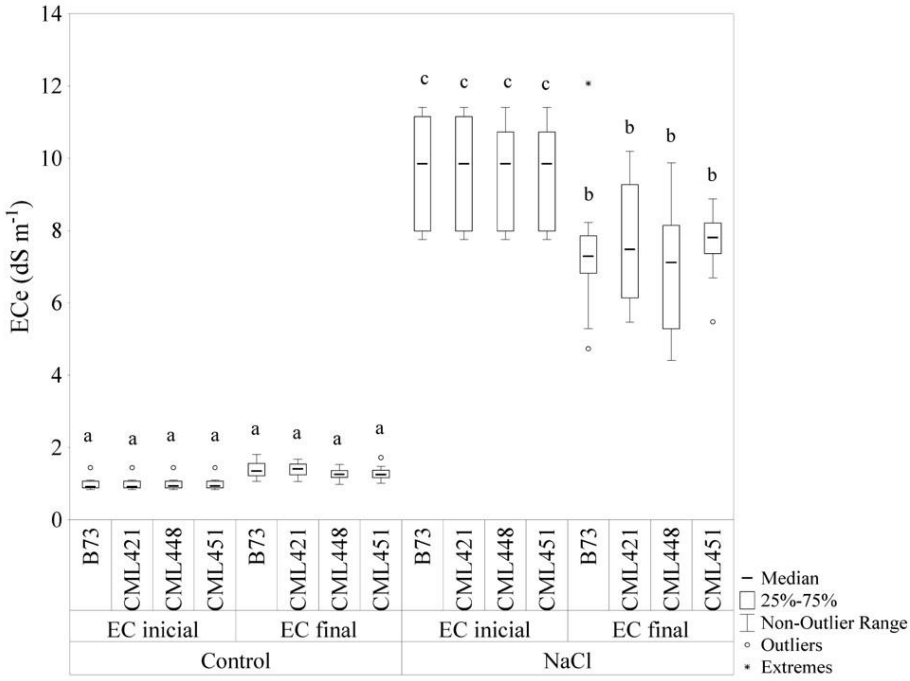

Figure 4.1 Electric conductivity (EC) of the soil mix with addition of NaCl or not (control). The EC was calculated by soil water suspensions (SWSs), with 1:5 soil to water ratio (EC1:5) and the values were converted using a regression equation, with the final EC in dS m-1 at 25◦C. Soil samples were measured at the beginning (ECinicial) and at the end (ECfinal) of the experiment. Means followed by the same letter did not differ according to the LSD test ($p \leq 0.05$). N = 6.

Physiological phenotyping of the four maize genotypes was performed not only to secure a link between agronomical effects of the salt stress and cellular phenotyping, but also to determine a specific time for sample collection. Therefore, seedlings were monitored weekly, by means of top images (Figure 4.2). At week 4, destructive samples were taken of the leaves, used for determination of the ion content, and of the roots to perform the proteome analysis. The first significant difference in projected leaf area between salt treated and non- treated plants occurred from the third to the fourth week after sowing (Figure 4.2).

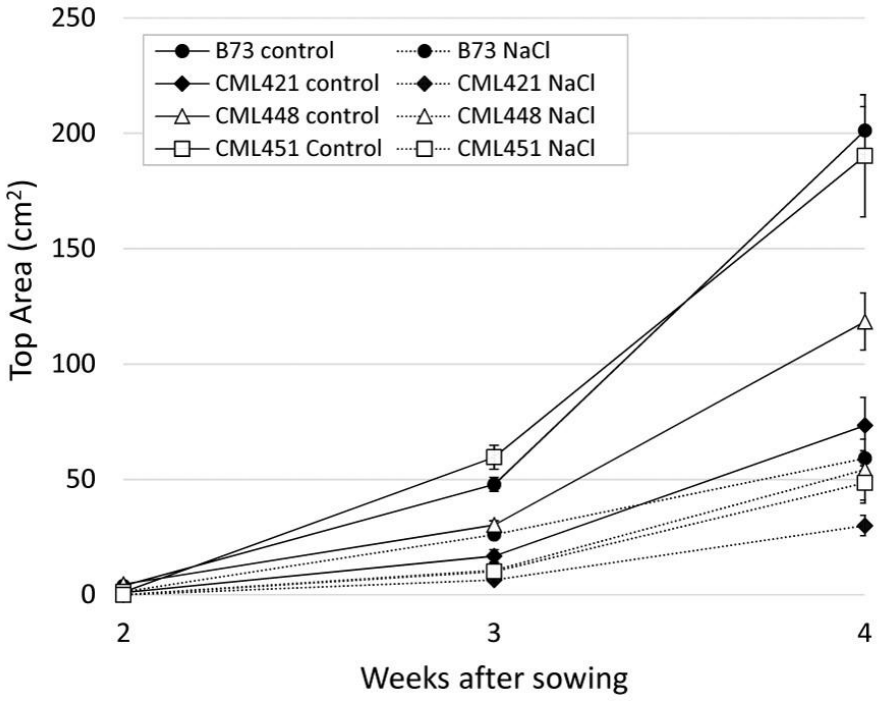

Figure 4.2 Tendency lines of the top area (cm2) of four maize genotypes in two different conditions, from second to fourth week after sowing. N= 6.

Featured in the ranking quadrant (Figure 4.3), CML421 plants are situated in the third quadrant, which means that each individual of this genotype, at each

treatment, had a lower leaf area than the median of all genotypes in the respective treatment. CML421 is characterized by the lowest growth in both conditions. B73 and CML 451 are represented in the first quadrant, which discriminates for relatively good growth and also displaying good vigor. The average leaf-area difference calculated between control and salt-stressed plants was biggest for genotype CML451 (76%), followed by B73 (70%), CML421 (57%) and CML448 (54%) (Figure 4.4).

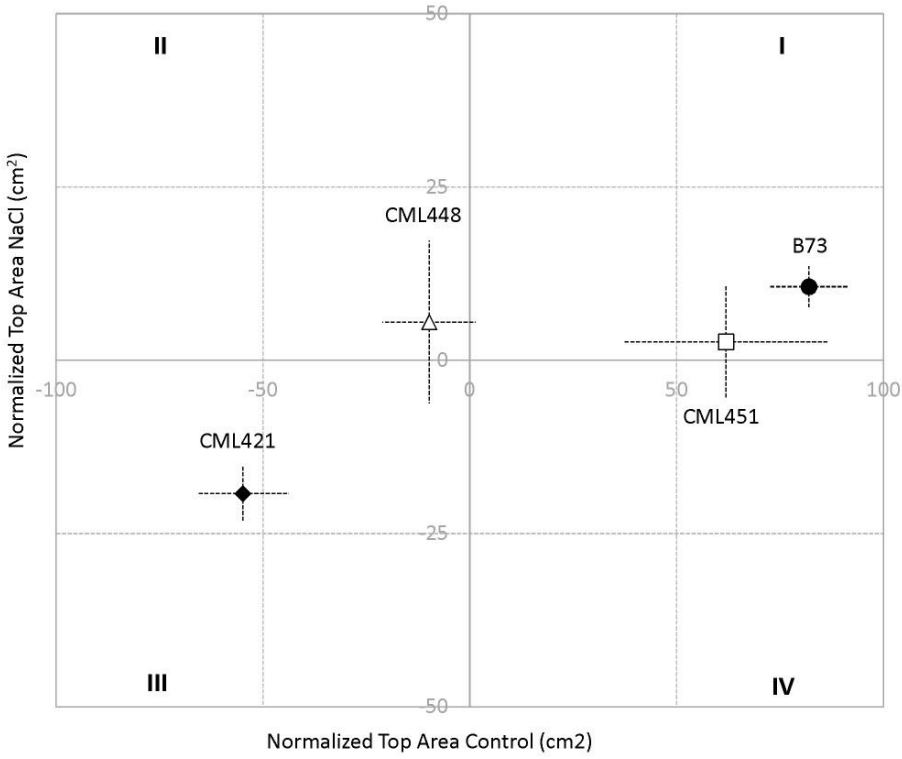

Figure 4.3 Quadrant ranking of maize genotypes on the fourth week after sowing, according to the total median top area (cm2) for each soil condition. Vertical and horizontal lines discriminate the growth potential of the plants in soil with or without salt, respectively. Dotted lines represent standard error. N = 6.

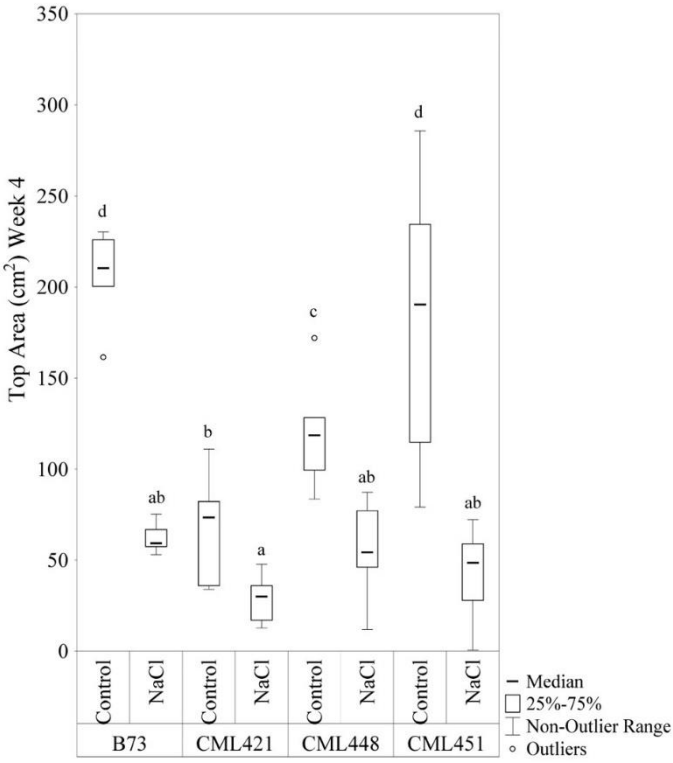

Figure 4.4 Top area (cm^2) of four maize genotypes treated with NaCl or not (control), at the fourth week after sowing. Means followed by the same letter did not differ according to the LSD test ($p < 0.05$). N = 6.

Root growth, determined by means of fresh weight at the fourth week (Figure 4.5) demonstrated a difference between treated and control plants, for all genotypes. Treated plants had significantly smaller roots than the ones not treated with salt and the average leaf-area differences are 39% for B73 and CML421, 46% for CML451 and 56% for CML448.

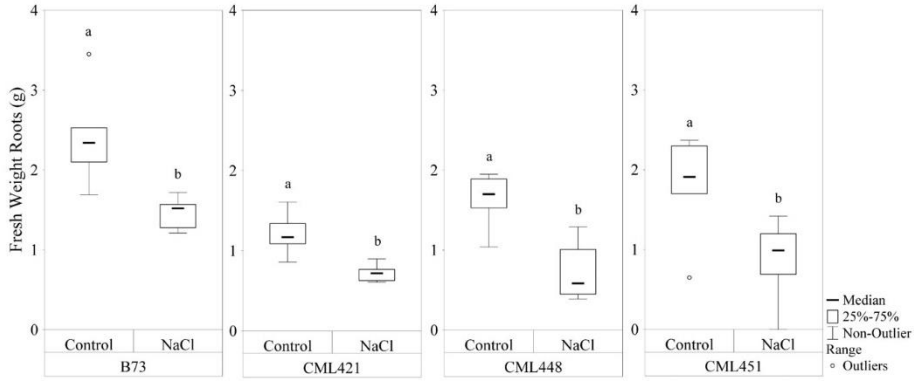

Figure 4.5 Fresh weight (g) of roots of four maize genotypes treated with NaCl or not (control), at the fourth week after sowing. Means followed by the same letter did not differ according to the LSD test ($p < 0.05$). N = 6.

4.2.2 Ion Content Determination

In the fourth week, sodium (Na^+) and chloride (Cl^-) showed a significant difference in the interaction of variables genotype and treatment (Figure 4.6). For the potassium concentration, there was a significant difference between control and treated plants for genotypes CML421 and CML448 (Figure 4.6).

There was a remarkable accumulation of both Na^+ and Cl^- ions in the leaves of genotype CML448 grown in saline conditions, which was the most pronounced among all four genotypes. In average, sodium was 97% higher and chloride, 57%, in the salt treated plants of this genotype. In CML451, the Na^+ and Cl^- concentrations were not significantly different between the NaCl-stress treatment and the control (Figure 4.6). Genotypes CML421 and CML448 exhibited a reduction in potassium content in salt treated leaves of 56 and 42%, respectively (Figure 4.6).

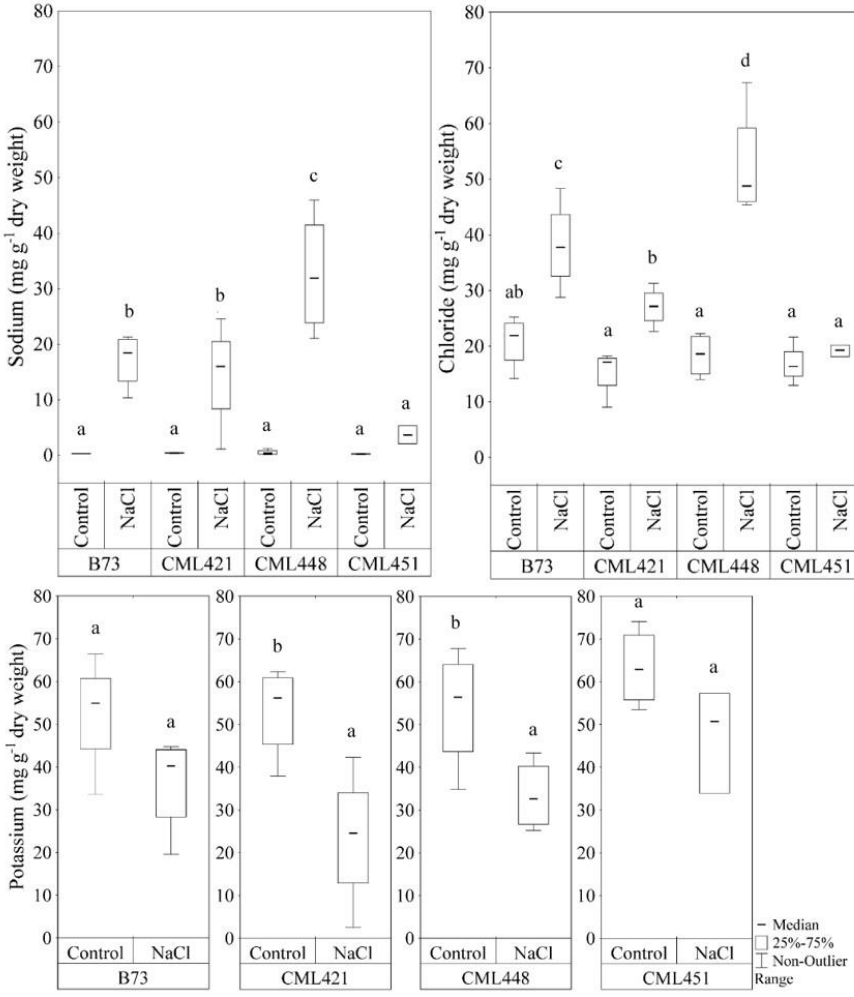

Figure 4.6 Sodium and chloride content (mg g^{-1} dry weight) in leaves of four maize genotypes, at the fourth week after sowing. Plants were grown in control or saline conditions (NaCl). Means followed by the same letter did not differ according to the LSD test ($p \leq 0.05$), calculated separately for each ion. For sodium and chloride, the interaction genotypes x treatment was significant, while for potassium, the significant difference between treatments occurred for each genotype. N = 4.

4.2.3 Protein identification and responsiveness to salt stress

The reference time for proteomics sampling was determined by the physiological phenotyping. Thus, at the fourth week after sowing, the roots

were collected, and the protein content was investigated. In total, 1,747 proteins were identified (Supplementary Table S4.1), at an FDR of 0% calculated by Scaffold, minimum of one identified peptide and best ion score from 25 upward. From this, 403 were significantly influenced by the stress treatment: 209 proteins were more abundant in the stressed plants, while 194 were more abundant in roots of control plants ($p < 0.05$) (Supplementary Table S4.1).

A Singular Enrichment Analysis (SEA) was performed for these 209 and 194 differentially abundant proteins. Enriched proteins with high abundance to salinity had 29 significant shared GO terms, and the category Biological Process (BP) included 19 significant GO terms. Enriched proteins with low abundance toward salt stress had 51 significant GO terms, from which 38 are in BP category.

For proteins less abundant in salt-stressed plants, the SEA showed that the major activated BPs categories were: (1) 'cellular process,' in which proteins are mainly involved in nucleosome assembly, (2) 'catabolic process' and (3) 'cellular metabolic process,' such as amino acid biosynthetic processes. As for salinity-activated BPs, the main categorization includes: (1) 'catabolic process,' (2) 'metabolic process,' where oxidation reduction processes and cellular respiration stood out, (3) 'response to stress,' including 'response to oxidative stress' and 'response to water' and (4) 'biological regulation' as 'cell redox homeostasis'.

Effects on class III plant peroxidase (POX) abundances are noteworthy. In total, 34 peroxidases belonging to this class were confidently identified in the roots (Supplementary Table S4.1), from which seven were highly accumulated in stressed plants (B4FNI0, B4FY83, B6T3V1, B6THU9, C0HHA6, D7NLB3, and B6U6W0) and ten in control (A5H452, A5H8G4, B4FCI9, B6T7B1,

K7U159, B1A9R4, B4FRD6, B6SIU4, B4FSW5, and Q9ZTS9) (Supplementary Table S4.1). The class III peroxidase genes found in this work are spread throughout the 10 chromosomes (chr), except chr4 and chr9. In total, 136 paralog genes were related to the class III peroxidases and a network of paralogs and proteins was created using Cytoscape (Figure 4.7). This network aggregated class III peroxidases according to their shared connections of paralogs, forming eight groups and one lone protein (K7UG68). From these, six groups gathered two or more proteins, and within three of them, class III peroxidases presented divergence in correlation to salt stress, groups 3, 4, and 5 (Figure 4.7). To better understand this big family and to be able to interpret the abundance divergence of proteins even within the same group (Figure 4.7), promoter analysis was conducted, comparing the sequences of those clusters. We focused on stress-related promoter elements present in genes of the peroxidases which were positively induced by salt stress. For group 4, the most significant motifs are MBS, which constitutes a MYB binding site involved in drought-inducibility, and TC-rich repeats, a cis-acting element involved in defense and stress responsiveness (Table 4.1). In group 5 promoters ABRE (ABA responsive elements) are present, which is a cis-acting element involved in the ABA responsiveness, DRECRTCOREAT (dehydration-responsive element/C-repeat), the core motif of DRE/CRT, and DRE2COREZMRAB17, a “DRE2” core found in maize rab17 gene promoter. Interestingly, in group 5 the promoter DRE2COREZMRAB17 is present exclusively in genes of salt stress positively induced class III peroxidase (B4FY83) (Table 4.1).

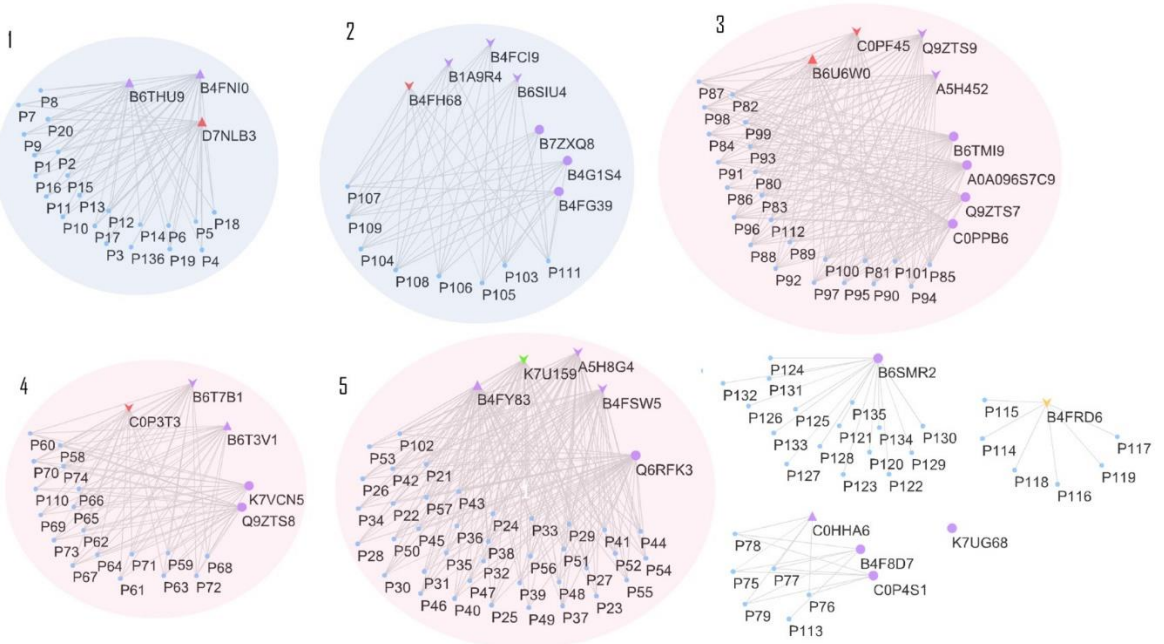

Figure 4.7 Cytoscape network relating class III peroxidase proteins and paralog genes. Proteins represented by purple triangles were positively correlated to salt stress, in all maize genotypes. Proteins represented by purple down arrows were negatively correlated to salt stress, for all maize genotypes Triangles and arrows in other colors than purple represents the class III peroxidases specifically differentiated to one genotype, being: colored red represents genotype CML421, green, genotype CML448 and orange, genotype CML451. Purple circles represent proteins that showed no difference in the relative abundance between control and treated plants. Clusters 1 and 2 gather proteins with no divergence in correlation to stress, while 3, 4, and 5, are groups that contain proteins negatively and positively correlated to stress. The paralog genes are displayed as a “P” plus a reference number.

Table 4.1 Promoter region analysis of genes expressing class III peroxidases that belong to the same paralogs cluster (Figure 4.7) and its relative abundance toward salt stress.

Protein	Salt stress induction	Promoter position and strand
Group 4 Class III peroxidases		
Promoter: MBS		
Function: MYB binding site involved in drought-inducibility		
B6T3V1	Positive	96 (+)
		1408 (-)
Q9ZTS8	Neutral	137 (+)
		1143 (+)
		787 (-)
		1030 (-)
K7VCN5	Neutral	1198 (-)
Promoter: TC-rich repeats		
Function: cis-acting element involved in defense and stress responsiveness		
B6T3V1	Positive	1237 (-)
B6T7B1	Negative	42 (+)
Q9ZTS8	Neutral	718 (+)
Group 5 Class III peroxidases		
Promoter: ABRE		
Function: cis-acting element involved in the abscisic acid responsiveness		
B4FY83	Positive	587 (+)
A5H8G4	Negative	940 (-)
		1042(-)
		1378 (-)
Promoter: DRECRTCOREAT		
Function: Core motif of DRE/CRT (dehydration-responsive element/C-repeat)		
B4FY83	Positive	264 (-)
A5H8G4	Negative	917 (+)
Promoter: DRE2COREZMRAB17		
Function: "DRE2" core found in maize (Z.M.) rab17 gene promoter		
B4FY83	Positive	690 (-)

4.2.4 Proteins differently abundant in response to salt stress, according to genotype

Regarding the variability among the genotypes, 84 proteins were found to be significantly different: 52 in CML421 plants; 13 in CML451; 6 in CML448; and 5 in B73 (Table 4.2). Uncharacterized proteins were searched via BlastP tool option from Gramene (http://www.gramene.org/), in which the sequences data were searched against *Zea mays* protein database.

From the 52 proteins differently accumulated in the slow growing genotype CML421, 34 were found to be highly abundant in response to salt stress and 18 lower abundant (Table 4.2). Salt stress abundant proteins for genotype CML421 are indicators of the stress impact, such as ROS, heat shock proteins (A0A096R6Z8, A0A096RB11, and C0PLX5) and one dehydrin RAB17 protein (A3KLI1) (Table 4.2 and Figure 4.8).

Genotype CML448 presented a heat-shock protein (HSP) 90-2 (A0A096RTH6), as possible evidence for the stress in salt- exposed plants (Table 4.2). One class III peroxidase (K7U159) was especially abundant in control plants of this genotype (Table 4.2).

Genotype CML451 presented a higher abundance of proteins involved in gene and protein regulation in treated plants (Table 4.2). Obviously, they are also found in other genotypes, but the relative abundance was the highest for CML451 in saline soil. Other possible salt-related response proteins had higher abundance in the control compared with salt-treated plants for this genotype, such as the 14-3-3-like protein (Table 4.2).

Five class III peroxidases reacted specifically to CML421 toward salt stress: C0P3T3, B4FH68, and C0PF45 were lower in salt-stressed plants, and

B6U6W0 and D7NLB3 were more abundant (Table 4.2). Other specific peroxidases that reacted negatively to salt stress were K7U159 in plants of genotype CML448 and B4FRD6 in genotype CML451.

Table 4.2 Significant proteins differentially abundant to each maize genotype, in response to salt stress.

Protein	Annotation	ANOVA	Number of identified peptides	Best ion score	Abundance in salt stress
List of Significant Proteins Differentially Abundant to Genotype B73 (p<0.05)					
B4FTS6	Endochitinase A	1,5E-03	10	71,23	High
A0A096RHR4	Glutathione S-transferase 12	7,6E-03	8	57,86	Low
A0A096RY69	Glutathione transferase 11	8,2E-03	9	61,44	Low
A0A096SXV5	Probable alpha-mannosidase	2,0E-06	25	81,34	Low
K7U0Q4	Germin-like protein subfamily 1 member 8	3,2E-03	3	44,78	Low
List of Significant Proteins Differentially Abundant to Genotype CML421 (p<0.05)					
A0A096PV29	Protein EXORDIUM	7,9E-03	2	91,58	High
A0A096QCP1	Alpha/beta-Hydrolases superfamily protein	1,0E-02	5	67,3	High
A0A096QF11	TolB protein-related	1,3E-02	17	87,95	High
A0A096QHE8	Glutathione S-transferase L2 chloroplastic	1,7E-02	4	29,94	High
A0A096R6Z8	Heat shock 70 kDa protein 6 chloroplastic	4,0E-02	1	61,39	High
A0A096RB11	17.4 kDa class III heat shock protein	1,0E-03	1	37,33	High
A0A096RUZ6	Bowman-Birk type trypsin inhibitor	1,2E-02	9	38,25	High

(Continued)

Table 4.2 Continued

A0A096S3X0	Succinate-semialdehyde dehydrogenase mitochondrial	1,8E-03	3	80,68	High
A0A096SQA7	Sarcosine oxidase	0,0E+00	8	73,2	High
A0A096SVP6	Octicosapeptide/Phox/Bem1p family protein	1,7E-02	3	45,02	High
A0A096TUS3	DPP6 N-terminal domain-like protein	2,4E-02	11	68,71	High
A0A096U7Y9	Adenosylmethionine aminotransferase 1	1,9E-03	6	102,82	High
A0A0A1P1P0	Cystatin protein	1,5E-02	2	32,5	High
A3KLI1	RAB17 protein	5,0E-04	9	66,41	High
B4F817	Dehydroascorbate reductase	1,6E-02	6	57,49	High
B4FI76	Adenylate kinase 4	1,3E-02	6	83,8	High
B4FPG2	Actin1 isoform 1	2,6E-03	6	74,27	High
B4FRS8	Germin-like protein subfamily T member 1	2,6E-03	4	55,02	High
B4G0K5	Hydroxyproline-rich glycoprotein family protein	0,0E+00	39	109,83	High
B5U8J9	Asparagine synthetase	7,0E-05	6	62,08	High
B6SIR9	1-aminocyclopropane-1-carboxylate oxidase	3,0E-02	3	64,43	High
B6SLU8	Putative uncharacterized protein	1,6E-04	6	69,92	High
B6SZY7	Glutathione S-transferase IV	1,0E-02	7	68,29	High
B6T033	Glutathione S-transferase GSTU6	2,1E-03	6	78,68	High

(Continued)

Table 4.2 Continued

B6T5H6	Auxin-induced protein PCNT115	2,2E-04	5	55,4	High
B6T916	N-acetyltransferase	1,5E-04	2	40,56	High
B6U9S6	APx1-Cytosolic Ascorbate Peroxidase	4,1E-03	10	72,86	High
C0PJR9	Putative alcohol dehydrogenase superfamily protein	1,4E-04	2	55,27	High
C0PLV4	Dihydroflavonol-4-reductase	1,1E-02	1	54,66	High
C0PLX5	17.4 kDa class I heat shock protein 3	1,0E-05	1	68,53	High
K7U935	Catalase	9,2E-04	12	93,3	High
K7VB29	Tryptophan synthase beta type 2	5,0E-05	3	27,57	High
K7VES9	Asparagine synthetase	4,0E-02	13	71,36	High
K7VHA0	5-pentadecatrienyl resorcinol O-methyltransferase	2,7E-02	1	34,54	High
A0A096PJN3	Heteroglycan glucosidase 1	1,5E-03	3	40,4	Low
A0A096T8I0	Cell number regulator 10	1,4E-02	1	52,01	Low
B4FH68	Peroxidase	3,5E-03	14	90,79	Low
B4FQE6	Uncharacterized protein	7,1E-03	1	45,13	Low
B4FVE1	NADPH quinone oxidoreductase 1	5,1E-03	13	96,74	Low
B6SWV1	Glucose-6-phosphate 1-dehydrogenase	8,0E-04	14	73,31	Low
B6T1G5	Histone H2B	3,0E-02	8	89,45	Low

(Continued)

Table 4.2 Continued

B6T8I3	Disease resistance response protein 206	1,1E-04	3	87,74	Low
B6UHQ8	Blue copper protein	3,1E-03	2	51,37	Low
C0P3T3	Peroxidase	8,0E-05	5	106,75	Low
C0PF45	Peroxidase	2,5E-03	7	89,2	Low
C0PGU8	Glycerophosphodiester phosphodiesterase GDPDL3	8,2E-03	8	112,35	Low
C4J4U3	GDSL esterase/lipase	3,6E-03	8	87,71	Low
K7V6Z1	Putative patellin family protein	2,3E-04	2	44,36	Low
K7VEJ7	Nicotianamine synthase 1	2,4E-02	2	36,61	Low
M1H779	Lipoxygenase (Fragment)	7,6E-03	1	44,4	Low
P51059	Phosphoenolpyruvate carboxylase 2	7,3E-03	3	22,92	Low
Q7XAT3	Glufosinate-resistant glutamine synthetase (Fragment)	3,5E-03	1	71,18	Low
List of Significant Proteins Differentially Abundant to Genotype CML448 (p<0.05)					
A0A096QYG0	NAD(P)-binding Rossmann-fold superfamily protein	2,0E-09	21	103,76	High
A0A096Q155	Beta-glucosidase aggregating factor-like protein	3,1E-04	1	67,1	High
A0A096RTH6	Heat shock protein 90-2	4,6E-02	21	106,84	High
C0HF51	Zinc finger (C3HC4-type RING finger) family protein	2,9E-05	18	66,66	High
B4FS90	Cysteine protease 1	1,3E-03	10	98,91	Low

(Continued)

Table 4.2 Continued

K7U159	Peroxidase	7,3E-03	5	32,28	Low
List of Significant Proteins Differentially Abundant to Genotype CML451 (p<0.05)					
B6SMC1	Thioredoxin	3,3E-03	3	49,05	High
B6T267	Ribosomal protein L15	9,1E-03	6	87,54	High
B6T2K5	60S ribosomal protein L35	1,4E-03	1	21,96	High
B6UH77	Histone H3	7,7E-03	11	56,75	High
C4J2M5	Pyruvate kinase	3,8E-03	5	101,31	High
A0A096QFM0	Guaiacol peroxidase 2	2,1E-03	6	71,84	Low
A0A096S9W1	Remorin	8,2E-04	5	30,12	Low
B4F935	Cystathionine gamma-synthase 1 chloroplastic	7,4E-03	5	43,29	Low
B4F9A4	NAD(P)-linked oxidoreductase superfamily protein	1,1E-03	16	63,73	Low
B6UGK8	3-isopropylmalate dehydratase small subunit 2	3,2E-02	4	67,87	Low
K7VC35	S-adenosylmethionine synthase	2,8E-03	18	66,87	Low
Q53WW9	Beta-D-glucosidase	8,2E-03	52	134,22	Low

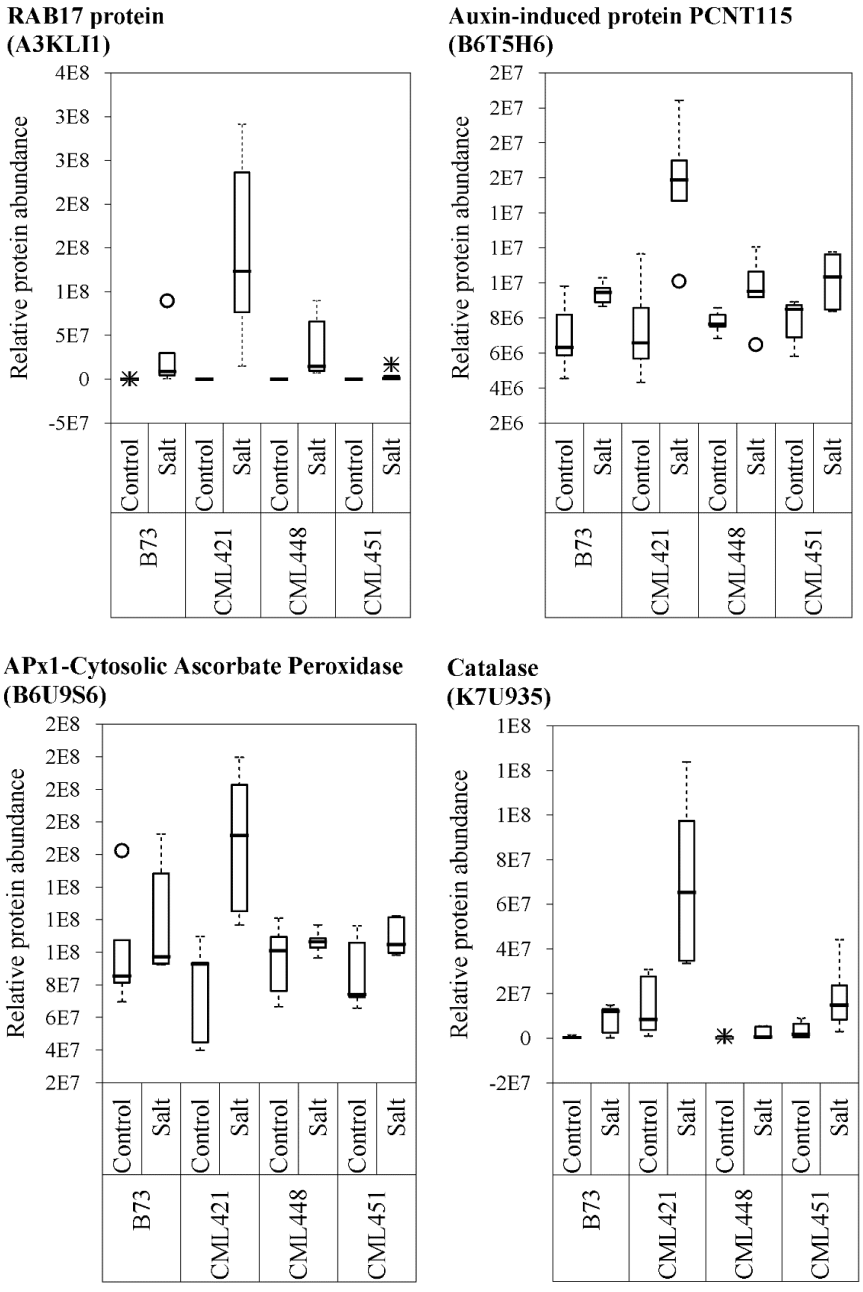

Figure 4.8 Variability plots of proteins selected by their genotype specificity and abundance toward salt stress. Relative abundance was calculated for the four maize genotypes, treated or not (control) with NaCl, at the fourth week after sowing.

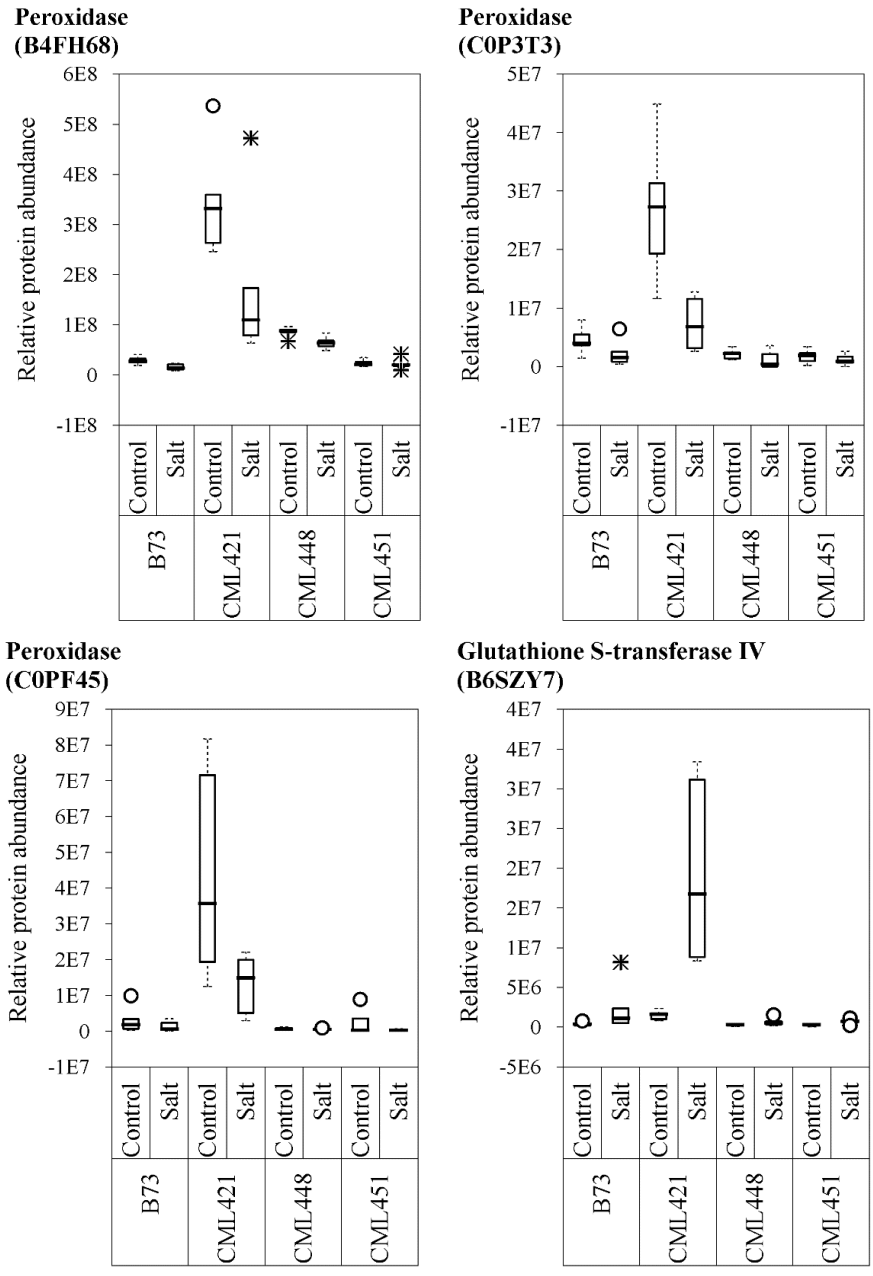

Figure 4.8 (continued) Variability plots of proteins selected by their genotype specificity and abundance toward salt stress. Relative abundance was calculated for the four maize genotypes, treated or not (control) with NaCl, at the fourth week after sowing.

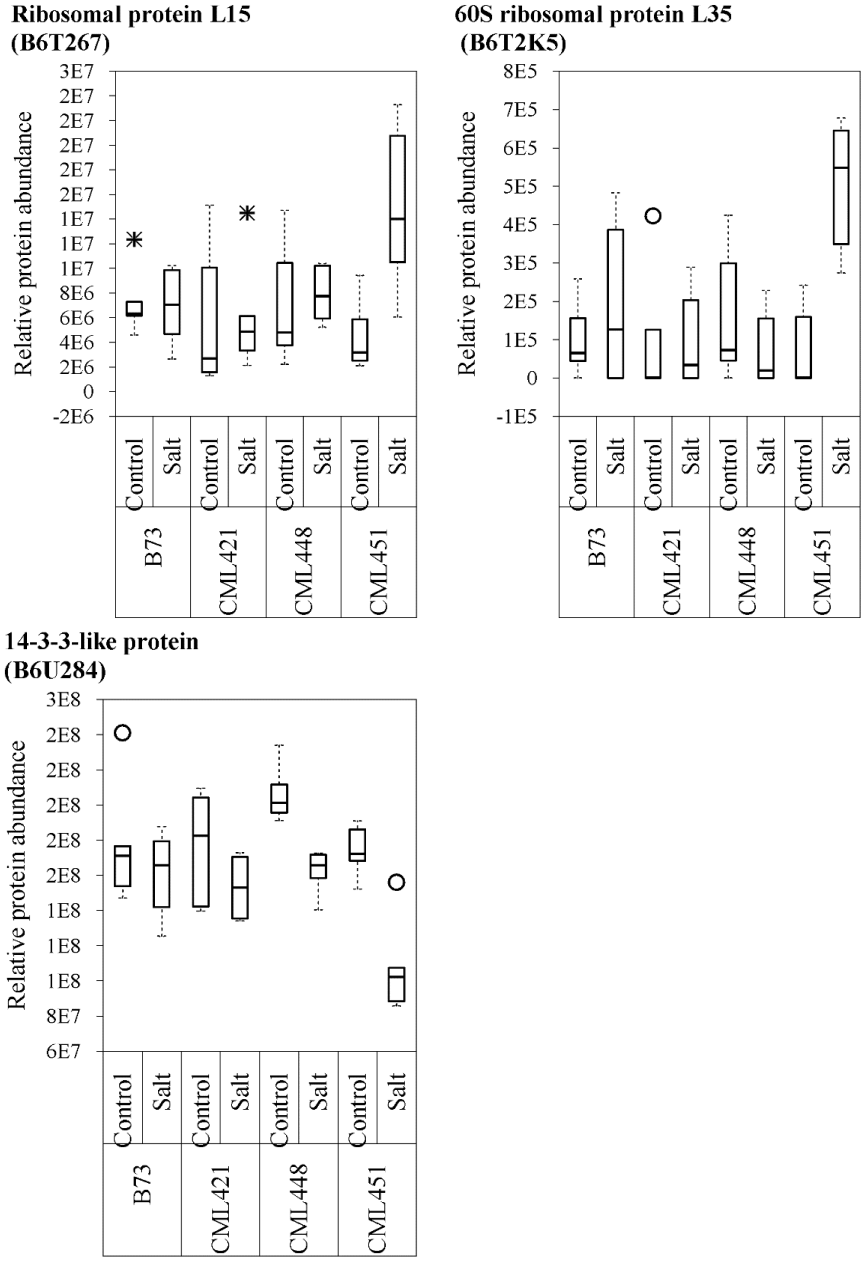

Figure 4.8 (continued) Variability plots of proteins selected by their genotype specificity and abundance toward salt stress. Relative abundance was calculated for the four maize genotypes, treated or not (control) with NaCl, at the fourth week after sowing.

4.3 Discussion

4.3.1 Growth impact caused by salt stress

The roots are the plant organs that first encounter salt in a saline environment. From there, signals that communicate the onset of salt stress spread systemically toward cells and organs that may be able to respond and anticipate. However, when the roots are hidden under the soil, the outcomes caused by salt stress are revealed to us in the aerial portion of the plant. In this work, the monitoring of the physiological changes through the monitoring of the physiological changes through images made it possible to describe a dynamic phenotyping, which led to the ranking of four maize genotypes regarding differing salt stress tolerance (Figure 4.3).

It is broadly known that salinity slows down leaf growth rates, either by transient osmotic imbalance on the cells, reduction of the cell elongation and division (Fricke and Peters, 2002) and/or cell wall stiffening (Geilfus et al., 2017). The slower growth of shoots was confirmed in our results (Figure 4.4). Although the stressed plants accumulated high amounts of ions in their leaves, they were still able to grow (Figure 4.4).

The growth limitation of plants in osmotic and ionic stress can be caused by an energy shortage due to a photosynthesis reduction or energy relocation into defense mechanisms (Munns and Gilliham, 2015). The growth maintenance, even if decelerated, requires sources of energy and thus, an increase in respiration can be induced in such circumstances (Zorrilla-fontanes et al., 2016). In our work, the salt treatment affected all genotypes and their root growth was significantly slower in comparison to control plants (Figure 4.5). Concomitantly, the same stressed plants presented a higher activation of processes involved in homeostasis regulation, response to oxidative stress,

response to water stress and cellular respiration. The pathways involved in cell division and biosynthetic processes were slowed down. Therefore, we reinforce the hypothesis of an increased energy demand related to stress and the subsequent enhanced respiration rates.

4.3.2 LEA proteins as markers of salt stress

We identified five different proteins belonging to the Late embryogenesis abundant proteins (LEA proteins) (B4F9K0, A3KLI0, A3KLI1, B7U627, and C4J477) (Supplementary Table S4.1), in response to salinity. Those play a role in acclimatization to stresses related to dehydration (Hong-bo et al., 2005). LEA proteins were found to be produced during dehydration and they are predicted to protect structures and molecules. In this way, they can contribute to coping with drought and salt stress in different plant species (Brini et al., 2007; Chen et al., 2002; Saavedra et al., 2006). Considering their function, they were suggested as excellent molecular markers for water stress (Hanin et al., 2011). Whether they are effective markers for salt tolerance is another issue.

4.3.3 Antioxidant responses

Gene ontology enrichment ‘response to oxidative stress’ and ‘cell redox homeostasis’ for proteins highly abundant in salt stress gathered several proteins: class III peroxidases (B6T3V1, B4FNI0, B6THU9, C0HHA6, B4FY83), APx1- cytosolic ascorbate peroxidases (B6U9S6, B6UB73), glutathione peroxidase (Q6JAH6), APx4-peroxisomal ascorbate peroxidase (B4FA06), protein disulfide isomerase (Q5EUE1, Q5EUD6, A5A5E7), Grx_C2.2-glutaredoxin subgroup I (B4FXZ3), thioredoxin h1 protein (Q4W1F7), and peroxiredoxin-5 (B6THT0). Sairam et al. (2002), working with wheat, demonstrated that their salt tolerant genotype had a lower decrease in biomass and grain yield, allied with a higher antioxidant activity when grown

in saline conditions. Thus, the activity of such detoxifying proteins is one of the mechanisms encountered in salt stressed plants contributing to their acclimation in that environment.

4.3.4 Class III plants peroxidase

Class III peroxidases are enzymes secreted into the apoplast, where they oxidize phenolics, lignin precursors or other secondary metabolites. They also oxidize the hormone auxin, as well as other substrates (Gaspar et al., 1982) and produce hydrogen peroxide (Blee et al., 2001) and hydroxyl radicals (Chen and Schopfer, 1999), two ROS involved in oxidative burst and in cell elongation. Class III peroxidases are multigenic complex family (Hiraga, 2001), with roles in several plant developmental processes, including regulation of cell elongation, cell wall formation and defense against pathogens (Mika et al., 2004; Passardi et al., 2004a). Cell wall stiffening is controlled by the cross-linkage of the peroxidase with compounds of the wall, such as extensin, lignin subunits and phenol molecules of the suberin constitution (Passardi et al., 2004b). Class III peroxidases can be induced by environmental stresses, participating direct- or indirectly of the plants responses (Cosio and Dunand, 2017).

Maize has 158 class III peroxidases (Koua et al., 2009). The complexity of diverse physiological roles and the number of genes suggests that each enzyme isoform went through a functional specialization (Cosio and Dunand, 2017). In this work, we present 34 class III peroxidases expressed in the roots, with peroxidases positively (B4FNI0, B4FY83, B6T3V1 B6THU9, C0HHA6, D7LNB3, and B6U6W0) and negatively (A5H452, A5H8G4, B4FCI9, B6T7B1, K7U159, B1A9R4, B4FRD6, B65IU4, B4FSW5, and Q9ZTS9) correlated to salt stress (Figure 4.7). The function of those class III peroxidases

negatively correlated to salt stress isoforms is predicted to be involved in cellular growth and elongation. The peroxidase isoforms positively correlated to stress, may be acting in the acclimation to salinity, e.g., helping in stiffening the root cell wall.

The 34 class III peroxidases identified belong to a group of 136 paralog genes connections, forming eight groups (Figure 4.7). Despite it is expected that closely related paralog groups have similar expression patterns and functionality (Du et al., 2012), we detected divergent abundance patterns within three clusters (Figure 4.7). By analyzing the promoters of divergent groups, we found that the MBS and TC-rich repeats motifs are in different positions and strands for the proteins of group 4 (Table 4.1). This difference in the promoter region might be a factor leading to a differential expression of these genes. In group 5 (Table 4.1), the ABRE and DRECRTCOREAT motifs were predicted. They are located in different positions and strands of the promoter regions. Remarkably, the motif DRE2COREZMRAB17 is present only in the promoter region of a gene expressing positively a peroxidase (B4FY83) to salt stress. This C-repeat/DRE motif is involved in dehydration and salinity stress processes, and it is participative of ABA induction in maize (Kizis, 2002). The presence of this motif in the promoter region of the salt-induced peroxidase B4FY83 might explain its higher relative abundance.

4.3.5 Genotype-specific reactions

We can say that despite that all genotypes started in similar conditions, they did not have the same salt-acclimatization level nor the same stress level, evidenced by the differential ion concentration in leaves (Figure 4.6), and the different leaf area and root FW produced under stress conditions (Figures 4.2, 4.5). Under stress, genotype CML448 showed a similar growth in comparison to control

condition plants, while it accumulated significantly more Na^+ and Cl^- ions (Figure 4.6). This indicates that CML448 tolerates higher amounts in its leaves and might have mechanisms for the partitioning of those ions away from the cytosol or away from the primary site of the photosynthesis and growing tissues.

Proteins APx1 cytosolic ascorbate peroxidase (B6U9S6), catalase (K7U935), RAB17 protein (A3KLI1), and glutathione S-transferase IV (B6SZY7) were found as a response to salinity in all genotypes, but for CML421 they were present in a higher abundance (Figure 4.8). Besides that, three HSPs (A0A096R6Z8, A0A096RB11, and C0PLX5) were also found in higher abundance in salt-stressed plants of this genotype (Table 4.2). HSPs have the important role of protein folding, assembly and translocation in plants under optimal and stress conditions. Their specific major function during abiotic stress includes aggregation prevention and stabilization of non-native proteins, as well as the following of signaling processes leading to the synthesis of stress-response proteins (Wang et al., 2004). Vanhove et al. (2015) identified a specific osmotic responsive HSP70 isoform, evidencing that the behavior of paralogs are not always similar toward a stress condition. Thus, for genotype CML421, the strongest response to ROS and dehydration, is displayed by the slowest growth under stress, and might indicate a higher stress level (Figure 4.3).

The 14-3-3-like protein (B6U284) was remarkably lower abundant in salt-stressed plants of genotype CML451 (Figure 4.8). This protein is known for its role in controlling K^+ channels (Van Den Wijngaard et al., 2005). It is also a key activator of H^+-ATPase activity (Fuglsang et al., 1999). We make a link between the lowest abundance of a 14-3-3-like protein (B6U284) in the roots of genotype CML451 and its remarkable low Na^+ concentration and no

alteration of potassium content in leaves of salt stressed plants (Figure 4.6). However, despite the fact that this genotype was able to avoid accumulating toxic ion contents in its leaves, this behavior has not translated into superior growth under stress (Figure 4.4).

Two ribosomal proteins were more abundant in response to salinity in plants of genotype CML451 (B6T267 and B6T2K5) (Figure 4.8). Abundance changes of proteins involved in protein synthesis have been reported in response to salt stress, including ribosomal proteins (Omidbakhshfard et al., 2012; Pang et al., 2010; Zörb et al., 2004). The role for ribosomal protein synthesis during periods of abiotic stress would be to maintain and regenerate plant protein synthesis mechanisms (Zörb et al., 2004). Under stress conditions, proteins assume important functions that confer enhanced tolerance to the plants, such as antioxidant activity, LEA proteins in osmotic adjustment, ion transporters, among several others (Kosová et al., 2013). Thus, the increased capacity to produce new proteins is directly related to the capacity to overcome salinity effects. Furthermore, Li et al. (2015) demonstrated that the regulation of vacuolar trafficking is likely to involve ribosomal proteins. As genotype CML451 presented the lowest leaf ion accumulation in salt treated plants (Figure 4.6), we speculate that they were compartmentalized in roots vacuoles, a strategic salt tolerance mechanism (Munns and Gilliham, 2015).

Three class III peroxidases (B4FH68, C0P3T3, and C0PF45) were significantly more abundant in genotype CML421 (Figure 4.8). They belong to three different subfamilies of the maize class III peroxidases (Figure 4.7). Cosio et al. (2008) demonstrated a negative regulation of a courgette class III peroxidase toward auxin, which led to growth suspension of the hypocotyl. Thus, the higher abundance of these three peroxidases in genotype CML421 may explain the slow general growth of this genotype (Figures 4.4).

4.4 Conclusions

This work has shown that phenotyping the above ground traits offers a relevant strategy to determine a good timing to conduct proteomics analyses of the roots. The study also demonstrates that phenotyping is also very useful for characterizing geno- and phenotype-specific stress-responses. Salinity is a complex form of stress, and tolerance is a multigenic trait, with several origins and levels. Tolerance is also a complex concept that is difficult to define.

Despite this challenging context for such stress-response studies, the work has revealed significant genotype-specific stress responses in maize, and also some elements of the underlying stress-response mechanisms. In this study, genotype CML448 tolerated the highest ion content in its leaves whilst still able to grow, suggesting some level of stress tolerance. However, CML448 also displayed reduced vigor under control conditions. Genotype CML451 avoided accumulation of ions in its shoots and displayed relatively strong vigor. Lower concentrations of a potentially channel-regulating protein and a higher abundance of proteins acting in protein synthesis and possible ion compartmentation were recorded in CML451. This might explain the low-ion accumulation phenotype. Genotype CML421 is the worst performing, since it displayed low vigor. The CML421 genotype stress-specific proteins are related to the anti-oxidative system and responses associated with dehydration. These proteins indicate that this genotype was more stressed despite all genotypes being exposed to the same saline conditions. A rigid classification of the genotypes as salt- tolerant is not possible and needs to be considered for each agro-ecological target area. Therefore, we ranked all genotypes according to their growth under both control and stressed conditions so that the general vigor can be determined. Further analyses are needed to elucidate hidden links of salt tolerance and acclimatization mechanisms.

Chapter 5 GROWTH ANALYSIS AND TISSUE PHENOTYPING OF ADDITIONAL MAIZE GENOTYPES DIFFERING IN SALT STRESS RESPONSES

5.1 *Introduction*

Crop domestication, initiated 10,000 years ago (Doebley et al., 2006), was an important milestone in human societies. Changes in the domesticated plants were conducted towards the selection of morphological and production traits specific to each environmental. Now the climate change is a serious threatening factor for crop production, since it is shifting climate conditions of production areas (IPCC, 2007).

In terms of energy intake, four crops are providers of 60% of human food needs: rice, wheat, potato and maize (http://www.fao.org/biodiversity/components/plants/en/). Despite our diet is relatively restricted, within each species there can be a great genetic diversity. This diversity represents an enormous potential to overcome a possible future feeding limitation generated by climate change and world population increase.

In this context, crop gene banks are important means for genetic diversity conservation. However, for many of them the genetic characterization seems to be a first priority and is currently far from being completed (McCouch et al., 2012b). The phenotypic evaluation for relevant agronomic traits is even a bigger challenge. Characterizing genetic resources produces the knowledge and identifies key features, including alleles of interest, playing an essential role in adaptation to environmental changes.

One of the greatest environmental threats is the soil salinization, which already affected 20% of the irrigated arable lands worldwide (FAO, 2016). Maize, despite being a major world consumed crop and a relative salt-sensitive species

(Zörb et al., 2004), counts with no commercialization release of salt-tolerant cultivars (Fita et al., 2015). Possessing an extremely rich genetic variability, with more than 135,000 accessions of maize crop diversity conserved worldwide (IPCC, 2007), maize provides us with great opportunities to uncover genetic information related to tolerance traits. The genetic and phenotypic characterization is of great value to cope with our current and future challenges.

In the chapter 4 of this thesis, we introduced and endorsed the link between physiological responses and molecular effects of 4 different maize genotypes With that, we not only were able to pick a time-point in which the plants proteome was being affected by the applied salt, but also to produce a genotype ranking of salt tolerance and characterize them towards this stress. However, all of the four genotypes were found to be rather sensitive to salt stress, by their relatively poor growth response when comparing to Across8023 and Across8024 used in chapter 3. Thus, our objectives with Chapter 5 experiments were to identify more salt-tolerant genotypes and characterize them towards salinity through whole plant phenotyping and different tissues proteomics. By including more salt tolerant genotypes and performing molecular analysis of an additional tissue, the leaves, we aimed to add information into the genotypes tolerance-ranking and to complete our knowledge about proteins and molecular networks involved in salt stress adaptation mechanisms.

5.2 *Results and discussion*

5.2.1 Physiological phenotyping

The calculated EC_e for controlled ($EC_{control}$) condition was 1 dS m^{-1} and for the treatment (EC_{NaCl}), 10 dS m^{-1}. Monitoring of the top area until the seventh week after sowing showed that salt-treated plants of genotypes B73, CML488 and CML491 had slower growth than non-treated plants (Figure 5.1). Genotypes

Across8024 and CML465 were the fastest growers among the control group, as well as within NaCl-treated group (Figure 5.1). From the sixth to the seventh week, Across8024 showed a break in the growth trend (Figure 5.1). At the seventh week, treated plants were 38% in average smaller than non-treated ones for this genotype, but there was no significant difference (Table 5.1). Genotype CML491 had the most affected top area by NaCl, with treated plants 88% smaller than control ones, followed by B73 (70%) and CML488 (66%) (Table 5.1). Salt-treated plants of genotype CML465 was only 18% in average smaller than non-treated ones at the seventh week (Table 5.1) and its growth trend did not show a slowdown during the experimental period (Figure 5.1).

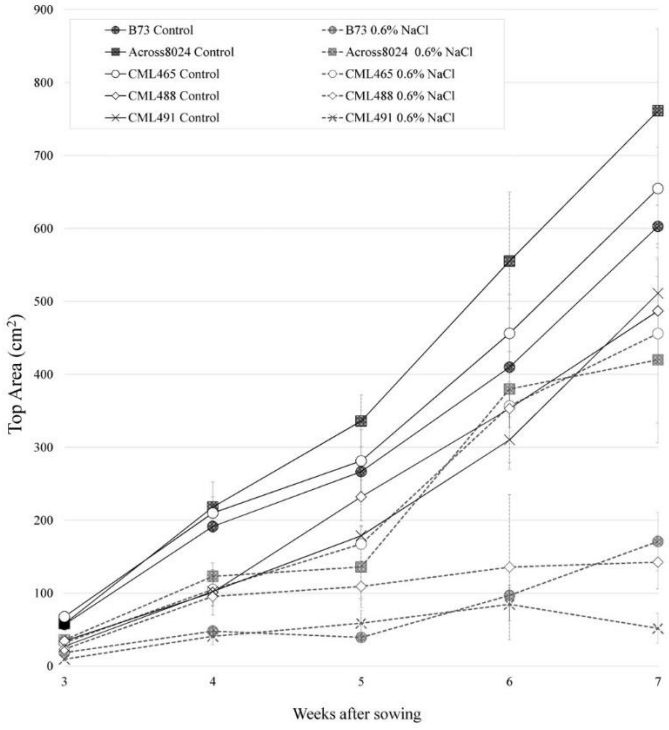

Figure 5.1 Trend lines of top area of five maize genotypes in control or saline condition. N = 6.

Table 5.1 Top area (cm^2) of three maize genotypes at the seventh experimental week, in control or saline condition.

GENOTYPES	TOP AREA (cm^2)	
	Control	NaCl
B73	620 b	188 a
Across8024	783 a	483 a
CML465	653 a	538 a
CML488	508 b	175 a
CML491	488 b	60 a

Means followed by the same letter did not differ according to the LSD test ($p \leq 0.05$), which compares treatments within each genotype.

Total FW and shoot FW of treated plants of genotypes B73, CML488 and CML491 were significant smaller than control, at the seventh week after sowing (Figure 5.2; Table 5.2). As for top area, Across8024 and CML465 did not suffer a significant reduction in total FW or shoot FW in salt stress condition (Figure 5.2; Table 5.2). However, for all genotypes, the roots FW was significantly reduced in saline condition, with genotype CML491 presenting the biggest reduction of 88% relative to control (Table 5.2). Genotype Across8024 had roots of treated plants reduced by 54%, followed by B73 and CML488 with 50% smaller roots and CML465, which had a reduction of 40% (Table 5.2).

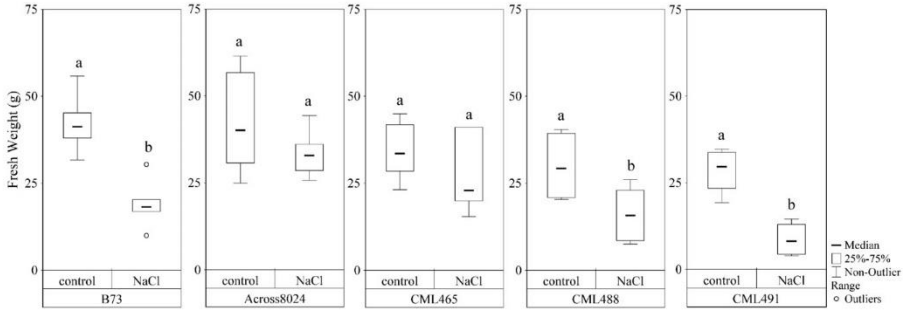

Figure 5.2 Total fresh weight (g) of five maize genotypes in different soil conditions. Means followed by the same letter did not differ according to the LSD test ($p \leq 0.05$), which compares treatments within each genotype. N = 6.

Table 5.2 Roots and shoot fresh weight (g) of five maize genotypes seven weeks after sowing, in different soil conditions.

GENOTYPES	FRESH WEIGHT (g)			
	Roots		Shoot	
	Control	NaCl	Control	NaCl
B73	6 b	3 a	36 B	16 A
Across8024	11 b	5 a	31 A	28 A
CML465	5 b	3 a	29 A	25 A
CML488	6 b	3 a	24 B	13 A
CML491	8 b	1 a	20 B	7 A

Means followed by the same letter did not differ according to the LSD test ($p \leq 0.05$), which compares treatments within each genotype.

The ranking quadrant highlights genotypes CML465 and Across8024 as the best relative growers, located in the first quadrant (Figure 5.3). They showed bigger median shoot area in saline and control conditions than the other genotypes. On the other hand, genotypes CML488 and CML491 are represented in the third quadrant as the slowest growers in both conditions, with CML491 presenting the worse relative growth in salt treatment (Figure 5.3).

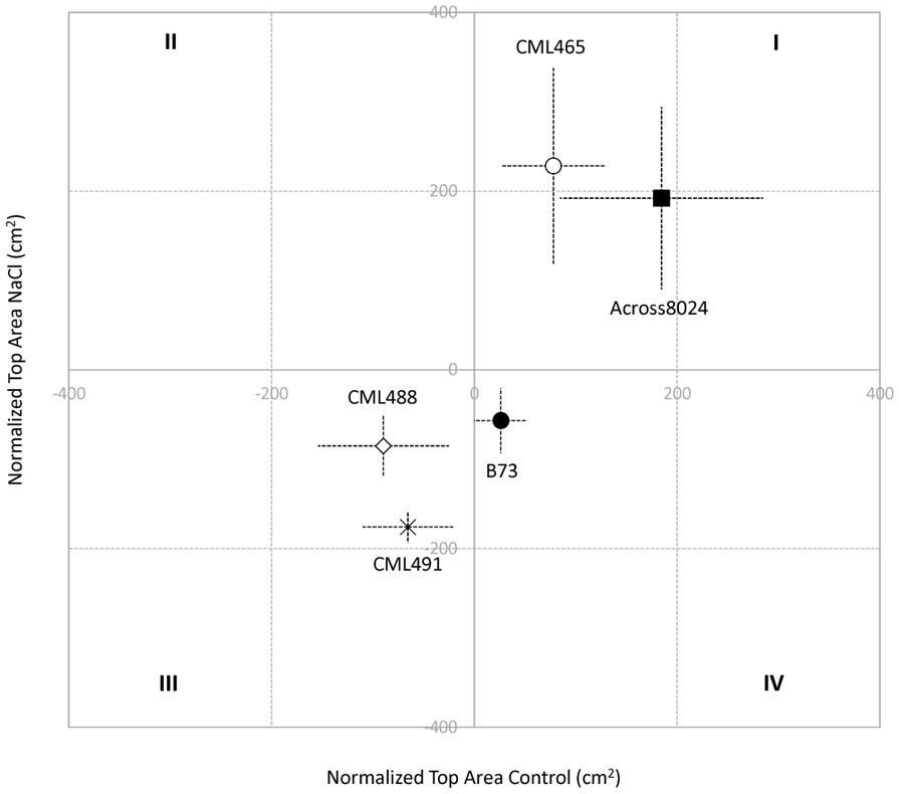

Figure 5.3 Quadrant rank of maize genotypes on the seventh week after sowing, according to the total median top area (cm^2) for each soil condition. Vertical and horizontal lines discriminate the growth potential of the plants in soil with or without salt, respectively. Dotted lines represent standard error. N = 6.

Regarding leaves ion accumulation, at the seventh experimental week, potassium (K^+) content was not significantly different when comparing treated and non-treated leaves for each and all genotypes (Figure 5.4). For sodium (Na^+) content, all genotypes presented significant higher amounts of this ion in leaves of salt-treated plants relative to control plants (Figure 5.4). For chloride (Cl^-), all genotypes had a significant increase of this ion in leaves of treated plants, except CML465, which did not present a statistical difference with the control plants (Figure 5.4).

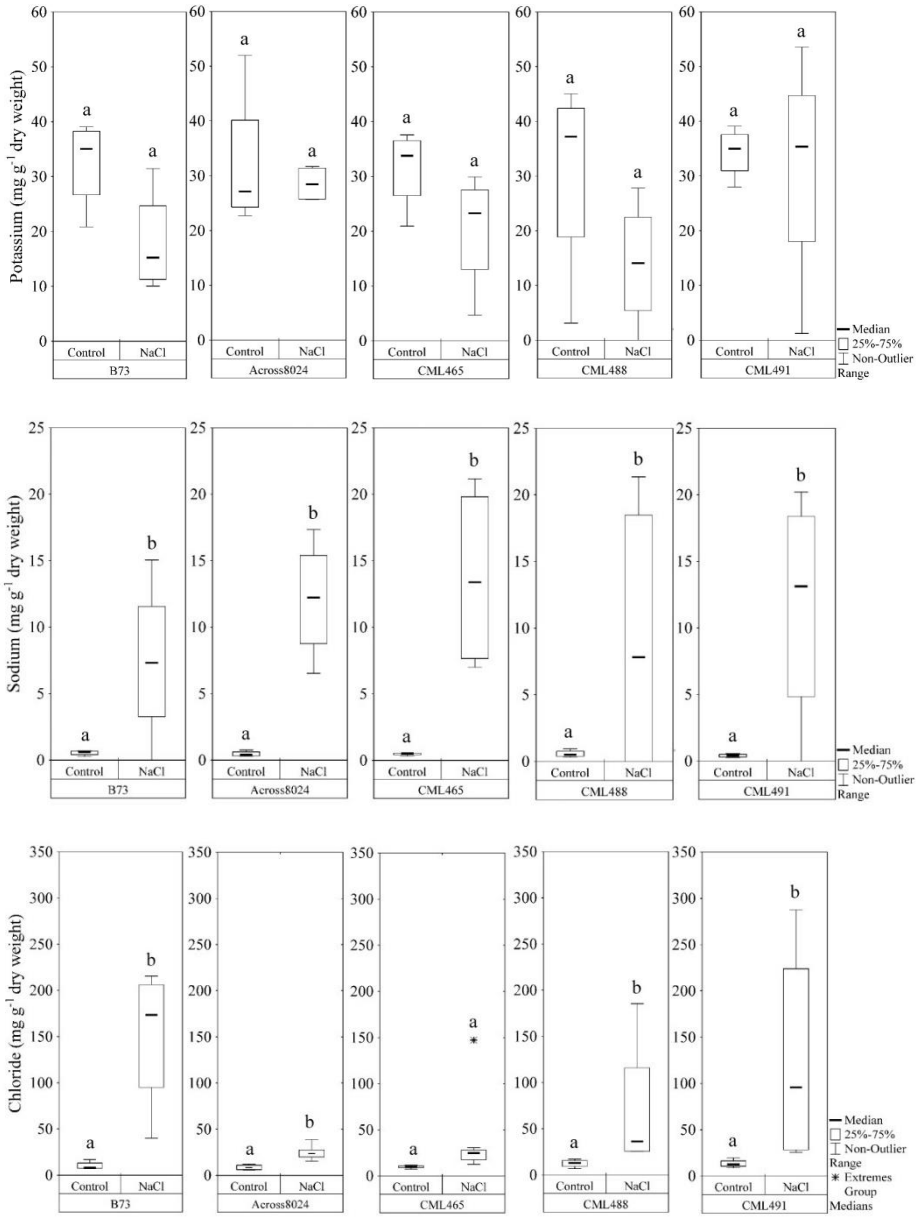

Figure 5.4 Potassium, sodium and chloride content (mg g^{-1} dry weight) in leaves of five maize genotypes, at the seventh week after sowing. Plants were grown in control or saline conditions (NaCl). Means followed by the same letter did not differ according to the LSD test ($p \leq 0.05$), which was calculated separately for each ion. N = 4.

Monitoring through time of the leaf area was suitable to identify differential growth trends of the genotypes according to the imposed salt stress (Figure 5.1). The genotype-reference B73 showed a similar growth behavior as in Chapter 3 experiments (Figure 3.3) and was highly affected by the salt stress. We observed the same trend for genotype Across8024, although the absolute area values were higher in Chapter 3 experiments, possibly due to the slightly lower calculated EC_{NaCl} (Figure 3.3). However, Across8024 once more maintained relatively good growth rate in saline condition and the sudden break from the sixth to the seventh week may be a specific ionic effect of the salt stress.

One of the salt tolerance indicators is the growth maintenance of a plant, despite having a relatively high ion content in leaves. This suggests vacuole compartmentalization, a strategy that prevents the built up of ions to a toxic level in the cytoplasm, as well as in the apoplast, which can lead to cell dehydration (Flowers and Yeo, 1986; Munns et al., 2016). In our work, salt treated plants of genotype CML465 maintained a growth trend (Figure 5.1) and a final shoot area (Table 5.1) approximate to the non-treated ones, whereas it accumulated significantly high Na^+ in their leaves (Figure 5.4). This has been previously reported for maize in a screening trial for salt tolerance (Alberico and Cramer, 1993). From the seven cultivars treated with 80 mM NaCl for 15 days, the five most tolerant in terms of biomass accumulation, had also the highest Na^+ shoot and root concentrations (Alberico and Cramer, 1993). In another study, James et al. (2006) showed that the salt-tolerant barley species (cv. Franklin) can tolerate high concentration of Na^+ and Cl^- in their leaves by vacuolar and cellular partitioning of these ions.

Regarding chloride concentration, genotype CML465 and genotype Across8024, accumulated much lower contents than in B73, CML488 and CML491 (Figure 5.4). During salt stress, one mechanism against ion

accumulation in plant shoot is the ion exclusion, in which its transport from the roots can be limited by, for example, the downregulation of transporters and channels (Li et al., 2017a; White and Broadley, 2001). At the same time, tonoplast chloride channels (CLC) can be upregulated for the vacuole sequestration of this ion in roots (Li et al., 2017a). The upregulation of a maize CLC (*ZmCLC-d*) was registered as response to salt stress and transgenic *ZmCLC-d*-over-expressing arabidopsis plants showed higher salinity resistance when growing in 100 mM NaCl (Wang et al., 2015b). In our study, the maize genotypes which better coped with salt stress, Across8024 and CML465, according to its top area (Figure 5.1) and FW (Figure 5.2) results, also presented the smallest accumulation of chloride in their leaves (Figure 5.4). Thus, we suggest a mechanism of transport control of chloride from the roots to shoot in these genotypes and vacuole compartmentalization in their roots as leaf ion exclusion strategy.

Genotype CML488 was previously classified as drought tolerant (Beyene et al., 2011, 2017). For that, we expected it to have a good growth maintenance during salt stress, possibly standing out at the first weeks from salt-sensitive genotypes. However, that was not the case in our experiment and salt treated plants of CML488 had an earlier growth break than genotypes CML465 and Across8024 (Figure 5.1). From the fourth week, CML488 showed reduced growth as an effect of salt stress, which may indicate a relatively early ion specific stress.

5.2.2 Tissue phenotyping toward salt stress

Physiological phenotyping lead to the sampling time for the proteomics studies. Samples were collected at the seventh week after sowing and leaves and roots were separately analyzed.

5.2.2.1 Leaves proteomics

A total of 1007 proteins were identified in the leaves (Supplementary Table S5.1), at an FDR of 0% calculated with Scaffold, and minimum of one identified peptide. 204 proteins responded significantly to the saline treatment, of which 88 had a high abundance and 116 were low abundant in salt stressed plants relative to the control ones ($p < 0.05$) (Supplementary Table S5.2).

We performed a Singular Enrichment Analysis (SEA) for each set of differentially abundant proteins. For proteins which were low abundant for salt stress, the SEA resulted in 31 significant GO terms ($p < 0.05$), in which 18 are from the biological processes (BPs) category. The main activated BPs for this group set were (1) 'regulation of biological quality' cluster, which includes 'cell redox homeostasis', (2) 'photosynthesis' within the cluster 'cellular metabolic process' and from within (3) 'localization' cluster, stands out 'transmembrane transport' and 'cation transport' (Figure 5.5).

The group set of enriched proteins related to photosynthesis was significantly higher for control plants, i.e., reduced in NaCl condition plants, in general (Figure 5.5). The decrease in photosynthesis-related proteins in salt stressed plants connects with the general reduction in growth of the genotypes (Figure 5.1). Photosynthesis is one of the first plant processes affected by salinity (Munns et al., 2006). The effects can be driven by different metabolic, physiological and biochemical alterations, such as stomatal closure and limitations on CO_2 diffusion (Flexas et al., 2004; Wilkinson and Davies, 1997), and oxidative stress as a secondary effect (Hossain and Dietz, 2016).

Related to the photosynthesis decrease in salt stressed plants, we can point out the enrichment of 'regulation of biological quality' cluster (Figure 5.5). The general reduction of proteins related to the cellular homeostasis complies with

the limitation of photosynthetic ability and corroborates with the perceived impact on growth, particularly in the genotypes B73, CML488 and CML491, but that also afflicted in a different scale or time CML468 and Across8024 (Figure 5.1). This is regarded with the production of ROS, which is inherent to aerobic metabolic processes. Because of the ROS capacity to produce oxidative damage and its constant generation, proteins related to the regulation of redox homeostasis are important players in the maintenance of ion homeostasis (Apel and Hirt, 2004; Hossain and Dietz, 2016). With the photosynthesis reduction in salt stressed plants in our work, it is deduced that the overall and relative abundance of proteins related to the redox homeostasis was also lowered for the general stress response. For stress specific response however, higher antioxidant activity was often related to an increased tolerance toward salt stress (Chaicherdsakul et al., 2017; de Azevedo Neto et al., 2006; Surender Reddy et al., 2015; Zhao et al., 2017).

The 'localization' cluster, notably 'transmembrane transport' and 'cation transport' enriched proteins, are also related to the photosynthetic metabolism and, as mentioned, were low abundant in salt stress. The groups comprehend mainly chloroplast ATP synthases (B6TQG0, C0P3K2 and C0P6Z6) (Supplementary Table S5.2) as well as a protein involved in ion homeostasis (P29036) (Supplementary Table S5.2). The production of ATP from ADP occurs via a proton gradient through the transmembrane enzyme ATP synthase (Taiz and Zeiger, 2010) and ATP synthase subunits (γ, δ, b) are involved in the photosystem electron-transfer reaction (Liu et al., 2014b). Thus, it is comprehensible that the related proteins are found in lower abundance in plants which exhibited lower photosynthetic activity (Figure 5.5). Mahler and colleagues (2007) discussed the correlation between singlet oxygen formation and ATP synthase. In their work, singlet oxygen was found to damage thylakoid

ATP synthase, leading to a positive effect on non- photochemical quenching (NPQ). As NPQ is a defense method in which the excessive energy can be dissipated by the form of heat, the ATP synthase damage caused by stress would be a protection mechanism to the photosynthetic apparatus (Mahler et al., 2007). However, whether the photosynthesis reduction is a consequence or a cause for ATP synthase lower abundance in saline condition in our work remains elusive.

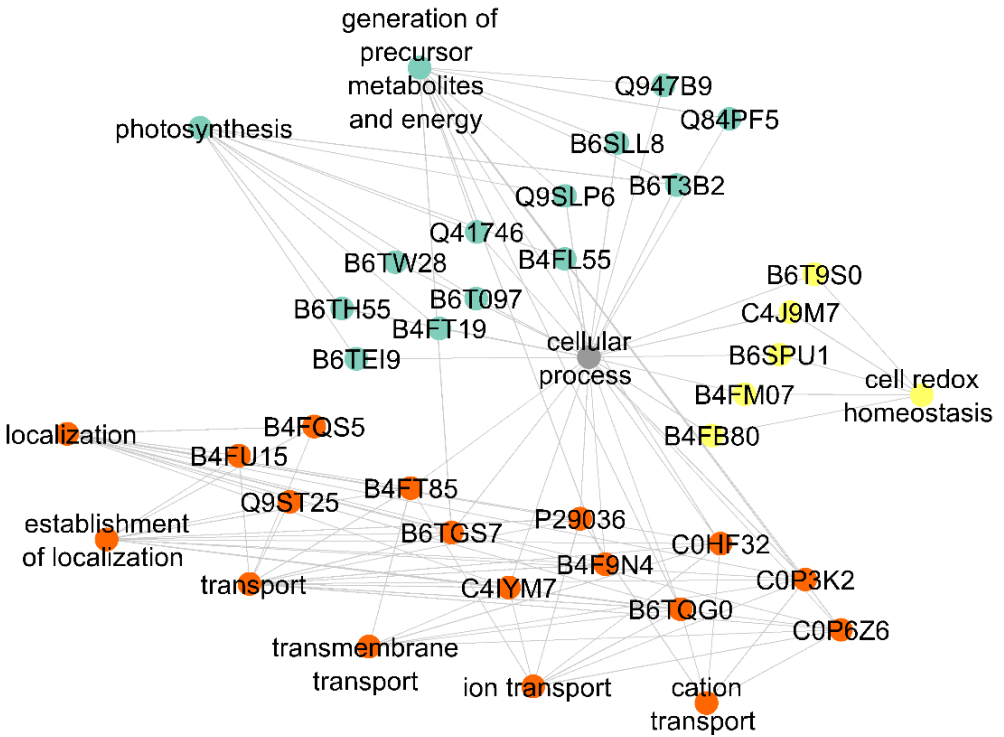

Figure 5.5 Cytoscape interaction network of low abundant proteins in response to salt stress and GO biological process (BP), enriched by singular enrichment analysis (SEA) ($p<0.05$) in leaves of maize genotypes.

For the 88 proteins highly abundant in response to salt stress, the SEA determined 35 significant shared GO terms ($p < 0.05$), from which 25 belonged to Biological Process (BP) category (Figure 5.6). The most relevant activated BPs were (1) 'cellular component biogenesis' cluster, including the 'nucleosome activity' BP, (2) 'generation of precursor metabolites and energy' and (3) 'translation' (Figure 5.6).

Regarding the 'generation of precursor metabolites and energy' cluster (Q947B9, Q84PF5, B6SLL8, B6T3B2, Q9SLP6, Q41746, B4FL55, B6TW28, B5T097, B6TH55, B4FT19, B6TEI9) (Supplementary Table S5.2), it formed a less complex interaction network and showed less enriched proteins than in control-abundant proteins (Figure 5.6). This indicates the general photosynthesis reduction in salt stressed plants. Salt stress also activated several proteins associated with gene expression and regulation, found in the 'translation' and 'cellular component biogenesis' clusters (Figure 5.6). Protein synthesis have been reported as a salt stress-responsive process, in which the capacity to produce new proteins is closely related to salinity tolerance (Kosová et al., 2013; Omidbakhshfard et al., 2012; Pang et al., 2010; Zörb et al., 2004). Thus, the higher abundance of proteins involved with the DNA structure, such as the histones H3 (B6SJQ5, B6UHK8, B6TTP0, B6SIV8) (Supplementary Table S5.2) and histones H2A (B6U5W4, C0HIB6, B6T7E7, B6SHX9, B6SI29) (Supplementary Table S5.2), and with the actual translation process, as ribosomal proteins (B6SIL9 and B4FNM4) (Supplementary Table S5.2) and elongation factors (Q9M7E4, B6T433, B6UHJ4) (Supplementary Table S5.2) in salt stressed plants, evince greater dynamism in protein synthesis as a stress response.

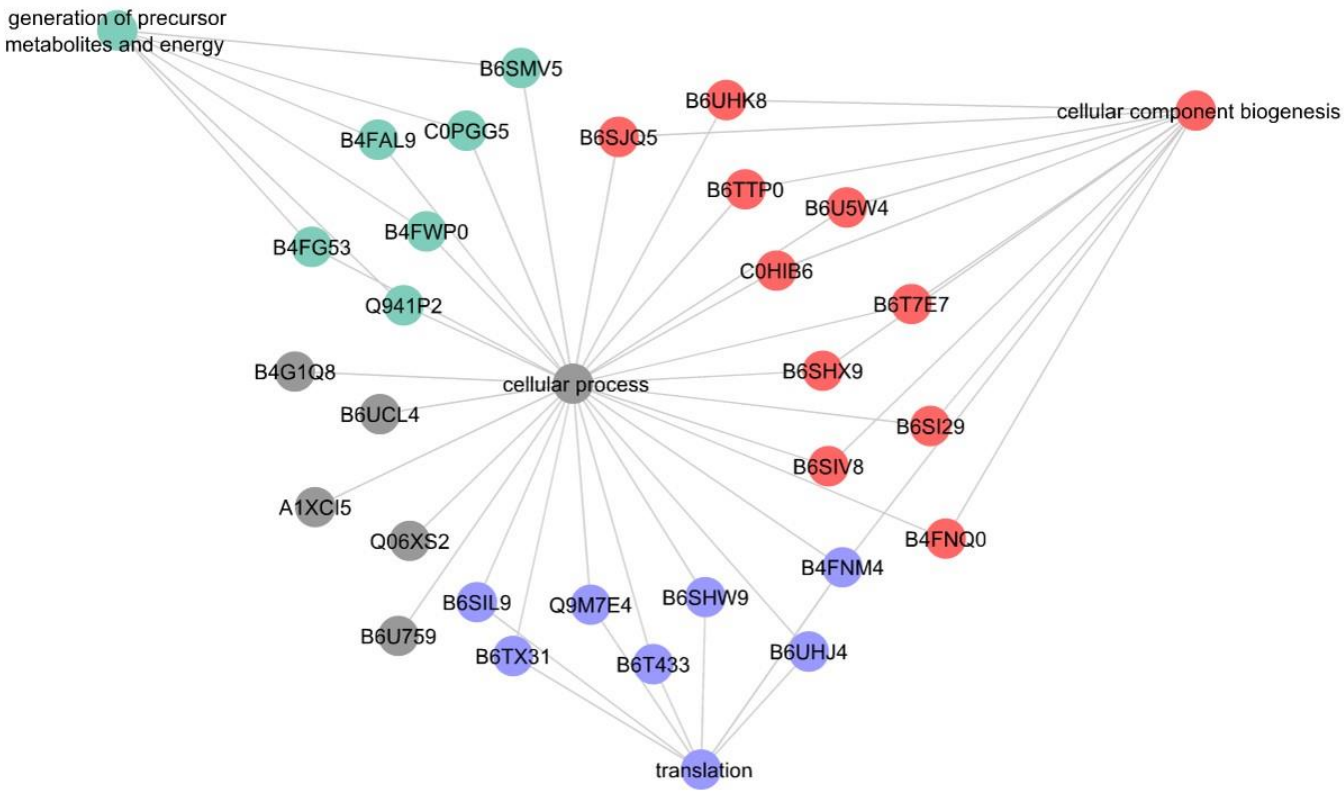

Figure 5.6 Cytoscape interaction network of highly abundant proteins in response to salt stress and GO biological process (BP), enriched by singular enrichment analysis (SEA) ($p<0.05$) in leaves of maize genotypes.

5.2.2.2 Genotype-specific differential protein abundance in leaves

Table 5.3 below lists the proteins which were significantly different and genotype specific. In total, we found five proteins that were significantly higher or lower abundant as a consequence of the salt stress and that specifically correlated to one genotype.

Genotype Across8024 and CML465 showed a different abundance trend for the chloroplastic Peroxiredoxin Q (Prx Q) (B4FS55) (Supplementary Table S5.2, Table 5.3). For these genotypes, the concentration of the enzyme was maintained relatively stable during salt stress, while for B73, CML488 and CML491, Prx Q demonstrated a significant reduction in response to the stress (Supplementary Table S5.2, Table 5.3). The plant peroxiredoxin family members act by detoxifying peroxidases substrates (Lim et al., 1993) and the subfamily Prx Q is specifically targeted to the plastids (Dietz, 2003). In a system which involves thioredoxin (Trx), Prx Q will reduce hydrogen peroxide (H_2O_2) and is regenerated by the Trx (Dietz, 2003). This Trx/Prx pathway is one of the main control points of protein thiol groups reduction, that are highly threatened by the H_2O_2 induced by salinity (Suo et al., 2017). Thus, the maintained abundance of Prx Q in Across8024 and CML465 as a response to salt stress may be one contributing factor to the relative salt tolerance of this genotype, which can have contributed to chloroplast redox homeostasis. In accordance with this, the work of Jing and colleagues (2006) with 4-weeks old *Arabidopsis* showed improved salt tolerance of mutants overexpressing a Prx Q gene, when exposed to 150 mM NaCl for two weeks.

Three proteins (A0A059Q8L8, A0A1D6K0D4 and A0A1D6QC17) (Supplementary Table S5.2) were highly abundant in salt stress for genotype CML465 (Table 5.3). The NAD(P)H-quinone oxidoreductase subunit 5

(A0A059Q8L8) (Supplementary Table S5.2) acts in the ATP synthesis coupled electron transport process, by shuttling electrons to quinone in the photosynthetic and, likely, in the chloroplast respiratory chains (Bateman et al., 2017). With the abundance increase of this protein, ATP production in cell will consequently be enhanced, probably improving the salt tolerance (Wang et al., 2015a). As noted in the physiological phenotyping, genotype CML465 showed the best relative growth in saline condition (Figure 5.3), which corroborates with the increase of a protein related with the energy metabolism.

Among the proteins with significant high abundance in salt stress, we observed the ATP-dependent Clp protease proteolytic subunit (A0A1D6K0D4) (Supplementary Table S5.2) in genotype CML465 (Table 5.3). Proteolytic enzymes have a range of functions and specific proteases will constantly degrade polypeptides both in normal and stressed conditions (Sjogren et al., 2006). The maintenance of proteostasis, checking of damaged proteins and all other proteolytic roles, occurs through the whole plant life and are especially important during stress periods, for the higher probability of protein damage (Nelson and Millar, 2015; Sjogren et al., 2006; Vierstra, 1996). One of these enzymes is the ATP-dependent Clp protease, also a partaker on protein turnover and involved in processes such as the regulation of enzymes and regulatory proteins (Vierstra, 1996). In saline conditions, the ATP-dependent Clp protease proteolytic subunit (*clpP*) was found to be upregulated in leaves of *Rhazya stricta*, a salt tolerant species, after 12 h in 500 mM NaCl (Hajrah et al., 2017). We now suggest a role of this enzyme in the relative salt tolerance of genotype CML465, which accumulated this protease in leaves of salt-treated plants.

The abundance of a plasma membrane (PM) H^+-ATPase (A0A1D6QC17) (Supplementary Table S5.2) was also significantly increased in response to salinity in genotype CML465 (Table 5.3). The PM H^+-ATPases, by exporting

protons from the cell, generates the transmembrane electrochemical gradient, which is the energy source for almost all transport proteins in the PM. Thus, this proton pump is considered a "powerhouse for plant growth" (Falhof et al., 2016). One specific process that utilizes electrochemical H^+ gradients from PM H^+-ATPases, is the extrusion of Na^+ to the apoplast (Ie et al., 2003), an important procedure during salinization to enhance plant tolerance. Furthermore, it is proposed a direct involvement of H^+-ATPases in growth and development regulation, through auxin activation. In the acid growth theory, the activation of H^+-ATPases by auxin leads to the acidification of the apoplast, activating cell wall loosening enzymes (Rayle and Cleland, 1992). Previous studies reported the increase of salt tolerance in plants which highly expressed PM H^+-ATPases, demonstrating growth maintenance under NaCl stress (Bose et al., 2015; Gevaudant et al., 2007; Wang et al., 2013). In maize, Geilfus et al. (2011) showed that the salt-tolerant hybrid SR03 had an upregulated total transcript expression of four PM H^+-ATPases when exposed to 100 mM NaCl.

Other two PM H^+-ATPases (A0A1D6DVJ8 and C0PDH2) (Supplementary Table S5.2) were found in leaves of these maize genotypes. However, they were not salt-stress responsive when compared to the non-treated plants, as A0A1D6QC17 (Supplementary Table S5.2, Table 5.3). Due to the broad range of physiological roles that PM H^+-ATPases can be involved in, and the fact that it is encoded by a multigene family in many species, plant PM H^+-ATPases are suggested to be regulated at several levels (Ie et al., 2003). Arango and colleagues (2003), discussing the different regulation forms this enzyme might go through according to the cell type it is present, argue that multiple promoters would be more efficient in its regulation under different conditions. With that, the response to different environmental factors would be fitted to the specific need of each plant. Thus, to investigate possible explanations to the divergence

on salt-responsiveness of the PM H^+-ATPases, we analyzed the promoters of the three enzymes, comparing position and strains of the most relevant ones (Table 5.4).

Promoters ABRE (cis-acting element involved in the abscisic acid responsiveness), ARE (cis-acting regulatory element essential for the anaerobic induction) and MBS (MYB binding site involved in drought-inducibility) were predicted for all three proteins (A0A1D6QC17, A0A1D6DVJ8 and C0PDH2) (Supplementary Table S5.2), though they are located in different positions and strands of the promoter regions. (Table 5.4). Promoters HSE (cis-acting element involved in heat stress responsiveness) and TC-rich repeats (cis-acting element involved in defense and stress responsiveness) are present on genes encoding for the proteins A0A1D6DVJ8 and A0A1D6QC17 (Supplementary Table S5.2) and also in different position and strains (Table 5.4). These results may explain the different responses of three PM H^+-ATPases to the same environmental stress, leading to a relative higher tolerance of the maize genotype CML465 to salinity. Therefore, we assume that an increased abundance of the PM H^+-ATPase in the salt stressed leaves of CML465 had a role in the relative tolerance of this genotype and might contribute to the excellent growth under salt stress.

.

Table 5.3 List of leaf proteins differentially abundant to each maize genotype, in response to salt stress. (c = control; s = salt treatment; N = 6)

List of Significant Proteins Differentially Abundant to Genotype CML465 (p<0.05)												
Protein	**Annotation**	**Identified peptides**	**Best ion score**	**Abundance in stress**	**B73**		**Across 8024**		**CML 465**		**CML 488**		**CML 491**	
					c	**s**	**c**	**s**	**c**	**s**	**c**	**s**	**c**	**s**
A0A059Q8L8	NAD(P)H-quinone oxidoreductase subunit 5, chloroplastic	4	37,4	High	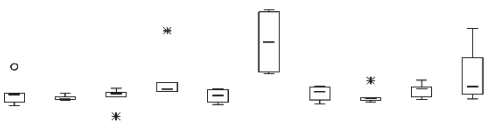									
B4FS55	Peroxiredoxin Q chloroplastic	12	115,2	High										
A0A1D6K0D4	ATP-dependent Clp protease proteolytic subunit	2	77,2	High	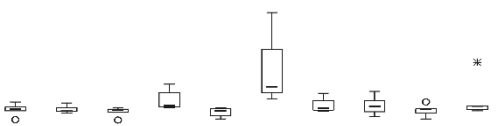									

Table 5.3 continued

List of Significant Proteins Differentially Abundant to Genotype CML465 (p<0.05)									
Protein	**Annotation**	**Identified peptides**	**Best ion score**	**Abundance in stress**	**B73**	**Across 8024**	**CML 465**	**CML 488**	**CML 491**
					c	**s**	**c**	**s**	**c**
A0A1D6QC17	Plasma membrane ATPase	4	32,2	High	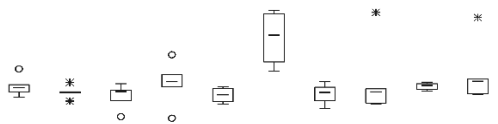				

List of Significant Proteins Differentially Abundant to Genotype Across 8024 (p<0.05)									
Protein	**Annotation**	**Identified peptides**	**Best ion score**	**Abundance in stress**	**B73**	**Across 8024**	**CML 465**	**CML 488**	**CML 491**
					c	**s**	**c**	**s**	**c**
B4FS55	Peroxiredoxin Q chloroplastic	12	115,2	High					

Table 5.4 Promoter region analysis of genes expressing PM H^+-ATPases, according to the response towards salinity treatment (0.6% NaCl).

PM H^+-ATPases		
Promoter: **ABRE**		
Function: cis-acting element involved in the abscisic acid responsiveness		
Protein	**Salt stress induction**	**Promoter position and strand**
A0A1D6QC1	Positive in CML465	750 (+)
		1353 (+)
		1215 (-)
		1431 (+)
C0PDH2	Neutral	1339 (+)
		1350 (-)
		1348 (-)
A0A1D6DVJ8	Neutral	490 (+)
		1379 (+)
		1195 (-)
		697 (+)
		1367 (-)
Promoter: **ARE**		
Function: cis-acting regulatory element essential for the anaerobic induction		
Protein	**Salt stress induction**	**Promoter position and strand**
A0A1D6QC17	Positive in CML465	542 (+)
		1266 (-)
C0PDH2	Neutral	836 (+)
		899 (+)
A0A1D6DVJ8	Neutral	335 (-)
		670 (-)

Table 5.4 continued

PM H^+-ATPases		
Promoter: **HSE**		
Function: cis-acting element involved in heat stress responsiveness		
Protein	**Salt stress induction**	**Promoter position and strand**
A0A1D6QC17	Positive in CML465	638 (-)
		1143 (-)
A0A1D6DVJ8	Neutral	629 (+)
Promoter: **MBS**		
Function: MYB binding site involved in drought-inducibility		
Protein	**Salt stress induction**	**Promoter position and strand**
A0A1D6QC17	Positive in CML465	233 (+)
C0PDH2	Neutral	396 (-)
A0A1D6DVJ8	Neutral	61 (+)
		960 (+)
		888 (+)
		1012 (+)
Promoter: **TC-rich repeats**		
Function: cis-acting element involved in defense and stress responsiveness		
A0A1D6QC17	Positive in CML465	1146 (+)
A0A1D6DVJ8	Neutral	176 (+)
		274 (-)

5.2.2.3 Roots proteomics

Roots proteomics resulted in a total of 2210 identified proteins at an FDR of 0% calculated with Scaffold, at least one identified peptide with confidence 0.95 (Supplementary Table S5.2). From this total, 493 proteins were significantly responsive to the saline treatments, being 382 highly abundant in salt stressed plants and 111 highly abundant in control plants, i.e., low abundant in NaCl stress ($p < 0.05$) (Supplementary Table S5.2).

From the SEA performed for the 111 proteins with low abundance in salt stress, we obtained 66 significant GO terms ($p < 0.05$), from which 25 are grouped within the BPs category. In this group set, the main BPs were (1) 'catabolic process', which includes the 'proteolysis' and the 'secondary metabolic process' clusters, (2) 'proteins complex biogenesis' and (3) 'response to oxidative stress' (Figure 5.7).

Salt stress induces metabolic disorders, either by a direct negative effect in sensitive genotypes or by tolerance or adaptive mechanisms in order to overpass the stress. There is also a link between protein turnover and metabolism, so that when there is no time to repair stress damaged proteins, there can be consequences to the metabolic pathway in which that proteins are involved (Nelson and Millar, 2015). Therefore, the low abundance of proteins related to the secondary metabolism and proteolysis in NaCl-stressed plants is an indicative of the salt effects over the maize genotypes in our work (Figure 5.7). Likewise, the decreased abundance of proteins of the cluster 'proteins complex biogenesis', is an evidence of the negative salt effects (Figure 5.7).

Control plants also showed higher abundance of five class III peroxidases (B4G1S4, Q6RFK0, B6T7B1, Q6RFK3 and B6T173) (Supplementary Table S5.2) when comparing to salt stress, within the 'response to oxidative stress'

GO term. Class III peroxidases are apoplast-secreting enzymes with multiples roles in developmental processes (Gaspar et al., 1982). Its multiplicity occurs due to its ability to neutralize ROS or to produce hydrogen peroxide (Blee et al., 2001) and hydroxyl radicals (Chen and Schopfer, 1999), which are involved in oxidative burst and in cell elongation (Passardi et al., 2004b, 2004a). By the cross-linkage of compounds of the cell wall and peroxidases, stiffening of the wall can be also controlled by the presence of this enzyme (Passardi et al., 2004b). Because of this diverse roles, and the fact that class III peroxidases constitute a complex family (Hiraga, 2001), it is suggested that each of the isoforms has undergone functional specialization (Cosio and Dunand, 2017). Thus, in our work it is likely that the peroxidases highly activated in control plants and lower abundant in salt stress are related with cellular growth and elongation.

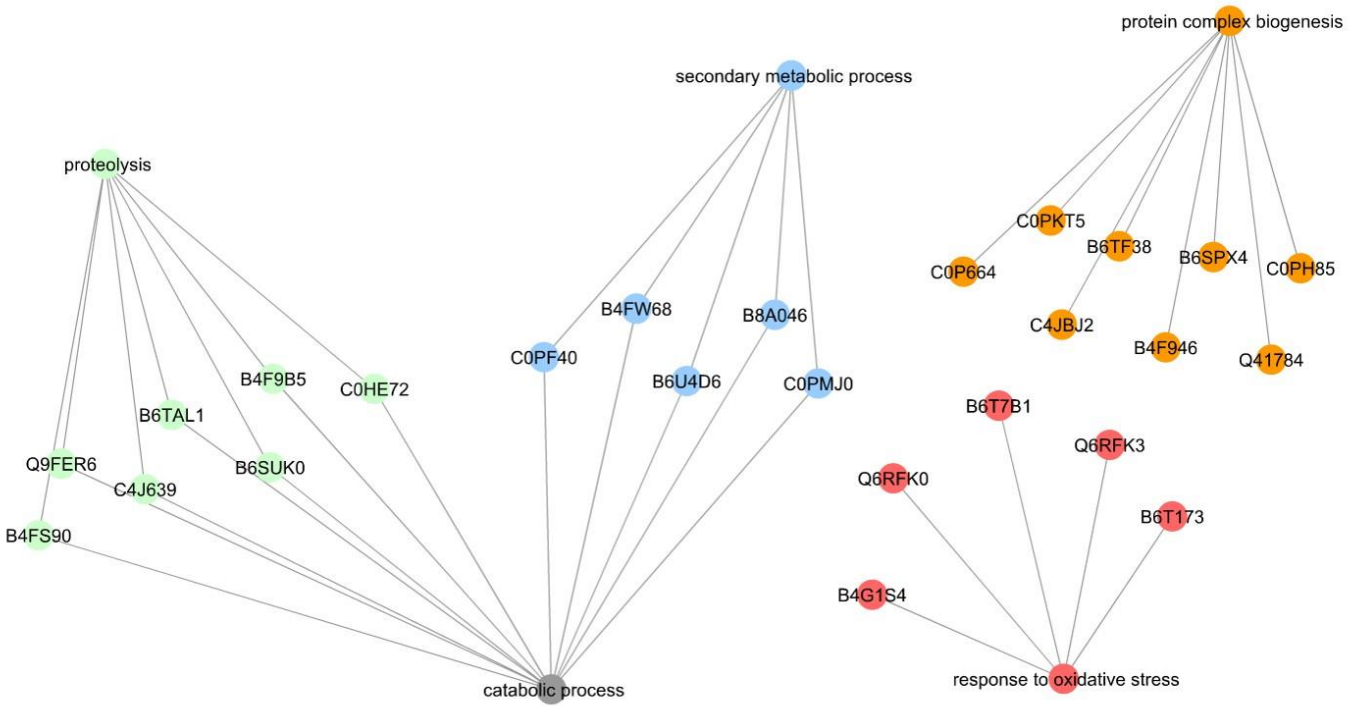

Figure 5.7 Cytoscape interaction network of low abundant proteins in response to salt stress and GO biological process (BP), enriched by singular enrichment analysis (SEA) ($p<0.05$) in roots of maize genotypes.

For the 382 salt-abundant proteins, the SEA resulted in 93 significant GO terms ($p < 0.05$), with 72 forming the BPs category and the most relevant being: (1) 'pentose-phosphate shunt' and 'NADPH regeneration', (2) glycolysis, (3) cellular amino acid biosynthetic process', (4) response to oxidative stress, (5) cell redox homeostasis and (6) translation (Figure 5.8).

Major metabolic pathways were responsive to salt stress in roots. The glycolysis, one of salt stress-activated pathways, accounted with six significantly high abundant proteins, B4FAE6 (pyrophosphate-fructose 6-phosphate 1-phosphotransferase subunit alpha) and C0PHB0 (2-oxoglutarate dehydrogenase E1 component and the isoforms B3GQB5 and Q8L5G8 (hexokinase), B4FWP0 and B4FAL9 (fructose-bisphosphate aldolase). In this pathway, soluble enzymes will carry out a series of reactions, being responsible for carbohydrate breakdown, yielding ATP, reducing power (NADH) and carbon skeletons. Glycolysis is also involved in acclimation under environmental stress, offering the demanded extra energy for suitable responses (Plaxton, 1996; Zorrilla-fontanes et al., 2016). In fact, in the work of Li et al. (2017b) on salt treated (300 mM NaCl) plants of the salt-tolerant species *Carex rigescens*, it was suggested that the strengthening of the glycolysis pathway in roots contributed to the plants tolerance. Likewise, this pathway is essential in sink tissues and plays a key role in a general salt-acclimation.

In parallel with glycolysis, the pentose phosphate pathway breaks down carbohydrates providing reducing power in the form of NADPH and biosynthetic intermediates, such as ribose-5-phosphate (Taiz and Zeiger, 2010b). Seven proteins (isoforms B6TX10, Q9ZTT0 and B4FSV6 - 6-phosphogluconate dehydrogenase, decarboxylating, C0PC61, B4FRC9 and B6TS84 - transaldolase 2, and C0PBH7 - ribose-5-phosphate isomerase) (Supplementary Table S5.2) associated with the pentose phosphate pathway

and its cluster tail, NADPH regeneration, were significantly more abundant in saline conditions (Figure 5.8). This pathway seems to be an important addition into the saline acclimation process, contributing with reducing power that is essential in sink tissues to generate ATP via respiration. This pentose phosphate pathway contribution to salt tolerance was reported in a salt tolerant maize genotype (Jing724), which showed an increase abundance of related proteins in 100 mM NaCl condition (Luo et al., 2018).

NAD(P)H increased production by glycolysis and the pentose phosphate pathway is also closely related with the stress-activated 'response to oxidative stress' cluster (Figure 5.8). Within this cluster, three glutathione peroxidases (Q6JAH6, B4FRF0 and Q7FS88) (Supplementary Table S5.2), an important antioxidant in scavenging ROS, were significantly more abundant in stress. Because the conversion of oxidized to reduced glutathione is NAD(P)H-dependent (Sharma et al., 2012), the production of the reduction power by glycolysis and the pentose phosphate pathway directly affects glutathione metabolism. In addition, three ascorbate peroxidases (B4FA06, B6TM55 and B6UB73) (Supplementary Table S5.2), an integral component of the ascorbate-glutathione cycle and important H_2O_2 scavenger (Sharma et al., 2012), were also more abundant in salt stress, enhancing the defenses against oxidative damage. Finally; one catalase (P12365) and two peroxidases (B6U6W0 and C0PEP6) (Supplementary Table S5.2) reinforced the team of antioxidant enzymes within the 'response to oxidative stress' cluster (Figure 5.8), indicating a general response of the genotypes against the salt stress.

Two SEA clusters are related to protein synthesis, 'cellular amino acid biosynthetic process', with 10 proteins enriched, and 'translation', that gathered 74 proteins (Figure 5.8). Due to the essential roles against abiotic stress, such as osmotic adjustment by LEA proteins and antioxidant activity, the

biosynthesis of these proteins is an indication for stress acclimatation and stress tolerance, including salinity (Kosová et al., 2013). In *Arabidopsis*, a strong enrichment of genes related with translation coincides with a root growth recovery phase after salt shock with 140 mM NaCl, suggesting a participation of novel proteins in the process (Geng et al., 2013). On the other hand, the low abundance of ribosomal proteins in the salt-tolerant maize genotype F63, as a response to salinity (160 mM NaCl), was interpreted as an ability to save energy by reducing the synthesis of redundant proteins (Cui et al., 2015). In our work, there was a high abundance of proteins related with proteins synthesis as a response to salt stress in roots of maize plants. However, all the genotypes had their roots negatively affected by NaCl (Table 5.2). Thus, despite being considered a factor for tolerance improvement and having an alleviation role on stress impacts, the high abundance of ribosomal proteins should not be considered in isolation as tolerance enhancer, as most probably other tolerance factors are working together. In addition, the energy cost of protein synthesis in a stress context should also been taken into account, as this process is largely energy consuming (Munns et al., 2019).

Ribosomes are constituted by two subunits differing in size. For eukaryotic organisms, the two subunits are the large 60S and the small 40S (Maguire and Zimmermann, 2001). Within the two SEA clusters ‘cellular amino acid biosynthetic process’ and ‘translation’ (Figure 5.8), 25 ribosomal small 40S subunits and 22 large 60S subunits were significantly more abundant as salt stress response for all maize genotypes. On the other hand, 13 small subunits and 17 large subunits did not show any effect to the salt treatment (Supplementary Table S5.1). To better understand why some subunits reacted in abundance to the NaCl treatment and others did not, we selected two very

similar large 60S subunits that differed in salt-reaction: the highly abundant B6T872 and the non-salt reactive B6SX67 (Supplementary Table S5.1).

An alignment analysis showed that B6T872 and B6SX67 have approximately 98% identity (uniprot.org) of their protein sequences. Thus, to have a better understanding of abundance differences of these two proteins in relation to salt stress, we analyzed stress-related promoter elements predicted for their genes. For the high-salt abundant subunit protein B6T872, the motifs ABRE (cis-acting element involved in the abscisic acid responsiveness), ABRE3a, ABRE4, ARE (cis-acting regulatory element essential for the anaerobic induction) and MBS (MYB binding site involved in drought-inducibility) were the most relevant found (Figure 5.9). The low-salt abundant B6SX67 presented as relevant motifs ABRE and ARE (Figure 5.10).

Despite the predicted motifs ABRE and ARE were present in both large subunits, their positions and strands are distinct, which could be a factor for differential expression of the two proteins (Figures 5.9 and 5.10). More interesting, MBS motif was found only in the highly abundant large subunit (B6T872). In a work of Tiwari and colleagues (2019), tobacco plants transformed with the *SbNHXI* promoter of a salt resistant species (*Salicornia brachiata*), presented a MBS recognition site, while in the wild plants it could not be identified when treated with 200 mM NaCl. Thus, this stress-responsive cis-regulatory motif may be one factor of salt tolerance improvement for this plant (Tiwari et al., 2019). In our work, the ribosomal large subunit that presented such promoter motif was highly abundant in salt stress, suggesting a correlation between the presence of this site and its protein synthesis.

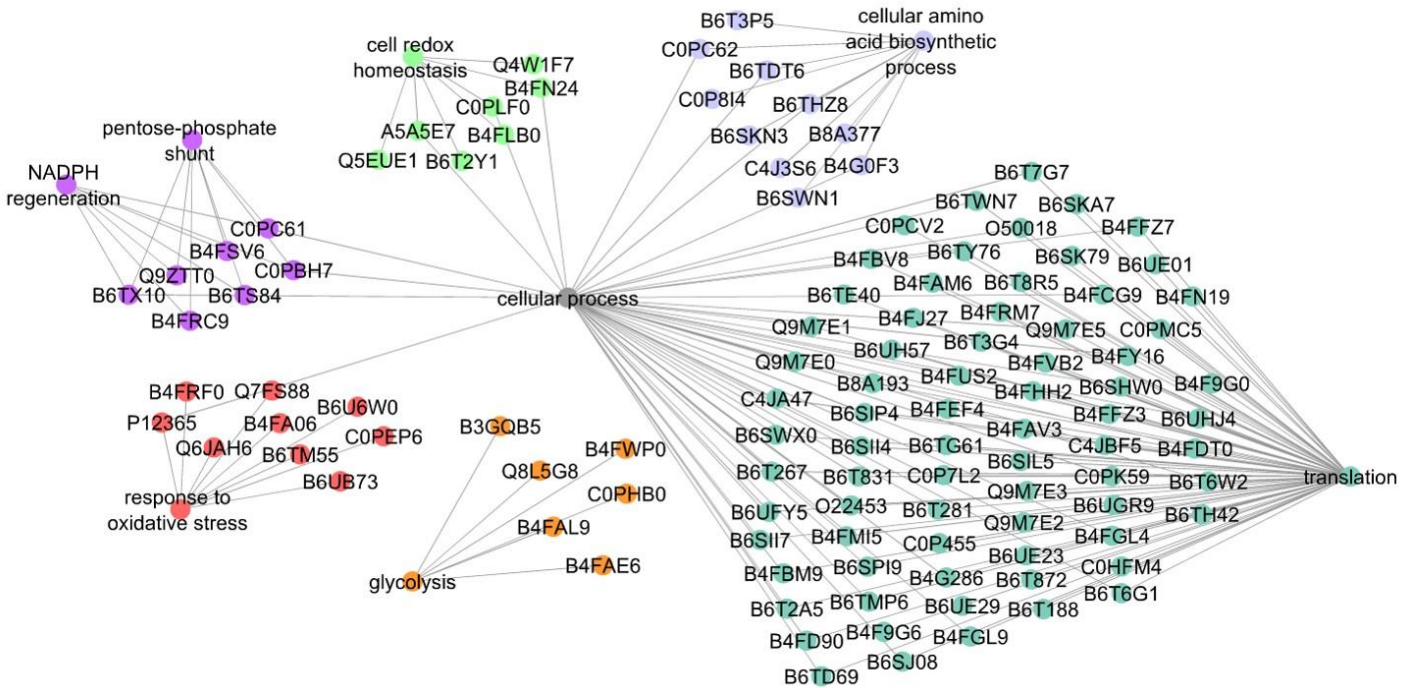

Figure 5.8 Cytoscape interaction network of highly abundant proteins in response to salt stress and GO biological process (BP), enriched by singular enrichment analysis (SEA) ($p<0.05$) in roots of maize genotypes.



Figure 5.9 Schematic representation of predicted promoters of the B6T872 ribosomal large 60S subunit protein, highly abundant in maize roots as salt stress response.



Figure 5.10 Schematic representation of predicted promoters of the B6SX67 ribosomal large 60S subunit protein with low abundance in maize roots as salt stress response.

5.2.2.4 Genotype-specific differential protein abundance in roots

In total, we found 17 genotype specific salt responsive protein abundances (Table 5.5). The genotype with the highest number genotype specific protein abundances is CML465, which also recorded the best leaf growth in salt stress (Figure 5.1, Table 5.5).

Three of the proteins highly activated in salt stress for genotype CML465 are the high mobility group I/Y-2 (HMG-I/Y) protein (Q9FYS5), the translation elongation factor EF1A (A0A096R9Y9) and the T-complex protein 1 subunit eta (B4FBP0) (Supplementary Table S5.2, Table 5.5). The HMG-I/Y protein is involved in the unfolding of the chromatin fiber by relieving the histone H1 (Zhao et al., 1993). It is suggested that they are implicated in the activation of gene transcription, by allowing transcription factors to access the DNA (Zhao and Grafi, 2000). The T-complex protein 1 subunit eta is a molecular chaperone, which assists the folding of proteins after they are translated (Bateman et al., 2017). The increase of these three proteins related with transcription regulation and biosynthesis of proteins corroborates with the prediction that enhancement of protein production is positively related with salt stress and most likely plays a crucial role in acclimation (Kosová et al., 2013), since they were highly abundant in the relative salt-tolerant genotype CML465.

One protein significantly high abundant during salt stress in CML465 is related with energy production, a cytochrome *c* oxidase subunit 5b-2 (COX5b-2) (K7V763) (Supplementary Table S5.2, Table 5.5). COX5b-2 is a subunit of the respiratory complex IV (cytochrome *c* oxidase - COX), where O_2 is reduced to H_2O in a process coupled with H^+ pump and resulting in ATP production (Taiz and Zeiger, 2010b). As a source of extra energy destined to growth or to a salt-acclimatation mechanism, the high abundant presence of COX5b-2 protein

specifically in stressed CML465 plants is an evidence of the maintenance ability of this genotype during salinity. In the work of Garcia et al. (2016), the overexpression of genes (*AtCOX17-1* and *AtCOX17-2*) involved in COX biogenesis in *Arabidopsis* positively affected salt stress tolerance and the rosette growth of these plants was less affected then the wild type plants under 150 mM NaCl treatment. Furthermore, a disturbance in the respiratory chain caused by stress damage of structural elements can lead to the accumulation of ROS. Thus, maintenance and replacement of COX assembly or structural proteins, such as the COX5b-2, is a possible strategy to avoid or limit the ROS generation during stress (Mansilla et al., 2018).

One aldehyde dehydrogenase (ALDH) (C0P7X2) is differentially accumulated in response to salt stress in roots of genotype CML465 (Supplementary Table S5.2, Table 5.5). ALDHs are enzymes which convert aldehydes to their corresponding carboxylic acids, using $NAD(P)^+$ as a cofactor and generating NAD(P)H (Končitíková et al., 2015). As aldehydes are highly reactive molecules and its accumulation can lead to a cell intoxication, ALDHs are important detoxifying agents. This function is especially important during oxidative stress, when oxidative degradation of lipid membranes produces reactive aldehydes, which can disturb the homeostasis (Brocker and Wang, 2014). ADLHs may also have a significant role in stress response by the production of the osmoprotectant glycine betaine (Brocker and Wang, 2014). Veeranagamallaiah and colleagues (2008) demonstrated the up-regulation of ADLH in the salt-tolerant foxtail millet during salt stress (100, 150 and 200 mM NaCl) suggesting it to be a strategy to reduce oxidative damage. Equivalently, in our work this enzyme may have had an important role in combating damaging salt effects in roots of genotype CML465.

Two antioxidant enzymes were found to be highly abundant in salt stressed CML465 plants, an ascorbate peroxidase (B4FA06) and a class III peroxidase (B4FG39) (Supplementary Table S5.2, Table 5.5). As previously mentioned, both enzymes are important ROS scavengers and are inducible by environmental stresses, bearing relevant stakes in the plant responses (Cosio and Dunand, 2017; Sharma et al., 2012). Thus, we predict the positive and protective effects the high accumulation of ascorbate peroxidase and the class III peroxidase are providing to the genotype CML465.

Finally, the α-L-arabinofuranosidase 1 (A0A1D6NQF3) and the brassinosteroid insensitive 1-associated receptor kinase 1 (BAK1) (B6SQE5) are related to root growth (Supplementary Table S5.2, Table 5.5). α-L-arabinofuranosidases are involved in the coordinated dissolution of the cell wall matrix, hydrolyzing terminal residues from arabinose-containing poly- and oligosaccharides (Kozlova et al., 2015). Kozlova et al. (2015) demonstrated that, in roots of maize, specific α-L-arabinofuranosidases genes up-regulation and activity were accompanied by elongation growth of cells. Regarding the BAK1, it was shown that it is a component of the brassinosteroids (BRs) signaling, which are important players in the growth and development processes in plants (Li et al., 2002). By the interaction of the cell-surface receptor brassinosteroid insensitive 1 (BRI1) with BAK1, several genes related with different physiological functions are regulated (Li et al., 2002). Due to the role of brassinosteroids in promoting roots growth (Mussig, 2003) and the involvment of BAK1 in its activation, as well as α-L-arabinofuranosidase 1 implication with elongation growth of roots cells, in our work the high abundance of these proteins as a salt stress response, can be related with the relative tolerance of genotype CML465 towards salt stress.

Thioredoxin, which scavenge H_2O_2 in the thioredoxin/peroxiredoxin system functioning as an electron donor, (Suo et al., 2017), was more abundant in genotypes, B73 (B4FH44) and CML488 (B6SMC1) (Supplementary Table S5.2, Table 5.5). Its high accumulation in two maize genotypes which had their growth significantly decreased in saline condition, highlights the complexity of the plants responses towards this stress. Because salt stress affects several different and interactive biochemical pathways, the production enhancement of a single protective protein is not enough to guarantee a good performance of a genotype in a stressful environment. The combination of adaptive mechanisms will dictate the success of a plant in saline condition, as in the case of genotype CML465, which gathered 12 salt stress-related proteins in their roots.

Table 5.5 List of root proteins differentially abundant to each maize genotype, in response to salt stress. (c = control; s = salt treatment; N = 6)

List of Significant Proteins Differentially Abundant to Genotype B73 (p<0.05)

Protein	Annotation	Identified peptides	Best ion score	Abundance in stress	B73		Across 8024		CML 465		CML 488		CML 491	
					c	s	c	s	c	s	c	s	c	s
B6SKW5	Inosine-5'-monophosphate dehydrogenase	4	45,21	High										
B4FH44	Thioredoxin	1	36,15	High										

List of Significant Proteins Differentially Abundant to Genotype CML465 (p<0.05)

Protein	Annotation	Identified peptides	Best ion score	Abundance in stress	B73		Across 8024		CML 465		CML 488		CML 491	
					c	s	c	s	c	s	c	s	c	s

A0A1D6NQF3	α- L - arabinofuranosidase 1	21	103,83	High	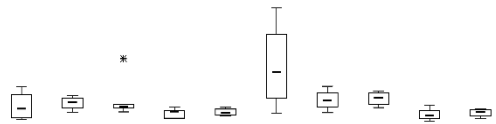
A0A096QP96	Blue copper protein	3	31,57	High	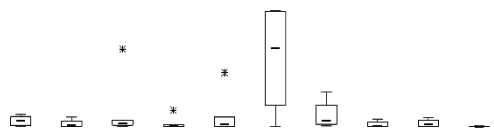
A0A096R9Y9	Translation elongation factor EF1A/initiation factor IF2gamma family protein	9	39,05	High	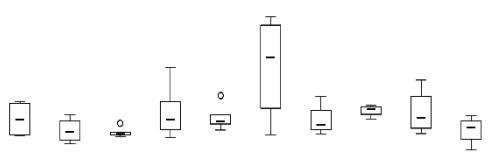
A0A096RRN7	Protein kinase superfamily protein	2	25,16	High	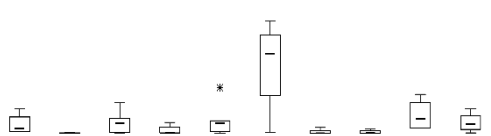

A0A096S029	Malic enzyme 5	5	31,27	High	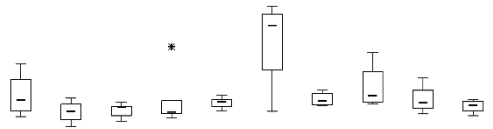
B4FA06	APx4-Peroxisomal Ascorbate Peroxidase	4	32,75	High	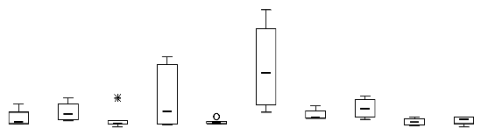
B4FBP0	T-complex protein 1 subunit eta	6	95,02	High	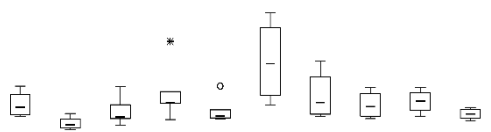
B4FG39	Peroxidase	24	119,81	High	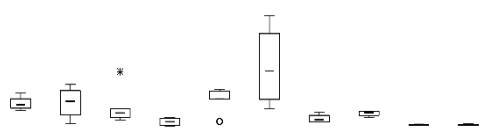

B6SQE5	Brassinosteroid insensitive 1-associated receptor kinase 1	3	77,22	High	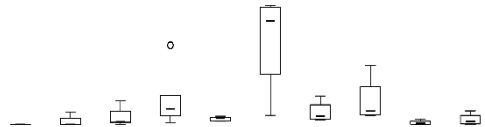
C0P7X2	Aldehyde dehydrogenase	4	36,74	High	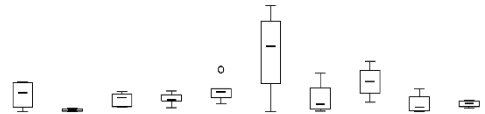
K7V763	Cytochrome c oxidase subunit 5b-2 mitochondrial	8	76,42	High	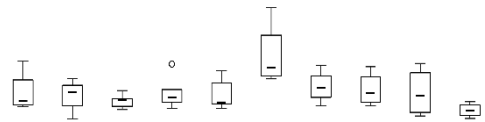
Q9FYS5	High mobility group I/Y-2	11	70,91	High	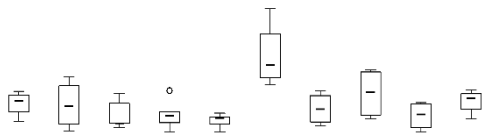

List of Significant Proteins Differentially Abundant to Genotype CML488 (p<0.05)

Protein	Annotation	Identified peptides	Best ion score	Abundance in stress	B73		Across 8024		CML 465		CML 488		CML 491	
					c	s	c	s	c	s	c	s	c	s
B6SMC1	Thioredoxin	2	42,81	High	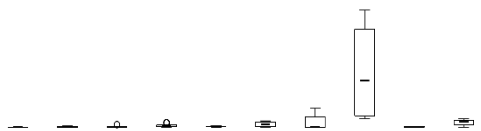									

List of Significant Proteins Differentially Abundant to Genotype CML491 (p<0.05)

Protein	Annotation	Identified peptides	Best ion score	Abundance in stress	B73		Across 8024		CML 465		CML 488		CML 491	
					c	s	c	s	c	s	c	s	c	s
A0A096PLW5	Tripeptidyl-peptidase 2	12	121,74	High	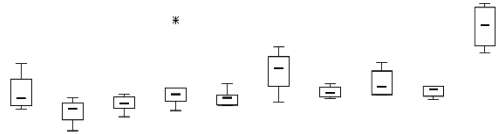									

C4J5Y0	Protein binding protein	28	79,67	High	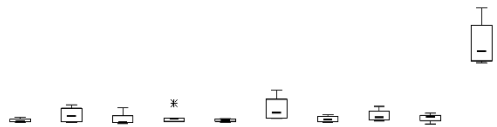

5.2.2.5 Molecular comparison between leaves and roots during salt stress

Besides the obvious differences between leaves and roots reactions to salt stress, such as photosynthesis mechanisms modifications, the parallel among these tissues reveals interesting information as general responses. Straightaway, the detected abundance of stress-responsive proteins was twice as large for roots than leaves, relatively. While for leaves 8.7% of the total proteome was found as highly abundant as a salinity response, for roots this number grows to 17.2% of the total. This result agrees with our expectations regarding the stress over the roots, since they are in direct contact with the salt-containing soil, which could trigger off higher stress deleterious effects and combat responses.

Within the stress-responsive proteins highly abundant in roots and leaves of the studied maize genotypes, a prominent group is formed by the ribosomal proteins. In roots, 25 ribosomal proteins were highly abundant in salt stress, being part of the 'translation' cluster of the Singular Enrichment Analysis (SEA) (Figure 5.8). The 'translation' cluster in leaves gathered less proteins and only two were the ribosomal proteins, also in high abundance in salinity (Figure 5.6). Given the importance of such proteins during salt stress, either by their role in protein synthesis (Zörb et al., 2004), salt-tolerance enhancement (Kosová et al., 2013), or as a possible involvement in regulation of vacuolar traffic (Li et al., 2015), we compared the detected ribosomal proteins for each tissue. Thereby, we found that both ribosomal proteins highly abundant in leaves of stressed plants (B4FMN4 and B6SIL9) (Supplementary Table S5.2) were, in our work, specific to this tissue. The expression data associated with B4FNM4 (60S acidic ribosomal protein P0) gene (Zm00001d035201) shows that its expression is widespread and the transcripts are found in most maize plant organs throughout the whole development period (Walley et al., 2016, maizegdb.org), being intensively expressed in root meristem and elongation

zones (qteller.maizegdb.org). Transcripts were also detected in relatively lower intensity in leaves of salt stressed maize, treated with 15 dS/m of a salt mix (Forestan et al., 2016b). For B6SIL9 (40S ribosomal protein S27a), its associated expression data is narrower, with transcripts of its gene (Zm00001d032616) remarkably detected in endosperm (Stelpflug et al., 2016), preligule (Johnston et al., 2014) mature leaf and root elongation zone (Walley et al., 2013a) (maizegdb.org).

5.3 Conclusions

We classified five maize genotypes according to their growth response during salt stress, grouping them as salt-tolerant (CML465 and Across8024) and salt-sensitive (B73, CML488 and CML491) (Figure 5.3). We suggest a transport regulation of chloride ions from roots to shoot in genotypes CML465 and Across8024, due to the very low accumulation in leaves of salt-stressed plants (Figure 5.4). Concomitantly, we suggest that CML465 presents a salt-tolerance mechanism which allows this genotype to maintain a relatively good growth (Figure 5.1) while having high sodium concentration in their leaves (Figure 5.4), most likely by ion compartmentalization.

Leaf proteomics showed a general and significant decrease in photosynthesis, regulation of biological quality and light harvesting ATP synthase activity for the salt-treated plants (Figure 5.5). On the other hand, salt-stress significantly resulted in greater abundance of proteins associated with gene expression and regulation, which may represent an adaptation defensive mechanism of the maize genotypes, as protein synthesis is reported as a salt stress-responsive process (Kosová et al., 2013; Omidbakhshfard et al., 2012; Pang et al., 2010; Zörb et al., 2004).

In roots, proteomics revealed that salt stress increased the abundance of proteins of more than three times as much as in the leaves. The salt-responsive proteins were mainly related to energy synthesis, antioxidant response and protein synthesis, the last one gathering 74 proteins with the 'translation' cluster (Figure 5.8). This, together with the growth disturbance caused by the salt stress in roots (Table 5.2), evidences that the roots were more strongly affected than the shoot.

Regarding the genotype-specific protein abundances, the genotype which demonstrated better growth in salt stress was also the one to accumulate more differential proteins, both in roots and shoot: the genotype CML465. In the leaves, the specific proteins were involved in the maintenance of proteostasis and energy production, which could have been reflected in the better adaptation of CML465 to the stress. Likewise, a set of proteins detected in roots of salt-stressed plants may have contributed to the relative tolerance of this genotype, which were involved in biosynthesis of proteins, extra energy production, antioxidant defense and growth and development processes. Thus, we reinforce that an improvement in salt-tolerance for non-halophytes consists of multiple factors that will lead to metabolic and pathways rearrangements, rather than of a single key event. To unravel and understand which factors are related to the salt-tolerance and how they are contributing to it, is an essential step for crop improvement.

Chapter 6 GENERAL CONCLUSIONS, DISCUSSION AND FUTURE RESEARCH

6.1 General conclusions and discussion

Maize is a very important crop, yet it is found in a relatively contradictory situation: despite the large number of accessions conserved worldwide, as far as we know there is no released commercial variety claiming salinity-tolerance, an abiotic stress that already affected 19.5% of irrigated lands (FAO, 2016). Some factors justify such contradiction, starting from the fact that salt stress triggers a complex multigenic response in plants, which is divided in two phases, the osmotic and the ionic stress (Munns, 1993), as well as the low interest of research investment towards tropical maize, especially by the private sector (Edmeades et al., 2017).

Besides the complexity and the gap within levels of knowledge, it is relevant to mention that phenotypic evaluation of crops facing abiotic stress have been left behind in comparison to genetic characterization of accessions in crop gene banks. Also, during the present research we encountered the challenge of working with non-sequenced maize cultivars, in order to identify genotypes presenting salt tolerance-metabolic routes. Providing phenotypical and molecular information of tolerance traits are key factors towards production of salt stress tolerant crops. The identification of tolerant genotypes, as well as the molecular mechanisms behind every adaptation or acclimatization event, are essential steps into this objective.

In this way, maize offers us a rich genetic variability, which increases the possibilities of new or complementing findings. Based on the hypothesis that uniting different knowledge scales of salt stress

response (whole plant and molecular) will help us to unravel aspects of tolerance mechanisms, our general aim was to provide a method that can be used on the long term to provide valuable information to farmers and germplasm banks to enhance food security, especially in less developed areas. For that purpose, it is necessary to unveil interesting cultivars within a crop. In this context, our specific aim was to understand the diversity in molecular mechanisms behind salt stress in maize, by digging into the dynamics of stress responses. For that, we established a low-cost maize salt stress phenotyping setup in the greenhouse, characterized and classified different genotypes and detected salt stress molecular reactions, identifying proteome-related responses.

To meet our objective, for the experiments of chapter 3, we selected two maize genotypes previously screened as salt-sensitive (Across8023) and salt-tolerant (Across8024), as well as a sequenced reference (B73), which we used in all experiments. In normal conditions, we defined a limit for growth monitoring time due to spatial limitations. A maize plant growing longer than nine weeks after sowing makes the measurement processes too laborious and impracticable in our greenhouse facilities. More importantly, the calculated top area becomes gradually less correlated with total leaf area in terms of sum of separate leaves with time (Figure 3.2A), possibly due to shadowing of older leaves by younger ones. In addition; we showed that modelled FW can be used in place of DW (Figure 3.2) for biomass calculation in control condition, with the advantage of being non-destructive. We determined top area, height and FW as feasible parameters to be used in our next experiments, able of distinguish the maize genotypes according to their growth rates (Figure 3.1).

In contextualizing our overall goal of generating relevant information of salt stress in tropical maize genotypes, chapter 3 delivers the important message that greenhouse phenotyping can be a low-cost process. Considering that tropical regions are often correlated to less developed countries, where we see a lack of research investments (Edmeades et al., 2017), the validation of such low-cost approach can be significant through the demonstration of possibilities.

Establishment of stress levels was also determined with the three mentioned genotypes (Across8024, Across8023 and B73), with the NaCl concentration of 0.6% settled as the most ideal compared to 1.2% and sufficient to rank our genotypes according to the level of tolerance. Thus, in chapter 3 we optimized a workflow for plant phenotyping in salt stress and gathered the first information on stress dynamics of different maize genotypes. With that, we ranked the maize genotypes according to the level of salt tolerance: Across8024 = Across8023 > B73. It is important to notice the discrepancy in salinity-related studies approaches and how a non-clear description can hinder the repeatability and validation of the results. Every research lab has its own approaches and techniques, and often the methodologies found in publications are not enough to repeat and reproduce the results. Furthermore, experiments in which the environment cannot be totally controlled, such as in a greenhouse, variation from one region to the other can be expected, influencing the research outcomes. In addition, when we compare different results from a similar experiment, we should take into account the aim of each research group. For instance, in our work we had the goal to avoid extreme stress, because we needed a clear separation of the genotypes according the salt tolerance. Other studies aiming for a higher stress level may obtain different conclusions from the same genotype. Thus, we suggest that each

research lab conducts a priori assays to determine the best approach and materials to match its own goals.

After having a whole plant phenotyping workflow that most probably can be extrapolated for all maize varieties, we aimed to integrate it with a cellular phenotyping optimized workflow. For that, in chapter 4 we investigated the salt stress responses of three additional tropical maize genotypes, totaling four (B73, CML421, CML448 and CML451), both at the plant level and at the molecular level. Based on the results regarding the differences in growth rate due to the imposed salinity, as was also the case in chapter 3, it directed to interesting time-pointing for proteomics sample collection for that genotype group. With that, we uncovered general molecular responses and stress markers for each genotype. These findings were strongly related to antioxidant and dehydration responses, as well as to differential expression of class III peroxidase isoforms as a consequence of the imposed salinity stress.

Chapter 5 experiments were conducted with the aim of reiterating the plant whole phenotyping linked with cellular phenotyping workflow built in chapters 3 and 4, adding more genotypes to the study and generating more valuable information for crop gene banks, in terms of growth and proteome responses. For that, five maize genotypes were screened, with B73 as the reference and Across8024, CML465, CML488 and CML491 composing the new experimental group set. As for chapter 4, trend lines of shoot growth, the biomass accumulation and ion content gave information about the physiological behavior of each maize genotype towards salt stress. Genotypes were clearly distinguished in terms of growth, with the ranking being, from the most to the least salt-tolerant: CML465 > Across8024 > B73 > CML488 >

CML491. Roots of all genotypes were significant and negatively affected by salt stress.

From whole plant phenotyping, we selected a time-point for proteomics sampling. General leaf protein abundance demonstrated reduced photosynthesis, increased quality control related to maintenance of ion homeostasis and high concentration of protein synthesis-related proteins. Roots were three times more affected than leaves by salinity regarding differential protein abundance in control and stressed plants, with proteins strongly related to energy, protein synthesis and antioxidant response.

Once more, genotype-specific molecular responses towards salinity was guided by plant phenotyping. Thus, the better grower genotype CML465 was the one to present the highest number of differential proteins, those being related to maintenance of proteostasis, energy production, biosynthesis of proteins and antioxidant defense.

To provide a general overview of the maize classification regarding salt-tolerance, we plotted the top area at the fourth week after sowing of all nine genotypes, having B73 as the reference (Figure 6.1). At this time-point, we can conclude that all the previously considered as the most sensitive (CML421 and CML491) or most tolerant (Across8024, Across8023 and CML465) genotypes are found in the same quadrants, III or I, respectively (Figure 6.1). For genotypes Across8024, Across8023 and CML465, there is a superiority in salt-tolerance, when compared to the other genotypes. On the other hand, CML421 and CML491 were the worse growers in both control and stress conditions at the fourth week after sowing and were classified as the most salt-sensitive ones of this maize group set (Figure 6.1).

The selection of the different maize genotypes for our salinity studies were based on: (1) previous researches which classified Across8023 and Across8024 as salt sensitive and salt tolerant, respectively (Hajibagheri et al., 1987; Pitann et al., 2013); (2) the classification of CML491 as drought tolerant genotype (Beyene et al., 2011), (3) CML465, CML488, CML421, CML448 and CML451, as well as the previously cited genotypes, being tropical climate adapted (CIMMYT, 2005); and (4) B73 as a sequenced reference. We expected genotypes CML491 and Across8024 to be tolerant to the applied salinity, and this was confirmed (Figure 6.1). Genotype Across8023 was classified in our work as a salt-tolerant one (Figure 6.1), which raised the discussion on selection of the stress level and too severe stress application (section 3.2.2 of chapter 3).

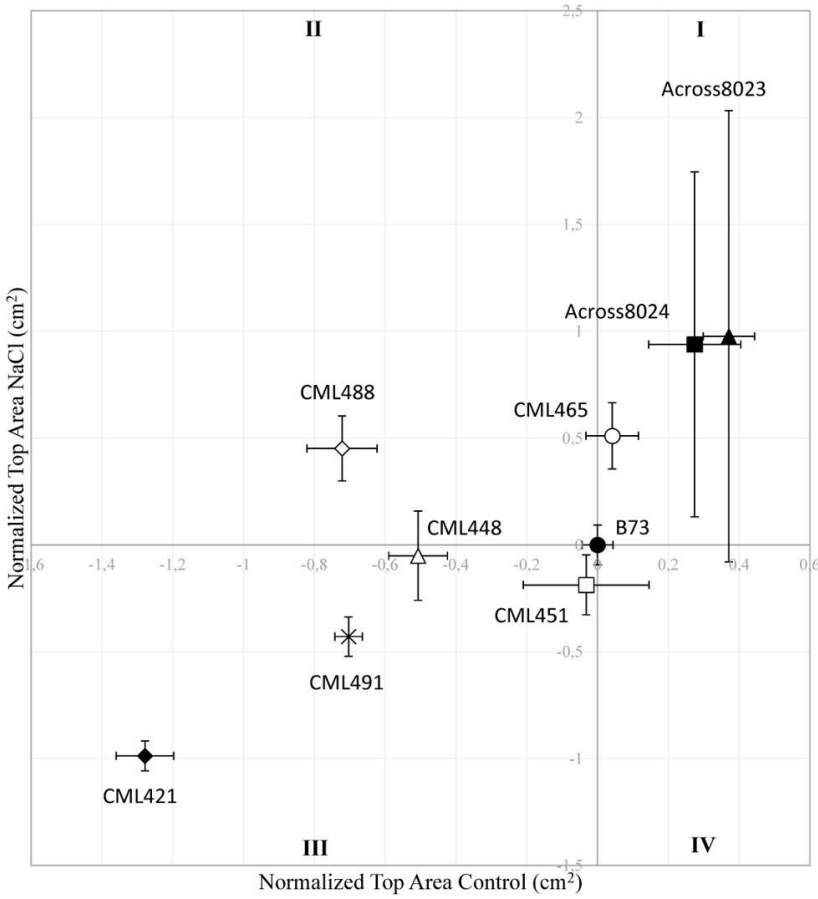

Figure 6.1 Quadrant rank of maize genotypes on the fourth week after sowing, according to the total median top area (cm^2) for each soil condition and with genotype B73 as reference. Vertical and horizontal lines discriminate the growth potential of the plants in soil with or without salt, respectively. Genotypes of experimental chapter 3: B73, Across8023 and Across8024. Genotypes of experimental chapter 4: B73, CML421, CML448 and CML451. Genotypes of experimental chapter 5: B73, Across8024, CML465, CNL488 and CML 491). Lines represent standard error. N = 6.

6.1.1 Salt stress related proteome responses - parallel between experimental chapters

Proteomics sampling time points of all experimental chapters were determined by the whole plant phenotyping and the shift in plant growth, which we assumed as an ionic effect of the salt stress. With this, proteomics analysis of each maize group set of genotypes were

conducted in a period of growth, with the time point being the fourth week for experimental chapter 4 and seventh week for chapter 5.

Phenotyping for determination of proteomics sampling time-point is an important step in salt-related studies. Due to the two-phases of stress that salinity imposes to plants, the osmotic and ionic stresses (Munns, 1993), to point out specific responses to ion accumulation, we have to be able to indicate when the shift of phases is happening within the plant. The stress phases can be detected when the applied stress is not too high, and the duration of each one is dependent of the salinity level and the plant tolerance, varying from days to weeks of difference (Munns et al., 1995). The built up of ions in leaves of maize genotype Across8023 until reaching toxic levels was calculated to happen between weeks 4 and 5 after the beginning of 100 mM NaCl treatment in greenhouse-pot experiment (Fortmeier and Schubert, 1995). In a hydroponically grown maize experiment, chloride-induced stress was detected in leaves after approximately 20 minutes after stressing the roots with 50 mM chloride containing salts and differences on the proteome of treated and non-treated plants were already encountered (Geilfus et al., 2017). However, the different methodologies and even subjective interpretation of the results have an influence in the determination of ionic-specific salt stress. Therefore, the whole plant phenotyping becomes a relevant procedure in studies that aim to interact physiological and cellular salt stress responses and, thus, the establishment of such a workflow is also essential.

It is important to notice that the selected time-pointing chosen for each genotype group for proteomics sampling was reasoned by the responses obtained from the whole plant phenotyping. For experimental chapter 4, the sampling took place at the fourth week,

while for experimental chapter 5, it happened at the seventh week after sowing. Because we had great interest in studying the ionic component of the salt stress, the tissue collection for proteomics was guided by the moment in which the growth of the genotypes differed statistically from each other as a possible consequence of ion accumulation. In addition, also an abrupt change in the growth trend was considered for each genotype. For that, we estimated the top area for all plants weekly under stress or not and calculated if and when the growth of salt treated plants presented a significant decrease from the control ones, and how this compared to the other genotypes. Thus, as it is possible to see on figures 4.2 and 5.1, these changes occurred from the third to the fourth week and the sixth to the seventh week at chapters 4 and 5, respectively. Of course, this brings some consequences for the comparison among all the nine studied genotypes. Proteomics analysis, for instance, will most probably generate different proteins or protein abundances at different durations of stress, as it was the case in our work.

A remarking general salt stress response of maize genotypes of chapter 5 (B73, Across8024, CML465, CML488 and CML491) was a high concentration of ribosomal proteins in roots of treated plants (Figure 5.8). Root proteomics responses of chapter 4 genotypes (B73, CML421, CML448 and CML451), gathered eight ribosomal proteins highly abundant in salt stress (B4G1B3, B6TRR4, B6T4E7, B6TAT4, B4FNM4, B6SLI1, B6SIG8, B6T831) and two with lower concentration (B6SH21 and K7TT73). When tracing the parallel, we can infer that the age difference plays an important part in the ribosomal protein response, In addition, we know that ribosomal proteins have important roles which confers tolerance enhancement to plants towards salinity by maintaining and regenerating plant protein

synthesis mechanisms (Zörb et al., 2004). The enhanced capacity of protein production during salinity is related to tolerance towards this stress due to the important roles they assume, such as LEA proteins in osmotic adjustment, ion transporters and antioxidant activity (Kosová et al., 2013). Furthermore, ribosomal proteins could play a role during salt stress to regulatevacuolar traffic (Li et al., 2015). Vacuolar traffic is regulated by the dynamics of its membrane which, in turn, is regulated by lipids content (Hawes et al., 1999). There are evidences that ribosomal proteins are involved in an auxin signal transduction, which ends up in the stimulation of lipids accumulation. The ribosomal proteins function then as a general regulator of the lipid metabolism working as a hub between lipid and auxin pathways (Li et al., 2015).

Salt stress also activated the response of class III peroxidases for both experimental chapters 4 and 5 (Table 6.1). In total, for experimental chapter 4, roots of salt stressed plants presented 34 class III peroxidases at the 4th week after sowing, from which 10 had low abundance and 7 were highly abundant (Table 6.1). Experimental chapter 5 salt stressed plants exhibited a total of 45 class III peroxidases at the seventh week, with 5 abundantly low as a response to salinity (Table 6.1).

Experimental chapter 4 plants presented 10 class III peroxidases in common with experimental chapter 5 that exclusively responded to salt stress: 3 were highly abundant (D7NLB3, C0HHA6 and B6U6W0), while 7 showed low abundance (Q9ZTS9, K7U159, B6SIU4, B4FRD6, B1A9R4, A5H8G4 and A5H452) (Table 6.1). Regarding this abundance difference of the same type of enzyme, in chapter 4 we predicted that isoforms abundantly low as salinity response are likely to be involved in cellular growth and elongation. Class III peroxidases highly abundant in salt stressed roots are then predicted to act in terms

of acclimation to salinity and would play a role in root cell wall stiffening. Considering the higher relative number of responsive enzymes for plants of experimental chapter 4, we can conclude that those genotypes were in general more affected by salt stress than for genotypes of chapter 5. This proteomics response is also reflected by the phenotype since all plants of experimental chapter 4 were the worst growers at the fourth week after sowing, except the most salt-sensitive genotype of experimental chapter 5 (Figure 6.1).

Class III peroxidases in common for experimental chapters 4 and 5 which responded similarly to salinity (Q6RFK3, B6T7B1 and B4G1S4), by a low abundance in response to salt stress, are presumably being involved in cellular growth and elongation, negatively affecting the root growth of all genotypes.

Table 6.1 Class III peroxidases found in roots of different maize genotypes, grown for four (experimental chapter 4) or seven (experimental chapter 5) weeks after sowing, in control or saline conditions. Arrows down represent class III peroxidases that positively responded to salt stress; arrows up represent negatively responsive class III peroxidases.

Class III peroxidases exclusively in the experimental chapter 4					
B4FSW5 ↓	B4FCI9 ↓	B4FNI0 ↑	Q9ZTS8	K7UG68	B6TMI9
Class III peroxidases exclusively in the experimental chapter 5					
Q6RFK0 ↓	B6T173 ↓	K7W888	K7VNV5	K7VH58	K7VDI6
K7UZ21	K7UV49	K7USX8	C0PEP6	C0HIT1	C0HGH8
C0HEE6	B6SIA9	B4FYD8	B4FVT1	B4FU88	
Class III peroxidases in both 4 and 5 experimental chapters					
Q9ZTS7	K7VCN5	C0PPB6	B7ZXQ8	B6SMR2	B4FH68
C0PF45	C0P4S1	C0P3T3	B4FG39	B4F8D7	
A0A096S7C9					
Class III peroxidases abundantly low in both 4 and 5 experimental chapters					
Q6RFK3 ↓		B6T7B1 ↓		B4G1S4 ↓	
Class III peroxidases in both 4 and 5 experimental chapters, highly abundant in experimental chapter 4					
D7NLB3 ↑		C0HHA6 ↑		B6U6W0 ↑	
Class III peroxidases in both 4 and 5 experimental chapters, abundantly low in experimental chapter 4					
Q9ZTS9 ↓	K7U159 ↓	B6SIU4 ↓	B4FRD6 ↓	B1A9R4 ↓	A5H8G4 ↓
A5H452 ↓					

6.2 Future research

The work presented in this thesis offered a feasible and relatively low-cost approach for application of whole plant phenotyping. Whole plant phenotyping was useful as a tool to interpret the molecular analysis, linking both as a reliable strategy for characterization and classification of maize genotypes towards salt stress. In terms of future directions, it will be essential to expand the identification of salt-tolerant maize genotypes in the greenhouse and, later on, to extend this workflow to the field for the selected genotypes. Ultimately, farmers and breeders must be able to access the information and choose for the most appropriate genotype according to their needs. For that, the identification of salt-tolerant genotypes in a greenhouse environment, should be validated in specific field conditions. Genotypes originated and adapted to tropical zones, for example, should be analyzed in those environmental conditions, despite the complexity of a salt stress field trial. Also, proteome effects of salinity under field conditions are important to be addressed and validated. Due to the many molecular pathways activated by salt stress plus the complexity of growth conditions in the field, it will be interesting and an important step for the validation of salt tolerance mechanisms.

It is known that the vegetative stage of maize is generally more salt sensitive than the reproductive one (Maas et al., 1983). However, in the field the soil contamination with salt is not only nonlinear, varying horizontal- and vertically, but can also increase or decrease, depending on weather conditions and farm management. Thus, it will be interesting that a field performance analysis takes into consideration the yield of the pre-selected tolerant genotypes. This would not only validate the predictive statement that correlates the growth trend and

the final yield for each tested genotype (Liebisch et al., 2015; Yin et al., 2011), but also assure farmers and breeders that the energy costs of salt tolerance mechanisms are not enough to disturb the yield capacity, when it is the case.

An important and interesting step to be further considered is the determination of subcellular ion content in roots and leaves of salt stressed plants through time. This can confirm the compartmentalization salt tolerance-strategy for the studied genotypes, in which excessive chloride, sodium or other ion, is sequestered in vacuoles (Apse et al., 1999; Blumwald et al., 2000). By using a scanning transmission electron microscope (STEM), it is possible to achieve high-spatial-resolution X-ray elemental imaging and quantification in plant tissues at subcellular levels, as described by Chen and colleagues (2014). Besides that, histological and chemical analysis would be an interesting method to study cell wall modifications stimulated by salinity, besides the Caspari strips, which controls the penetration rate of ions towards other tissues.

For the future, an increase in the number of whole genome sequenced maize genotypes will be interesting and necessary. Proteomics is a resourceful tool for the understanding of molecular dynamics and stress effects over multiple pathways. It targets the functional fraction of the genetics, the proteins, which gives us precise information of the cellular situation on certain conditions and time period. With the release of more sequenced genotypes, we will be able to use this tool to have access to important information, such as specific allele mutations that may influence the tolerance levels of different maize (Campos et al., 2018; Carpentier et al., 2011; Cenci et al., 2019; Van Wesemael et al., 2018).

In our work, our efforts were directed into fully scanning the proteins related to the applied stress and which were relevant within a tolerance context or as a stress marker. With that, we described interesting proteins and protein families that should be further and more deeply researched. As a next step, the study of causal inference aims to explore and confirm the assumptions concerning stress-related biomolecular mechanisms, obtained with statistical associations that resulted in descriptive proteomics. Causality have the "task of uncovering regulatory relationships between components of biomolecular pathways and networks" (Ness et al., 2016). Pinu and colleagues (2019) proposes methods for the task of genotype and phenotype causal inference and functional associations, by the use of multi-omics integration. In a top-down data reduction approach, genomics or transcriptomics data are firstly used as predictors of phenotypic responses and, following, proteomics (or metabolomics) will validate and quantify the functionality of detected pathways (Pinu et al., 2019). Alternatively, the bottom-up data reduction has metabolomics as a starting point, targeting subsequent proteomics (or transcriptomics) analyses (Pinu et al., 2019). Ness and colleagues (2016) suggests key practical approaches for causal inference in large-scale proteomic data sets to overcome usual problems when working with large and complex data.

As well as causal inference for the confirmation of suggested protein interaction and networks, other analysis can take place for proteomics and phenotyping validation. In vivo photosynthesis estimation tools, for instance, can support the observations of photosynthesis reduction in salt stressed plants of experimental chapter 5, which was addressed through relative photosynthetic protein abundance. Techniques of gas exchange measurement (O_2 production or CO_2 assimilation) or light-

based biophysical probes, such as chlorophyll fluorescence and leaf spectroscopy, are some of the options for in vivo photosynthesis estimation that comprises an wide array of instruments (Walker et al., 2018).

In the context of proteomics validation, now regarding the abundance of enzymes participating in the respiratory chain and the correlation with ATP production capacity (Chapter 4), causal inference analysis can be very useful in determining factors which could be interfering or crossing over its pathway. Furthermore, Mookerjee and colleagues (2017) describe a method for the calculation of ATP generation by glycolysis and oxidative phosphorylation separately, by concomitantly measuring extracellular acidification and oxygen consumption. Using this approach, we can better understand the responses of respiratory chain enzymes and its connection with salt stress in maize.

Concerning cis responsive elements in promoter genes, more specifically ABRE motifs predicted in class III peroxidases (chapter 4) and PM H^+-ATPases (chapter 5), the next step would be the verification of its relevance in salt-stress responses for maize. For that, we suggest the transcriptional profiling of genes containing ABRE promoter, by applying exogenous ABA in plants under salinity treatment. Once changes in gene expression can be induced by ABA response, this approach can validate the relevance of ABRE in the expression of salt-responsiveness genes

Throughout our scanning analysis of the proteomics data, we found protein groups that could compose new branches of study for future research. For example, class III peroxidases and ribosomal proteins, found in high abundance as a response to salinity in chapters 4 and 5, respectively, are interesting proteins families to consider for a deeper

investigation. Class III peroxidases are remarkable for having multiple functions and participating of several metabolic pathways, including oxidation of auxin, cell elongation and formation of cell wall (Mika et al., 2004; Passardi et al., 2004a). RedoxiBase (http://peroxibase.toulouse.inra.fr), a database dedicated to information compiling and centralization of peroxidases and other oxido-reductase enzymes, is a central point for the study of this protein family and reinforces the importance of this class for plant biological processes, including salt stress. As we found a considerable abundance of this proteins with opposite responses to salt stress, even when grouped within the same paralog group (Figure 4.7), it would be interesting to study the different roles, by, for example, knocking out detected isoforms.

Ribosomal proteins were detected in salt-stress studies (Cui et al., 2015; Geilfus et al., 2017; Zörb et al., 2004) and may be related to vacuole trafficking (Li et al., 2015), a process that can be important for conferring tolerance to plants when ions are compartmentalized into this organelle (Greenway and Munns, 1980; Munns and Tester, 2008). Thus, as future perspective, we propose a study to investigate the correlation among ribosomal protein response to salinity and its function in vacuolar traffic.

After linking whole plant phenotyping with cellular phenotyping, going through the steps of field validation of possible salt tolerant genotypes and further investigation of molecular mechanisms by subcellular ion content determination, specific allele mutations detection and functional association of responsive proteins, the next phase is the genome engineering. Clustered regularly interspaced short palindromic repeat (CRISPR)/CRISPR-associated protein 9 (Cas9)

system is an example of precise editing of sequences in which mutations and regulatory proteins can be targeted to specific sites in a genome. Thus, non-transgenic but genetically altered crops can be produced (Lozano-Juste and Cutler, 2014). In the case of our work, this possibility enlightens the pathway of developing salt-tolerant maize, which preserves adaptive characteristics from its own region. However, taking into account that tropical maize research is already neglected, possible by its connection with less developed world areas, the feasibility of the introduction of such technology must be carefully considered and studied.

Reference List

Abogadallah, G. M. (2010). Antioxidative defense under salt stress. *Plant Signal. Behav.* 5, 369–374. doi:10.4161/psb.5.4.10873.

Abrol, I. P., Yadav, J. S. P., and Massoud, F. I. (1988). "Saline Soils and Their Management," in *FAO Soils Bulletin 39*, 1–32.

Aguilar-Rangel, M. R., Chávez Montes, R. A., González-Segovia, E., Ross-Ibarra, J., Simpson, J. K., and Sawers, R. J. H. (2017). Allele specific expression analysis identifies regulatory variation associated with stress-related genes in the Mexican highland maize landrace Palomero Toluqueño. *PeerJ* 5, e3737. doi:10.7717/peerj.3737.

Aharon, R., Shahak, Y., Wininger, S., Bendov, R., and Kapulnik, Y. (2003). Overexpression of a Plasma Membrane Aquaporin in Transgenic Tobacco Improves Plant Vigor under Favorable Growth Conditions but Not under Drought or Salt Stress. 15, 439–447. doi:10.1105/tpc.009225.component.

Ahmad, P., Abdel Latef, A. A. H., Rasool, S., Akram, N. A., Ashraf, M., and Gucel, S. (2016). Role of Proteomics in Crop Stress Tolerance. *Front. Plant Sci.* 7, 1–14. doi:10.3389/fpls.2016.01336.

Akram, M., Ashraf, M. Y., Ahmad, R., Waraich, E. A., Iqbal, J., and Mohsan, M. (2010). Screening for salt tolerance in maize (Zea mays L.) hybrids at an early seedling stage. *Pakistan J. Bot.* 42, 141–154.

Alberico, G. J., and Cramer, G. R. (1993). Is the Salt Tolerance of Maize Related To Sodium Exclusion .1. Preliminary Screening of 7 Cultivars. *J. Plant Nutr.* 16, 2289–2303.

Amthor, J. S. (2000). The McCree-de Wit-Penning de Vries-Thornley Respiration Paradigms: 30 Years Later. *Ann. Bot.* 86, 1–20. doi:10.1006/anbo.2000.1175.

Apel, K., and Hirt, H. (2004). Reactive Oxygen Species: Metabolism, Oxidative Stress, and Signal Transduction. *Annu. Rev. Plant Biol.* 55, 373–399. doi:10.1146/annurev.arplant.55.031903.141701.

Apse, M. P., Aharon, G. S., Snedden, W. A., and Blumwald, E. (1999). Salt tolerance conferred by overexpression of a vacuolar Na^+/H^+ antiport in *Arabidopsis*. *Science (80-.).* 285, 1256–1258. doi:7771 [pii].

Arber, A. (1925). *Monocotyledons : A Morphological Study*. Cramer.

Ashwin, N. M. R., Barnabas, L., Ramesh Sundar, A., Malathi, P., Viswanathan, R., Masi, A., et al. (2017). Advances in proteomic technologies and their scope of application in understanding plant–pathogen interactions. *J. Plant Biochem. Biotechnol.* 26, 371–386. doi:10.1007/s13562-017-0402-1.

Baerenfaller, K., Massonnet, C., Walsh, S., Baginsky, S., Bühlmann, P., Hennig, L., et al. (2012). Systems-based analysis of Arabidopsis leaf growth reveals adaptation to water deficit. *Mol. Syst. Biol.* 8. doi:10.1038/msb.2012.39.

Barros, E., Lezar, S., Anttonen, M. J., Van Dijk, J. P., Röhlig, R. M., Kok, E. J., et al. (2010). Comparison of two GM maize varieties with a near-isogenic non-GM variety using transcriptomics, proteomics and metabolomics. *Plant Biotechnol. J.* 8, 436–451. doi:10.1111/j.1467-7652.2009.00487.x.

Bateman, A., Martin, M. J., O'Donovan, C., Magrane, M., Alpi, E., Antunes, R., et al. (2017). UniProt: The universal protein knowledgebase. *Nucleic Acids Res.* 45, D158–D169. doi:10.1093/nar/gkw1099.

Beavis, W. D., Grant, D., Albertsen, M., and Fincher, R. (1991). Quantitative Trait Loci for Plant Height in 4 Maize Populations and Their Associations with Qualitative Genetic-Loci. *Theor Appl Genet* 83, 141–145.

Berger, B., Parent, B., and Tester, M. (2010). High-throughput shoot imaging to study drought responses. *J. Exp. Bot.* 61, 3519–3528. doi:10.1093/jxb/erq201.

Bernstein, L., and Hayward, H. E. (1958). Physiology of Salt Tolerance. *Annu. Rev. Plant Physiol.* 9, 25–46. doi:10.1146/annurev.pp.09.060158.000325.

Beyene, Y., Mugo, S., Oikeh, S. O., Juma, C., and Olsen, M. (2017). Hybrids performance of doubled haploid lines derived from 10 tropical bi-parental maize populations evaluated in contrasting environments in Kenya. 16, 371–379. doi:10.5897/AJB2016.15697.

Beyene, Y., Mugo, S., Pillay, K., Tefera, T., Ajanga, S., Njoka, S., et al. (2011). Testcross performance of doubled haploid maize lines derived from tropical adapted backcross populations. *Maydica* 56, 351–358.

Blee, K. A., Jupe, S. C., Richard, G., Zimmerlin, A., Davies, D. R., and Bolwell, G. P. (2001). Molecular identification and expression of the peroxidase responsible for the oxidative burst in French bean

(Phaseolus vulgaris L .) and related members of the gene family. 607–620.

Blokhina, O., and Fagerstedt, K. V (2010). Reactive oxygen species and nitric oxide in plant mitochondria : origin and redundant regulatory systems. 447–462. doi:10.1111/j.1399-3054.2009.01340.x.

Blumwald, E., Aharon, G. S., and Apse, M. P. (2000). Sodium transport in plant cells. *Biochim. Biophys. Acta* 1465, 140–151. doi:10.1016/S0005-2736(00)00135-8.

Bose, J., Rodrigo-moreno, A., Lai, D., Xie, Y., Shen, W., and Shabala, S. (2015). Rapid regulation of the plasma membrane H 1 -ATPase activity is essential to salinity tolerance in two halophyte species , Atriplex lentiformis and Chenopodium quinoa. 481–494. doi:10.1093/aob/mcu219.

Boyne, M. T., Garcia, B. A., Li, M., Zamdborg, L., Wenger, C. D., Babai, S., et al. (2009). NIH Public Access. *Proteome* 8, 374–379. doi:10.1021/pr800635m.Tandem.

Brini, F., Hanin, M., Lumbreras, V., Amara, I., Khoudi, H., Hassairi, A., et al. (2007). Overexpression of wheat dehydrin DHN-5 enhances tolerance to salt and osmotic stress in Arabidopsis thaliana. *Plant Cell Rep.* 26, 2017–2026. doi:10.1007/s00299-007-0412-x.

Brocker, C., and Wang, X. (2014). NIH Public Access. 237, 189–210. doi:10.1007/s00425-012-1749-0.Aldehyde.

Cai, G., Wang, G., Wang, L., Liu, Y., Pan, J., and Li, D. (2014). A maize mitogen-activated protein kinase kinase, ZmMKK1, positively regulated the salt and drought tolerance in transgenic Arabidopsis. *J. Plant Physiol.* 171, 1003–1016. doi:10.1016/j.jplph.2014.02.012.

Cai, H., Chu, Q., Yuan, L., Liu, J., Chen, X., Chen, F., et al. (2012). Identification of quantitative trait loci for leaf area and chlorophyll content in maize (Zea mays) under low nitrogen and low phosphorus supply. *Mol. Breed.* 30, 251–266. doi:10.1007/s11032-011-9615-5.

Cai, R., Dai, W., Zhang, C., Wang, Y., Wu, M., Zhao, Y., et al. (2017). The maize WRKY transcription factor ZmWRKY17 negatively regulates salt stress tolerance in transgenic Arabidopsis plants. *Planta* 246, 1215–1231. doi:10.1007/s00425-017-2766-9.

Calligaris, D., Villard, C., and Lafitte, D. (2011). Advances in top-

down proteomics for disease biomarker discovery. *J. Proteomics* 74, 920–934. doi:10.1016/j.jprot.2011.03.030.

Campos, A., Swennen, R., and Carpentier, S. C. (2018). The Plantain Proteome , a Focus on Allele Specific Proteins Obtained from Plantain Fruits. *Proteomics* 1700227, 1–5. doi:10.1002/pmic.201700227.

Cannon, J., Lohnes, K., Wynne, C., Wang, Y., Edwards, N., and Fenselau, C. (2010). High-throughput middle-down analysis using an orbitrap. *J. Proteome Res.* 9, 3886–3890. doi:10.1021/pr1000994.

Carpentier, S. C., Panis, B., Renaut, J., Samyn, B., Vertommen, A., Vanhove, A. C., et al. (2011). The use of 2D-electrophoresis and de novo sequencing to characterize inter- and intra-cultivar protein polymorphisms in an allopolyploid crop. *Phytochemistry* 72, 1243–1250. doi:10.1016/j.phytochem.2010.10.016.

Carpentier, S. C., Panis, B., Vertommen, A., Swennen, R., Sergeant, K., Renaut, J., et al. (2008). Proteome Analysis of Non-Model Plants: a Challenging But Powerful Approach. *Mass Spectrom. Rev.* 27, 354–377.

Carpentier, S. C., Witters, E., Laukens, K., Deckers, P., Swennen, R., and Panis, B. (2005). Preparation of protein extracts from recalcitrant plant tissues: An evaluation of different methods for two-dimensional gel electrophoresis analysis. *Proteomics* 5, 2497–2507. doi:10.1002/pmic.200401222.

Cattivelli, L., Rizza, F., Badeck, F. W., Mazzucotelli, E., Mastrangelo, A. M., Francia, E., et al. (2008). Drought tolerance improvement in crop plants: An integrated view from breeding to genomics. *F. Crop. Res.* 105, 1–14. doi:10.1016/j.fcr.2007.07.004.

Cenci, A., Hueber, Y., Zorrilla-Fontanesi, Y., Van Wesemael, J., Kissel, E., Gislard, M., et al. (2019). Effect of paleopolyploidy and allopolyploidy on gene expression in banana. *BMC Genomics* 20, 1–12. doi:10.1186/s12864-019-5618-0.

Cha-um, S., and Kirdmanee, C. (2009). Effect of salt stress on proline accumulation , photosynthetic ability and growth characters in two maize cultivars. *Pakistan J. Bot.* 41, 87–98.

Chaicherdsakul, T., Yuenyong, W., Roytrakul, S., Chadchawan, S., Wutipraditkul, N., Limpaseni, T., et al. (2017). Proteomic analysis of transgenic rice overexpressing a calmodulin calcium sensor reveals its effects on redox signaling and homeostasis. *J. Plant Biochem. Biotechnol.* 26, 235–245. doi:10.1007/s13562-

016-0386-2.

Chakraborty, K., Sairam, R. K., and Bhattacharya, R. C. (2012). Plant Physiology and Biochemistry Differential expression of salt overly sensitive pathway genes determines salinity stress tolerance in Brassica genotypes. *Plant Physiol. Biochem.* 51, 90–101. doi:10.1016/j.plaphy.2011.10.001.

Chelius, D., and Bondarenko, P. V. (2002). Quantitative profiling of proteins in complex mixtures using liquid chromatography and mass spectrometry. *J. Proteome Res.* 1, 317–323. doi:10.1021/pr025517j.

Chen, D., Neumann, K., Friedel, S., Kilian, B., Chen, M., Altmann, T., et al. (2014a). Dissecting the Phenotypic Components of Crop Plant Growth and Drought Responses Based on High-Throughput Image Analysis. *Plant Cell Online* 26, 4636–4655. doi:10.1105/tpc.114.129601.

Chen, J., Yu, F., Liu, Y., Du, C., Li, X., Zhu, S., et al. (2016). FERONIA interacts with ABI2-type phosphatases to facilitate signaling cross-talk between abscisic acid and RALF peptide in Arabidopsis. *Proc. Natl. Acad. Sci.* 113, E5519–E5527. doi:10.1073/pnas.1608449113.

Chen, M., Chen, Q., Niu, X., Zhang, R., Lin, H., Xu, C., et al. (2007). Expression of OsNHX1 gene in maize confers salt tolerance and promotes plant growth in the field. *Plant, Soil Environ.* 53, 490–498.

Chen, S., Diekmann, H., Janz, D., and Polle, A. (2014b). Quantitative X-ray Elemental Imaging in Plant Materials at the Subcellular Level with a Transmission Electron Microscope: Applications and Limitations. in, 3160–3175. doi:10.3390/ma7043160.

Chen, S. X., and Schopfer, P. (1999). Hydroxyl-radical production in physiological reactions. A novel function of peroxidase. *Eur. J. Biochem.* 260, 726–735. doi:10.1046/j.1432-1327.1999.00199.x.

Chen, Y. H., Cao, Y. Y., Wang, L. J., Li, L. M., Yang, J., and Zou, M. X. (2018). Identification of MYB transcription factor genes and their expression during abiotic stresses in maize. *Biol. Plant.* 62, 222–230. doi:10.1007/s10535-017-0756-1.

Chen, Z. Q., Liu, Q., Zhu, Y. S., and Li, Y. X. (2002). Wheat LEA genes PMA80 and PMA 1959, enhance dehydration tolerance of transgenic rice (Oryza sativa L.). *Mol. Breed.* 10, 71–82. doi:10.1023/A:1020329401191.

Cheng, Y., Chen, G., Hao, D., Lu, H., Shi, M., Mao, Y., et al. (2014). Salt-induced root protein profile changes in seedlings of maize inbred lines with differing salt tolerances. *Chil. J. Agric. Res.* 74, 468–476. doi:10.4067/S0718-58392014000400014.

Chia, J., Song, C., Bradbury, P. J., Costich, D., Leon, N. De, Doebley, J., et al. (2012). Maize HapMap2 identifies extant variation from a genome in flux. *Nat. Genet.* 44, 803–807. doi:10.1038/ng.2313.

Choi, H., Fermin, D., and Nesvizhskii, A. I. (2008). Significance Analysis of Spectral Count Data in Label-free Shotgun Proteomics. *Mol. Cell. Proteomics* 7, 2373–2385. doi:10.1074/mcp.M800203-MCP200.

Christin, C., Bischoff, R., and Horvatovich, P. (2011). Data processing pipelines for comprehensive profiling of proteomics samples by label-free LC-MS for biomarker discovery. *Talanta* 83, 1209–1224. doi:10.1016/j.talanta.2010.10.029.

CIMMYT (2005). Maize Inbred Lines I Released By CIMMYT.

Claeys, H., Landeghem, V., Dubois, M., Maleux, K., Inzé, D., Van Landeghem, S., et al. (2014). What is Stress? Dose-Response Effects in Commonly Used In Vitro Stress Assays. *Plant Physiol.* 165, 519–527. doi:10.1104/pp.113.234641.

Colasanti, J., and Muszynski, M. (2009). "The Maize Floral Transition," in *Handbook of Maize: Its Biology*, eds. J. L. Bennetzen and S. C. Hake (Springer Science), 41–55.

Colmenero-Flores, J. M., Martínez, G., Gamba, G., Vázquez, N., Iglesias, D. J., Brumós, J., et al. (2007). Identification and functional characterization of cation-chloride cotransporters in plants. *Plant J.* 50, 278–292. doi:10.1111/j.1365-313X.2007.03048.x.

Conn, S., and Gilliham, M. (2010). Comparative physiology of elemental distributions in plants. *Ann. Bot.* 105, 1081–1102. doi:10.1093/aob/mcq027.

Cosio, C., and Dunand, C. (2017). Specific functions of individual class III peroxidase genes. 60, 391–408. doi:10.1093/jxb/ern318.

Cosio, C., Vuillemin, L., Meyer, M. De, Kevers, C., Penel, C., and Dunand, C. (2009). An anionic class III peroxidase from zucchini may regulate hypocotyl elongation through its auxin oxidase activity. 823–836. doi:10.1007/s00425-008-0876-0.

Costa, C., Schurr, U., Loreto, F., Menesatti, P., and Carpentier, S. (2019). Plant Phenotyping Research Trends , a Science Mapping

Approach. 9, 1–11. doi:10.3389/fpls.2018.01933.

Csiszár, J., Horváth, E., Váry, Z., Gallé, Á., Bela, K., Brunner, S., et al. (2014). Glutathione transferase supergene family in tomato: Salt stress-regulated expression of representative genes from distinct GST classes in plants primed with salicylic acid. *Plant Physiol. Biochem.* 78, 15–26. doi:10.1016/j.plaphy.2014.02.010.

Cubero-Font, P., Maierhofer, T., Jaslan, J., Rosales, M. A., Espartero, J., Díaz-Rueda, P., et al. (2016). Silent S-Type Anion Channel Subunit SLAH1 Gates SLAH3 Open for Chloride Root-to-Shoot Translocation. *Curr. Biol.* 26, 2213–2220. doi:10.1016/j.cub.2016.06.045.

Cui, D., Wu, D., Liu, J., Li, D., Xu, C., Li, S., et al. (2015). Proteomic Analysis of Seedling Roots of Two Maize Inbred Lines That Differ Significantly in the Salt Stress Response. 1–13. doi:10.1371/journal.pone.0116697.

Davenport, R. (2002). Glutamate receptors in plants. *Ann. Bot.* 90, 549–557. doi:10.1093/aob/mcf228.

Davenport, R. J., Muñoz-Mayor, A., Jha, D., Essah, P. A., Rus, A., and Tester, M. (2007). The Na+ transporter AtHKT1;1 controls retrieval of Na+ from the xylem in Arabidopsis. *Plant. Cell Environ.* 30, 497–507. doi:10.1111/j.1365-3040.2007.01637.x.

de Azevedo Neto, A. D., Prisco, J. T., Enéas-Filho, J., Abreu, C. E. B. De, and Gomes-Filho, E. (2006). Effect of salt stress on antioxidative enzymes and lipid peroxidation in leaves and roots of salt-tolerant and salt-sensitive maize genotypes. *Environ. Exp. Bot.* 56, 87–94. doi:10.1016/j.envexpbot.2005.01.008.

Dellaporta, S. L., and Calderon-urrea, A. (1994). The Sex Determination Process in Maize. *Science (80-.).* 266, 1501–1505.

Demidchik, V., and Maathuis, F. J. M. M. (2007). Physiological roles of nonselective cation channels in plants: From salt stress to signalling and development. *New Phytol.* 175, 387–404. doi:10.1111/j.1469-8137.2007.02128.x.

Dickens, F. (1933). Interaction of halogenacetates and SH compounds. *Biochem. J.* 27, 1141–1151. doi:10.1042/bj0271141.

Dietz, K.-J. (2003). Plant Peroxiredoxins. *Annu. Rev. Plant Biol.* 54, 93–107. doi:10.1146/annurev.arplant.54.031902.134934.

Doebley, J. F., Gaut, B. S., and Smith, B. D. (2006). Review The Molecular Genetics of Crop Domestication. 1309–1321.

Driscoll, S. P., Prins, A., Olmos, E., Kunert, K. J., and Foyer, C. H.

(2006). Specification of adaxial and abaxial stomata , epidermal structure and photosynthesis to CO2 enrichment in maize leaves. *J. Exp. Bot.* 57, 381–390. doi:10.1093/jxb/erj030.

Du, H., Feng, B.-R., Yang, S.-S., Huang, Y.-B., and Tang, Y.-X. (2012). The R2R3-MYB Transcription Factor Gene Family in Maize. *PLoS One* 7, e37463. doi:10.1371/journal.pone.0037463.

Edmeades, G. O., Trevisan, W., Prasanna, B. M., and Campos, H. (2017). "Tropical Maize (Zea mays L.)," in *Genetic Improvement of Tropical Crops*, eds. H. Campos and P. D. S. Caligari (Springer International Publishing), 57–109.

El-Aneed, A., Cohen, A., and Banoub, J. (2009). Mass spectrometry, review of the basics: Electrospray, MALDI, and commonly used mass analyzers. *Appl. Spectrosc. Rev.* 44, 210–230. doi:10.1080/05704920902717872.

Evans, A. R., Hall, D., Pritchard, J., and Newbury, H. J. (2012). The roles of the cation transporters CHX21 and CHX23 in the development of Arabidopsis thaliana. *J. Exp. Bot.* 63, 59–67. doi:10.1093/jxb/err271.

Evans, G. C. (1972). *The Quantitative Analysis of Plant Growth*.

Fahlgren, N., Gehan, M. A., and Baxter, I. (2015). Lights, camera, action: High-throughput plant phenotyping is ready for a close-up. *Curr. Opin. Plant Biol.* 24, 93–99. doi:10.1016/j.pbi.2015.02.006.

Falhof, J., Pedersen, J. T., Fuglsang, A. T., and Palmgren, M. (2016). Plasma Membrane H + -ATPase Regulation in the Center of Plant Physiology. *Mol. Plant* 9, 323–337. doi:10.1016/j.molp.2015.11.002.

FAO (2009). Global agriculture towards 2050. *High Lev. Expert Forum-How to Feed world 2050*, 1–4. doi:http://www.fao.org/fileadmin/templates/wsfs/docs/Issues_papers/HLEF2050_Global_Agriculture.pdf.

FAO (2015). *FAO Statistical Pocketbook 2015*. doi:978-92-5-108802-9.

FAO (2016). FAO Soils Portal.

Feki, K., Quintero, F. J., Pardo, J. M., and Masmoudi, K. (2011a). Regulation of c-myc transcription and mRNA abundance by serum growth factors and cell contact. *Plant Mol. Biol.* 76, 545–556. doi:10.1007/s11103-011-9787-8.

Feki, K., Quintero, F. J., Pardo, J. M., and Masmoudi, K. (2011b).

Regulation of durum wheat Na + / H + exchanger TdSOS1 by phosphorylation. 545–556. doi:10.1007/s11103-011-9787-8.

Feldman, L. (1994). "The Maize Root," in *The maize hand*, eds. M. Freeling and V. Walbot (New York: Springer), 29–37.

Felle, H. H. (1994). The H+/CI' Symporter. 1131–1136.

Felle, H. H. (2001). pH: Signal and messenger in plant cells. *Plant Biol.* 3, 577–591. doi:10.1055/s-2001-19372.

Fenn, J. B., Mann, M., Meng, C. K., Wong, S. F., and Whitehouse, C. M. (1989). Electrospray ionization for mass spectrometry of large biomolecules. *Science (80-.).* 246, 64–71. doi:10.1126/science.2675315.

Finkel, E. (2009). With ' Phenomics ,' Plant Scientists Hope to Shift Breeding Into Overdrive Data Integrity Report Sends Journals Back to the Drawing Board. *Science (80-.).*, 380–381.

Fiorani, F., and Schurr, U. (2013). Future Scenarios for Plant Phenotyping. *Annu. Rev. Plant Biol.* 64, 267–291. doi:10.1146/annurev-arplant-050312-120137.

Fita, A., Rodríguez-Burruezo, A., Boscaiu, M., Prohens, J., and Vicente, O. (2015). Breeding and Domesticating Crops Adapted to Drought and Salinity: A New Paradigm for Increasing Food Production. *Front. Plant Sci.* 6, 1–14. doi:10.3389/fpls.2015.00978.

Flexas, J., Bota, J., Loreto, F., Cornic, G., and Sharkey, T. D. (2004). Diffusive and Metabolic Limitations to Photosynthesis under Drought and Salinity in C 3 Plants. 6. doi:10.1055/s-2004-820867.

Flowers, T. J. (1972). Salt tolerance in Suaeda maritima (L.) dum: the effect of sodium chloride on growth, respiration, and soluble enzymes in a comparative study with Pisum sativum L. *J. Exp. Bot.* 23, 310–321. doi:10.1093/jxb/23.2.310.

Flowers, T. J. (2004). Improving crop salt tolerance. *J. Exp. Bot.* 55, 307–319. doi:10.1093/jxb/erh003.

Flowers, T. J., and Flowers, S. A. (2005). Why does salinity pose such a difficult problem for plant breeders? *Agric. Water Manag.* 78, 15–24. doi:10.1016/j.agwat.2005.04.015.

Flowers, T. J., Troke, P. F., and Yeo, A. R. (1977). The mechanism of salt tolerance in halophytes. *Annu. Rev. Plant Physiol.* 28, 89–121.

Flowers, T. J., and Yeo, A. R. (1986). Ion Relations of Plants under Drought and Salinity. *Aust. J. Plant Physiol* 13, 75–91. doi:10.1071/PP9860075.

Forestan, C., Aiese Cigliano, R., Farinati, S., Lunardon, A., Sanseverino, W., Varotto, S., et al. (2016a). Stress-induced and epigenetic-mediated maize transcriptome regulation study by means of transcriptome reannotation and differential expression analysis. *Sci. Rep.* 6, 30446. doi:10.1038/srep30446.

Forestan, C., Cigliano, R. A., Farinati, S., Lunardon, A., Sanseverino, W., and Varotto, S. (2016b). Stress-induced and epigenetic-mediated maize transcriptome regulation study by means of transcriptome reannotation and differential expression analysis. *Nat. Publ. Gr.*, 1–20. doi:10.1038/srep30446.

Forieri, I., Hildebrandt, U., and Rostás, M. (2016). Salinity stress effects on direct and indirect defence metabolites in maize. *Environ. Exp. Bot.* 122, 68–77. doi:10.1016/j.envexpbot.2015.09.007.

Fortmeier, R., and Schubert, S. (1995). Salt tolerance of maize (Zea mays L.): the role of sodium exclusion. *Plant. Cell Environ.* 18, 1041–1047.

Fricke, W., and Peters, W. S. (2002). The Biophysics of Leaf Growth in Salt-Stressed Barley . A Study at the Cell Level 1. doi:10.1104/pp.001164.With.

Fu, J., Zhang, D., Liu, Y., Ying, S., Shi, Y., Song, Y., et al. (2012). Isolation and Characterization of Maize PMP3 Genes Involved in Salt Stress Tolerance. *PLoS One* 7, e31101. doi:10.1371/journal.pone.0031101.

Fuglsang, A. T., Visconti, S., Drumm, K., Jahn, T., Stensballe, A., Mattei, B., et al. (1999). Binding of 14-3-3 Protein to the Plasma Membrane H ⁺-ATPase AHA2 Involves the Three C-terminal Residues Tyr 946 -Thr-Val and Requires Phosphorylation of Thr 947 *. *Biochemistry* 274, 36774–36780. doi:10.1074/jbc.274.51.36774.

Fukuda, A., Yazaki, Y., Ishikawa, T., Koike, S., and Tanaka, Y. (1998). N a + / H + Antiporter in Tonoplast Vesicles from Rice Roots. *Plant Cell Physiol.* 39, 196–201.

Garcia, L., Welchen, E., Gey, U., Arce, A. L., Steinebrunner, I., and Gonzalez, D. H. (2016). The cytochrome c oxidase biogenesis factor AtCOX17 modulates stress responses in Arabidopsis. 628–644. doi:10.1111/pce.12647.

Gaspar, T., Penel, C., and Thorpe, T. A. (1982). *Peroxidases, 1970-1980: a survey of their biochemical and physiological roles in higher plants*. Genève : Université de Genève. Centre de botanique.

Gaut, B. S., and Doebley, J. F. (1997). DNA sequence evidence for the segmental allotetraploid origin of maize. *Proc. Natl. Acad. Sci. U. S. A.* 94, 6809–14. doi:10.1073/pnas.94.13.6809.

Geilfus, C.-M. M., Tenhaken, R., and Carpentier, S. C. (2017). Transient alkalinization of the leaf apoplast stiffens the cell wall during onset of chloride salinity in corn leaves. *J. Biol. Chem.* 292, 18800–18813. doi:10.1074/jbc.M117.799866.

Geilfus, C. M. (2018). Chloride: From Nutrient to Toxicant. *Plant Cell Physiol.* 59, 877–886. doi:10.1093/pcp/pcy071.

Geilfus, C. M., Mith, A., Muehling, K. H., Mithöfer, A., Ludwig-Müller, J., Zörb, C., et al. (2015). Chloride-inducible transient apoplastic alkalinizations induce stomata closure by controlling abscisic acid distribution between leaf apoplast and guard cells in salt-stressed Vicia faba. *New Phytol.* 208, 803–816. doi:10.1111/nph.13507.

Geilfus, C. M., and Mühling, K. H. (2012). Transient alkalinization in the leaf apoplast of Vicia faba L. depends on NaCl stress intensity: an in situ ratio imaging study. *Plant, Cell Environ.* 35, 578–587. doi:10.1111/j.1365-3040.2011.02437.x.

Geilfus, C. M., Zörb, C., Neuhaus, C., Hansen, T., Lüthen, H., and Mühling, K. H. (2011). Differential Transcript Expression of Wall-loosening Candidates in Leaves of Maize Cultivars Differing in Salt Resistance. *J. Plant Growth Regul.* 30, 387–395. doi:10.1007/s00344-011-9201-4.

Geilfus, C., Zörb, C., and Mühling, K. H. (2010). Plant Physiology and Biochemistry Salt stress differentially affects growth-mediating b -expansins in resistant and sensitive maize (Zea mays L .). *Plant Physiol. Biochem.* 48, 993–998. doi:10.1016/j.plaphy.2010.09.011.

Geng, Y., Wu, R., Wee, C. W., Xie, F., Wei, X., Chan, P. M. Y., et al. (2013). A Spatio-Temporal Understanding of Growth Regulation during the Salt Stress Response in Arabidopsis. *Plant Cell* 25, 2132–2154. doi:10.1105/tpc.113.112896.

Gevaudant, F., Duby, G., von Stedingk, E., Zhao, R., Morsomme, P., and Boutry, M. (2007). Expression of a Constitutively Activated Plasma Membrane H+-ATPase Alters Plant Development and

Increases Salt Tolerance. *Plant Physiol.* 144, 1763–1776. doi:10.1104/pp.107.103762.

Ghanem, M. E., Marrou, H., and Sinclair, T. R. (2015). Physiological phenotyping of plants for crop improvement. *Trends Plant Sci.* 20, 139–144. doi:10.1016/j.tplants.2014.11.006.

Giaveno, C. D., Ribeiro, R. V., Souza, G. M., and Oliveira, R. F. De (2007). Screening of tropical maize for salt stress tolerance. *Crop Breed. Appl. Biotechnol.* 7, 304–313.

Gilliham, M., and Tester, M. (2005). The regulation of anion loading to the maize root xylem. *Plant Physiol.* 137, 819–828. doi:10.1104/pp.104.054056.

Gong, F. P., Yang, L., Tai, F. J., Hu, X. L., and Wang, W. (2014). "Omics" of Maize Stress Response for Sustainable Food Production: Opportunities and Challenges. *Omi. J. Integr. Biol.* 18, 714–732. doi:Doi 10.1089/Omi.2014.0125.

Granier, C., Aguirrezabal, L., Chenu, K., Cookson, S. J., Dauzat, M., Hamard, P., et al. (2006). PHENOPSIS, an automated platform for reproducible phenotyping of plant responses to soil water deficit in Arabidopsis thaliana permitted the identification of an accession with low sensitivity to soil water deficit. *New Phytol.* 169, 623–635. doi:10.1111/j.1469-8137.2005.01609.x.

Greenway, H., and Munns, R. (1980). Mechanisms of salt tolerance in nonhalophytes. *Revis. Plant Physiol.* 31, 149–190.

Griffiths, A., Wessler, S., Lewontin, R., Gelbart, W., Suzuki, D., and Miller, J. (2005). An introduction to genetic analysis. *Vasa*, 706.

Gu, Y., Zhao, C., He, L., Yan, B., Dong, J., Li, Z., et al. (2018). Genome-wide identification and abiotic stress responses of DGK gene family in maize. *J. Plant Biochem. Biotechnol.* 27, 156–166. doi:10.1007/s13562-017-0424-8.

Gupta, A. K., and Kaur, N. (2005). Sugar signalling and gene expression in relation to carbohydrate metabolism under abiotic stresses in plants. *J. Biosci.* 30, 761–776. doi:10.1007/BF02703574.

Hainey, C., Rafalski, J. A., Hanafey, M., Zhang, Y., Krespan, W., Luck, S. D., et al. (2015). "Genomic distribution of genetic diversity in elite maize germplasm," in *Genetics, Genomics and Breeding of Maize*, eds. R. Wusirika, M. Bohn, J. Lai, and C. Kole (CRC Press), 51–63. doi:10.2135/cropsci2015.11.0003br.

Hajibagheri, M. A., Harvey, D. M. R., and Flowers, T. J. (1987).

Quantitative Ion Distribution Within Root-Cells of Salt-Sensitive and Salt-Tolerant Maize Varieties. *New Phytol.* 105, 367–379. doi:10.1111/j.1469-8137.1987.tb00874.x.

Hajrah, N. H., Obaid, A. Y., Atef, A., Ramadan, A. M., Arasappan, D., Nelson, C. A., et al. (2017). Transcriptomic analysis of salt stress responsive genes in Rhazya stricta. 1–18.

Halfter, U., Ishitani, M., and Zhu, J. K. (2000). The Arabidopsis SOS2 protein kinase physically interacts with and is activated by the calcium-binding protein SOS3. *Proc Natl Acad Sci* 97, 3735–3740. doi:10.1073/pnas.040577697.

Han, Y., Wang, W., Sun, J., Ding, M., Zhao, R., Deng, S., et al. (2013). Populus euphratica XTH overexpression enhances salinity tolerance by the development of leaf succulence in transgenic tobacco plants. 64, 4225–4238. doi:10.1093/jxb/ert229.

Hanin, M., Brini, F., Ebel, C., Toda, Y., Takeda, S., and Masmoudi, K. (2011). Versatile proteins for complex mechanisms Plant dehydrins and stress tolerance. 1503–1509. doi:10.4161/psb.6.10.17088.

Hanway, J. J. (1966). *How a Corn Plant Develops*. Iowa State University. Cooperative Extension Service.

Hartmann, A., Czauderna, T., Hoffmann, R., Stein, N., and Schreiber, F. (2011). HTPheno: An image analysis pipeline for high-throughput plant phenotyping. *BMC Bioinformatics* 12. doi:10.1186/1471-2105-12-148.

Hasanuzzaman, M., Nahar, K., Fujita, M., Ahmad, P., Chandna, R., Prasad, M. N. V, et al. (2013). "Enhancing Plant Productivity Under Salt Stress: Relevance of Poly-omics," in *Salt Stress in Plants: Signalling, Omics and Adaptations*, eds. P. Ahmad, M. M. Azooz, and M. N. V Prasad (New York, NY: Springer New York), 113–156. doi:10.1007/978-1-4614-6108-1_6.

Hawes, C. R., Brandizzi, F., and Andreeva, A. V (1999). Endomembranes and vesicle trafficking. *Curr. Opin. Plant Biol.* 2, 454–461.

Henry, C., Bledsoe, S. W., Griffiths, C. A., Kollman, A., Paul, M. J., Sakr, S., et al. (2015). Differential Role for Trehalose Metabolism in Salt-Stressed Maize. *Plant Physiol.* 169, 1072–89. doi:10.1104/pp.15.00729.

Henry, C., Morgan, D., Weekes, R., Daniels, R., and Boffey, C. (2003). Farm scale evaluations of GM crops: monitoring gene flow from

GM crops to non-GM equivalent crops in the vicinity. Part I: Forage Maize. Dorchester.

Henryk Eisenberg (2002). Macromolecular marvels. *Nature* 415, 261–262. doi:10.1038/415261a.

Henzel, W. J., Billeci, T. M., Stults, J. T., Wong, S. C., Grimley, C., and Watanabe, C. (1993). Identifying proteins from two-dimensional gels by molecular mass searching of peptide fragments in protein sequence databases. *Proc. Natl. Acad. Sci. U. S. A.* 90, 5011–5. doi:10.1073/pnas.90.11.5011.

Heyno, E., Mary, V., Schopfer, P., and Krieger-Liszkay, A. (2011). Oxygen activation at the plasma membrane : relation between superoxide and hydroxyl radical production by isolated membranes. *Planta* 234, 35–45. doi:10.1007/s00425-011-1379-y.

Hippeli, S., and Elstner, E. F. (1996). Mechanisms of Oxygen Activation during Plant Stress: Biochemical Effects of Air Pollutants. *J. Plant Physiol.* 148, 249–257. doi:10.1016/S0176-1617(96)80250-1.

Hiraga, S. (2001). A Large Family of Class III Plant Peroxidases. *Plant Cell Physiol.* 42, 462–468. doi:10.1093/pcp/pce061.

Hmida-Sayari, A., Gargouri-Bouzid, R., Bidani, A., Jaoua, L., Savouré, A., and Jaoua, S. (2005). Overexpression of Δ1-pyrroline-5-carboxylate synthetase increases proline production and confers salt tolerance in transgenic potato plants. *Plant Sci.* 169, 746–752. doi:10.1016/j.plantsci.2005.05.025.

Hochholdinger, F. (2009). "The Maize Root System: Morphology, Anatomy, and Genetics," in *Handbook of Maize: Its Biology*, eds. J. L. Bennetzen and S. C. Hake (Springer Science), 145–160. doi:10.1007/978-0-387-79418-1.

Hoffmann, E. de, and Stroobant, V. (2007a). "Ion Sources," in *Mass Spectrometry: Principles and Applications* (John Wiley & Sons), 15–83.

Hoffmann, E. de, and Stroobant, V. (2007b). "Mass Analysers," in *Mass Spectrometry: Principles and Applications* (John Wiley & Sons), 85–170. doi:10.1007/978-3-642-10711-5.

Hong-bo, S., Zong-suo, L., and Ming-an, S. (2005). LEA proteins in higher plants : Structure , function , gene expression and regulation. 45, 131–135. doi:10.1016/j.colsurfb.2005.07.017.

Horie, T., Yoshida, K., Nakayama, H., Yamada, K., Oiki, S., and

Shinmyo, A. (2001). Two types of HKT transporters with different properties of Na+ and K+ transport in Oryza sativa. *Plant J.* 27, 129–138. doi:10.1046/j.1365-313X.2001.01077.x.

Hossain, M. S., and Dietz, K. (2016). Tuning of Redox Regulatory Mechanisms , Reactive Oxygen Species and Redox Homeostasis under Salinity Stress. 7. doi:10.3389/fpls.2016.00548.

Hu, Y., and Schmidhalter, U. (1997). Interactive effects of salinity and macronutrient level on wheat . II . Composition Macronutrient Level on Wheat . *J. Plant Nutr.* 20, 1169–1182. doi:10.1080/01904169709365325.

Hussain Wani, S., Brajendra Singh, N., Haribhushan, A., and Iqbal Mir, J. (2013). Compatible Solute Engineering in Plants for Abiotic Stress Tolerance - Role of Glycine Betaine. *Curr. Genomics* 14, 157–165. doi:10.2174/1389202911314030001.

Hustoft, H. K., Malerod, H., Wilson, S. R., Reubsaet, L., Lundanes, E., and Greibrokk, T. (2012). "A Critical Review of Trypsin Digestion for LC-MS Based Proteomics," in *Integrative Proteomics*, ed. H.-C. Leung (InTech), 74–92.

Ie, E. V, Arango, M., Oufattole, F. M., and Boutry, M. (2003). The plasma membrane proton pump ATPase : the significance of gene subfamilies. 355–365. doi:10.1007/s00425-002-0856-8.

IPCC (2007). *Climate Change 2007: The Physical Science Basis*. , eds. S. Solomon, D. Qin, M. Manning, M. Marquis, K. Averyt, M. M. B. Tignor, et al. Geneva: IPCC Secretariat doi:10.1017/CBO9781107415324.004.

Ishitani, M., Liu, J., Halfter, U., Kim, C.-S., Shi, W., and Zhu, J. (2000). SOS3 Function in Plant Salt Tolerance Requires N-Myristoylation and Calcium Binding. *Plant Cell* 12, 1667–1678. doi:10.1105/tpc.12.9.1667.

Jackson, D., and Hake, S. (1999). Control of phyllotaxy in maize by the abphyl1 gene. *Development* 126, 315–323.

James, P., Quadroni, M., Carafoli, E., and Gonnet, G. (1993). Protein identification by mass profile fingerprinting. *Biochem. Biophys. Res. Commun.* 195, 58–64. doi:10.1006/bbrc.1993.2009.

James, R. A., Munns, R., Caemmerer, S. V. O. N., Trejo, C., Miller, C., and Condon, T. A. G. (2006). Photosynthetic capacity is related to the cellular and subcellular partitioning of Na + , K + and Cl - in salt-affected barley and durum wheat. 2185–2197. doi:10.1111/j.1365-3040.2006.01592.x.

Jandera, P., and Henze, G. (2012). "Liquid Chromatography, 1. Fundamentals, History, Instrumentation, Materials," in *Ullmann's Encyclopedia of Industrial Chemistry* (Weinheim: Wiley-VCH), 85–138. doi:10.1002/14356007.b05.

Jennings, D. H. (1976). The Effects of Sodium Chloride on Higher Plants. *Biol. Rev.* 51, 453–486. doi:10.1111/j.1469-185X.1976.tb01064.x.

Jian, Y., Xu, C., Guo, Z., Wang, S., Xu, Y., and Zou, C. (2017). Maize (Zea mays L .) genome size indicated by 180-bp knob abundance is associated with flowering time. *Sci. Rep.* 7, 1–9. doi:10.1038/s41598-017-06153-8.

Jing, L. W., Chen, S. H., Guo, X. L., Zhang, H., and Zhao, Y. X. (2006). Overexpression of a chloroplast-located peroxiredoxin Q gene, SsPrxQ, increases the salt and low-temperature tolerance of Arabidopsis. *J. Integr. Plant Biol.* 48, 1244–1249. doi:10.1111/j.1744-7909.2006.00357.x.

Johannsen, W. L. (1909). *Elemente der exakten Erblichkeitslehre*. Jena: Gustav Fischer.

Johnston, R., Wang, M., Sun, Q., Sylvester, A. W., Hake, S., and Scanlon, M. J. (2014). Transcriptomic analyses indicate that maize ligule development recapitulates gene expression patterns that occur during lateral organ initiationw open. *Plant Cell* 26, 4718–4732. doi:10.1105/tpc.114.132688.

Karas, M., and Hillenkamp, F. (1988). Laser Desorption Ionization of Proteins with Molecular Masses Exceeding 10 000 Daltons. *Anal. Chem.* 60, 2299–2301. doi:10.1021/ac00171a028.

Karpievitch, Y. V, Polpitiya, A. D., Anderson, G. A., Smith, R. D., and Dabney, A. R. (2011). Liquid Chromatography Mass Spectrometry-Based Proteomics: Biological and Technological Aspects. *Ann Appl Stat* 4, 1797–1823. doi:10.1214/10-AOAS341.Liquid.

Kasukabe, Y., He, L. X., Nada, K., Misawa, S., Ihara, I., and Tachibana, S. (2004). Overexpression of spermidine synthase enhances tolerance to multiple environmental stresses and up-regulates the expression of various stress regulated genes in transgenic Arabidopsis thaliana. *Plant Cell Physiol.* 45, 712–722. doi:10.1093/pcp/pch083.

Khan, M. S., Khan, M. A., and Ahmad, D. (2016). Assessing Utilization and Environmental Risks of Important Genes in Plant Abiotic Stress Tolerance. *Front. Plant Sci.* 7, 1–13.

doi:10.3389/fpls.2016.00792.

Kissel, E., van Asten, P., Swennen, R., Lorenzen, J., and Carpentier, S. C. (2015). Transpiration efficiency versus growth: Exploring the banana biodiversity for drought tolerance. *Sci. Hortic. (Amsterdam)*. 185, 175–182. doi:10.1016/j.scienta.2015.01.035.

Kizis, D. (2002). Maize DRE binding proteins DBF1 and DBF2 are involved in rab17 regulation through the drought responsive element in an ABA dependent pathway. *Plant J.* 30, 679–689.

Klug, W. S., Cummings, M. R., Spencer, C. A., and Palladino, M. A. (2015). *Concepts of Genetics*. 11th ed. Pearson doi:10.1017/CBO9781107415324.004.

Končitíková, R., Vigouroux, A., Kopečná, M., Andree, T., Bartoš, J., Šebela, M., et al. (2015). Role and structural characterization of plant aldehyde dehydrogenases from family 2 and family 7. *Biochem. J.* 468, 109–23. doi:10.1042/BJ20150009.

Kong, X., Pan, J., Zhang, M., Xing, X. I. N., Zhou, Y. A. N., Liu, Y., et al. (2011). ZmMKK4, a novel group C mitogen-activated protein kinase kinase in maize (Zea mays), confers salt and cold tolerance in transgenic Arabidopsis. *Plant. Cell Environ.* 34, 1291–1303. doi:10.1111/j.1365-3040.2011.02329.x.

Kosová, K., Prášil, I. T., and Vítámvás, P. (2013). Protein Contribution to Plant Salinity Response and Tolerance Acquisition. 6757–6789. doi:10.3390/ijms14046757.

Koua, D., Cerutti, L., Falquet, L., Sigrist, C. J. A., Hulo, N., and Dunand, C. (2009). PeroxiBase : a database with new tools for peroxidase family classification. 37, 261–266. doi:10.1093/nar/gkn680.

Kozlova, L. V., Gorshkov, O. V., Mokshina, N. E., and Gorshkova, T. A. (2015). Differential expression of α-l-arabinofuranosidases during maize (Zea mays L.) root elongation. *Planta* 241, 1159–1172. doi:10.1007/s00425-015-2244-1.

Kuleshov, N. N. (1933). World's diversity of phenotypes of maize. *J. Am. Soc. Agron.*

Kutschera, U., and Schopfer, P. (1986). Effect of auxin and abscisic acid on cell wall extensibility in maize coleoptiles. *Planta* 167, 527–535.

Laboratory, U. S. (1954). *Diagnosis and Improvement of Saline and Alkaline Soils*. , ed. L. A. Richards doi:10.2136/sssaj1954.03615995001800030032x.

Laborda, P. R., Oliveira, K. M., Garcia, A. A. F., Paterniani, M. E. A. G. Z., and De Souza, A. P. (2005). Tropical maize germplasm: What can we say about its genetic diversity in the light of molecular markers? *Theor. Appl. Genet.* 111, 1288–1299. doi:10.1007/s00122-005-0055-7.

Lacan, D., and Durand, M. (1996). Na + -K + Exchange at the XylemlSymplast Boundary Its Significance in the Salt Sensitivity of Soybean. *Plant Physiol.* 110, 705–711.

Lange, E., Tautenhahn, R., Neumann, S., and Gröpl, C. (2008). Critical assessment of alignment procedures for LC-MS proteomics and metabolomics measurements. *BMC Bioinformatics* 9, 1–19. doi:10.1186/1471-2105-9-375.

Langridge, P., and Fleury, D. (2011). Making the most of "omics" for crop breeding. *Trends Biotechnol.* 29, 33–40. doi:10.1016/j.tibtech.2010.09.006.

Lawson, S. S., and Michler, C. H. (2014). Overexpression of At STO1 leads to improved salt tolerance in Populus tremula 3 P . alba. doi:10.1007/s11248-014-9808-x.

Leister, D., Varotto, C., Pesaresi, P., Niwergall, A., and Salamini, F. (1999). Large-scale evaluation of plant growth in Arabidopsis thaliana by non-invasive image analysis. *Plant Physiol. Biochem.* 37, 671–678. doi:10.1016/S0981-9428(00)80097-2.

Leroy, B., Houyoux, N., Matallana-Surget, S., and Wattiez, R. (2012). "Gel-Free Proteome Analysis Isotopic Labelling Vs. Label-Free Approaches for Quantitative Proteomics," in *Integrative Proteomics*, ed. H.-C. Leung (InTech), 327–346.

Lescot, M., Déhais, P., Thijs, G., Marchal, K., Moreau, Y., Peer, Y. Van de, et al. (2002). PlantCARE, a database of plant cis-acting regulatory elements and a portal to tools for in silico analysis of promoter sequences. *Nucleic Acids Res.* 30, 325–327. doi:10.1093/nar/30.1.325.

Lewontin, R. C. (1992). "Genotype and phenotype," in *Keywords in Evolutionary Biology*, eds. E. F. Keller and E. Lloyd (Harvard University Press), 137–144.

Li, B., Tester, M., and Gilliham, M. (2017a). Chloride on the Move. *Trends Plant Sci.* 22, 236–248. doi:10.1016/j.tplants.2016.12.004.

Li, J., Wen, J., Lease, K. A., Doke, J. T., Tax, F. E., and Walker, J. C. (2002). BAK1 , an Arabidopsis LRR Receptor-like Protein

Kinase , Interacts with BRI1 and Modulates Brassinosteroid Signaling. 110, 213–222.

Li, M., Zhang, K., Long, R., Sun, Y., Kang, J., Zhang, T., et al. (2017b). iTRAQ-based comparative proteomic analysis reveals tissue-speci fi c and novel early-stage molecular mechanisms of salt stress response in Carex rigescens. *Environ. Exp. Bot.* 143, 99–114. doi:10.1016/j.envexpbot.2017.08.010.

Li, R., Sun, R., Hicks, G. R., and Raikhel, N. V (2015). Arabidopsis ribosomal proteins control vacuole trafficking and developmental programs through the regulation of lipid metabolism. 112, 19537–19544. doi:10.1073/pnas.1500941112.

Li, W. Y. F., Wong, F. L., Tsai, S. N., Phang, T. H., Shao, G., and Lam, H. M. (2006). Tonoplast-located GmCLC1 and GmNHX1 from soybean enhance NaCl tolerance in transgenic bright yellow (BY)-2 cells. *Plant, Cell Environ.* 29, 1122–1137. doi:10.1016/j.diamond.2005.12.024.

Liebisch, F., Kirchgessner, N., Schneider, D., Walter, A., and Hund, A. (2015). Remote, aerial phenotyping of maize traits with a mobile multi-sensor approach. *Plant Methods* 11. doi:10.1186/s13007-015-0048-8.

Lim, G., Zhang, X., Chung, M., Lee, D. J., Woo, Y., Cheong, H., et al. (2010). A putative novel transcription factor , AtSKIP , is involved in abscisic acid signalling and confers salt and osmotic tolerance in Arabidopsis. 103–113.

Lim, Y. S., Cha, M. K., Kim, H. K., Uhm, T. B., Park, J. W., Kim, K., et al. (1993). Removals of hydrogen peroxide and hydroxyl radical by thiol-specific antioxidant protein as a possible role in vivo. *Biochem. Biophys. Res. Commun.* 192, 273–280. doi:10.1006/bbrc.1993.1410.

Link, A. J., Eng, J., Schieltz, D. M., Carmack, E., Mize, G. J., Morris, D. R., et al. (1999). Direct analysis of protein complexes using mass spectrometry. *Nat. Biotechnol.* 17, 676–682. doi:10.1038/10890.

Liska, A. J., and Shevchenko, A. (2003). Expanding the organismal scope of proteomics: Cross-species protein identification by mass spectrometry and its implications. *Proteomics* 3, 19–28. doi:10.1002/pmic.200390004.

Liu, G., Li, X., Jin, S., Liu, X., Zhu, L., Nie, Y., et al. (2014a). Overexpression of Rice NAC Gene SNAC1 Improves Drought and Salt Tolerance by Enhancing Root Development and

Reducing Transpiration Rate in Transgenic Cotton. 9. doi:10.1371/journal.pone.0086895.

Liu, G., Ma, L., Duan, W., Wang, B., Li, J., Xu, H., et al. (2014b). Differential proteomic analysis of grapevine leaves by iTRAQ reveals responses to heat stress and subsequent recovery. 1–17. doi:10.1186/1471-2229-14-110.

Liu, H., Sadygov, R. G., and Yates, J. R. (2004). A model for random sampling and estimation of relative protein abundance in shotgun proteomics. *Anal. Chem.* 76, 4193–4201. doi:10.1021/ac0498563.

Liu, Y., and He, C. (2016). Regulation of plant reactive oxygen species (ROS) in stress responses: learning from AtRBOHD. *Plant Cell Rep.* 35, 995–1007. doi:10.1007/s00299-016-1950-x.

Lockhart, D. J., and Winzeler, E. A. (2000). Genomics, gene expression and DNA arrays. 405.

Lodish, H. F. (1981). Post-translational modification of proteins. *Enzym. Microb. Technol.* 3, 178–188. doi:10.1016/0141-0229(81)90084-3.

Lohaus, G., Hussmann, M., Pennewiss, K., Schneider, H., Zhu, J. J., and Sattelmacher, B. (2000). Solute balance of a maize (Zea mays L.) source leaf as affected by salt treatment with special emphasis on phloem retranslocation and ion leaching. *J. Exp. Bot.* 51, 1721–32. doi:10.1093/jexbot/51.351.1721.

Lozano-Juste, J., and Cutler, S. R. (2014). Plant genome engineering in full bloom. *Trends Plant Sci.* 19, 284–287. doi:10.1016/j.tplants.2014.02.014.

Lu, Y., Shah, T., Hao, Z., Taba, S., Zhang, S., Gao, S., et al. (2011). Comparative SNP and haplotype analysis reveals a higher genetic diversity and rapider LD decay in tropical than temperate germplasm in maize. *PLoS One* 6. doi:10.1371/journal.pone.0024861.

Luo, M., Zhao, Y., Wang, Y., Shi, Z., Zhang, P., Zhang, Y., et al. (2018). Comparative Proteomics of Contrasting Maize Genotypes Provides Insights into Salt-Stress Tolerance Mechanisms. doi:10.1021/acs.jproteome.7b00455.

Maas, E. V., and Hoffman, G. J. (1977). Crop Salt Tolerance–Current Assessment. *J. Irrig. Drain. Div.* 103, 115–134.

Maas, E. V., Hoffman, G. J., Chaba, G. D., Poss, J. A., and Shannon, M. C. (1983). Salt sensitivity of corn at various growth stages.

Irrig. Sci. 4, 45–57.

Maathuis, F. J. M., Ahmad, I., and Patishtan, J. (2014). Regulation of Na+ fluxes in plants. *Front. Plant Sci.* 5, 1–9. doi:10.3389/fpls.2014.00467.

Magalhães, P. C., and Souza, T. C. de (2011). Cultivo do Milho - Ecofisiologia. *Sist. Produção-Cultivo do Milho*, 1–17.

Maguire, B. A., and Zimmermann, R. A. (2001). The ribosome in focus. *Cell* 104, 813–816. doi:10.1016/S0092-8674(01)00278-1.

Mahler, H., Wuennenberg, P., Linder, M., Przybyla, D., Zoerb, C., Landgraf, F., et al. (2007). Singlet oxygen affects the activity of the thylakoid ATP synthase and has a strong impact on its subunit. *Planta* 225, 1073–1083. doi:10.1007/s00425-006-0416-8.

Mahner, M., and Kary, M. (1997). What exactly are genomes, genotypes and phenotypes? And what about phenomes? *J. Theor. Biol.* 186, 55–63. doi:10.1006/jtbi.1996.0335.

Makarov, A. A. (1999). Mass spectrometer.

Mann, M., and Jensen, O. N. (2003). Proteomic analysis of post-translational modifications. 21, 255–261.

Mansilla, N., Racca, S., Gras, D. E., Gonzalez, D. H., and Welchen, E. (2018). The Complexity of Mitochondrial Complex IV : An Update of Cytochrome c Oxidase Biogenesis in Plants. doi:10.3390/ijms19030662.

Marion, G. M., and Babcock, K. L. (1976). Predicting specific condutance and salt concentration in dilute aqueous solutions. *Soil Sci.* 122, 181–187. doi:10.1097/00010694-197610000-00001.

Matsuoka, Y., Mitchell, S. E., Kresovich, S., Goodman, M., and Doebley, J. (2002). Microsatellites in Zea - Variability, patterns of mutations, and use for evolutionary studies. *Theor. Appl. Genet.* 104, 436–450. doi:10.1007/s001220100694.

McCormack, A. L., Schieltz, D. M., Goode, B., Yang, S., Barnes, G., Drubin, D., et al. (1997). Direct Analysis and Identification of Proteins in Mixtures by LC/MS/MS and Database Searching at the Low-Femtomole Level. *Anal. Chem.* 69, 767–776. doi:10.1021/ac960799q.

McCouch, S. R., McNally, K. L., Wang, W., and Hamilton, R. S. (2012a). Genomics of gene banks: A case study in rice. *Am. J. Bot.* 99, 407–423. doi:10.3732/ajb.1100385.

McCouch, S. R., McNally, K. L., Wang, W., and Hamilton, R. S. (2012b). Genomics of gene banks: A case study in rice. *Am. J. Bot.* 99, 407–423. doi:10.3732/ajb.1100385.

McCully, M. E., and Canny, M. J. (1988). Pathways and processes of water and nutrient movement in roots. *Plant Soil* 111, 159–170.

Meloni, D. A., Oliva, M. A., Ruiz, H. A., and Martinez, C. A. (2001). Contribution of Proline and Inorganic Solutes To Osmotic Adjustment in Cotton Under Salt Stress. *J. Plant Nutr.* 24, 599–612. doi:10.1081/PLN-100104983.

Melorose, J., Perroy, R., and Careas, S. (2015). World population prospects. *United Nations* 1, 587–92. doi:10.1017/CBO9781107415324.004.

Mian, A., Oomen, R. J. F. J., Isayenkov, S., Sentenac, H., Maathuis, F. J. M., Véry, A. A., et al. (2011). Over-expression of an Na +- and K +-permeable HKT transporter in barley improves salt tolerance. *Plant J.* 68, 468–479. doi:10.1111/j.1365-313X.2011.04701.x.

Mika, A., Minibayeva, F., Beckett, R., and Lüthje, S. (2004). Possible functions of extracellular peroxidases in stress-induced generation and detoxification of active oxygen species. 173–193.

Mittler, R. (2002). Oxidative stress, antioxidants and stress tolerance. *Trends Plant Sci.* 7, 405–410.

Moller, I. S., Gilliham, M., Jha, D., Mayo, G. M., Roy, S. J., Coates, J. C., et al. (2009). Shoot Na+ Exclusion and Increased Salinity Tolerance Engineered by Cell Type-Specific Alteration of Na+ Transport in Arabidopsis. *Plant Cell Online* 21, 2163–2178. doi:10.1105/tpc.108.064568.

Mookerjee, S. A., Gerencser, A. A., Nicholls, D. G., and Brand, M. D. (2017). Quantifying intracellular rates of glycolytic and oxidative ATP production and consumption using extracellular flux measurements. *J. Biol. Chem.* 292, 7189–7207. doi:10.1074/jbc.M116.774471.

Morari, F., Meggio, F., Lunardon, A., Scudiero, E., and Forestan, C. (2015). Time course of biochemical , physiological , and molecular responses to field-mimicked conditions of drought , salinity , and recovery in two maize lines. 6, 1–15. doi:10.3389/fpls.2015.00314.

Morgante, M., Paoli, E. De, and Radovic, S. (2007). Transposable elements and the plant pan-genomes. *Curr. Opin. Plant Biol.* 10,

149–155. doi:10.1016/j.pbi.2007.02.001.

Moya, J. L., Primo-Millo, E., and Talon, M. (1999). Morphological factors determining salt tolerance in citrus seedlings: The shoot to root ratio modulates passive root uptake of chloride ions and their accumulation in leaves. *Plant, Cell Environ.* 22, 1425–1433. doi:10.1046/j.1365-3040.1999.00495.x.

Munns, R. (1993). Physiological processes limiting plant growth in saline soils: some dogmas and hypotheses. *Plant. Cell Environ.* 16, 15–24.

Munns, R. (2002a). Comparative physiology of salt and water stress. *Plant. Cell Environ.* 25, 239–250. doi:10.1046/j.0016-8025.2001.00808.x.

Munns, R. (2002b). Comparative physiology of salt and water stress. *Plant Cell Env.* 25, 239–250. doi:10.1046/j.0016-8025.2001.00808.x.

Munns, R. (2005). Genes and Salt Tolerance. *New Phytol.* 167, 645–663.

Munns, R., Day, D. A., Fricke, W., Watt, M., Arsova, B., Barkla, B. J., et al. (2019). Energy costs of salt tolerance in crop plants. *New Phytol.* doi:10.1111/nph.15864.

Munns, R., and Gilliham, M. (2015). Salinity tolerance of crops - what is the cost ? Tansley insight Salinity tolerance of crops – what is the cost ? doi:10.1111/nph.13519.

Munns, R., James, R. A., Gilliham, M., Flowers, T. J., and Colmer, T. D. (2016). Tissue tolerance: an essential but elusive trait for salt-tolerant crops. *Funct. Plant Biol.* 43, 1103–1113. doi:10.1071/FP16187.

Munns, R., James, R. A., and Läuchli, A. (2006). Approaches to increasing the salt tolerance of wheat and other cereals. *J. Exp. Bot.* 57, 1025–1043. doi:10.1093/jxb/erj100.

Munns, R., Schachtman, D. P., and Condon, A. G. (1995). The Significance of a Two-Phase Growth Response to Salinity in Wheat and Barley. *Aust. J. Plant Physiol.* 22, 561–569. doi:10.1071/PP9950561.

Munns, R., and Tester, M. (2008). Mechanisms of salinity tolerance. *Annu. Rev. Plant Biol.* 59, 651–81. doi:10.1146/annurev.arplant.59.032607.092911.

Murillo-Amador, B., Troyo-Diéguez, E., García-Hernández, J. L., López-Aguilar, R., Ávila-Serrano, N. Y., Zamora-Salgado, S., et

al. (2006). Effect of NaCl salinity in the genotypic variation of cowpea (Vigna unguiculata) during early vegetative growth. *Sci. Hortic. (Amsterdam).* 108, 423–431. doi:10.1016/j.scienta.2006.02.010.

Mussig, C. (2003). Brassinosteroids Promote Root Growth in Arabidopsis. *Plant Physiol.* 133, 1261–1271. doi:10.1104/pp.103.028662.

Nahnsen, S., Bielow, C., Reinert, K., and Kohlbacher, O. (2013). Tools for Label-free Peptide Quantification <sup/>. *Mol. Cell. Proteomics* 12, 549–556. doi:10.1074/mcp.R112.025163.

Nannas, N. J., and Dawe, R. K. (2015). Genetic and Genomic Toolbox of Zea mays. *Genetics* 199, 655–669. doi:10.1534/genetics.114.165183.

Negi, N. P., Shrivastava, D. C., Sharma, V., Sarin, N. B., Prabha, N., Divya, N., et al. (2015). Overexpression of CuZnSOD from Arachis hypogaea alleviates salinity and drought stress in tobacco. *Plant Cell Rep.* 34, 1109–1126. doi:10.1007/s00299-015-1770-4.

Negrão, S., Schmöckel, S. M., and Tester, M. (2017). Evaluating physiological responses of plants to salinity stress. *Ann. Bot.* 119, 1–11. doi:10.1093/aob/mcw191.

Neilson, K. A., Ali, N. A., Muralidharan, S., Mirzaei, M., Mariani, M., Assadourian, G., et al. (2011). Less label, more free: Approaches in label-free quantitative mass spectrometry. *Proteomics* 11, 535–553. doi:10.1002/pmic.201000553.

Nelson, C. J., and Millar, A. H. (2015). Protein turnover in plant biology. 1, 1–7. doi:10.1038/NPLANTS.2015.17.

Ness, R. O., Sachs, K., and Vitek, O. (2016). From Correlation to Causality: Statistical Approaches to Learning Regulatory Relationships in Large-Scale Biomolecular Investigations. *J. Proteome Res.* 15, 683–690. doi:10.1021/acs.jproteome.5b00911.

Neto, A. D. de A., Prisco, J. T., Enéas-Filho, J., Lacerda, C. F. De, De Azevedo Neto, A. D., Prisco, J. T., et al. (2004). Effects of salt stress on plant growth, stomatal response and solute accumulation of different maize genotypes. *Brazilian J. Plant Physiol.* 16, 31–38. doi:10.1590/S1677-04202004000100005.

Neumann, P. M., Azaizeh, H., and Leon, D. (1994). Hardening of root cell walls: a growth inhibitory response to salinity stress. *Plant.*

Cell Environ. 17, 303–309.

Newton, R. P., and Smith, C. J. (2004). Cyclic nucleotides. *Phytochemistry* 65, 2423–2437. doi:10.1016/j.phytochem.2004.07.026.

Nguyen, H. T., Leipner, J., Stamp, P., and Guerra-Peraza, O. (2009). Plant Physiology and Biochemistry Low temperature stress in maize (Zea mays L .) induces genes involved in photosynthesis and signal transduction as studied by suppression subtractive hybridization. *Plant Physiol. Biochem.* 47, 116–122. doi:10.1016/j.plaphy.2008.10.010.

Niu, G., Xu, W., Rodriguez, D., and Sun, Y. (2012). Growth and Physiological Responses of Maize and Sorghum Genotypes to Salt Stress. *ISRN Agron.* 2012, 1–12. doi:10.5402/2012/145072.

Nogueira, S. S. S., Nagai, V., Braga, N. R., Novo, M. D. O. C. S. S., and Camargo, M. B. P. (1994). Growth analysis of chickpea (Cicer arietinum L .). *Sci. Agric.* 51, 430–435.

Nohzadeh Malakshah, S., Habibi Rezaei, M., Heidari, M., and Hosseini Salekdeh, G. (2007). Proteomics Reveals New Salt Responsive Proteins Associated with Rice Plasma Membrane. *Biosci. Biotechnol. Biochem.* 71, 2144–2154. doi:10.1271/bbb.70027.

O'Farrell, P. H. (1975). High resolution two-dimensional electrophoresis of proteins. *J. Biol. Chem.* 250, 4007–4021. doi:10.1016/j.bbi.2008.05.010.

Oliver, S. (2000). Guilt-by-association goes global. 403, 601–603.

Olsen, J. V., Ong, S.-E., and Mann, M. (2004). Trypsin Cleaves Exclusively C-terminal to Arginine and Lysine Residues. *Mol. Cell. Proteomics* 3, 608–614. doi:10.1074/mcp.T400003-MCP200.

Omidbakhshfard, M. A., Omranian, N., Ahmadi, F. S., Nikoloski, Z., and Mueller-Roeber, B. (2012). Effect of salt stress on genes encoding translation-associated proteins in Arabidopsis thaliana. *Plant Signal. Behav.* 7, 1095–102. doi:10.4161/psb.21218.

Pang, Q., Chen, S., Dai, S., Chen, Y., Wang, Y., and Yan, X. (2010). Comparative Proteomics of Salt Tolerance in Arabidopsis thaliana and Thellungiella halophila research articles. 2584–2599.

Pappin, D. J. C., Hojrup, P., and Bleasby, A. J. (1993). Rapid identification of proteins by peptide-mass fingerprinting. *Curr. Biol.* 3, 327–332. doi:10.1016/0960-9822(93)90195-T.

Passardi, F., Longet, D., Penel, C., and Dunand, C. (2004a). The class III peroxidase multigenic family in rice and its evolution in land plants q , qq. *Phytochemistry* 65, 1879–1893. doi:10.1016/j.phytochem.2004.06.023.

Passardi, F., Penel, C., and Dunand, C. (2004b). Performing the paradoxical : how plant peroxidases modify the cell wall. 9. doi:10.1016/j.tplants.2004.09.002.

Passioura, J. B. (2012). Phenotyping for drought tolerance in grain crops. *Funct. Plant Biol.* 39, 851–859.

Passioura, J. B., and Munns, R. (2000). Rapid environmental changes that affect leaf water status induce transient surges or pauses in leaf expansion rate. *Aust. J. Plant Physiol.* 27, 941–948. doi:10.1071/PP99207.

Patterson, S. D., and Aebersold, R. H. (2003). Proteomics: The first decade and beyond. *Nat. Genet.* 33, 311–323. doi:10.1038/ng1106.

Pearce, G., Moura, D. S., Stratmann, J., and Ryan, C. a (2001). RALF, a 5-kDa ubiquitous polypeptide in plants, arrests root growth and development. *PNAS* 98, 12843–12847 PLANT.

Peng, X., Ding, X., Chang, T., Wang, Z., Liu, R., Zeng, X., et al. (2014). Overexpression of a Vesicle Trafficking Gene , OsRab7 , Enhances Salt Tolerance in Rice. 2014.

Permentier, H. P., and Bruins, A. P. (2004). Electrochemical oxidation and cleavage of proteins with on-line mass spectrometric detection: Development of an instrumental alternative to enzymatic protein digestion. *J. Am. Soc. Mass Spectrom.* 15, 1707–1716. doi:10.1016/j.jasms.2004.09.003.

Permentier, H. P., Jurva, U., Barroso, B., and Bruins, A. P. (2003). Electrochemical oxidation and cleavage of peptides analyzed with on-line mass spectrometric detection. *Rapid Commun. Mass Spectrom.* 17, 1585–1592. doi:10.1002/rcm.1090.

Pingali, P. L., and Pandey, S. (2000). Meeting World Maize Needs: Technological Opportunities and Priorities for the Public Sector. *2000 CIMMYT World Maize Facts Trends*.

Pinu, F. R., Beale, D. J., Paten, A. M., Kouremenos, K., Swarup, S., Schirra, H. J., et al. (2019). Systems biology and multi-omics integration: Viewpoints from the metabolomics research community. *Metabolites* 9, 1–31. doi:10.3390/metabo9040076.

Pitann, B., Mohamed, A. K., Neubert, A. B., and Schubert, S. (2013).

Tonoplast Na+/H+ antiporters of newly developed maize (Zea mays) hybrids contribute to salt resistance during the second phase of salt stress. *J. Plant Nutr. Soil Sci.* 176, 148–156. doi:10.1002/jpln.201200597.

Plaxton, W. C. (1996). The organization and regulation of plant glycolysis. *Annu. Rev. Plant Physiol. Plant Mol. BioI* 47, 185–214.

Podwojski, K., Eisenacher, M., Kohl, M., Turewicz, M., Meyer, H. E., Rahnenführer, J., et al. (2010). Peek a peak: A glance at statistics for quantitative label-free proteomics. *Expert Rev. Proteomics* 7, 249–261. doi:10.1586/epr.09.107.

Ponnala, L., Wang, Y., Sun, Q., and Van Wijk, K. J. (2014). Correlation of mRNA and protein abundance in the developing maize leaf. *Plant J.* 78, 424–440. doi:10.1111/tpj.12482.

Poorter, H., Niinemets, Ü., Poorter, L., Wright, I. J., Villar, R., Niinemets, U., et al. (2009). Causes and consequences of variation in leaf mass per area (LMA):a meta-analysis. *New Phytol.* 182, 565–588. doi:10.1111/j.1469-8137.2009.02830.x.

Potts, S. G., Imperatriz-fonseca, V., Ngo, H. T., Aizen, M. A., Biesmeijer, J. C., and Breeze, T. D. (2016). Safeguarding pollinators and their values to human well-being. *Nat. Publ. Gr.* 540, 220–229. doi:10.1038/nature20588.

Prasanna, B. M. (2012). Diversity in global maize germplasm: Characterization and utilization. *J. Biosci.* 37, 843–855. doi:10.1007/s12038-012-9227-1.

Qiu, J., Henderson, S. W., Tester, M., Roy, S. J., and Gilliham, M. (2017). SLAH1, a homologue of the slow type anion channel SLAC1, modulates shoot Cl-accumulation and salt tolerance in Arabidopsis thaliana. *J. Exp. Bot.* 68, 4495–4505. doi:10.1093/jxb/erw237.

Qiu, Q.-S., Guo, Y., Dietrich, M. A., Schumaker, K. S., and Zhu, J.-K. (2002). Regulation of SOS1, a plasma membrane Na+/H+ exchanger in Arabidopsis thaliana, by SOS2 and SOS3. *Proc. Natl. Acad. Sci.* 99, 8436–8441. doi:10.1073/pnas.122224699.

Ramesh, S. A., Tyerman, S. D., Xu, B., Bose, J., Kaur, S., Conn, V., et al. (2015). GABA signalling modulates plant growth by directly regulating the activity of plant-specific anion transporters. *Nat. Commun.* 6, 1–10. doi:10.1038/ncomms8879.

Rao, A. Q., Din, S. ud, Akhtar, S., Sarwar, M. B., Ahmed, M., Rashid,

B., et al. (2016). “Genomics of Salinity Tolerance in Plants,” in *Plant Genomics*, ed. I. Y. Abdurakhmonov (IntechOpen), 273–299.

Rao, S. A., and Mcneilly, T. (1999). Genetic basis of variation for salt tolerance in maize (Zea mays L). *Euphytica* 108, 145–150. doi:10.1023/a:1003612411293.

Raven, J. (1985). Regulation of pH and generation of osmolarity in vascular plants: a cost-benefit analysis in relation to efficiency of use of energy, nitrogen and water. *New Phytol.* 101, 25–77. doi:10.1111/j.1469-8137.1985.tb02816.x.

Rayle, D. L., and Cleland, R. E. (1992). The Acid Growth Theory of auxin-induced cell elongation is alive and well. *Plant Physiol.* 99, 1271–1274. doi:10.1104/pp.99.4.1271.

Rea, P. A., and Poole, R. J. (1993). Vacuolar H+ -Translocating Pyrophosphatase. *Annu. Rev. Plant Physiol. Plant Mol. BioI* 44, 157–80. doi:10.1146/annurev.pp.44.060193.001105.

Ren, Z. H., Gao, J. P., Li, L. G., Cai, X. L., Huang, W., Chao, D. Y., et al. (2005). A rice quantitative trait locus for salt tolerance encodes a sodium transporter. *Nat. Genet.* 37, 1141–1146. doi:10.1038/ng1643.

Rengasamy, P., Chittleborough, D., and Helyar, K. (2003). Root-zone constraints and plant-based solutions for dryland salinity. *Plant Soil* 257, 249–260.

Rieger, R., Michaelis, A., and Green, M. M. (1991). *Glossary of Genetics: Classical and Molecular*. Springer-Verlag Berlin Heidelberg doi:10.1016/0307-4412(91)90089-Q.

Río, L. A. del, Sandalio, L. M., Corpas, F. J., Palma, M., and Barroso, J. B. (2006). Reactive Oxygen Species and Reactive Nitrogen Species in Peroxisomes. Production, Scavenging, and Role in Cell Signaling. 141, 330–335. doi:10.1104/pp.106.078204.

Rodriguez, H. G., Roberts, J., Jordan, W. R., and Drew, M. C. (1997). Growth, water relations, and accumulation of organic and inorganic solutes in roots of maize seedlings during salt stress. *Plant Physiol.* 113, 881–893. doi:10.1104/PP.113.3.881.

Roshandel, P., and Flowers, T. (2009). The ionic effects of NaCl on physiology and gene expression in rice genotypes differing in salt tolerance. 135–147. doi:10.1007/s11104-008-9738-6.

Roy, S. J., Negrão, S., Tester, M., and Roy, S. J. (2014). Salt resistant crop plants. *Curr. Opin. Biotechnol.* 26, 115–124.

doi:10.1016/j.copbio.2013.12.004.

Ryan, C. A., Pearce, G., Scheer, J., and Moura, D. S. (2001). Polypeptide hormones. *Plant Physiol.* 28 Suppl, 65–68. doi:10.1105/tpc.010484.

Saavedra, L., Svensson, J., Carballo, V., and Izmendi, D. (2006). A dehydrin gene in Physcomitrella patens is required for salt and osmotic stress tolerance. 237–249. doi:10.1111/j.1365-313X.2005.02603.x.

Sairam, R. K., Rao, K. V, and Srivastava, G. C. (2002). Differential response of wheat genotypes to long term salinity stress in relation to oxidative stress, antioxidant activity and osmolyte concentration. *Plant Sci.* 163, 1037–1046. doi:10.1016/S0168-9452(02)00278-9.

Saneoka, H., Nagasaka, C., Hahn, D. T., Yang, W., Premachandra, G. S., Joly, R. J., et al. (1995). Salt Tolerance of Glycinebetaine-Deficient and -Containing. *Plant Physiol.* 107, 631–638.

Sawahel, W. A., and Hassan, A. H. (2002). Generation of transgenic wheat plants producing high levels of the osmoprotectant proline. *Biotechnol. Lett.* 24, 721–725. doi:10.1023/A:1015294319114.

Saxena, M., Roy, S. D., Sopory, S. K., and Bhalla-sarin, N. (2011). Overexpression of the Glyoxalase II Gene Leads to Enhanced Salinity Tolerance in Brassica Juncea. 23–28.

Scudiero, E., Skaggs, T. H., and Corwin, D. L. (2015). Regional-scale soil salinity assessment using Landsat ETM+ canopy reflectance. *Remote Sens. Environ.* 169, 335–343. doi:10.1016/j.rse.2015.08.026.

Shabala, S. (2013). Learning from halophytes: Physiological basis and strategies to improve abiotic stress tolerance in crops. *Ann. Bot.* 112, 1209–1221. doi:10.1093/aob/mct205.

Shabala, S., Chakraborty, K., Bose, J., Shabala, L., and Eyles, A. (2016). Evaluating relative contribution of osmotolerance and tissue tolerance mechanisms toward salinity stress tolerance in three Brassica species. *Physiol. Plant.* 158, 135–151. doi:10.1111/ppl.12447.

Shannon, P., Markiel, A., Owen Ozier, Baliga, N. S., Wang, J. T., Ramage, D., et al. (2003). Cytoscape: a software environment for integrated models of biomolecular interaction networks. *Genome Res.* 13, 2498–2504. doi:10.1101/gr.1239303.metabolite.

Sharma, P., Jha, A. B., Dubey, R. S., and Pessarakli, M. (2012).

Reactive Oxygen Species, Oxidative Damage, and Antioxidative Defense Mechanism in Plants under Stressful Conditions. *J. Bot.* 2012, 1–26. doi:10.1155/2012/217037.

Sharp, R. E., Poroyko, V., Hejlek, L. G., Spollen, W. G., Springer, G. K., Bohnert, H. J., et al. (2018). Root growth maintenance during water deficits : physiology to functional genomics *. 55, 2343–2351. doi:10.1093/jxb/erh276.

Shendure, J., and Ji, H. (2008). Next-generation DNA sequencing. 26, 1135–1145. doi:10.1038/nbt1486.

Shi, H., Quintero, F. J., Pardo, J. M., and Zhu, J. K. (2002). The putative plasma membrane Na^+/H^+ antiporter SOS1 controls long-distance Na^+transport in plants. *Plant Cell* 14, 465–477. doi:10.1105/tpc.010371.et.

Shirasawa, K., Takabe, T., Takabe, T., and Kishitani, S. (2006). Accumulation of glycinebetaine in rice plants that overexpress choline monooxygenase from spinach and evaluation of their tolerance to abiotic stress. *Ann. Bot.* 98, 565–571. doi:10.1093/aob/mcl126.

Singh, M., Kumar, J., Singh, S., Singh, V. P., and Prasad, S. M. (2015). Roles of osmoprotectants in improving salinity and drought tolerance in plants: a review. *Rev. Environ. Sci. Biotechnol.* 14, 407–426. doi:10.1007/s11157-015-9372-8.

Sjogren, L. L. E., Stanne, T. M., Zheng, B., Sutinen, S., and Clarke, A. K. (2006). Structural and Functional Insights into the Chloroplast ATP-Dependent Clp Protease in Arabidopsis. *Plant Cell Online* 18, 2635–2649. doi:10.1105/tpc.106.044594.

Slabu, C., Zörb, C., Steffens, D., and Schubert, S. (2009). Is salt stress of faba bean (Vicia faba) caused by Na + or Cl – toxicity ? 644–650. doi:10.1002/jpln.200900052.

Smithies, O., and Poulik, M. (1956). Two-Dimensional Electrophoresis of Serum Proteins. *Nature* 177, 1033. doi:10.1038/1771033a0.

Sonmez, S., Buyuktas, D., Okturen, F., and Citak, S. (2008). Assessment of different soil to water ratios (1:1, 1:2.5, 1:5) in soil salinity studies. *Geoderma* 144, 361–369. doi:10.1016/j.geoderma.2007.12.005.

Staal, M., Maathuis, F. J. M., Elzenga, J. T. M., Overbeek, J. H. M., and Prins, H. B. A. (1991). Na+/H+ antiport activity in tonoplast vesicles from roots of the salt-tolerant Plantago maritima and the salt-sensitive Plantago media. *Physiol. Plant.* 82, 179–184.

doi:10.1111/j.1399-3054.1991.tb00078.x.

Stelpflug, S. C., Sekhon, R. S., Vaillancourt, B., Hirsch, C. N., Buell, C. R., de Leon, N., et al. (2016). An expanded maize gene expression atlas based on RNA sequencing and its use to explore root development. *Plant Genome* 9. doi:10.3835/plantgenome2015.04.0025.

Stephenson, E., Estrada, S., Meng, X., Ourada, J., Muszynski, G., Habben, J. E., et al. (2019). Over-expression of the photoperiod response regulator ZmCCT10 modifies plant architecture , flowering time and inflorescence morphology in maize. 1–32.

Sul, J.-Y., Wu, C. K., Zeng, F., Jochems, J., Lee, M. T., Kim, T. K., et al. (2009). Transcriptome transfer produces a predictable cellular phenotype. *Proc. Natl. Acad. Sci. U. S. A.* 106, 7624–9. doi:10.1073/pnas.0902161106.

Sunarpi, Horie, T., Motoda, J., Kubo, M., Yang, H., Yoda, K., et al. (2005). Enhanced salt tolerance mediated by AtHKT1 transporter-induced Na+unloading from xylem vessels to xylem parenchyma cells. *Plant J.* 44, 928–938. doi:10.1111/j.1365-313X.2005.02595.x.

Suo, J., Zhao, Q., David, L., Chen, S., and Dai, S. (2017). Salinity response in chloroplasts: Insights from gene characterization. *Int. J. Mol. Sci.* 18. doi:10.3390/ijms18051011.

Surekha, C., Kumari, K. N., Aruna, L. V., Suneetha, G., Arundhati, A., and Kavi Kishor, P. B. (2014). Expression of the Vigna aconitifolia P5CSF129A gene in transgenic pigeonpea enhances proline accumulation and salt tolerance. *Plant Cell. Tissue Organ Cult.* 116, 27–36. doi:10.1007/s11240-013-0378-z.

Surender Reddy, P., Jogeswar, G., Rasineni, G. K., Maheswari, M., Reddy, A. R., Varshney, R. K., et al. (2015). Proline over-accumulation alleviates salt stress and protects photosynthetic and antioxidant enzyme activities in transgenic sorghum [Sorghum bicolor (L.) Moench]. *Plant Physiol. Biochem.* 94, 104–113. doi:10.1016/j.plaphy.2015.05.014.

Swanson-wagner, R. A., Eichten, S. R., Kumari, S., Tiffin, P., Stein, J. C., Ware, D., et al. (2010). Pervasive gene content variation and copy number variation in maize and its undomesticated progenitor. *Genome Res.* 20, 1689–1699. doi:10.1101/gr.109165.110.20.

Switzar, L., Giera, M., and Niessen, W. M. A. (2013). Protein digestion: An overview of the available techniques and recent

developments. *J. Proteome Res.* 12, 1067–1077. doi:10.1021/pr301201x.

Tackenberg, O. (2007). A new method for non-destructive measurement of biomass, growth rates, vertical biomass distribution and dry matter content based on digital image analysis. *Ann. Bot.* 99, 777–783. doi:10.1093/aob/mcm009.

Taiz, L., and Zeiger, E. (2002). "Photosynthesis: The Light Reactions," in *Plant Physiology, 3rd Edition* (Sinauer Associates Inc), 111–143. doi:10.1136/bmj.2.4842.923-b.

Taiz, L., and Zeiger, E. (2010a). "Abscisic Acid: A Seed Maturation and Antistress Signal," in *Plant Physiology* (Sinauer Associates, Inc.), 539–558.

Taiz, L., and Zeiger, E. (2010b). "Respiration and lipid metabolism," in *Plant Physiology* (Sinauer Associates Inc), 223–258.

Tan, M. (2010). Plant Physiology and Biochemistry Analysis of DNA methylation of maize in response to osmotic and salt stress based on methylation-sensitive ampli fi ed polymorphism. *Plant Physiol. Biochem.* 48, 21–26. doi:10.1016/j.plaphy.2009.10.005.

Tang, M., Liu, X., Deng, H., and Shen, S. (2011). Plant Science Over-expression of JcDREB , a putative AP2 / EREBP domain-containing transcription factor gene in woody biodiesel plant Jatropha curcas , enhances salt and freezing tolerance in transgenic Arabidopsis thaliana. *Plant Sci.* 181, 623–631. doi:10.1016/j.plantsci.2011.06.014.

Tavakkoli, E., Rengasamy, P., and Mcdonald, G. K. (2010). High concentrations of Na+ and Cl- ions in soil solution have simultaneous detrimental effects on growth of faba bean under salinity stress. *J. Exp. Bot.* 61, 4449–4459. doi:10.1093/jxb/erq251.

Teakle, N. L., and Tyerman, S. D. (2010). Mechanisms of Cl - transport contributing to salt tolerance. *Plant, cell Environ. Environ.* 33, 566–589. doi:10.1111/j.1365-3040.2009.02060.x.

Tessmer, O. L., Jiao, Y., Cruz, J. A., Kramer, D. M., and Chen, J. (2013). Functional approach to high-throughput plant growth analysis. *BMC Syst. Biol.* 7, S17. doi:10.1186/1752-0509-7-S6-S17.

Tester, M., and Davenport, R. (2003). Na+ Tolerance and Na+ Transport in Higher Plants. *Ann. Bot.* 91, 503–527. doi:10.1093/aob/mcg058.

Tiwari, V., Patel, M. K., Chaturvedi, A. K., Mishra, A., and Jha, B. (2019). Cloning and functional characterization of the Na+/H+ antiporter (NHX1) gene promoter from an extreme halophyte Salicornia brachiata. *Gene* 683, 233–242. doi:10.1016/j.gene.2018.10.039.

Torres, M. A., and Dangl, J. L. (2005). Functions of the respiratory burst oxidase in biotic interactions , abiotic stress and development. *Curr. Opin. Plant Biol.* 8, 397–403. doi:10.1016/j.pbi.2005.05.014.

Troyer, A. F., and Larkins, J. R. (1985). Selection for Early Flowering in Corn: 10 Late Synthetics. *Crop Sci.* 25, 695—697. doi:10.2135/cropsci1985.0011183X002500040029x.

Ünlü, M., Morgan, M. E., and Minden, J. S. (1997). Difference gel electrophoresis: A single gel method for detecting changes in protein extracts. *Electrophoresis* 18, 2071–2077. doi:10.1002/elps.1150181133.

Valdez-aguilar, L. A., Grieve, C. M., Razak-mahar, A., Mcgiffen, M. E., and Merhaut, D. J. (2011). Growth and Ion Distribution Is Affected by Irrigation with Saline Water in Selected Landscape Species Grown in Two Consecutive Growing Seasons : Spring – summer and Fall – winter. 46, 632–642.

Van Den Wijngaard, P. W. J., Sinnige, M. P., Roobeek, I., Reumer, A., Schoonheim, P. J., Mol, J. N. M., et al. (2005). Abscisic acid and 14-3-3 proteins control K+ channel activity in barley embryonic root. *Plant J.* 41, 43–55. doi:10.1111/j.1365-313X.2004.02273.x.

Van Wesemael, J., Hueber, Y., Kissel, E., Campos, N., Swennen, R., and Carpentier, S. (2018). Homeolog expression analysis in an allotriploid non-model crop via integration of transcriptomics and proteomics. *Sci. Rep.* 8, 1–11. doi:10.1038/s41598-018-19684-5.

Vanhove, A. C., Vermaelen, W., Cenci, A., Swennen, R., and Carpentier, S. C. (2015). A look behind the screens: Characterization of the HSP70 family during osmotic stress in a non-model crop. *J. Proteomics* 119, 10–20. doi:10.1016/j.dib.2015.01.008.

Veeranagamallaiah, G., Jyothsnakumari, G., Thippeswamy, M., Chandra Obul Reddy, P., Surabhi, G. K., Sriranganayakulu, G., et al. (2008). Proteomic analysis of salt stress responses in foxtail millet (Setaria italica L. cv. Prasad) seedlings. *Plant Sci.* 175, 631–641. doi:10.1016/j.plantsci.2008.06.017.

Vierstra, R. D. (1996). Proteolysis in plants: Mechanisms and

functions. *Plant Mol. Biol.* 32, 275–302. doi:10.1007/BF00039386.

Volkov, V. (2015). Salinity tolerance in plants. Quantitative approach to ion transport starting from halophytes and stepping to genetic and protein engineering for manipulating ion fluxes. *Front. Plant Sci.* 6, 873. doi:10.3389/fpls.2015.00873.

Vollbrecht, E., and Schmidt, R. J. (2003). "Development of the Inflorescences," in *Handbook of Maize: Its Biology*, eds. J. L. Bennetzen and S. C. Hake (Springer), 13–40.

Voyksner, R. D., and Lee, H. (1999). Investigating the use of an octupole ion guide for ion storage and high-pass mass filtering to improve the quantitative performance of electrospray ion trap mass spectrometry. *Rapid Commun. Mass Spectrom.* 13, 1427–1437. doi:10.1002/(SICI)1097-0231(19990730)13:14<1427::AID-RCM662>3.0.CO;2-5.

Walker, B. J., Busch, F. A., Driever, S. M., Kromdijk, J., and Lawson, T. (2018). "Survey of tools for measuring in vivo photosynthesis," in *Methods in Molecular Biology*, ed. Sarah Covshoff (ed.) (Springer Science+Business Media), 3–24. doi:10.1007/978-1-4939-7786-4_1.

Walley, J. W., Sartor, R. C., Shen, Z., Schmitz, R. J., Ecker, J. R., and Briggs, S. P. (2013a). Integration of omic networks in a developmental atlas of maize. 0–5. doi:10.5061/dryad.v8969.

Walley, J. W., Shen, Z., Sartor, R., Wu, K. J., Osborn, J., Smith, L. G., et al. (2013b). Reconstruction of protein networks from an atlas of maize seed proteotypes. *Proc. Natl. Acad. Sci.* 110, E4808–E4817. doi:10.1073/pnas.1319113110.

Walls, D., and Loughran, S. (2017). *Methods in Molecular Biology: Protein Chromatography*. , eds. D. Walls and S. T. Loughran New York, NY: Humana Press doi:10.1007/978-1-4939-6412-3.

Walter, A., Liebisch, F., and Hund, A. (2015). Plant phenotyping: From bean weighing to image analysis. *Plant Methods* 11, 1–11. doi:10.1186/s13007-015-0056-8.

Wang, D. G., Fan, J., Siao, C., Berno, A., Young, P., Sapolsky, R., et al. (1998). Large-Scale Identification , Mapping , and Genotyping of Single-Nucleotide Polymorphisms in the Human Genome. *Science (80-.).* 280, 1077–1082.

Wang, J., Ding, H., Zhang, A., Ma, F., Cao, J., and Jiang, M. (2010). A Novel Mitogen-Activated Protein Kinase Gene in Maize (Zea

mays), ZmMPK3 , is Involved in Response to Diverse Environmental Cues. *J. Integr. Plant Biol.* 52, 442–452. doi:10.1111/j.1744-7909.2010.00906.x.

Wang, J., Meng, Y., Li, B., Ma, X., Lai, Y., Si, E., et al. (2015a). Physiological and proteomic analyses of salt stress response in the halophyte Halogeton glomeratus. 655–669. doi:10.1111/pce.12428.

Wang, M., Wang, Y., Sun, J., Ding, M., Deng, S., Hou, P., et al. (2013). Plant Physiology and Biochemistry Overexpression of PeHA1 enhances hydrogen peroxide signaling in salt-stressed Arabidopsis. *Plant Physiol. Biochem.* 71, 37–48. doi:10.1016/j.plaphy.2013.06.020.

Wang, M., Zhao, X., Xiao, Z., Yin, X., Xing, T., and Xia, G. (2016). A wheat superoxide dismutase gene TaSOD2 enhances salt resistance through modulating redox homeostasis by promoting NADPH oxidase activity. *Plant Mol. Biol.* 91, 115–130. doi:10.1007/s11103-016-0446-y.

Wang, S., Su, S. Z., Wu, Y., Li, S. P., Shan, X. H., Liu, H. K., et al. (2015b). Overexpression of maize chloride channel gene ZmCLC-d in Arabidopsis thaliana improved its stress resistance. 59, 55–64. doi:10.1007/s10535-014-0468-8.

Wang, W., Chen, D., Zhang, X., Liu, D., and Cheng, Y. (2018). Role of plant respiratory burst oxidase homologs in stress responses. *Free Radic. Res.* 52, 826–839. doi:10.1080/10715762.2018.1473572.

Wang, W., Vinocur, B., Shoseyov, O., and Altman, A. (2004). Role of plant heat-shock proteins and molecular chaperones in the abiotic stress response. 9, 13–15. doi:10.1016/j.tplants.2004.03.006.

Washburn, M. P., Wolters, D., and Yates, J. R. (2001). Large-scale analysis of the yeast proteome by multidimensional protein identification technology. *Nat. Biotechnol.* 19, 242–247. doi:10.1038/85686.

White, P. J., and Broadley, M. R. (2001). Chloride in Soils and its Uptake and Movement within the Plant : A Review. *Ann. Bot.* 88, 967–988. doi:10.1006/anbo.2001.1540.

Wilkins, M. R., and Hochstrasser, D. F. (1997). “Introduction to the proteome,” in *Proteome research: new frontiers in functional genomics*, eds. M. R. Wilkins, K. L. Williams, R. D. Appel, and D. F. Hochstrasser (Springer Heidelberg), 1–11.

Wilkinson, S., and Davies, W. J. (1997). Xylem Sap pH Increase: A Drought Signal Received at the Apoplastic Face of the Guard Cell That Involves the Suppression of Saturable Abscisic Acid Uptake by the Epidermal Symplast. *Plant Physiol.* 113, 559–573. doi:10.1104/PP.113.2.559.

Wilm, M. (2011). Principles of Electrospray Ionization. *Mol. Cell. Proteomics* 10, M111.009407. doi:10.1074/mcp.M111.009407.

Wu, C., Tran, J. C., Zamdborg, L., Durbin, K. R., Li, M., Ahlf, D. R., et al. (2012). A protease for "middle-down" proteomics. *Nat. Methods* 9, 822–824. doi:10.1038/nmeth.2074.

Wu, S. L., Hühmer, A. F. R., Hao, Z., and Karger, B. L. (2007). On-line LC-MS approach combining collision-induced dissociation (CID), electron-transfer dissociation (ETD), and CID of an isolated charge-reduced species for the trace-level characterization of proteins with post-translational modifications. *J. Proteome Res.* 6, 4230–4244. doi:10.1021/pr070313u.

Wu, S. L., Kim, J., Hancock, W. S., and Karger, B. (2005). Extended Range Proteomic Analysis (ERPA): A new and sensitive LC-MS platform for high sequence coverage of complex proteins with extensive post-translational modifications-comprehensive analysis of beta-casein and Epidermal Growth Factor Receptor (EGFR). *J. Proteome Res.* 4, 1155–1170. doi:10.1021/pr050113n.

Xu, J., Xing, X. J., Tian, Y. S., Peng, R. H., Xue, Y., Zhao, W., et al. (2015). Transgenic Arabidopsis plants expressing tomato glutathione S-transferase showed enhanced resistance to salt and drought stress. *PLoS One* 10, 1–16. doi:10.1371/journal.pone.0136960.

Yan, J., Tang, H., Huang, Y., Shi, Y., Li, J., and Zheng, Y. (2003). Dynamic analysis of QTL for plant height at different developmental stages in maize (Zea mays L.). *Chinese Sci. Bull.* 48, 2601–2607. doi:10.1360/03wc0044.

Yang, X., Liang, Z., Wen, X., and Lu, C. (2008). Genetic engineering of the biosynthesis of glycinebetaine leads to increased tolerance of photosynthesis to salt stress in transgenic tobacco plants. *Plant Mol. Biol.* 66, 73–86. doi:10.1007/s11103-007-9253-9.

Yeo, A. R., and Flowers, T. J. (1983). Varietal differences in the toxicity of sodium ions in rice leaves. *Physiol. Plant.* 59, 189–195. doi:10.1111/j.1399-3054.1983.tb00756.x.

Yin, X., McClure, M. A., Jaja, N., Tyler, D. D., and Hayes, R. M.

(2011). In-season prediction of corn yield using plant height under major production systems. *Agron. J.* 103, 923–929. doi:10.2134/agronj2010.0450.

Ying, H., Xiao-xia, Z., Yi-hong, L. I., Jian-zhou, D., Han-mei, D. U., Zhuo, Z., et al. (2018). Overexpression of the Suaeda salsa SsNHX1 gene confers enhanced salt and drought tolerance to transgenic Zea mays. *J. Integr. Agric.* 17, 2612–2623. doi:10.1016/S2095-3119(18)61998-7.

Yu, Y., Li, Y., Jia, F., Zhao, M., Li, W., Sun, Q., et al. (2017). ZmFKBP20-1 improves the Drought and Salt Tolerance of Transformed Arabidopsis. *J. Plant Biol.* 60, 558–570. doi:10.1007/s12374-017-0262-1.

Yu, Y., Zhang, H., Li, W., Mu, C., Zhang, F., Wang, L., et al. (2012). Genome-wide analysis and environmental response pro fi ling of the FK506-binding protein gene family in maize (Zea mays L .). *Gene* 498, 212–222. doi:10.1016/j.gene.2012.01.094.

Zhang, M., Cao, Y., Wang, Z., Wang, Z., Shi, J., Liang, X., et al. (2018). A retrotransposon in an HKT1 family sodium transporter causes variation of leaf Na + exclusion and salt tolerance in maize. *New Phytol.* 217, 1161–1176. doi:10.1111/nph.14882.

Zhao, J., and Grafi, G. (2000). The high mobility group I/Y protein is hypophosphorylated in endoreduplicating maize endosperm cells and is involved in alleviating histone H1-mediated transcriptional repression. *J. Biol. Chem.* 275, 27494–27499. doi:10.1074/jbc.M001711200.

Zhao, K., Käs, E., Gonzalez, E., and Laemmli, U. K. (1993). SAR-dependent mobilization of histone H1 by HMG-I/Y in vitro: HMG-I/Y is enriched in H1-depleted chromatin. *EMBO J.* 12, 3237–47.

Zhao, X., Wei, P., Liu, Z., Yu, B., and Shi, H. (2017). Soybean Na + / H + antiporter GmsSOS1 enhances antioxidant enzyme activity and reduces Na + accumulation in Arabidopsis and yeast cells under salt stress. 1–11. doi:10.1007/s11738-016-2323-3.

Zhou, S., Chen, X., Zhang, X., and Li, Y. (2008). Improved salt tolerance in tobacco plants by co-transformation of a betaine synthesis gene BADH and a vacuolar Na+/H+antiporter gene SeNHX1. *Biotechnol. Lett.* 30, 369–376. doi:10.1007/s10529-007-9548-6.

Zhu, J. (2002). Salt and Drought Stress Signal Transduction in Plants. *Annu Rev Plant Biol* 53, 247–273.

doi:10.1146/annurev.arplant.53.091401.143329.Salt.

Zhu, M., Zhou, M., Shabala, L., and Shabala, S. (2017). Physiological and molecular mechanisms mediating xylem Na+ loading in barley in the context of salinity stress tolerance. *Plant Cell Environ.* 40, 1009–1020. doi:10.1111/pce.12727.

Zhu, W., Smith, J. W., and Huang, C. M. (2010). Mass spectrometry-based label-free quantitative proteomics. *J. Biomed. Biotechnol.* 2010. doi:10.1155/2010/840518.

Zivy, M., Wienkoop, S., Renaut, J., Pinheiro, C., Goulas, E., and Carpentier, S. (2015a). The quest for tolerant varieties: the importance of integrating "omics" techniques to phenotyping. *Front. Plant Sci.* 6, 448. doi:10.3389/fpls.2015.00448.

Zivy, M., Wienkoop, T., Renaut, J., Pinheiro, C., Goulas, E., and Carpentier, S. (2015b). The quest for tolerant varieties: the importance of integrating "omics" techniques to phenotyping. *Front. Plant Sci.* 6, 1–11. doi:10.3389/fpls.2015.00448.

Zo, C., Schubert, S., Neubert, A., Schierholt, A., and Su, A. (2009). Plant Science Development of salt-resistant maize hybrids : The combination of physiological strategies using conventional breeding methods. 177, 196–202. doi:10.1016/j.plantsci.2009.05.011.

Zörb, C., Schmitt, S., and Mühling, K. H. (2010). Proteomic changes in maize roots after short-term adjustment to saline growth conditions. *Proteomics* 10, 4441–4449. doi:10.1002/pmic.201000231.

Zörb, C., Schmitt, S., Neeb, A., Karl, S., Linder, M., and Schubert, S. (2004). The biochemical reaction of maize (Zea mays L.) to salt stress is characterized by a mitigation of symptoms and not by a specific adaptation. *Plant Sci.* 167, 91–100. doi:10.1016/j.plantsci.2004.03.004.

Zorrilla-fontanes, Y., Rouard, M., Cenci, A., Kissel, E., Do, H., Dubois, E., et al. (2016). Differential root transcriptomics in a polyploid non-model crop: the importance of respiration during osmotic stress. *Nature* 6, 1–15. doi:10.1038/srep22583.

Supplementary Table S4.1 List of proteins found in roots of four maize genotypes at the fourth week after sowing (Chapter 4).

In addition, the relative abundance of proteins as a response to applied salt stress.

Protein	Annotation	Response to salt stress	ANOVA
A0A096PJN2	Uncharacterized protein	High Abundance	6,3E-03
A0A096PPZ7	Uncharacterized protein	High Abundance	2,1E-02
A0A096PSR5	Uncharacterized protein	High Abundance	2,6E-04
A0A096PV29	Uncharacterized protein	High Abundance	1,0E-02
A0A096PVG9	Uncharacterized protein	High Abundance	1,6E-02
A0A096Q4N0	Uncharacterized protein	High Abundance	1,4E-02
A0A096Q7W9	Uncharacterized protein	High Abundance	1,3E-03
A0A096QCP1	Uncharacterized protein	High Abundance	9,1E-03
A0A096QDJ2	Uncharacterized protein	High Abundance	4,7E-03
A0A096QF11	Uncharacterized protein	High Abundance	2,7E-03
A0A096QG13	Uncharacterized protein	High Abundance	2,3E-04
A0A096QHE8	Uncharacterized protein	High Abundance	1,6E-02

Protein	Annotation	Response to salt stress	ANOVA
A0A096QM72	Uncharacterized protein	High Abundance	1,6E-02
A0A096QN33	Uncharacterized protein	High Abundance	1,3E-02
A0A096QVG7	Uncharacterized protein	High Abundance	1,6E-04
A0A096QYG0	Uncharacterized protein	High Abundance	2,1E-04
A0A096R6Z8	Heat shock 70 kDa protein 6 chloroplastic	High Abundance	8,5E-03
A0A096R8Z3	Uncharacterized protein	High Abundance	6,1E-03
A0A096R8Z6	Uncharacterized protein	High Abundance	1,5E-03
A0A096RA51	Uncharacterized protein	High Abundance	1,1E-02
A0A096RAH6	Uncharacterized protein	High Abundance	1,4E-04
A0A096RB11	Uncharacterized protein	High Abundance	9,4E-03
A0A096RCF3	Uncharacterized protein	High Abundance	7,7E-05
A0A096RD67	Uncharacterized protein	High Abundance	2,4E-02
A0A096RE30	Uncharacterized protein	High Abundance	2,8E-04
A0A096RTH6	Uncharacterized protein	High Abundance	1,0E-04

Protein	Annotation	Response to salt stress	ANOVA
A0A096RUZ6	Uncharacterized protein	High Abundance	4,0E-04
A0A096S105	Uncharacterized protein	High Abundance	1,4E-03
A0A096S3Y4	Uncharacterized protein	High Abundance	4,9E-04
A0A096S9Y5	Uncharacterized protein	High Abundance	4,1E-03
A0A096SCS1	Uncharacterized protein	High Abundance	6,3E-03
A0A096SDT4	Uncharacterized protein	High Abundance	3,8E-02
A0A096SGZ3	Uncharacterized protein	High Abundance	2,8E-02
A0A096SH08	Uncharacterized protein	High Abundance	2,6E-04
A0A096SIT0	Uncharacterized protein	High Abundance	3,6E-03
A0A096SKV8	Uncharacterized protein	High Abundance	1,3E-03
A0A096SLY9	Uncharacterized protein	High Abundance	8,9E-03
A0A096SQA7	Uncharacterized protein	High Abundance	5,1E-04
A0A096SVP6	Octicosapeptide /Phox/Bem1p family protein	High Abundance	1,5E-03
A0A096T0B4	Uncharacterized protein	High Abundance	3,3E-03

Protein	Annotation	Response to salt stress	ANOVA
A0A096T792	Uncharacterized protein	High Abundance	2,7E-03
A0A096TB53	Uncharacterized protein	High Abundance	1,0E-03
A0A096TCG5	Uncharacterized protein	High Abundance	9,5E-04
A0A096TDT7	Uncharacterized protein	High Abundance	1,2E-03
A0A096TIB6	Uncharacterized protein	High Abundance	4,3E-03
A0A096TJB4	Uncharacterized protein	High Abundance	4,9E-03
A0A096TMB6	Uncharacterized protein	High Abundance	9,6E-04
A0A096TME2	Uncharacterized protein	High Abundance	1,3E-03
A0A096TRU3	Uncharacterized protein	High Abundance	2,6E-02
A0A096TUS3	Uncharacterized protein	High Abundance	1,0E-03
A0A096U7P6	Uncharacterized protein	High Abundance	1,3E-04
A0A096U7Y9	Uncharacterized protein	High Abundance	6,1E-04
A0A096U8U9	Uncharacterized protein	High Abundance	3,4E-02
A0A097PRQ9	EMB1873 protein (Fragment)	High Abundance	4,1E-03

Protein	Annotation	Response to salt stress	ANOVA
A0A0A1P1P0	Cystatin protein	High Abundance	2,6E-02
A3KLI1	RAB17 protein	High Abundance	2,6E-04
A5A5E7	Protein disulfide-isomerase	High Abundance	3,6E-02
B1PEY4	Superoxide dismutase [Cu-Zn]	High Abundance	1,5E-02
B4F7V1	2-dehydro-3-deoxyphosphooctonate aldolase	High Abundance	2,2E-02
B4F817	Dehydroascorbate reductase	High Abundance	3,3E-04
B4F8V5	NADH dehydrogenase [ubiquinone] iron-sulfur protein 1 mitochondrial	High Abundance	4,2E-02
B4F925	Superoxide dismutase	High Abundance	6,3E-04
B4F932	Putative mitochondrial-processing peptidase subunit beta mitochondrial	High Abundance	1,3E-02

Protein	Annotation	Response to salt stress	ANOVA
B4F9G1	Aspartate aminotransferase	High Abundance	4,3E-02
B4F9K0	Late embryogenesis abundant protein group 2	High Abundance	3,5E-04
B4FA06	APx4-Peroxisomal Ascorbate Peroxidase	High Abundance	4,7E-03
B4FAD9	UDP-glucose pyrophosphorylase2	High Abundance	6,2E-04
B4FAJ4	2-hydroxyphytanoyl-CoA lyase	High Abundance	1,5E-03
B4FAV5	Germin-like protein 1	High Abundance	1,3E-03
B4FB35	Translation machinery-associated protein 22	High Abundance	2,2E-02
B4FFF1	Ran-binding protein 1 homolog a	High Abundance	3,3E-03
B4FFZ7	60S ribosomal protein L32-1	High Abundance	1,1E-02
B4FG03	Uncharacterized protein	High Abundance	2,8E-07

Protein	Annotation	Response to salt stress	ANOVA
B4FGF5	Hydroxyacylglutathione hydrolase cytoplasmic	High Abundance	1,1E-03
B4FGM4	Endothelial differentiation-related factor 1	High Abundance	2,5E-03
B4FH88	C-1-tetrahydrofolate synthase, cytoplasmic	High Abundance	2,0E-02
B4FI47	Arginine/serine-rich splicing factor RSZ20 transcript I	High Abundance	3,3E-03
B4FI68	Uncharacterized protein	High Abundance	4,5E-03
B4FIE5	Nascent polypeptide-associated complex subunit beta	High Abundance	1,3E-03
B4FIH9	Xylose isomerase	High Abundance	3,7E-04
B4FK69	Acyl carrier protein	High Abundance	3,8E-03
B4FL28	Isovaleryl-CoA dehydrogenase mitochondrial	High Abundance	6,1E-03

Protein	Annotation	Response to salt stress	ANOVA
B4FMB6	Induced stolen tip protein TUB8	High Abundance	2,0E-03
B4FNI0	Peroxidase	High Abundance	7,2E-03
B4FNK1	Uncharacterized protein	High Abundance	9,6E-03
B4FNL7	MAP3K-like protein kinase	High Abundance	1,6E-02
B4FNM4	60S acidic ribosomal protein P0	High Abundance	1,0E-02
B4FPZ7	GrpE protein homolog	High Abundance	2,1E-03
B4FQK5	Eukaryotic peptide chain release factor subunit 1-1	High Abundance	3,3E-02
B4FRQ7	Proteasome subunit beta type	High Abundance	1,6E-02
B4FS99	ATP synthase D chain, mitochondrial	High Abundance	8,6E-03
B4FSR6	Glutathione S-transferase	High Abundance	3,8E-03
B4FT31	Dehydroascorbate reductase	High Abundance	4,2E-04
B4FTS6	Endochitinase A	High Abundance	1,2E-02

Protein	Annotation	Response to salt stress	ANOVA
B4FUT3	Germin-like protein subfamily 1 member 17	High Abundance	4,8E-02
B4FV48	Multidomain cystatin	High Abundance	9,8E-04
B4FVB2	Elongation factor Tu	High Abundance	8,5E-04
B4FW90	ER luminal binding protein	High Abundance	3,3E-03
B4FX25	Putative UDP-arabinopyranose mutase 5	High Abundance	3,0E-04
B4FXZ3	Grx_C2.2-glutaredoxin subgroup I	High Abundance	1,0E-02
B4FY74	Retrotransposon protein Ty1-copia subclass	High Abundance	1,3E-04
B4FY83	Peroxidase	High Abundance	2,3E-04
B4FYN6	Uncharacterized protein	High Abundance	6,0E-03
B4FZ29	Argininosuccinate synthase	High Abundance	4,8E-04
B4FZA1	Mitochondrial glycoprotein	High Abundance	6,7E-03
B4G0K5	Uncharacterized protein	High Abundance	2,2E-05

Protein	Annotation	Response to salt stress	ANOVA
B4G1B3	60S acidic ribosomal protein P3	High Abundance	3,0E-03
B5U8J9	Asparagine synthetase	High Abundance	3,1E-04
B6SHD3	Malate dehydrogenase	High Abundance	4,2E-04
B6SIG5	Triosephosphate isomerase	High Abundance	1,3E-03
B6SIG8	60S acidic ribosomal protein P2A	High Abundance	1,4E-04
B6SIL7	Eukaryotic translation initiation factor 5A	High Abundance	3,1E-04
B6SIR9	1-aminocyclopropane-1-carboxylate oxidase	High Abundance	3,2E-03
B6SJS7	Nascent polypeptide-associated complex subunit beta	High Abundance	5,4E-04
B6SK54	Superoxide dismutase [Cu-Zn]	High Abundance	3,3E-03

Protein	Annotation	Response to salt stress	ANOVA
B6SLI1	40S ribosomal protein S30	High Abundance	3,6E-03
B6SLU8	Putative uncharacterized protein	High Abundance	7,2E-04
B6SMQ5	Triosephosphate isomerase	High Abundance	3,6E-04
B6SPX4	Tubulin alpha-3 chain	High Abundance	3,4E-04
B6SUK9	GNAT transcription factor	High Abundance	2,6E-02
B6SXA8	Ubiquitin-fold modifier 1	High Abundance	4,5E-02
B6SZY7	Glutathione S-transferase IV	High Abundance	1,3E-04
B6T3V1	Peroxidase	High Abundance	2,2E-03
B6T4E7	40S ribosomal protein S6	High Abundance	3,8E-03
B6T4Q3	Plasminogen activator inhibitor 1 RNA-binding protein	High Abundance	4,3E-04
B6T4Q5	Pro-resilin	High Abundance	5,3E-04
B6T5H6	Auxin-induced protein PCNT115	High Abundance	9,4E-04

Protein	Annotation	Response to salt stress	ANOVA
B6T5R1	Ran-binding protein 1	High Abundance	5,1E-04
B6T7A4	Glyceraldehyde -3-phosphate dehydrogenase	High Abundance	1,9E-03
B6T7C2	Eucaryotic translation initiation factor5 isoform 1	High Abundance	1,9E-02
B6T831	60S ribosomal protein L37a	High Abundance	1,7E-02
B6T8F4	Ran-binding protein 1	High Abundance	3,3E-02
B6T8U5	ER6 protein	High Abundance	9,1E-04
B6T916	N-acetyltransferase	High Abundance	7,2E-04
B6T9A1	Co-chaperone protein SBA1	High Abundance	1,9E-04
B6TAT4	60S ribosomal protein L36	High Abundance	1,3E-02
B6TBW4	Proliferation-associated protein 2G4	High Abundance	1,1E-04
B6TCR9	Mitochondrial ATP synthase	High Abundance	2,2E-02
B6TDW7	Secretory protein	High Abundance	3,2E-03

Protein	Annotation	Response to salt stress	ANOVA
B6TEM6	Acyl carrier protein	High Abundance	2,2E-02
B6TEX6	Cytochrome b-c1 complex subunit 7	High Abundance	4,6E-02
B6TFX9	Legumin-like protein	High Abundance	1,4E-02
B6TGF0	Proteasome subunit alpha type	High Abundance	2,9E-03
B6THT0	Peroxiredoxin-5	High Abundance	8,3E-03
B6THU5	Elongation factor 1-delta 1	High Abundance	1,4E-03
B6THU9	Peroxidase	High Abundance	1,6E-03
B6TL91	Hsc70-interacting protein	High Abundance	2,2E-02
B6TLU5	Lipid binding protein	High Abundance	2,2E-04
B6TMF3	Wound/stress protein	High Abundance	5,2E-04
B6TNF1	Calnexin	High Abundance	4,9E-03
B6TP19	Thioredoxin-like protein 5	High Abundance	3,9E-03
B6TQC0	3-N-debenzoyl-2-deoxytaxol N-	High Abundance	4,0E-02

Protein	Annotation	Response to salt stress	ANOVA
	benzoyltransferase		
B6TR38	Basic endochitinase A	High Abundance	2,6E-02
B6TRR4	60S ribosomal protein L36	High Abundance	1,5E-02
B6TRW8	Dihydrolipoylly sine-residue succinyltransfer ase component of 2-oxoglutarate dehydrogenase complex	High Abundance	1,6E-02
B6TVC7	Ferredoxin	High Abundance	2,7E-03
B6U7P4	Nonspecific lipid-transfer protein AKCS9	High Abundance	4,0E-02
B6U9S6	APx1-Cytosolic Ascorbate Peroxidase	High Abundance	1,2E-04
B6UB73	APx1-Cytosolic Ascorbate Peroxidase	High Abundance	8,0E-04
B6UHB6	Histone H1	High Abundance	3,4E-02
B7U627	DHN2-like protein	High Abundance	3,6E-04

Protein	Annotation	Response to salt stress	ANOVA
B8A0Q6	Succinate dehydrogenase [ubiquinone] flavoprotein subunit, mitochondrial (EC 1.3.5.1)	High Abundance	3,3E-04
B8A306	Phosphoglycerate mutase1	High Abundance	6,1E-03
C0HHA6	Peroxidase	High Abundance	1,6E-04
C0HHC4	Nucleoside diphosphate kinase	High Abundance	2,0E-03
C0P7J4	Aminopeptidase P1	High Abundance	6,8E-03
C0P9J6	Aminoaldehyde dehydrogenase 1	High Abundance	8,3E-03
C0PBY7	Nucleoside diphosphate kinase	High Abundance	1,4E-02
C0PJR9	Putative alcohol dehydrogenase superfamily protein	High Abundance	3,1E-03
C0PK05	Lactoylglutathione lyase	High Abundance	3,2E-03
C0PK55	Cytochrome c-2	High Abundance	1,4E-03

Protein	Annotation	Response to salt stress	ANOVA
C0PLX5	Uncharacterized protein	High Abundance	9,1E-03
C1K9J1	Heat shock protein 90	High Abundance	1,1E-02
C3UZ63	HSP protein	High Abundance	5,0E-03
C4J2M5	Pyruvate kinase	High Abundance	2,3E-02
C4J477	Dehydrin	High Abundance	1,5E-04
C4J9R0	PLAT domain-containing protein 3	High Abundance	1,0E-04
C4JBX2	Uncharacterized protein	High Abundance	2,9E-03
K7TSU4	Putative O-Glycosyl hydrolase superfamily protein	High Abundance	1,3E-02
K7U5W7	Wound/stress protein	High Abundance	6,0E-03
K7U935	Catalase	High Abundance	1,5E-03
K7UGU4	Putative WD40-like beta propeller repeat family protein	High Abundance	2,7E-03
K7US39	Dihydrolipoyl dehydrogenase	High Abundance	2,0E-04

Protein	Annotation	Response to salt stress	ANOVA
K7UX34	Uncharacterized protein	High Abundance	1,5E-03
K7UXM3	Putative thioredoxin superfamily protein	High Abundance	3,2E-03
K7UZN5	Putative oxidoreductase, aldo/keto reductase family protein	High Abundance	4,3E-03
K7UZU9	Uncharacterized protein	High Abundance	1,4E-04
K7V435	Cyclin4	High Abundance	1,4E-02
K7V5R7	Acetyltransferase component of pyruvate dehydrogenase complex	High Abundance	2,0E-03
K7V794	Enolase1	High Abundance	1,5E-03
K7VB29	Uncharacterized protein	High Abundance	1,6E-02
K7VES9	Asparagine synthetase	High Abundance	7,2E-03
K7VHA0	5-pentadecatrienyl resorcinol O-	High Abundance	1,1E-02

Protein	Annotation	Response to salt stress	ANOVA
	methyltransferase		
K7W544	Gibberellin receptor GID1L2	High Abundance	2,4E-03
P00333	Alcohol dehydrogenase 1	High Abundance	2,3E-02
P26301	Enolase 1	High Abundance	1,7E-03
P29185	Chaperonin CPN60-1, mitochondrial	High Abundance	7,8E-03
Q06XS2	Lipoxygenase	High Abundance	1,6E-03
Q43274	Aldehyde dehydrogenase	High Abundance	3,1E-03
Q43298	Chaperonin CPN60-2, mitochondrial	High Abundance	1,6E-03
Q4W1F7	Thioredoxin	High Abundance	6,1E-04
Q5EUD6	Protein disulfide isomerase	High Abundance	4,5E-04
Q5EUE1	Protein disulfide-isomerase	High Abundance	2,0E-02
Q5GA18	Putative uncharacterized protein adh1F	High Abundance	7,7E-04

Protein	Annotation	Response to salt stress	ANOVA
Q5GAU1	Putative alanine aminotransferase	High Abundance	1,7E-03
Q6JAH6	Glutathione peroxidase	High Abundance	2,0E-04
Q8W0Q2	Putative aldehyde dehydrogenase MIS1	High Abundance	4,3E-04
Q94KT5	Alpha-expansin 3	High Abundance	8,4E-03
Q9SWR9	Acetyltransferase component of pyruvate dehydrogenase complex	High Abundance	4,2E-03
A0A075T3E7	Pyrabactin resistance-like protein	Low Abundance	9,2E-03
A0A096PJN3	Uncharacterized protein	Low Abundance	2,2E-02
A0A096PQJ8	Uncharacterized protein	Low Abundance	3,4E-04
A0A096PQU4	Uncharacterized protein	Low Abundance	2,5E-02
A0A096PVE7	Uncharacterized protein	Low Abundance	1,9E-02
A0A096QCN9	Uncharacterized protein	Low Abundance	3,7E-04

Protein	Annotation	Response to salt stress	ANOVA
A0A096QFM0	Uncharacterized protein	Low Abundance	9,5E-04
A0A096QK67	Uncharacterized protein	Low Abundance	3,7E-03
A0A096QLU9	Uncharacterized protein	Low Abundance	9,4E-03
A0A096QNY2	Uncharacterized protein	Low Abundance	1,2E-03
A0A096QRL3	Uncharacterized protein	Low Abundance	9,8E-03
A0A096QYB2	Uncharacterized protein	Low Abundance	2,2E-03
A0A096RDN9	Uncharacterized protein	Low Abundance	5,2E-04
A0A096RFR6	Eukaryotic translation initiation factor 3 subunit A	Low Abundance	1,3E-02
A0A096RFZ7	Uncharacterized protein	Low Abundance	3,3E-03
A0A096RHA4	Uncharacterized protein	Low Abundance	7,2E-03
A0A096RHZ7	Uncharacterized protein	Low Abundance	7,7E-03
A0A096RIM2	Uncharacterized protein (Fragment)	Low Abundance	3,7E-02
A0A096RLS0	Uncharacterized protein	Low Abundance	3,2E-04

Protein	Annotation	Response to salt stress	ANOVA
A0A096RP94	Uncharacterized protein	Low Abundance	3,4E-02
A0A096RPU1	Uncharacterized protein	Low Abundance	2,8E-02
A0A096RT35	Uncharacterized protein	Low Abundance	3,6E-04
A0A096RY69	Uncharacterized protein	Low Abundance	1,4E-02
A0A096RYJ7	Uncharacterized protein	Low Abundance	3,0E-02
A0A096RZC8	Uncharacterized protein	Low Abundance	7,5E-04
A0A096S1K7	Uncharacterized protein	Low Abundance	6,8E-04
A0A096S9W1	Uncharacterized protein	Low Abundance	1,5E-04
A0A096SA13	Uncharacterized protein	Low Abundance	1,0E-04
A0A096SBV9	Uncharacterized protein	Low Abundance	1,6E-02
A0A096SCG9	Uncharacterized protein	Low Abundance	8,7E-04
A0A096SF47	Uncharacterized protein	Low Abundance	4,0E-03
A0A096SFR9	Uncharacterized protein	Low Abundance	3,0E-03
A0A096SMM7	Uncharacterized protein	Low Abundance	1,1E-03
A0A096T5T9	Uncharacterized protein	Low Abundance	3,1E-03

Protein	Annotation	Response to salt stress	ANOVA
A0A096T5Y3	Uncharacterized protein	Low Abundance	2,4E-03
A0A096T7J3	Uncharacterized protein	Low Abundance	1,1E-04
A0A096T8I0	Cell number regulator 10	Low Abundance	4,7E-03
A0A096TG88	Uncharacterized protein	Low Abundance	5,8E-03
A0A096TLY3	Uncharacterized protein	Low Abundance	5,3E-04
A0A096TPX1	Uncharacterized protein	Low Abundance	2,9E-02
A0A096TSW5	Uncharacterized protein	Low Abundance	4,1E-03
A0A096U3B2	Uncharacterized protein	Low Abundance	1,7E-04
A0A096UEP2	Uncharacterized protein	Low Abundance	2,7E-02
A0A096UEQ1	Uncharacterized protein	Low Abundance	3,6E-02
A0A096UJ90	Uncharacterized protein	Low Abundance	1,7E-03
A0A097C0X0	Sus1	Low Abundance	2,3E-04
A5H452	Peroxidase 70	Low Abundance	5,5E-04
A5H8G4	Peroxidase 1	Low Abundance	2,1E-03
B1A9R4	Peroxidase	Low Abundance	1,2E-03
B4F891	Uncharacterized protein	Low Abundance	1,9E-03
B4F8U2	Uncharacterized protein	Low Abundance	4,2E-02

Protein	Annotation	Response to salt stress	ANOVA
B4F935	Uncharacterized protein	Low Abundance	4,9E-04
B4F9A4	Uncharacterized protein	Low Abundance	3,8E-04
B4F9J5	Glutamate dehydrogenase	Low Abundance	4,0E-07
B4FAB0	Uncharacterized protein	Low Abundance	7,0E-03
B4FAD1	S-adenosylmethionine synthase	Low Abundance	1,3E-03
B4FAG0	Uncharacterized protein	Low Abundance	1,3E-03
B4FB55	Ras-related protein ARA-3	Low Abundance	2,5E-02
B4FB81	Uncharacterized protein	Low Abundance	6,9E-03
B4FC92	Nuclear transport factor 2	Low Abundance	1,1E-02
B4FCI9	Peroxidase	Low Abundance	7,1E-04
B4FDH5	Histone H2B	Low Abundance	2,9E-04
B4FEZ1	Uncharacterized protein	Low Abundance	2,1E-02
B4FF24	UDP-glucuronic acid decarboxylase 1 isoform 1	Low Abundance	7,8E-03

Protein	Annotation	Response to salt stress	ANOVA
B4FFI2	Nitrilase-associated protein	Low Abundance	1,5E-02
B4FHN3	Uncharacterized protein	Low Abundance	1,6E-02
B4FIA6	Histone H2A	Low Abundance	3,0E-03
B4FIZ5	Uncharacterized protein	Low Abundance	8,7E-04
B4FLE0	O-methyltransferase ZRP4	Low Abundance	1,0E-03
B4FLS8	Uncharacterized protein	Low Abundance	2,1E-04
B4FMH5	Histone H2A	Low Abundance	1,2E-02
B4FMJ0	ADP-ribosylation factor 1	Low Abundance	1,1E-02
B4FP94	Uncharacterized protein	Low Abundance	1,6E-02
B4FQC6	Glucose-6-phosphate isomerase	Low Abundance	6,6E-03
B4FQE6	Uncharacterized protein	Low Abundance	3,8E-04
B4FQK0	Uncharacterized protein	Low Abundance	1,0E-04
B4FQV3	Uncharacterized protein	Low Abundance	5,4E-03
B4FR08	Cysteine synthase	Low Abundance	1,9E-03

Protein	Annotation	Response to salt stress	ANOVA
B4FR89	Phosphomannomutase	Low Abundance	1,3E-03
B4FRS6	Uncharacterized protein	Low Abundance	1,3E-02
B4FS90	Cysteine protease 1	Low Abundance	8,2E-04
B4FSE9	Histone H2B	Low Abundance	1,9E-02
B4FT82	Uncharacterized protein	Low Abundance	2,8E-02
B4FU52	Histone H2A	Low Abundance	1,3E-02
B4FUC4	Uncharacterized protein	Low Abundance	4,0E-04
B4FUE0	Obg-like ATPase 1	Low Abundance	2,0E-02
B4FV46	Rapid alkalinization factor 1	Low Abundance	7,7E-04
B4FVE1	NADPH quinone oxidoreductase 1	Low Abundance	1,1E-04
B4FWI4	Uncharacterized protein	Low Abundance	2,3E-03
B4FZM9	DNA repair protein RAD23	Low Abundance	8,2E-04
B4G029	3-N-debenzoyl-2-deoxytaxol N-benzoyltransferase	Low Abundance	7,1E-04

Protein	Annotation	Response to salt stress	ANOVA
B4G195	Aspartate aminotransferase	Low Abundance	1,6E-02
B4G1B5	Uncharacterized protein	Low Abundance	1,8E-02
B6SHZ1	40S ribosomal protein S5	Low Abundance	3,3E-02
B6SI11	Actin-2	Low Abundance	1,2E-04
B6SIR7	Uncharacterized protein	Low Abundance	3,4E-02
B6SIU1	Ubiquitin-conjugating enzyme E2-17 kDa 9	Low Abundance	1,4E-02
B6SKN3	1,2-dihydroxy-3-keto-5-methylthiopentene dioxygenase	Low Abundance	1,4E-03
B6SP74	Glycine-rich RNA-binding protein 2	Low Abundance	2,7E-03
B6SRI4	14-3-3-like protein	Low Abundance	1,3E-02
B6SWV1	Glucose-6-phosphate 1-dehydrogenase	Low Abundance	1,9E-02
B6SXE9	Chemocyanin	Low Abundance	2,3E-04
B6SY01	Ferredoxin--nitrite reductase	Low Abundance	4,1E-03

Protein	Annotation	Response to salt stress	ANOVA
B6SYY0	Beta-fructofuranosidase, insoluble isoenzyme 7	Low Abundance	4,5E-03
B6T0Q2	Histone H2A	Low Abundance	1,7E-02
B6T1G5	Histone H2B	Low Abundance	1,5E-02
B6T3E9	Histone H2A	Low Abundance	1,5E-03
B6T3J3	Histone H2A	Low Abundance	3,2E-03
B6T4U8	Calmodulin	Low Abundance	8,4E-03
B6T6B3	Eukaryotic translation initiation factor 3 subunit M	Low Abundance	6,8E-03
B6T6D2	Disease resistance response protein 206	Low Abundance	1,0E-04
B6T7B1	Peroxidase	Low Abundance	3,4E-04
B6T7G7	Elongation factor 1-gamma 3	Low Abundance	2,1E-03
B6T7H0	Glutathione S-transferase 6	Low Abundance	1,0E-04
B6T8I3	Disease resistance response protein 206	Low Abundance	3,8E-04
B6TBA8	Aspartic proteinase nepenthesin-2	Low Abundance	4,6E-02

Protein	Annotation	Response to salt stress	ANOVA
B6TBH5	Cortical cell-delineating protein	Low Abundance	4,4E-02
B6TDT6	Methylthioribose kinase	Low Abundance	2,4E-03
B6TEC1	Sorbitol dehydrogenase	Low Abundance	7,9E-03
B6TF12	Glycine-rich RNA-binding protein 8	Low Abundance	1,2E-02
B6TIL6	3-ketoacyl-CoA thiolase 2, peroxisomal	Low Abundance	1,4E-03
B6TJ90	Histone H4	Low Abundance	3,7E-02
B6TK17	DREPP2 protein	Low Abundance	1,1E-04
B6TNI6	DREPP4 protein	Low Abundance	1,2E-03
B6TNY0	Aquaporin TIP2.1	Low Abundance	2,2E-02
B6TQ08	Actin-1	Low Abundance	3,6E-03
B6TVU2	Prefoldin subunit 5	Low Abundance	4,6E-02
B6TXX0	Ribose-phosphate pyrophosphokinase 4	Low Abundance	4,7E-04
B6TYW3	Ribonuclease 1	Low Abundance	1,4E-02

Protein	Annotation	Response to salt stress	ANOVA
B6TZD1	Methylthioribose-1-phosphate isomerase	Low Abundance	1,2E-02
B6U118	T-complex protein 1 subunit zeta	Low Abundance	1,4E-02
B6U242	Uncharacterized protein	Low Abundance	2,0E-02
B6U284	14-3-3-like protein	Low Abundance	1,7E-02
B6U3H8	Lipid transfer protein	Low Abundance	2,8E-03
B6U4D6	Phenylalanine ammonia-lyase	Low Abundance	1,7E-02
B6U579	Thaumatin-like protein	Low Abundance	1,1E-02
B6UEB0	Lipid binding protein	Low Abundance	4,3E-04
B6UEL1	Germin-like protein subfamily 1 member 11	Low Abundance	2,9E-06
B6UF55	5-methyltetrahydropteroyltriglutamate--homocysteine methyltransferase	Low Abundance	3,6E-02

Protein	Annotation	Response to salt stress	ANOVA
B6UG09	Putative uncharacterized protein	Low Abundance	3,1E-02
B6UG81	Cortical cell-delineating protein	Low Abundance	2,5E-03
B6UGK8	3-isopropylmalate dehydratase small subunit 2	Low Abundance	5,7E-03
B6UH77	Histone H3	Low Abundance	3,2E-03
B6UHQ8	Blue copper protein	Low Abundance	2,6E-04
B7ZY79	Putative leucine-rich repeat receptor-like protein kinase family protein	Low Abundance	5,1E-03
B8A046	Phenylalanine ammonia-lyase	Low Abundance	1,6E-02
B8A068	S-adenosylmethionine synthase	Low Abundance	1,3E-03
B8A0S8	Uncharacterized protein	Low Abundance	1,1E-03
B8A1C0	Proliferating cell nuclear antigen	Low Abundance	3,1E-03

Protein	Annotation	Response to salt stress	ANOVA
C0P2K9	Uncharacterized protein	Low Abundance	2,0E-02
C0P3K6	Uncharacterized protein	Low Abundance	1,3E-02
C0P3Z8	Uncharacterized protein	Low Abundance	8,0E-04
C0P4T5	Uncharacterized protein	Low Abundance	2,2E-03
C0P5C0	Importin subunit alpha	Low Abundance	1,6E-02
C0PA44	Uncharacterized protein	Low Abundance	5,2E-03
C0PD45	Uncharacterized protein	Low Abundance	6,1E-03
C0PD71	Uncharacterized protein	Low Abundance	2,4E-02
C0PDB6	Uncharacterized protein	Low Abundance	6,6E-04
C0PFF5	Proteasome subunit beta type	Low Abundance	2,0E-02
C0PFJ2	Succinate dehydrogenase [ubiquinone] iron-sulfur subunit, mitochondrial	Low Abundance	7,6E-04
C0PGU8	Uncharacterized protein	Low Abundance	2,8E-03

Protein	Annotation	Response to salt stress	ANOVA
C0PHH5	Dihydrolipoyl dehydrogenase	Low Abundance	2,8E-02
C0PI43	Uncharacterized protein	Low Abundance	1,2E-03
C0PL35	Glyoxysomal fatty acid beta-oxidation multifunctional protein MFP-a	Low Abundance	3,0E-03
C0PNK2	Uncharacterized protein	Low Abundance	1,8E-02
C4J3E2	Uncharacterized protein	Low Abundance	8,6E-03
C4J4U3	Uncharacterized protein	Low Abundance	4,5E-03
C4J4W3	Uncharacterized protein	Low Abundance	1,5E-04
K7TL05	14-3-3-like protein GF14-12	Low Abundance	2,0E-04
K7TT73	40S ribosomal protein S3	Low Abundance	1,5E-02
K7TY03	Alanine--tRNA ligase	Low Abundance	1,3E-02
K7U0Q0	Putative sucrose synthase family protein	Low Abundance	7,3E-03
K7U0Q4	Uncharacterized protein	Low Abundance	2,0E-03
K7U159	Peroxidase	Low Abundance	6,3E-03

Protein	Annotation	Response to salt stress	ANOVA
K7UDG5	Uncharacterized protein	Low Abundance	1,1E-02
K7ULE9	Uncharacterized protein	Low Abundance	3,5E-03
K7URF9	Uncharacterized protein	Low Abundance	4,9E-04
K7US09	Uncharacterized protein	Low Abundance	3,1E-02
K7UXK5	Putative alcohol dehydrogenase superfamily protein	Low Abundance	1,5E-04
K7V6Z1	Putative patellin family protein	Low Abundance	6,0E-04
K7VC35	S-adenosylmethionine synthase	Low Abundance	4,9E-02
K7VEJ7	Uncharacterized protein	Low Abundance	4,2E-03
K7VIL3	Methionine S-methyltransferase	Low Abundance	1,3E-03
K7VKX8	Uncharacterized protein	Low Abundance	4,2E-02
K7VNE0	Uncharacterized protein	Low Abundance	3,7E-04
K7VP18	Putative leucine-rich repeat receptor-like protein	Low Abundance	1,0E-02

Protein	Annotation	Response to salt stress	ANOVA
	kinase family protein		
K7W3A9	Ras protein Rab11C	Low Abundance	2,7E-02
K7WDG3	Uncharacterized protein	Low Abundance	1,8E-02
K7WE51	Uncharacterized protein	Low Abundance	6,8E-03
P51059	Phosphoenolpyruvate carboxylase 2	Low Abundance	5,7E-03
Q3S3T0	Hemoglobin 2	Low Abundance	3,6E-02
Q7FU57	Bowman-Birk type wound-induced proteinase inhibitor WIP1	Low Abundance	7,6E-04
Q8W4W3	Putative gamma-glutamylcysteine synthetase	Low Abundance	2,2E-04
Q9FQC6	Glutathione S-transferase GST 13	Low Abundance	4,9E-04
A0A096PJN2	Uncharacterized protein	High Abundance	6,3E-03
A0A096PPZ7	Uncharacterized protein	High Abundance	2,1E-02
A0A096PSR5	Uncharacterized protein	High Abundance	2,6E-04

Protein	Annotation	Response to salt stress	ANOVA
A0A096PII0	Uncharacterized protein		
A0A096PJC5	Uncharacterized protein		
A0A096PLH9	Uncharacterized protein		
A0A096PLW5	Uncharacterized protein		
A0A096PMM2	Uncharacterized protein		
A0A096PNV5	Uncharacterized protein		
A0A096PQ28	Uncharacterized protein		
A0A096PQR0	Uncharacterized protein		
A0A096PQS4	Uncharacterized protein		
A0A096PR13	Uncharacterized protein		
A0A096PRG4	Uncharacterized protein		
A0A096PTL9	Uncharacterized protein		
A0A096PU33	Uncharacterized protein		
A0A096PU41	Uncharacterized protein		
A0A096PUN1	Uncharacterized protein		

Protein	Annotation	Response to salt stress	ANOVA
A0A096PW86	Uncharacterized protein		
A0A096PX16	Uncharacterized protein		
A0A096PXW1	Uncharacterized protein		
A0A096PXZ0	Uncharacterized protein		
A0A096PYB4	Uncharacterized protein		
A0A096PYV1	Uncharacterized protein		
A0A096PYV5	Uncharacterized protein		
A0A096PZ84	Uncharacterized protein		
A0A096PZA7	Uncharacterized protein		
A0A096PZG1	Uncharacterized protein		
A0A096PZT8	Uncharacterized protein		
A0A096Q027	Uncharacterized protein		
A0A096Q0H4	Uncharacterized protein		
A0A096Q0P9	Uncharacterized protein		
A0A096Q0T1	Uncharacterized protein		

Protein	Annotation	Response to salt stress	ANOVA
A0A096Q155	Uncharacterized protein		
A0A096Q1Q2	Uncharacterized protein		
A0A096Q1T0	Uncharacterized protein		
A0A096Q1Z5	Uncharacterized protein		
A0A096Q240	Uncharacterized protein		
A0A096Q2C3	Uncharacterized protein		
A0A096Q2E3	Uncharacterized protein		
A0A096Q3K5	Uncharacterized protein		
A0A096Q4Q2	Uncharacterized protein		
A0A096Q5Z9	Uncharacterized protein		
A0A096Q6B7	Uncharacterized protein		
A0A096Q701	Uncharacterized protein		
A0A096Q770	Uncharacterized protein		
A0A096Q783	Uncharacterized protein		
A0A096Q7L4	Uncharacterized protein		

Protein	Annotation	Response to salt stress	ANOVA
A0A096Q8J4	Uncharacterized protein		
A0A096Q8Q2	Uncharacterized protein		
A0A096Q8R5	Uncharacterized protein		
A0A096Q8T5	Uncharacterized protein		
A0A096Q9D6	Uncharacterized protein		
A0A096Q9F9	Uncharacterized protein		
A0A096Q9I4	Uncharacterized protein		
A0A096Q9I5	Uncharacterized protein		
A0A096Q9X1	Uncharacterized protein		
A0A096QA11	Uncharacterized protein		
A0A096QA17	Uncharacterized protein		
A0A096QAF4	Uncharacterized protein		
A0A096QAP5	Uncharacterized protein		
A0A096QAW4	Uncharacterized protein		
A0A096QB84	Uncharacterized protein		

Protein	Annotation	Response to salt stress	ANOVA
A0A096QB86	Uncharacterized protein		
A0A096QBH5	Uncharacterized protein		
A0A096QC57	Uncharacterized protein		
A0A096QCL2	Uncharacterized protein		
A0A096QCV9	Uncharacterized protein		
A0A096QCW0	Uncharacterized protein		
A0A096QCX3	Uncharacterized protein		
A0A096QDZ2	Uncharacterized protein		
A0A096QE21	Uncharacterized protein		
A0A096QE36	Uncharacterized protein		
A0A096QEM9	Uncharacterized protein		
A0A096QEY4	Uncharacterized protein		
A0A096QG19	Uncharacterized protein		
A0A096QG39	Uncharacterized protein		
A0A096QGZ6	Uncharacterized protein		

Protein	Annotation	Response to salt stress	ANOVA
A0A096QH03	Uncharacterized protein		
A0A096QHC2	Uncharacterized protein		
A0A096QHG4	Uncharacterized protein		
A0A096QHH6	Uncharacterized protein		
A0A096QHM6	Uncharacterized protein		
A0A096QHZ1	Uncharacterized protein		
A0A096QHZ2	Uncharacterized protein		
A0A096QHZ4	Uncharacterized protein		
A0A096QIH2	30S ribosomal protein S11, chloroplastic		
A0A096QIX6	Uncharacterized protein		
A0A096QJW7	Uncharacterized protein		
A0A096QK58	Uncharacterized protein		
A0A096QLV9	Uncharacterized protein		
A0A096QN00	Uncharacterized protein		

Protein	Annotation	Response to salt stress	ANOVA
A0A096QNP1	Uncharacterized protein		
A0A096QQU0	Uncharacterized protein		
A0A096QRB1	Uncharacterized protein		
A0A096QRU9	Uncharacterized protein		
A0A096QS94	Uncharacterized protein		
A0A096QSC1	Uncharacterized protein		
A0A096QSW5	Uncharacterized protein		
A0A096QSZ4	Uncharacterized protein		
A0A096QSZ8	Uncharacterized protein		
A0A096QUZ5	Uncharacterized protein		
A0A096QV74	Uncharacterized protein		
A0A096QVH3	Uncharacterized protein		
A0A096QWG0	Uncharacterized protein		
A0A096QX18	Uncharacterized protein		
A0A096QXB7	Uncharacterized protein		

Protein	Annotation	Response to salt stress	ANOVA
A0A096QXJ5	Uncharacterized protein		
A0A096QXN0	Uncharacterized protein		
A0A096QY57	Uncharacterized protein		
A0A096QYR1	Uncharacterized protein		
A0A096QYW3	Uncharacterized protein		
A0A096R049	Uncharacterized protein		
A0A096R091	Uncharacterized protein		
A0A096R0C8	Uncharacterized protein		
A0A096R0R6	Uncharacterized protein		
A0A096R148	Uncharacterized protein		
A0A096R1Q6	Tubulin beta-6 chain		
A0A096R2T3	Uncharacterized protein		
A0A096R3F8	Uncharacterized protein		
A0A096R3G2	Uncharacterized protein		
A0A096R3R4	Uncharacterized protein		

Protein	Annotation	Response to salt stress	ANOVA
A0A096R3R9	Uncharacterized protein		
A0A096R4T9	Uncharacterized protein		
A0A096R4U1	Uncharacterized protein		
A0A096R557	Uncharacterized protein		
A0A096R5T7	Uncharacterized protein		
A0A096R737	Uncharacterized protein		
A0A096R8B3	Uncharacterized protein		
A0A096R8F6	Uncharacterized protein		
A0A096R9B8	Uncharacterized protein		
A0A096R9Y2	Uncharacterized protein		
A0A096RA88	Uncharacterized protein		
A0A096RAP0	Uncharacterized protein		
A0A096RBS9	Uncharacterized protein		
A0A096RDT6	Uncharacterized protein		
A0A096RDV2	Uncharacterized protein		

Protein	Annotation	Response to salt stress	ANOVA
A0A096RDX9	Uncharacterized protein		
A0A096RE21	Uncharacterized protein		
A0A096RFZ9	Uncharacterized protein		
A0A096RG34	Uncharacterized protein		
A0A096RG76	Uncharacterized protein		
A0A096RGR3	Uncharacterized protein		
A0A096RH42	Uncharacterized protein (Fragment)		
A0A096RHR4	Uncharacterized protein		
A0A096RHS1	Uncharacterized protein		
A0A096RHZ4	Uncharacterized protein		
A0A096RK85	Inosine-5'-monophosphate dehydrogenase		
A0A096RLG5	Uncharacterized protein		
A0A096RLJ6	Uncharacterized protein		
A0A096RLJ7	Uncharacterized protein		

Protein	Annotation	Response to salt stress	ANOVA
A0A096RLY4	Eukaryotic translation initiation factor 3 subunit D		
A0A096RM05	Uncharacterized protein		
A0A096RM44	Uncharacterized protein		
A0A096RMS8	Uncharacterized protein		
A0A096RN19	Uncharacterized protein		
A0A096RN43	Uncharacterized protein		
A0A096RNV3	Uncharacterized protein		
A0A096RQ47	Uncharacterized protein		
A0A096RQA9	Uncharacterized protein		
A0A096RQS3	Uncharacterized protein		
A0A096RR57	Uncharacterized protein		
A0A096RRD2	Uncharacterized protein		
A0A096RSM5	Uncharacterized protein		
A0A096RSS7	Uncharacterized protein		

Protein	Annotation	Response to salt stress	ANOVA
A0A096RTC3	Uncharacterized protein		
A0A096RTH2	Uncharacterized protein		
A0A096RTN1	Uncharacterized protein		
A0A096RU40	Uncharacterized protein		
A0A096RVM3	Uncharacterized protein		
A0A096RVP9	Uncharacterized protein		
A0A096RW01	Uncharacterized protein		
A0A096RWY9	Uncharacterized protein		
A0A096RX71	Uncharacterized protein		
A0A096RX91	Uncharacterized protein		
A0A096RY70	Uncharacterized protein		
A0A096RY98	Uncharacterized protein		
A0A096RYL4	Uncharacterized protein		
A0A096RYS3	Uncharacterized protein		
A0A096RYU5	Uncharacterized protein		

Protein	Annotation	Response to salt stress	ANOVA
A0A096RYZ1	Uncharacterized protein		
A0A096RZB1	Uncharacterized protein		
A0A096S0A2	Uncharacterized protein		
A0A096S0J0	Uncharacterized protein		
A0A096S0N9	Uncharacterized protein		
A0A096S188	Uncharacterized protein		
A0A096S1G2	Uncharacterized protein		
A0A096S1K8	Uncharacterized protein		
A0A096S386	Uncharacterized protein		
A0A096S3X0	Uncharacterized protein		
A0A096S499	Uncharacterized protein		
A0A096S4A0	Uncharacterized protein		
A0A096S5A7	Uncharacterized protein		
A0A096S5M0	Uncharacterized protein		
A0A096S6K6	Uncharacterized protein		

Protein	Annotation	Response to salt stress	ANOVA
A0A096S6Q1	Uncharacterized protein		
A0A096S6X8	Uncharacterized protein		
A0A096S756	Uncharacterized protein		
A0A096S7C9	Peroxidase 66		
A0A096S842	Uncharacterized protein		
A0A096S8H2	Uncharacterized protein		
A0A096S8Y8	Uncharacterized protein		
A0A096S9C5	Uncharacterized protein		
A0A096SAK5	Uncharacterized protein		
A0A096SAP4	Uncharacterized protein		
A0A096SB59	Uncharacterized protein		
A0A096SBR4	Uncharacterized protein		
A0A096SC11	Uncharacterized protein		
A0A096SCE8	Uncharacterized protein		
A0A096SCH4	Uncharacterized protein		

Protein	Annotation	Response to salt stress	ANOVA
A0A096SE28	Uncharacterized protein		
A0A096SFW3	Uncharacterized protein		
A0A096SGI5	Uncharacterized protein		
A0A096SH62	Uncharacterized protein		
A0A096SHX7	Uncharacterized protein		
A0A096SIN0	Uncharacterized protein		
A0A096SIZ0	Uncharacterized protein		
A0A096SKA6	Uncharacterized protein		
A0A096SKE9	Eukaryotic translation initiation factor 3 subunit L		
A0A096SKY9	Uncharacterized protein		
A0A096SMD9	Uncharacterized protein		
A0A096SMR9	Uncharacterized protein		
A0A096SMS0	Uncharacterized protein		
A0A096SMW4	Uncharacterized protein		

Protein	Annotation	Response to salt stress	ANOVA
A0A096SPM8	Uncharacterized protein		
A0A096SPX6	Uncharacterized protein		
A0A096SRH7	Uncharacterized protein		
A0A096SSA4	Uncharacterized protein		
A0A096SSH2	Uncharacterized protein		
A0A096SSR2	Uncharacterized protein		
A0A096ST25	Uncharacterized protein		
A0A096ST53	Uncharacterized protein		
A0A096ST65	Uncharacterized protein		
A0A096STN8	Uncharacterized protein		
A0A096STP3	Uncharacterized protein		
A0A096SUU7	Uncharacterized protein		
A0A096SVV9	Uncharacterized protein		
A0A096SW39	Uncharacterized protein		
A0A096SWH3	Uncharacterized protein		

Protein	Annotation	Response to salt stress	ANOVA
A0A096SWM8	Uncharacterized protein		
A0A096SWY6	Uncharacterized protein		
A0A096SXT9	Uncharacterized protein		
A0A096SXV5	Uncharacterized protein		
A0A096SYA9	Uncharacterized protein		
A0A096SZL6	Uncharacterized protein		
A0A096SZS3	Uncharacterized protein		
A0A096T094	Uncharacterized protein		
A0A096T0B7	Uncharacterized protein		
A0A096T178	Uncharacterized protein (Fragment)		
A0A096T1A5	Uncharacterized protein		
A0A096T1H2	Uncharacterized protein		
A0A096T1S3	Uncharacterized protein		
A0A096T1S5	Uncharacterized protein		

Protein	Annotation	Response to salt stress	ANOVA
A0A096T1T5	Uncharacterized protein		
A0A096T241	Uncharacterized protein		
A0A096T366	Glyceraldehyde -3-phosphate dehydrogenase 2, cytosolic		
A0A096T433	Uncharacterized protein		
A0A096T4B5	Uncharacterized protein		
A0A096T4L3	Uncharacterized protein		
A0A096T4N9	Uncharacterized protein		
A0A096T4U7	Uncharacterized protein		
A0A096T4Z5	Uncharacterized protein		
A0A096T8E0	Uncharacterized protein		
A0A096T8M4	Uncharacterized protein		
A0A096T8W7	Uncharacterized protein		
A0A096T8Z3	Uncharacterized protein		
A0A096T909	Uncharacterized protein		

Protein	Annotation	Response to salt stress	ANOVA
A0A096T9R8	Uncharacterized protein		
A0A096TA12	Uncharacterized protein		
A0A096TA45	Uncharacterized protein		
A0A096TAC4	Uncharacterized protein		
A0A096TAP2	Uncharacterized protein		
A0A096TBI8	Uncharacterized protein		
A0A096TBV3	Uncharacterized protein		
A0A096TCF9	Uncharacterized protein		
A0A096TDC4	Uncharacterized protein		
A0A096TEB2	Uncharacterized protein (Fragment)		
A0A096TED8	Uncharacterized protein		
A0A096TEK8	Uncharacterized protein		
A0A096TIE6	Uncharacterized protein		
A0A096TIX9	Uncharacterized protein		

Protein	Annotation	Response to salt stress	ANOVA
A0A096TJA2	Uncharacterized protein		
A0A096TKD1	Uncharacterized protein		
A0A096TKT9	Uncharacterized protein		
A0A096TMA9	Uncharacterized protein		
A0A096TMX7	Uncharacterized protein		
A0A096TN76	Uncharacterized protein		
A0A096TPW8	Uncharacterized protein		
A0A096TQZ6	Uncharacterized protein		
A0A096TS52	Uncharacterized protein		
A0A096TS88	Uncharacterized protein		
A0A096TSJ8	Uncharacterized protein		
A0A096TTJ9	Uncharacterized protein		
A0A096TU86	Uncharacterized protein		
A0A096TUD0	Uncharacterized protein		
A0A096TUQ9	Uncharacterized protein		

Protein	Annotation	Response to salt stress	ANOVA
A0A096TUS0	Histone H3.2		
A0A096TUV6	Uncharacterized protein		
A0A096TV80	Uncharacterized protein		
A0A096TVF7	Uncharacterized protein (Fragment)		
A0A096TXA8	Uncharacterized protein		
A0A096TY27	Uncharacterized protein		
A0A096TY66	Uncharacterized protein		
A0A096U0D4	Uncharacterized protein		
A0A096U158	Uncharacterized protein		
A0A096U258	Uncharacterized protein		
A0A096U2E6	Uncharacterized protein		
A0A096U2Y1	Uncharacterized protein		
A0A096U487	Uncharacterized protein		
A0A096U6B0	Uncharacterized protein		
A0A096U902	Uncharacterized protein		

Protein	Annotation	Response to salt stress	ANOVA
A0A096U9I4	Uncharacterized protein		
A0A096UA28	Uncharacterized protein		
A0A096UAK8	Uncharacterized protein		
A0A096UCG5	Uncharacterized protein		
A0A096UCP4	Uncharacterized protein		
A0A096UCP7	Uncharacterized protein		
A0A096UCQ5	Uncharacterized protein		
A0A096UDB7	Uncharacterized protein		
A0A096UDS3	Uncharacterized protein		
A0A096UE42	Uncharacterized protein		
A0A096UG04	Uncharacterized protein		
A0A096UGV3	Uncharacterized protein		
A0A096UHC7	Uncharacterized protein		
A0A096UJ03	Uncharacterized protein		
A0A096UJ49	Uncharacterized protein		

Protein	Annotation	Response to salt stress	ANOVA
A0A097C0T5	Sus1		
A0A097PKB3	Homoserine kinase (Fragment)		
A0A097PLA8	Nitrilase/cyanide hydratase and apolipoprotein N-acyltransferase family protein (Fragment)		
A2T1W7	Aldose reductase		
A3FMB9	Proteasome subunit alpha type		
A6YSM3	PL3K2		
A8IK79	Asr protein		
B1P123	TRIBOA-glucoside O-methyltransferase BX7		
B2XWS5	Isopentenyl transferase IPT4		
B4F7S3	Plasma membrane intrinsic protein1		
B4F7T1	Uncharacterized protein		

Protein	Annotation	Response to salt stress	ANOVA
B4F7U0	Proteasome subunit alpha type		
B4F7V3	Orphans transcription factor		
B4F7X5	Reticulon-like protein		
B4F820	Triosephosphate isomerase		
B4F848	Chaperonin		
B4F861	Uncharacterized protein		
B4F871	Uncharacterized protein		
B4F8B9	Uncharacterized protein		
B4F8D7	Peroxidase		
B4F8J8	Pyruvate kinase		
B4F8K1	60S ribosomal protein L7-2		
B4F8X3	Acyl-coenzyme A oxidase		
B4F946	Uncharacterized protein		
B4F957	Uncharacterized protein		
B4F972	Glutamate decarboxylase		

Protein	Annotation	Response to salt stress	ANOVA
B4F987	Uncharacterized protein		
B4F9B2	Acetyl-CoA acetyltransferase, cytosolic 1		
B4F9B5	Uncharacterized protein		
B4F9G0	Uncharacterized protein		
B4F9G8	Pyruvate kinase		
B4F9H1	Uncharacterized protein		
B4F9I2	Uncharacterized protein		
B4F9I5	ATP synthase delta chain		
B4F9K2	Uncharacterized protein		
B4F9T3	Uncharacterized protein		
B4F9U8	Uncharacterized protein		
B4F9U9	Uncharacterized protein		
B4F9X0	Alpha-galactosidase		
B4FA21	Purple acid phosphatase		
B4FA63	Uncharacterized protein		

Protein	Annotation	Response to salt stress	ANOVA
B4FA76	Dolichyl-diphosphooligosaccharide--protein glycosyltransferase 48 kDa subunit		
B4FAD4	Isocitrate dehydrogenase [NAD] subunit, mitochondrial		
B4FAE1	Ras protein RIC1		
B4FAE5	Uncharacterized protein		
B4FAF8	Uncharacterized protein		
B4FAL9	Fructose-bisphosphate aldolase		
B4FAM6	Uncharacterized protein		
B4FAP8	Erwinia induced protein 2		
B4FAV3	40S ribosomal protein S3a		
B4FB65	Uncharacterized protein		
B4FB66	Uncharacterized protein		

Protein	Annotation	Response to salt stress	ANOVA
B4FBC2	Uncharacterized protein		
B4FBC9	Uncharacterized protein		
B4FBD5	Uncharacterized protein		
B4FBF2	Carboxypeptidase		
B4FBF4	Serine hydroxymethyltransferase		
B4FBF6	Uncharacterized protein		
B4FBJ5	Uncharacterized protein		
B4FBK3	Eukaryotic initiation factor 4A		
B4FBN8	Chitinase 1		
B4FBP0	Putative TCP-1/cpn60 chaperonin family protein isoform 1		
B4FBQ8	Cytochrome b-c1 complex subunit Rieske, mitochondrial		
B4FBV8	Eukaryotic translation		

Protein	Annotation	Response to salt stress	ANOVA
	initiation factor 3 subunit G		
B4FBW5	Mannitol dehydrogenase		
B4FBY5	40S ribosomal protein S23		
B4FBY6	Uncharacterized protein		
B4FCG9	60S ribosomal protein L11-1		
B4FCK9	60S ribosomal protein L22-2		
B4FCM4	Prenylated Rab receptor 2		
B4FCQ4	Cytochrome c oxidase subunit		
B4FCR7	Soluble inorganic pyrophosphatase		
B4FD74	Uncharacterized protein		
B4FD90	40S ribosomal protein S19		
B4FDG2	Acyl carrier protein		
B4FDN9	Uncharacterized protein		

Protein	Annotation	Response to salt stress	ANOVA
B4FDY6	Proteasome subunit alpha type		
B4FE18	Histone H2B		
B4FE30	Chaperonin		
B4FE49	Uncharacterized protein		
B4FEJ6	Actin-depolymerizing factor 3		
B4FEN3	Uncharacterized protein		
B4FER8	Acyl-CoA-binding protein		
B4FF57	Uncharacterized protein		
B4FF65	Uncharacterized protein		
B4FF86	Uncharacterized protein		
B4FFA7	Enoyl-[acyl-carrier-protein] reductase isoform 1		
B4FFE7	Acyl carrier protein		
B4FFG8	Uncharacterized protein		
B4FFH8	Adenosine kinase 2		

Protein	Annotation	Response to salt stress	ANOVA
B4FFJ9	Uncharacterized protein		
B4FFP2	Glutamate dehydrogenase		
B4FFV3	Malate dehydrogenase		
B4FFX7	Proteasome subunit alpha type		
B4FFZ2	Ketol-acid reductoisomerase		
B4FFZ3	Uncharacterized protein		
B4FFZ6	60S ribosomal protein L3		
B4FG22	40S ribosomal protein S25-1		
B4FG39	Peroxidase		
B4FG53	Malate dehydrogenase		
B4FGA3	Uncharacterized protein		
B4FGC8	40S ribosomal protein S12		
B4FGF1	Non-green plastid inner envelope membrane protein		

Protein	Annotation	Response to salt stress	ANOVA
B4FGL4	60S ribosomal protein L23		
B4FH44	Thioredoxin		
B4FH55	Histone H2A		
B4FH57	Elongation factor Tu		
B4FH68	Peroxidase		
B4FH98	Uncharacterized protein		
B4FHE4	Uncharacterized protein		
B4FHH4	Triosephosphate isomerase		
B4FHM1	Uncharacterized protein		
B4FHM5	60S ribosomal protein L37a		
B4FHT1	Annexin		
B4FHZ4	NADH ubiquinone oxidoreductase B14 subunit		
B4FI76	Uncharacterized protein		
B4FI86	Proteasome subunit beta type		
B4FIC7	Superoxide dismutase [Cu-Zn]		

Protein	Annotation	Response to salt stress	ANOVA
B4FID1	Uncharacterized protein		
B4FID4	Putative oxidoreductase, aldo/keto reductase family protein		
B4FIE9	S-adenosylmethionine synthase		
B4FIT7	CHY1		
B4FJ27	40S ribosomal protein S24		
B4FJA8	Uncharacterized protein		
B4FJL0	Serine/threonine-protein phosphatase		
B4FJY1	Uncharacterized protein		
B4FK84	Uncharacterized protein		
B4FKA5	Small nuclear ribonucleoprotein Sm D3		
B4FKD5	Eukaryotic translation initiation factor 6		
B4FKH7	Cytochrome b5		

Protein	Annotation	Response to salt stress	ANOVA
B4FKI3	60S ribosomal protein L23a		
B4FKM1	Guanine nucleotide-binding protein beta subunit-like protein		
B4FKW0	Uncharacterized protein		
B4FL17	Translationally-controlled tumor protein		
B4FL36	Uncharacterized protein		
B4FL64	Ribosomal protein L19		
B4FL79	Uncharacterized protein		
B4FLA1	Uncharacterized protein		
B4FLA2	Chorismate synthase		
B4FLB0	Uncharacterized protein		
B4FLB2	Adenylosuccinate lyase		
B4FLH5	Uncharacterized protein		
B4FLH6	NADH-ubiquinone		

Protein	Annotation	Response to salt stress	ANOVA
	oxidoreductase B18 subunit		
B4FLJ3	Isocitrate dehydrogenase [NADP]		
B4FLN7	PUR ALPHA-1		
B4FLQ8	26S proteasome non-ATPase regulatory subunit 14		
B4FM12	Esterase isoform 1		
B4FM15	60S ribosomal protein L28 isoform 1		
B4FM49	Import receptor subunit TOM40		
B4FMI5	40S ribosomal protein S4		
B4FML8	40S ribosomal protein S13		
B4FML9	Pyruvate dehydrogenase E1 component subunit alpha		
B4FMP6	Putative oxidoreductase, aldo/keto reductase family protein		

Protein	Annotation	Response to salt stress	ANOVA
B4FMR9	Uncharacterized protein		
B4FMS7	Mitochondrial prohibitin complex protein 2		
B4FMS8	Uncharacterized protein		
B4FMV3	Uncharacterized protein		
B4FMX4	Glutamine synthetase		
B4FMY6	Uncharacterized protein		
B4FN17	USP family protein		
B4FN19	Uncharacterized protein		
B4FN24	Peroxiredoxin-5		
B4FN28	Ribosomal protein		
B4FNC9	Small ubiquitin-related modifier		
B4FNG6	Uncharacterized protein		
B4FNK8	Uncharacterized protein		
B4FNQ8	Calmodulin		
B4FP25	40S ribosomal protein S19		

Protein	Annotation	Response to salt stress	ANOVA
B4FPA0	Uncharacterized protein		
B4FPB7	60S ribosomal protein L7a		
B4FPD1	Membrane steroid-binding protein 1		
B4FPE4	Uncharacterized protein		
B4FPG2	Actin1 isoform 1		
B4FPJ2	U6 snRNA-associated Sm-like protein LSm3		
B4FPK8	Cytochrome b5		
B4FPL1	Bowman-Birk type wound-induced proteinase inhibitor WIP1		
B4FPM8	Uncharacterized protein		
B4FPX5	Uncharacterized protein		
B4FQ03	60S ribosomal protein L7-2		
B4FQ61	40S ribosomal protein S15a		

Protein	Annotation	Response to salt stress	ANOVA
B4FQ71	Uncharacterized protein		
B4FQ98	NADH-ubiquinone oxidoreductase 51 kDa subunit		
B4FQA5	Uncharacterized protein		
B4FQC4	Uncharacterized protein		
B4FQH2	Uncharacterized protein		
B4FQJ6	Uncharacterized protein		
B4FQL2	SEC13-related protein		
B4FQM2	Pyrophosphate--fructose 6-phosphate 1-phosphotransferase beta subunit		
B4FQP4	Uncharacterized protein		
B4FQQ1	Uncharacterized protein		
B4FQS9	Putative cytochrome P450 superfamily protein		

Protein	Annotation	Response to salt stress	ANOVA
B4FQW8	Aquaporin PIP1.1		
B4FQX1	Uncharacterized protein		
B4FQZ2	Uncharacterized protein		
B4FR02	Uncharacterized protein		
B4FR57	Eukaryotic translation initiation factor 3 subunit H		
B4FR70	26S proteasome non-ATPase regulatory subunit 8		
B4FR72	Purple acid phosphatase		
B4FR90	Uncharacterized protein		
B4FR99	Uncharacterized protein		
B4FRC2	Uncharacterized protein		
B4FRC6	Uncharacterized protein		
B4FRC9	Transaldolase 2		
B4FRF0	Glutathione peroxidase		

Protein	Annotation	Response to salt stress	ANOVA
B4FRG1	14-3-3-like protein		
B4FRG8	Uncharacterized protein		
B4FRI1	Phosphoserine aminotransferase		
B4FRK0	Uncharacterized protein		
B4FRM7	60S ribosomal protein L12		
B4FRR1	Uncharacterized protein		
B4FRS1	Ras-related protein Rab-6A		
B4FRS8	Uncharacterized protein		
B4FS42	Aquaporin PIP2.4		
B4FS65	Uncharacterized protein		
B4FS84	Uncharacterized protein		
B4FSA7	ADP,ATP carrier protein		
B4FSF1	Uncharacterized protein		
B4FSG4	Jasmonate-induced protein		

Protein	Annotation	Response to salt stress	ANOVA
B4FSJ1	Uncharacterized protein		
B4FSL2	Uncharacterized protein		
B4FSN1	Uncharacterized protein		
B4FSQ4	40S ribosomal protein SA		
B4FSS8	Uncharacterized protein		
B4FST4	SKP1-like protein 1A		
B4FSV6	6-phosphogluconate dehydrogenase, decarboxylating		
B4FSW0	Uncharacterized protein		
B4FSW5	Peroxidase		
B4FSZ7	Uncharacterized protein		
B4FT32	Diaminopimelate decarboxylase		
B4FT61	Uncharacterized protein		
B4FT62	Uncharacterized protein		
B4FT85	Isochorismate synthase 1		

Protein	Annotation	Response to salt stress	ANOVA
B4FTA3	60S ribosomal protein L27		
B4FTB5	Proteasome subunit beta type		
B4FTD1	Glutathione S-transferase III		
B4FTD2	40S ribosomal protein SA		
B4FTJ6	Uncharacterized protein		
B4FTK9	1,4-beta-D-glucanase		
B4FTM3	Haloacid dehalogenase-like hydrolase domain-containing protein 1A		
B4FTM9	Uncharacterized protein		
B4FTW4	Uncharacterized protein		
B4FTW5	60S ribosomal protein L7-1		
B4FTW8	Uncharacterized protein		
B4FTX3	Uncharacterized protein		

Protein	Annotation	Response to salt stress	ANOVA
B4FTY8	Harpin inducing protein		
B4FU56	Uncharacterized protein		
B4FUA9	60 ribosomal protein L14		
B4FUB4	60S acidic ribosomal protein P1		
B4FUH2	Aspartate aminotransferase		
B4FUK2	Peptidyl-prolyl cis-trans isomerase		
B4FUK7	Uncharacterized protein		
B4FUM4	Plasma membrane intrinsic protein1 isoform 1		
B4FUR2	Uncharacterized protein		
B4FUR6	Uncharacterized protein		
B4FUS2	40S ribosomal protein S18		
B4FUS5	ATP-dependent Clp protease		

Protein	Annotation	Response to salt stress	ANOVA
	proteolytic subunit		
B4FUZ2	Uncharacterized protein		
B4FV68	Profilin		
B4FV82	Uncharacterized protein		
B4FV91	Uncharacterized protein		
B4FVB1	Uncharacterized protein		
B4FVD5	Uncharacterized protein		
B4FVD6	Uncharacterized protein		
B4FVH1	Malate dehydrogenase		
B4FVJ0	Uncharacterized protein		
B4FVL1	26S proteasome non-ATPase regulatory subunit 6		
B4FVN5	Uncharacterized protein		
B4FW57	Uncharacterized protein		
B4FWD0	Minor allergen Alt a 7		

Protein	Annotation	Response to salt stress	ANOVA
B4FWP0	Fructose-bisphosphate aldolase		
B4FWR7	60S ribosomal protein L13		
B4FWU6	Uncharacterized protein		
B4FWY4	Uncharacterized protein		
B4FX16	Macrophage migration inhibitory factor		
B4FX40	Uncharacterized protein		
B4FXW5	Uncharacterized protein		
B4FY16	Elongation factor 1-alpha		
B4FY63	Annexin		
B4FYA3	Uncharacterized protein		
B4FYN0	Mitochondrial import inner membrane translocase subunit Tim13		
B4FYV4	Saposin-like type B, region 1 family protein		

Protein	Annotation	Response to salt stress	ANOVA
B4FZ84	40S ribosomal protein SA		
B4FZN6	40S ribosomal protein S7		
B4FZU8	Malate dehydrogenase		
B4FZU9	Uncharacterized protein		
B4FZZ2	Peptidyl-prolyl cis-trans isomerase		
B4G031	Uncharacterized protein		
B4G039	Uncharacterized protein		
B4G043	Uncharacterized protein		
B4G066	Uncharacterized protein		
B4G072	DIMBOA UDP-glucosyltransferase BX9		
B4G080	Caffeoyl-CoA O-methyltransferase 1		
B4G087	Uncharacterized protein		
B4G0F3	Probable bifunctional		

Protein	Annotation	Response to salt stress	ANOVA
	methylthioribulose-1-phosphate dehydratase/enolase-phosphatase E1		
B4G0H3	Uncharacterized protein		
B4G0N0	Glucose-6-phosphate isomerase		
B4G0Q9	Abscisic stress ripening protein 2		
B4G0R0	60S ribosomal protein L33-B		
B4G0V4	Coatomer subunit delta		
B4G0V9	Lipase/lipooxygenase, PLAT/LH2		
B4G0Z5	60S ribosomal protein L27a-3		
B4G137	Uncharacterized protein		
B4G177	Uncharacterized protein		
B4G194	40S ribosomal protein SA		
B4G1B0	Remorin		

Protein	Annotation	Response to salt stress	ANOVA
B4G1C1	Uncharacterized protein		
B4G1C2	Uncharacterized protein		
B4G1D2	CBS domain protein		
B4G1G0	Uncharacterized protein		
B4G1H1	Uncharacterized protein		
B4G1L5	Uncharacterized protein		
B4G1P1	Glutamine synthetase		
B4G1P9	3-N-debenzoyl-2-deoxytaxol N-benzoyltransferase		
B4G1S4	Peroxidase		
B4G1T3	Uncharacterized protein		
B4G1V7	Uncharacterized protein		
B4G1Y5	Uncharacterized protein		
B4G1Z0	Alpha-L-fucosidase 2		
B4G1Z2	Xyloglucan endotransglucosylase/hydrolase		

Protein	Annotation	Response to salt stress	ANOVA
B4G286	40S ribosomal protein S18		
B5AK47	Dhurrinase-like B-glucosidase		
B5U8J8	Asparagine synthetase		
B6SGB6	Pyrophosphate--fructose 6-phosphate 1-phosphotransferase alpha subunit		
B6SGK5	Uncharacterized protein		
B6SGM5	Putative oxidoreductase, aldo/keto reductase family protein		
B6SGP2	Ras-related protein RGP1		
B6SGY0	Subtilisin-chymotrypsin inhibitor CI-1B		
B6SH12	Uncharacterized protein		
B6SHF6	Mitochondrial-processing peptidase alpha subunit		

Protein	Annotation	Response to salt stress	ANOVA
B6SHM7	40S ribosomal protein S7		
B6SHT0	OB-fold nucleic acid binding domain containing protein		
B6SHT6	PVR3-like protein		
B6SHW0	60S ribosomal protein L6		
B6SHY0	ATOZI1		
B6SI49	Ras-related protein Rab-2-A		
B6SIA2	40S ribosomal protein S26		
B6SIC6	Putative ubiquitin-conjugating enzyme family		
B6SIF0	Glycine-rich RNA-binding protein 2		
B6SII4	40S ribosomal protein S15		
B6SII7	40S ribosomal protein S15		
B6SIL5	40S ribosomal protein S11		

Protein	Annotation	Response to salt stress	ANOVA
B6SIM0	Cytochrome c oxidase polypeptide Vb		
B6SIM7	Proteasome subunit beta type		
B6SIP0	NHP2-like protein 1		
B6SIP2	Hydrogen-transporting ATP synthase, rotational mechanism		
B6SIP4	40S ribosomal protein S26		
B6SIU4	Peroxidase		
B6SIU9	Glycine-rich RNA-binding protein 2		
B6SIX3	40S ribosomal protein S24		
B6SIY6	60S ribosomal protein L44		
B6SJ21	Guanine nucleotide-binding protein beta subunit-like protein		
B6SJC1	RALF		

Protein	Annotation	Response to salt stress	ANOVA
B6SJC8	60S ribosomal protein L18		
B6SJF5	Acyl carrier protein		
B6SJJ1	60S ribosomal protein L31		
B6SJJ4	Jasmonate-induced protein		
B6SJN1	Auxin-repressed 12.5 kDa protein		
B6SJQ5	Histone H3		
B6SJS2	Protein Z		
B6SJY2	Putative uncharacterized protein		
B6SJZ5	Histone H2B		
B6SJZ8	Glyceraldehyde -3-phosphate dehydrogenase		
B6SK03	Ubiquitin-conjugating enzyme spm2		
B6SK48	Late embryogeneis abundant protein		
B6SKA0	Glutathione S-transferase GSTF2		

Protein	Annotation	Response to salt stress	ANOVA
B6SKA7	Elongation factor 1-alpha		
B6SKW0	Histone H4		
B6SLK4	Elongation factor 1-beta		
B6SLX1	Chaperonin		
B6SM71	Uncharacterized protein		
B6SMC1	Thioredoxin		
B6SMR2	Peroxidase		
B6SN85	H/ACA ribonucleoprotein complex subunit 3-like protein		
B6SNG5	6,7-dimethyl-8-ribityllumazine synthase		
B6SNI9	Cytochrome b5		
B6SNL8	60S ribosomal protein L38		
B6SNM4	Protein transport protein Sec61 beta subunit		
B6SPB2	Flavoprotein wrbA		
B6SPL7	Copper chaperone		
B6SPR5	Fb14		

Protein	Annotation	Response to salt stress	ANOVA
B6SPZ2	Glyceraldehyde -3-phosphate dehydrogenase		
B6SQE5	BRASSINOSTEROID INSENSITIVE 1-associated receptor kinase 1		
B6SQI1	Bundle sheath cell specific protein 1		
B6SQM6	Pathogeneis protein 10		
B6SR40	Putative uncharacterized protein		
B6SRE7	Peptidyl-prolyl cis-trans isomerase		
B6SRL2	Aconitate hydratase		
B6SS03	Arogenate dehydrogenase isoform 2		
B6SS27	AMP-binding protein		
B6SS48	Outer mitochondrial		

Protein	Annotation	Response to salt stress	ANOVA
	membrane protein porin		
B6SSB6	Eukaryotic translation initiation factor 3 subunit I		
B6SSJ6	Protein P21		
B6SST9	ATP synthase delta chain		
B6ST04	Beta-hexosaminidase		
B6ST82	Putative uncharacterized protein		
B6STA5	Glycine-rich RNA-binding protein 2		
B6STJ0	Pleckstrin homology domain containing, family A		
B6STR1	dTDP-4-dehydrorhamnose reductase		
B6STY9	Salt tolerance protein		
B6SU31	Glutathione peroxidase		

Protein	Annotation	Response to salt stress	ANOVA
B6SUB6	Anthocyanidin 5,3-O-glucosyltransferase		
B6SUD1	Alcohol dehydrogenase 2		
B6SUK0	LOL3		
B6SUV6	Hypersensitive-induced response protein		
B6SV64	Heat shock 70 kDa protein 4		
B6SVE1	Carboxypeptidase		
B6SVV9	ATP synthase subunit beta		
B6SWZ4	Propionyl-CoA carboxylase beta chain		
B6SXF5	Pathogenesis-related protein 1		
B6SXV4	Peroxisomal fatty acid beta-oxidation multifunctional protein		
B6SXW8	RuBisCO large subunit-binding		

Protein	Annotation	Response to salt stress	ANOVA
	protein subunit alpha		
B6SYF5	Peptidyl-prolyl cis-trans isomerase		
B6SYW0	40S ribosomal protein S26		
B6SZ69	Heat shock cognate 70 kDa protein 2		
B6SZ83	Actin-7		
B6SZB9	14-3-3-like protein		
B6SZK9	Coatomer subunit epsilon		
B6SZZ6	Nonspecific lipid-transfer protein		
B6T033	Glutathione S-transferase GSTU6		
B6T056	Superoxide dismutase [Cu-Zn]		
B6T0X0	Histone H4		
B6T0Y2	ATP synthase epsilon chain, mitochondrial		
B6T0Z9	60S ribosomal protein L27a-3		

Protein	Annotation	Response to salt stress	ANOVA
B6T188	40S ribosomal protein S26		
B6T198	40S ribosomal protein S26		
B6T1G6	60S ribosomal protein L24		
B6T1H0	40S ribosomal protein S6		
B6T1K2	60S acidic ribosomal protein P1		
B6T1L8	60S ribosomal protein L33-B		
B6T1V6	Calmodulin		
B6T267	Ribosomal protein L15		
B6T281	40S ribosomal protein S14		
B6T291	Actin-depolymerizing factor 3		
B6T2A5	40S ribosomal protein S11		
B6T2A6	Stem-specific protein TSJT1		
B6T2R4	IQ calmodulin-binding motif family protein		

Protein	Annotation	Response to salt stress	ANOVA
B6T2S0	26S protease regulatory subunit 4		
B6T2Y1	Peroxiredoxin-5		
B6T2Z0	B12D protein		
B6T329	Nuclease PA3		
B6T3B4	Putative uncharacterized protein		
B6T3D4	Methionyl-tRNA synthetase		
B6T433	Elongation factor 1-alpha		
B6T451	Importin subunit alpha		
B6T4G7	Fibrillarin-2		
B6T4H7	60S ribosomal protein L27a-3		
B6T4P9	Esterase		
B6T4R2	Flavoprotein wrbA		
B6T4R3	UTP--glucose-1-phosphate uridylyltransferase		
B6T533	Ribosomal protein		
B6T574	Pyruvate kinase		

Protein	Annotation	Response to salt stress	ANOVA
B6T595	60S ribosomal protein L17		
B6T5F2	60S ribosomal protein L13		
B6T5Q6	Uncharacterized protein		
B6T5U0	Uncharacterized protein		
B6T638	Tyrosyl-tRNA synthetase		
B6T6G1	60S ribosomal protein L12		
B6T6H3	Pyruvate dehydrogenase E1 component subunit beta		
B6T6Y2	S-glutathione dehydrogenase/ class III alcohol dehydrogenase		
B6T706	Aspartic proteinase oryzasin-1		
B6T711	DNA repair protein RAD23		
B6T715	Aldehyde dehydrogenase		
B6T766	60S ribosomal protein L21		

Protein	Annotation	Response to salt stress	ANOVA
B6T769	60S ribosomal protein L7a		
B6T7B2	40S ribosomal protein S9		
B6T7B6	Glutathione S-transferase, C-terminal-like		
B6T7B8	Aquaporin PIP2.2		
B6T7C6	Putative uncharacterized protein		
B6T7E7	Histone H2A		
B6T7H7	Protein LRP16		
B6T7J7	Serine hydroxymethyltransferase		
B6T7L9	14-3-3-like protein		
B6T7Q7	Serine hydroxymethyltransferase		
B6T7Z2	Cytochrome b5		
B6T828	Grx_C4-glutaredoxin subgroup I		
B6T834	40S ribosomal protein S3a		
B6T856	L-lactate dehydrogenase		

Protein	Annotation	Response to salt stress	ANOVA
B6T872	60S ribosomal protein L32		
B6T8C6	Ribosomal protein		
B6T8F6	Uncharacterized protein		
B6T8K2	40S ribosomal protein S20		
B6T8M9	Mitochondrial prohibitin complex protein 2		
B6T8R5	60S ribosomal protein L34		
B6T8U0	Plasminogen activator inhibitor 1 RNA-binding protein		
B6T904	UMP-CMP kinase		
B6T969	Proteasome subunit alpha type		
B6T9C0	Uncharacterized protein		
B6T9P7	Cycloartenol-C-24-methyltransfera se 1		

Protein	Annotation	Response to salt stress	ANOVA
B6T9T0	O-methyltransferase ZRP4		
B6T9W6	Charged multivesicular body protein 1b		
B6TA81	GDP-mannose 4,6 dehydratase 2		
B6TAA7	Chaperonin		
B6TAJ3	Proteasome subunit alpha type		
B6TAL1	Vacuolar processing enzyme		
B6TB29	Fructokinase-2		
B6TB39	Fructokinase-2		
B6TB84	Soluble inorganic pyrophosphatase		
B6TBM1	Alpha-soluble NSF attachment protein		
B6TBW2	ATP synthase delta chain		
B6TBX3	GTP-binding nuclear protein Ran-A1		

Protein	Annotation	Response to salt stress	ANOVA
B6TBY8	UDP-glucose 6-dehydrogenase		
B6TC92	60S ribosomal protein L35		
B6TC95	Histone H1		
B6TCE9	Peptidyl-prolyl cis-trans isomerase		
B6TCK3	NADH-cytochrome b5 reductase		
B6TD54	ATP-citrate synthase		
B6TD62	Membrane steroid-binding protein 1		
B6TD69	40S ribosomal protein S17-4		
B6TDA9	2-cys peroxiredoxin BAS1		
B6TDF2	Riboflavin synthase alpha chain		
B6TDF8	Glyceraldehyde -3-phosphate dehydrogenase		
B6TDG5	Protein pob		
B6TDH1	DAG protein		

Protein	Annotation	Response to salt stress	ANOVA
B6TDH5	Ubiquitin-conjugating enzyme E2-17 kDa		
B6TE40	60S ribosomal protein L22-2		
B6TEP5	Triose phosphate/phosphate translocator, non-green plastid,chloroplast		
B6TET7	Abscisic stress ripening protein 1		
B6TF15	Xylose isomerase		
B6TF69	Ketol-acid reductoisomerase		
B6TFE4	Ribokinase		
B6TFN1	Minor allergen Alt a 7		
B6TFS9	14-3-3-like protein A		
B6TFY4	40S ribosomal protein S27		
B6TG61	40S ribosomal protein S16		

Protein	Annotation	Response to salt stress	ANOVA
B6TG70	Mitochondrial-processing peptidase beta subunit		
B6TG98	Copper ion binding protein		
B6TGG2	2,3-bisphosphoglycerate-independent phosphoglycerate mutase		
B6TGG7	3-oxoacyl-[acyl-carrier-protein] synthase		
B6TGS7	Cytochrome c		
B6TGS8	6,7-dimethyl-8-ribityllumazine synthase		
B6TH42	60S ribosomal protein L9		
B6TH57	Succinyl-CoA ligase alpha-chain 2		
B6TH64	40S ribosomal protein S9		
B6TH67	MFP1 attachment factor 1		

Protein	Annotation	Response to salt stress	ANOVA
B6THH7	Isoamyl acetate-hydrolyzing esterase		
B6THJ2	Mitochondrial uncoupling protein 3		
B6THM9	60S ribosomal protein L22-2		
B6THR9	3-isopropylmalate dehydrogenase		
B6THZ8	Threonine synthase		
B6TIG6	Transaminase/ transferase, transferring nitrogenous groups		
B6TIL4	GDP-mannose 3,5-epimerase 2		
B6TIM2	Deoxyribodipyrimidine photolyase		
B6TIQ8	ATP/GTP binding protein		
B6TIR4	Ribulose-phosphate 3-epimerase		
B6TIY2	Transposon protein		

Protein	Annotation	Response to salt stress	ANOVA
B6TJ22	Glutathione S-transferase parA		
B6TJ40	Lipid transfer protein		
B6TJ78	3-N-debenzoyl-2-deoxytaxol N-benzoyltransferase		
B6TJ93	40S ribosomal protein S15a		
B6TJB6	Proteasome subunit alpha type		
B6TJM1	Isocitrate dehydrogenase [NAD] subunit, mitochondrial		
B6TJY4	Dihydrolipoyllysine-residue acetyltransferase component of pyruvatedehydrogenase complex		
B6TK27	Glutathione S-transferase GSTU6		
B6TKR7	Jasmonate-induced protein		

Protein	Annotation	Response to salt stress	ANOVA
B6TKY3	Putative TCP-1/cpn60 chaperonin family protein		
B6TKZ3	Hydrolase, carbon-nitrogen family		
B6TL24	Glyoxylate reductase		
B6TL26	NADPH quinone oxidoreductase 2		
B6TLM5	Glutathione S-transferase GSTU6		
B6TLX0	NADH-ubiquinone oxidoreductase 10.5 kDa subunit		
B6TLX2	Fiber protein Fb15		
B6TLX4	Jasmonate-induced protein		
B6TM00	60 ribosomal protein L14		
B6TM55	APx1-Cytosolic Ascorbate Peroxidase		

Protein	Annotation	Response to salt stress	ANOVA
B6TMA0	Dehydrin 13		
B6TMB2	PDIL2-2-Zea mays protein disulfide isomerase		
B6TMC1	DAG protein		
B6TMG9	Mitochondrial NADH ubiquinone oxidoreductase 29 kDa subunit		
B6TN41	4-hydroxy-4-methyl-2-oxoglutarate aldolase		
B6TN48	3-hydroxyisobutyryl-CoA hydrolase/ catalytic		
B6TNC0	Ankyrin repeat domain-containing protein 2		
B6TNR8	40S ribosomal protein S2		
B6TNS0	Nucleolar protein Nop56		
B6TNT5	Peptide methionine		

Protein	Annotation	Response to salt stress	ANOVA
	sulfoxide reductase		
B6TP36	Prohibitin		
B6TP58	Histone H3		
B6TP60	CSD transcription factor		
B6TPA4	Carnitine racemase/ catalytic		
B6TPG2	60S ribosomal protein L26-1		
B6TPP7	Threonine synthase		
B6TQ36	Pyruvate dehydrogenase E1 component subunit beta		
B6TQ65	Proteasome subunit beta type		
B6TQB3	Ran-binding protein 1		
B6TQN7	60S acidic ribosomal protein P1		
B6TQW0	Carboxypeptidase		

Protein	Annotation	Response to salt stress	ANOVA
B6TRL2	Brain acid soluble protein 1		
B6TRM9	Mitochondrial-processing peptidase alpha subunit		
B6TRQ7	Pre-mRNA-splicing factor 19		
B6TS21	Succinyl-CoA ligase subunit beta		
B6TS22	O-methyltransferase ZRP4		
B6TS83	Aquaporin PIP2.1		
B6TS84	Transaldolase 2		
B6TS91	Glutathione S-transferase		
B6TSB3	Glucose-6-phosphate 1-dehydrogenase		
B6TSH6	60S ribosomal protein L21		
B6TSQ9	Aspartic proteinase oryzasin-1		
B6TTP0	Histone H3		

Protein	Annotation	Response to salt stress	ANOVA
B6TTP1	Non-specific lipid-transfer protein		
B6TTW1	Cyanate hydratase		
B6TU33	Rapid alkalinization factor 1		
B6TUA2	Acetyltransferase component of pyruvate dehydrogenase complex		
B6TV07	Glutamate decarboxylase		
B6TV55	Stem 28 kDa glycoprotein		
B6TVD6	3-isopropylmalate dehydrogenase		
B6TVP8	Stromal cell-derived factor 2		
B6TW65	Beta-glucosidase		
B6TWE1	USP family protein		
B6TWW1	Aspartate-semialdehyde dehydrogenase		

Protein	Annotation	Response to salt stress	ANOVA
B6TXH5	Transaminase/ transferase, transferring nitrogenous groups		
B6TXM6	10-deacetylbaccatin III 10-O-acetyltransferase		
B6TXS9	ATP synthase subunit gamma		
B6TYG2	Enoyl-[acyl-carrier-protein] reductase [NADH]		
B6TZS3	Uncharacterized protein		
B6TZY4	60S ribosomal protein L28		
B6U0P4	RHM1		
B6U0S1	Elongation factor 2		
B6U0T2	Putative uncharacterized protein		
B6U1C5	Uncharacterized protein		

Protein	Annotation	Response to salt stress	ANOVA
B6U3A0	Glycine-rich RNA-binding protein 7		
B6U474	Minor allergen Alt a 7		
B6U4D9	Protein ROOT HAIR DEFECTIVE 3 homolog		
B6U543	Versicolorin reductase		
B6U5I0	Mitochondrial import inner membrane translocase subunit Tim10		
B6U5W6	Mitochondrial import inner membrane translocase subunit Tim9		
B6U6W0	Peroxidase		
B6U724	Flavoprotein wrbA		
B6U7D8	Cinnamyl alcohol dehydrogenase		
B6U7Y1	Activator of 90 kDa heat shock protein ATPase		

Protein	Annotation	Response to salt stress	ANOVA
B6U8P6	ABA-responsive protein		
B6U990	Ankyrin repeat domain-containing protein 2		
B6U9K5	Oxysterol-binding protein		
B6U9X1	Cytidine deaminase		
B6UBG1	Putative uncharacterized protein		
B6UC34	Glutaminyl-tRNA synthetase		
B6UCR8	Proteasome subunit alpha type		
B6UCV5	Shikimate biosynthesis protein aroDE		
B6UD26	O-methyltransferase ZRP4		
B6UD80	Glutathione S-transferase		
B6UDG4	Malic enzyme		

Protein	Annotation	Response to salt stress	ANOVA
B6UDS5	Glutamine synthetase		
B6UDY2	60S ribosomal protein L17		
B6UE00	Soluble inorganic pyrophosphatase		
B6UE01	40S ribosomal protein S29		
B6UE23	60S ribosomal protein L18a		
B6UEA6	40S ribosomal protein S28		
B6UEG5	Mitochondrial import inner membrane translocase subunit Tim9		
B6UES0	Charged multivesicular body protein 4b		
B6UF43	Calcium-dependent protein kinase, isoform 2		
B6UFB3	Stromal 70 kDa heat shock-related protein		

Protein	Annotation	Response to salt stress	ANOVA
B6UGM5	60S ribosomal protein L21		
B6UGQ9	Rhicadhesin receptor		
B6UGR9	60S ribosomal protein L10-3		
B6UHP9	Programmed cell death protein 5		
B6UHU1	Catalase		
B6UIM2	40S ribosomal protein S10		
B7ZWY9	Citrate synthase		
B7ZX06	Uncharacterized protein		
B7ZXQ8	Peroxidase		
B7ZZ04	Uncharacterized protein		
B7ZZ42	Uncharacterized protein		
B7ZZJ0	3-oxoacyl-[acyl-carrier-protein] synthase		
B7ZZZ2	Uncharacterized protein		
B8A095	Uncharacterized protein		
B8A0P7	Uncharacterized protein		

Protein	Annotation	Response to salt stress	ANOVA
B8A1K3	Uncharacterized protein		
B8A1K8	Uncharacterized protein		
B8A1M2	Thioredoxin-like protein 5		
B8A1R0	Putative O-Glycosyl hydrolase superfamily protein		
B8A324	Uncharacterized protein		
B8A367	Cysteine synthase		
B8A377	Cysteine synthase		
B8A390	Uncharacterized protein		
B8A3K0	Uncharacterized protein		
B9TSW5	Glutamine synthetase		
C0HDZ6	Uncharacterized protein		
C0HE15	Uncharacterized protein		
C0HE58	Uncharacterized protein		

Protein	Annotation	Response to salt stress	ANOVA
C0HER4	Aconitate hydratase		
C0HF32	ATP synthase subunit beta		
C0HF51	Uncharacterized protein		
C0HF92	Uncharacterized protein		
C0HFM4	Uncharacterized protein		
C0HFP5	Uncharacterized protein		
C0HFU7	Phospholipase D		
C0HGE1	Uncharacterized protein		
C0HGT5	T-complex protein 1 subunit delta		
C0HGT6	Uncharacterized protein		
C0HGV5	Uncharacterized protein		
C0HHJ2	Uncharacterized protein		
C0HHR4	Uncharacterized protein		
C0HHT0	Phospholipase D		

Protein	Annotation	Response to salt stress	ANOVA
C0HHT5	Glutamate decarboxylase		
C0HHU2	Uncharacterized protein		
C0HHY2	Purple acid phosphatase		
C0HJ33	Uncharacterized protein		
C0HJ53	Uncharacterized protein		
C0P2E2	60S ribosomal protein L21		
C0P3Q1	Uncharacterized protein		
C0P3T3	Peroxidase		
C0P429	Uncharacterized protein		
C0P455	Uncharacterized protein		
C0P488	Uncharacterized protein		
C0P4C5	Aquaporin TIP2-3		
C0P4G2	Putative cytochrome P450 superfamily protein		
C0P4K4	Uncharacterized protein		

Protein	Annotation	Response to salt stress	ANOVA
C0P4M0	Uncharacterized protein		
C0P4S1	Peroxidase		
C0P4T2	Uncharacterized protein		
C0P4U8	ATP synthase		
C0P4Z1	Uncharacterized protein		
C0P516	Uncharacterized protein		
C0P530	Putative TCP-1/cpn60 chaperonin family protein isoform 1		
C0P539	Uncharacterized protein		
C0P558	Uncharacterized protein		
C0P567	Uncharacterized protein		
C0P568	NADH ubiquinone oxidoreductase 13kD-like subunit		
C0P5B0	Asparaginyl-tRNA synthetase, cytoplasmic 3		

Protein	Annotation	Response to salt stress	ANOVA
C0P5U8	Glutathione S-transferase 4		
C0P638	Uncharacterized protein		
C0P664	Uncharacterized protein		
C0P6I5	Uncharacterized protein		
C0P6S7	Uncharacterized protein		
C0P758	Malic enzyme		
C0P790	Eukaryotic translation initiation factor 3 subunit B		
C0P7E7	Uncharacterized protein		
C0P7J5	Acyl-coenzyme A oxidase		
C0P7Q1	Uncharacterized protein		
C0P820	Uncharacterized protein		
C0P840	Lipoxygenase		
C0P848	Formate dehydrogenase		
C0P869	Uncharacterized protein		
C0P8C6	Uncharacterized protein		

Protein	Annotation	Response to salt stress	ANOVA
C0P8K7	Uncharacterized protein		
C0P8R6	Uncharacterized protein		
C0P930	Uncharacterized protein		
C0P9K2	Uncharacterized protein		
C0P9T1	Uncharacterized protein		
C0PA04	Uncharacterized protein		
C0PAH7	Uncharacterized protein		
C0PAJ9	Uncharacterized protein		
C0PAS6	Uncharacterized protein		
C0PAU7	Glucose-6-phosphate isomerase		
C0PB15	Uncharacterized protein		
C0PB44	Transaminase/transferase		
C0PBH7	Ribose-5-phosphate isomerase		
C0PBL7	Uncharacterized protein		

Protein	Annotation	Response to salt stress	ANOVA
C0PC61	Transaldolase 2		
C0PC62	Uncharacterized protein		
C0PC75	Putative thioredoxin superfamily protein		
C0PCQ6	Uncharacterized protein		
C0PCV2	40S ribosomal protein S8		
C0PCX2	Cysteine synthase		
C0PCY1	Ubiquitin carboxyl-terminal hydrolase		
C0PD27	Isocitrate dehydrogenase [NADP]		
C0PD90	Uncharacterized protein		
C0PDA6	Uncharacterized protein		
C0PDG3	Uncharacterized protein		
C0PDM0	Uncharacterized protein		

Protein	Annotation	Response to salt stress	ANOVA
C0PDV3	MYB-related transcription factor		
C0PF40	Uncharacterized protein		
C0PF45	Peroxidase		
C0PFA1	Adenylosuccinate synthetase, chloroplastic		
C0PFK3	Proteasome subunit alpha type		
C0PFM8	Uncharacterized protein		
C0PFX0	Glucose-6-phosphate 1-dehydrogenase		
C0PG78	Uncharacterized protein		
C0PGB5	Pyruvate kinase		
C0PGM6	Uncharacterized protein		
C0PGQ1	Uncharacterized protein		
C0PH06	Uncharacterized protein		
C0PH85	Uncharacterized protein		
C0PHB0	Uncharacterized protein		

Protein	Annotation	Response to salt stress	ANOVA
C0PHC0	Putative ATPase, V1 complex, subunit A protein		
C0PHL2	Uncharacterized protein		
C0PHR4	Adenosylhomocysteinase		
C0PHR9	Uncharacterized protein		
C0PHV6	Uncharacterized protein		
C0PIM0	Uncharacterized protein		
C0PJ26	Uncharacterized protein		
C0PJ41	Putative ubiquitin-conjugating enzyme family		
C0PJQ8	Uncharacterized protein		
C0PKD2	Uncharacterized protein		
C0PKT5	Uncharacterized protein		
C0PLF0	Protein disulfide-isomerase		

Protein	Annotation	Response to salt stress	ANOVA
C0PLI2	Uncharacterized protein		
C0PLV4	Uncharacterized protein		
C0PM03	Uncharacterized protein		
C0PM74	Uncharacterized protein		
C0PMC5	Uncharacterized protein		
C0PMH6	Glucose-6-phosphate/phosphate translocator 2Glucose-6-phosphate/phosphate-translocator		
C0PMJ0	Phenylalanine ammonia-lyase		
C0PN38	Uncharacterized protein		
C0PN94	Ras protein RIC2		
C0PNL5	Uncharacterized protein		
C0PNT2	40S ribosomal protein S24		
C0PPB6	Peroxidase		

Protein	Annotation	Response to salt stress	ANOVA
C0PPD4	Uncharacterized protein		
C4IYE1	Uncharacterized protein		
C4IYM7	Uncharacterized protein		
C4IZW9	Malate dehydrogenase		
C4IZZ9	Uncharacterized protein		
C4J030	Uncharacterized protein		
C4J0D4	Putative cytochrome P450 superfamily protein		
C4J2K0	Uncharacterized protein		
C4J3S6	Uncharacterized protein		
C4J410	Heat shock protein1		
C4J4E4	Uncharacterized protein		
C4J4M8	Histone H2B		
C4J6I7	Uncharacterized protein		

Protein	Annotation	Response to salt stress	ANOVA
C4J6K9	Rab GDP dissociation inhibitor alpha		
C4J6R6	Uncharacterized protein		
C4J748	Uncharacterized protein		
C4J757	Uncharacterized protein		
C4J929	Ribosomal protein		
C4J986	Uncharacterized protein		
C4J9A9	Superoxide dismutase [Cu-Zn]		
C4JA36	Putative RNA recognition motif containing family protein		
C4JA40	Phosphoribosylformylglycinamidine cyclo-ligase		
C4JAU6	Plasma membrane intrinsic protein2		
C4JB73	Uncharacterized protein		

Protein	Annotation	Response to salt stress	ANOVA
C4JBB8	Uncharacterized protein		
C4JBE3	Aminomethyltransferase		
C4JBF5	60S ribosomal protein L9, mRNA		
C4JBJ2	Uncharacterized protein		
C4JBL9	Glycine cleavage system H protein 1		
C4JBS8	Glyceraldehyde-3-phosphate dehydrogenase		
C4JC09	Uncharacterized protein		
D1ME28	Uncharacterized protein		
D2DMN0	QM-like protein		
D2JSQ1	ATP synthase subunit 4		
D2JSQ3	ATP synthase subunit 8		
D7NLB3	Peroxidase		
D9IZY9	Pathogenesis-related protein 5		
E7DDW6	Putative uncharacterized protein		

Protein	Annotation	Response to salt stress	ANOVA
G2XK63	Putative uncharacterized protein		
H2BJB6	Acyl-CoA-like protein		
H9BG22	Fatty acid alpha-dioxygenase		
K7TI14	Clathrin heavy chain		
K7TIN2	Glycine cleavage complex P-protein		
K7TJS0	Uncharacterized protein		
K7TJV6	Uncharacterized protein		
K7TM64	Pyruvate kinase		
K7TMY3	Uncharacterized protein		
K7TNB3	Uncharacterized protein		
K7TNK3	Uncharacterized protein		
K7TP58	Cysteine protease 1		
K7TPR9	Pyruvate kinase		
K7TQJ7	Uncharacterized protein		

Protein	Annotation	Response to salt stress	ANOVA
K7TSA0	Uncharacterized protein		
K7TSX2	Uncharacterized protein		
K7TT00	Uncharacterized protein		
K7TU57	Uncharacterized protein		
K7TVZ1	6-phosphogluconate dehydrogenase, decarboxylating		
K7TWV7	Peptidyl-prolyl cis-trans isomerase		
K7TX67	Plasma membrane H+-transporting ATPase-like protein		
K7U078	Uncharacterized protein		
K7U0Y8	Serine/threonine-protein phosphatase		
K7U735	Uncharacterized protein		
K7U795	Putative MADS-box		

Protein	Annotation	Response to salt stress	ANOVA
	transcription factor family protein		
K7U850	ADP,ATP carrier protein 2, mitochondrial		
K7U9C9	Putative DEAD-box ATP-dependent RNA helicase family protein		
K7U9N2	Putative subtilase family protein		
K7U9T3	Uncharacterized protein		
K7UAJ5	Uncharacterized protein		
K7UB12	Calcium-transporting ATPase		
K7UB20	Uncharacterized protein		
K7UBP7	Uncharacterized protein		
K7UC74	Putative oxidoreductase, aldo/keto reductase family protein		

Protein	Annotation	Response to salt stress	ANOVA
K7UCH1	Putative TCP-1/cpn60 chaperonin family protein		
K7UDE7	Uncharacterized protein		
K7UEU8	Uncharacterized protein		
K7UFB4	Putative ATPase, V1 complex, subunit A protein		
K7UFV4	Uncharacterized protein		
K7UGR2	Putative TCP-1/cpn60 chaperonin family protein isoform 1		
K7UH13	Uncharacterized protein		
K7UND8	Uncharacterized protein		
K7UNP2	Uncharacterized protein (Fragment)		
K7UP24	Benzoxazinone synthesis8		

Protein	Annotation	Response to salt stress	ANOVA
K7UPD0	Putative TCP-1/cpn60 chaperonin family protein		
K7UQS6	Heterogeneous nuclear ribonucleoprotein A3		
K7UQT7	Elongation factor 1-gamma 2		
K7URE0	Aconitate hydratase		
K7US79	GTP-binding protein SAR1A		
K7UTZ0	Hexose transporter		
K7UVD7	Uncharacterized protein		
K7UWM4	40S ribosomal protein S8		
K7UX63	Phenylalanine ammonia-lyase		
K7UX79	Dynamin protein 1A		
K7UY19	Fructose-bisphosphate aldolase		

Protein	Annotation	Response to salt stress	ANOVA
K7UY44	Nucleoside diphosphate kinase		
K7UYX2	Uncharacterized protein		
K7V067	Isocitrate dehydrogenase [NADP]		
K7V0F3	Uncharacterized protein		
K7V0P3	Uncharacterized protein		
K7V106	Phosphoglycerate kinase		
K7V1I3	Uncharacterized protein		
K7V355	Uncharacterized protein		
K7V3I5	Beta tubulin2		
K7V4Q5	Proteasome subunit alpha type		
K7V5H4	Phosphoenolpyruvate carboxylase isoform 1		
K7V6X2	Sulfurtransferase		
K7V763	Uncharacterized protein		

Protein	Annotation	Response to salt stress	ANOVA
K7V7I6	Uncharacterized protein		
K7V9X0	Uncharacterized protein		
K7VA33	Uncharacterized protein		
K7VBB8	3-phosphoshikimate 1-carboxyvinyltransferase		
K7VCJ9	Uncharacterized protein		
K7VCN5	Peroxidase		
K7VDR8	Shrunken1 isoform 1		
K7VEB9	Importin subunit alpha		
K7VG53	Uncharacterized protein		
K7VHM9	Uncharacterized protein		
K7VI04	Uncharacterized protein		
K7VIK9	Uncharacterized protein		
K7VJC3	Uncharacterized protein		
K7VLR0	Uncharacterized protein		

Protein	Annotation	Response to salt stress	ANOVA
K7VNQ7	Uncharacterized protein		
K7VQ65	Putative translation elongation factor family protein		
K7VQA7	Uncharacterized protein		
K7VQL1	Uncharacterized protein		
K7VQR1	Uncharacterized protein		
K7VRI2	Uncharacterized protein		
K7VT74	Uncharacterized protein		
K7VVS6	Serine-threonine kinase receptor-associated protein		
K7VVT1	Putative translation elongation factor Tu family protein isoform 1		
K7VW90	Uncharacterized protein		

Protein	Annotation	Response to salt stress	ANOVA
K7VWT6	Uncharacterized protein		
K7W515	Plasma membrane intrinsic protein1		
K7W6W9	Root cap-specific protein		
K7WBY4	Pyrabactin resistance-like protein		
K7WDF1	Uncharacterized protein		
K7WG82	40S ribosomal protein S3a		
L7WLJ8	Clathrin heavy chain		
M1H779	Lipoxygenase (Fragment)		
M4QAY6	Clathrin heavy chain		
O22453	40S ribosomal protein S4		
O22499	Cysteine proteinase Mir2		
O24449	Translational initiation factor eIF-4A		

Protein	Annotation	Response to salt stress	ANOVA
O24573	60S acidic ribosomal protein P0		
O49010	Herbicide safener binding protein		
O50018	Elongation factor 1-alpha		
O81217	Bowman-Birk type bran trypsin inhibitor		
O82086	Pathogenesis related protein-1		
P00761	Trypsin OS=Sus scrofa PE=1 SV=1		
P02538	Keratin, type II cytoskeletal 6A OS=Homo sapiens GN=KRT6A PE=1 SV=3		
P04264	Keratin, type II cytoskeletal 1 OS=Homo sapiens GN=KRT1 PE=1 SV=6		
P08727	Keratin, type I cytoskeletal 19		

Protein	Annotation	Response to salt stress	ANOVA
	OS=Homo sapiens GN=KRT19 PE=1 SV=4		
P13646	Keratin, type I cytoskeletal 13 OS=Homo sapiens GN=KRT13 PE=1 SV=4		
P13647	Keratin, type II cytoskeletal 5 OS=Homo sapiens GN=KRT5 PE=1 SV=3		
P35527	Keratin, type I cytoskeletal 9 OS=Homo sapiens GN=KRT9 PE=1 SV=3		
P35908	Keratin, type II cytoskeletal 2 epidermal OS=Homo sapiens GN=KRT2 PE=1 SV=2		

Protein	Annotation	Response to salt stress	ANOVA
P38559	Glutamine synthetase root isozyme 1		
P38563	Glutamine synthetase root isozyme 5		
P80607	Alpha-1,4-glucan-protein synthase [UDP-forming]		
P93633	Actin (Fragment)		
P93638	Actin (Fragment)		
P93639	Actin (Fragment)		
Q0PCF2	Deoxymugineic acid synthase1		
Q10724	Peptidyl-prolyl cis-trans isomerase, microsomal (Fragment)		
Q2MJJ9	Putative RH2 protein		
Q41798	Calnexin (Fragment)		
Q41870	Aquaporin PIP1-1		

Protein	Annotation	Response to salt stress	ANOVA
Q42420	Proteinase inhibitor		
Q43260	Glutamate dehydrogenase		
Q43261	Histone H2B.3		
Q43271	H(+)-transporting ATPase		
Q4A1J8	Putative cystatin (Fragment)		
Q4W1F6	Thioredoxin		
Q53WW9	Beta-D-glucosidase		
Q5EBY7	Heat shock protein 70 (Fragment)		
Q5EUD5	Protein disulfide isomerase		
Q5G1U0	Malic enzyme		
Q5I204	Brain acid soluble protein 1		
Q5IBC6	DANA2		
Q5K097	NADH dehydrogenase, subunit 9		
Q6E0J0	U1 snRNP		
Q6LCT7	Ubiquitin fusion protein		

Protein	Annotation	Response to salt stress	ANOVA
Q6PLR9	14-3-3-like protein		
Q6QP36	26S proteasome regulatory complex ATPase RPT3		
Q6R979	NADH-ubiquinone oxidoreductase chain 6		
Q6R985	Cytochrome c oxidase subunit 2		
Q6R987	ATP synthase subunit alpha		
Q6R9G1	NADH dehydrogenase subunit 7		
Q6R9H4	NADH-ubiquinone oxidoreductase chain 5		
Q6RFK3	Peroxidase (Fragment)		
Q6RW09	Allene oxide cyclase		
Q6VWE6	O-methyltransferase		

Protein	Annotation	Response to salt stress	ANOVA
Q6VWF1	O-methyltransferase (Fragment)		
Q6VWF7	O-methyltransferase		
Q6VWG3	Brown midrib3		
Q6VWJ0	Caffeoyl-CoA 3-O-methyltransferase 1		
Q6XZ78	Fructokinase-2		
Q7FS88	Glutathione peroxidase		
Q7SIC9	Transketolase, chloroplastic		
Q7XAT3	Glufosinate-resistant glutamine synthetase (Fragment)		
Q84JX6	Phosphoglycerate kinase (Fragment)		
Q84RL8	Plasma membrane intrinsic protein		
Q84TL7	Legumin-like protein		

Protein	Annotation	Response to salt stress	ANOVA
Q8S2X6	Glycine-rich RNA binding protein (Fragment)		
Q8S4W9	Pyruvate decarboxylase		
Q8S531	Cytosolic aldehyde dehydrogenase RF2C		
Q8W0V2	Lipoxygenase		
Q94G64	T-cytoplasm male sterility restorer factor 2		
Q94IQ8	Putative methyl-binding domain protein MBD106		
Q9ATL8	Aquaporin TIP2-2		
Q9FQA3	Glutathione transferase GST 23		
Q9FYS5	High mobility group I/Y-2		
Q9LKL4	Lipoxygenase		
Q9M7E5	Elongation factor 1-alpha		

Protein	Annotation	Response to salt stress	ANOVA
Q9SAZ6	Phosphoenolpyruvate carboxylase		
Q9SE94	Methylenetetrahydrofolate reductase 1		
Q9SPD7	Outer mitochondrial membrane protein porin		
Q9SYS1	Beta-amylase		
Q9T0N7	Phytase		
Q9XF58	Aquaporin PIP2-5		
Q9ZP62	Glutathione transferase III(A)		
Q9ZPN0	NADH-cytochrome b5 reductase		
Q9ZTS7	Peroxidase		

Supplementary Table S5.1 List of proteins found in leaves of five maize genotypes at the seventh week after sowing (Chapter 5).

In addition, the relative abundance as a response to applied salt stress.

Protein	Annotation	Response to salt stress	ANOVA
A0A059Q6U2	Photosystem I P700 chlorophyll a apoprotein A2	High abundance	9,2E-03
A0A059Q6X7	50S ribosomal protein L33, chloroplastic	High abundance	2,6E-02
A0A059Q8J6	Photosystem II CP43 reaction center protein	High abundance	2,1E-02
A0A059Q8L8	NAD(P)H-quinone oxidoreductase subunit 5, chloroplastic	High abundance	2,2E-03
A0A096RG04	SOUL heme-binding family protein	High abundance	2,7E-02
A0A0B4J3C2	Elongation factor 1-alpha	High abundance	3,1E-02
A0A1D6E6B3	Isocitrate dehydrogenase [NADP]	High abundance	2,7E-02
A0A1D6E6W1	60S ribosomal protein L23a-1	High abundance	1,4E-02

Protein	Annotation	Response to salt stress	ANOVA
A0A1D6EBC0	Histone H3.2	High abundance	1,2E-02
A0A1D6EPE4	Enolase	High abundance	4,1E-02
A0A1D6ES23	Heat shock protein 90-2	High abundance	7,7E-03
A0A1D6EXF1	PDK regulatory protein1	High abundance	1,0E-02
A0A1D6EY66	Elongation factor 1-alpha	High abundance	7,7E-03
A0A1D6F5B9	Protein disulfide-isomerase	High abundance	7,3E-03
A0A1D6FKF4	Aspartic proteinase A1	High abundance	1,3E-02
A0A1D6FVK9	Dehydroascorbate reductase like1	High abundance	4,6E-02
A0A1D6GMN4	Heat shock 70 kDa protein	High abundance	5,2E-03
A0A1D6H4B4	Lipoxygenase	High abundance	3,1E-02
A0A1D6H614	Phosphoenolpyruvate carboxylase2	High abundance	2,0E-02
A0A1D6I1V4	Phosphoenolpyruvate carboxylase3	High abundance	1,7E-02
A0A1D6I2R4	Proton-dependent oligopeptide	High abundance	4,0E-02

Protein	Annotation	Response to salt stress	ANOVA
	transport (POT) family protein		
A0A1D6I588	BRCT domain-containing DNA repair protein	High abundance	3,2E-02
A0A1D6J3D1	Acetyl-coenzyme A carboxylase1	High abundance	1,9E-02
A0A1D6K0D4	ATP-dependent Clp protease proteolytic subunit	High abundance	3,1E-03
A0A1D6KIN1	PfkB-like carbohydrate kinase family protein	High abundance	9,5E-03
A0A1D6KLF7	ATP synthase subunit d, mitochondrial	High abundance	2,1E-02
A0A1D6KNP3	Peptidylprolyl isomerase	High abundance	9,3E-03
A0A1D6LC90	PGR5-like protein 1B chloroplastic	High abundance	1,1E-02
A0A1D6LCQ1	Uncharacterized protein	High abundance	1,8E-02
A0A1D6LH59	Protein disulfide isomerase-like 1-2	High abundance	2,7E-02

Protein	Annotation	Response to salt stress	ANOVA
A0A1D6LHL0	Aspartic proteinase A1	High abundance	9,9E-03
A0A1D6LPG1	40S ribosomal protein S14-3	High abundance	2,0E-02
A0A1D6M0I7	Carboxypeptidase	High abundance	2,6E-02
A0A1D6MJX7	Double Clp-N motif-containing P-loop nucleoside triphosphate hydrolase superfamily protein	High abundance	8,3E-03
A0A1D6NV44	Lipase-like	High abundance	3,0E-02
A0A1D6NZT1	Proton-dependent oligopeptide transport (POT) family protein	High abundance	3,2E-02
A0A1D6P1B2	Beta-glucosidase 11	High abundance	1,6E-02
A0A1D6PTR0	HSP20-like chaperones superfamily protein	High abundance	2,1E-02
A0A1D6QC17	Plasma membrane ATPase	High abundance	3,8E-03

Protein	Annotation	Response to salt stress	ANOVA
A0A1D6QPU0	Phosphoenolpyruvate carboxylase isoform 1	High abundance	5,8E-03
A0A1D6QSB3	Glyceraldehyde-3-phosphate dehydrogenase GAPCP1 chloroplastic	High abundance	9,6E-03
A1XCI5	Lipoxygenase	High abundance	3,3E-02
A8IK79	Abscisic acid stress ripening5	High abundance	3,7E-02
B4F7V3	Protein phosphatase 2C isoform epsilon	High abundance	5,6E-03
B4FAL9	Fructose-bisphosphate aldolase	High abundance	3,4E-02
B4FG53	Malate dehydrogenase	High abundance	3,8E-02
B4FNM4	60S acidic ribosomal protein P0	High abundance	2,7E-02
B4FNQ0	Uncharacterized protein	High abundance	1,5E-02
B4FPG2	Actin-1	High abundance	2,1E-02
B4FPT7	Polyubiquitin 2	High abundance	9,4E-03

Protein	Annotation	Response to salt stress	ANOVA
B4FWP0	Fructose-bisphosphate aldolase	High abundance	2,3E-02
B4G1Q8	Uncharacterized protein	High abundance	9,3E-03
B6SHW9	Ubiquitin fusion protein	High abundance	4,5E-02
B6SHX8	Putative uncharacterized protein	High abundance	1,3E-02
B6SHX9	Histone H2A	High abundance	3,1E-02
B6SI29	Histone H2A	High abundance	2,6E-02
B6SIL9	40S ribosomal protein S27a	High abundance	1,0E-02
B6SIV8	Histone H3	High abundance	1,2E-02
B6SJQ5	Histone H3	High abundance	1,7E-02
B6SMV5	Chlorophyll a-b binding protein, chloroplastic	High abundance	2,7E-02
B6T291	Actin-depolymerizing factor 3	High abundance	2,5E-02
B6T433	Elongation factor 1-alpha	High abundance	4,1E-02
B6T4Q5	Pro-resilin	High abundance	3,8E-02
B6T7E7	Histone H2A	High abundance	2,1E-02

Protein	Annotation	Response to salt stress	ANOVA
B6T8U0	Plasminogen activator inhibitor 1 RNA-binding protein	High abundance	1,1E-02
B6TLX3	Putative uncharacterized protein	High abundance	3,1E-02
B6TTP0	Histone H3	High abundance	1,2E-02
B6TX31	Putative uncharacterized protein	High abundance	1,5E-02
B6U0S1	Elongation factor 2	High abundance	2,5E-03
B6U5W4	Histone H2A	High abundance	2,1E-02
B6U759	Bifunctional 3-phosphoadenosine 5-phosphosulfate synthetase	High abundance	1,8E-02
B6UCL4	Outer mitochondrial membrane protein porin	High abundance	2,3E-02
B6UHJ4	Elongation factor 1-alpha	High abundance	3,2E-02
B6UHK8	Histone H3	High abundance	1,8E-02

Protein	Annotation	Response to salt stress	ANOVA
B7ZZ42	Heat shock 70 kDa protein 3	High abundance	2,7E-02
C0HIB6	Histone H2A	High abundance	2,8E-02
C0P4Q4	Uncharacterized protein	High abundance	2,3E-02
C0PGG5	Pyruvate kinase	High abundance	3,6E-02
C0PNZ2	Uncharacterized protein	High abundance	6,5E-03
C3VQ48	Ascorbate peroxidase	High abundance	2,2E-02
C4J4E4	Monodehydroascorbate reductase homolog1	High abundance	2,2E-03
C4J9E9	Uncharacterized protein	High abundance	4,5E-02
K7VCJ9	Phosphoenolpyruvate carboxylase 3	High abundance	2,0E-02
K7VW90	Putative mediator of RNA polymerase II transcription subunit 37c	High abundance	1,6E-02
Q06XS2	Lipoxygenase	High abundance	2,5E-02
Q4W437	Vacuolar H+-translocating	High abundance	5,1E-03

Protein	Annotation	Response to salt stress	ANOVA
	inorganic pyrophosphatase		
Q941P2	Glucose-1-phosphate adenylyltransferase	High abundance	7,2E-03
Q9M7E4	Elongation factor 1 alpha	High abundance	6,8E-03
A0A059Q6M5	ATP synthase subunit beta, chloroplastic	Low abundance	4,8E-03
A0A059Q6T6	NAD(P)H-quinone oxidoreductase subunit K, chloroplastic	Low abundance	2,7E-02
A0A059Q6V5	NAD(P)H-quinone oxidoreductase subunit I, chloroplastic	Low abundance	7,3E-03
A0A059Q7F0	ATP synthase epsilon chain, chloroplastic	Low abundance	9,0E-04
A0A059Q7I6	Photosystem I iron-sulfur center	Low abundance	4,6E-03

Protein	Annotation	Response to salt stress	ANOVA
A0A059Q8H6	Cytochrome b559 subunit alpha	Low abundance	6,5E-03
A0A096QB26	Thiol disulfide interchange protein txlA	Low abundance	2,0E-02
A0A096QRW1	Chlorophyll a-b binding protein, chloroplastic	Low abundance	3,0E-02
A0A1D6DW07	D-3-phosphoglycerate dehydrogenase	Low abundance	1,5E-02
A0A1D6EVV4	Photosynthetic NDH subunit of subcomplex B 3 chloroplastic	Low abundance	2,9E-02
A0A1D6EWW7	ATP synthase gamma chain 1 chloroplastic	Low abundance	3,2E-02
A0A1D6FJP5	ATP synthase subunit beta	Low abundance	1,0E-02
A0A1D6FKP2	Protease Do-like 1 chloroplastic	Low abundance	1,2E-02
A0A1D6FKW0	Malate dehydrogenase	Low abundance	2,7E-02
A0A1D6FPJ1	Glucose-1-phosphate adenylyltransfer	Low abundance	6,9E-04

Protein	Annotation	Response to salt stress	ANOVA
	ase small subunit chloroplastic		
A0A1D6FQN6	Malic enzyme	Low abundance	1,0E-03
A0A1D6GCA1	Malic enzyme	Low abundance	9,0E-04
A0A1D6GTJ8	40S ribosomal protein S14	Low abundance	1,8E-02
A0A1D6H1R5	V-type proton ATPase catalytic subunit A	Low abundance	4,5E-02
A0A1D6H2K7	Nucleoid-associated protein chloroplastic	Low abundance	2,6E-02
A0A1D6H9Z3	Uncharacterized protein	Low abundance	3,3E-02
A0A1D6HBD7	Photosynthetic NDH subunit of lumenal location 2 chloroplastic	Low abundance	7,2E-03
A0A1D6HKL3	ATP synthase chloroplast subunit1	Low abundance	1,4E-02
A0A1D6HL34	Presequence protease 2 chloroplastic/mitochondrial	Low abundance	4,1E-03

Protein	Annotation	Response to salt stress	ANOVA
A0A1D6HT76	Protein containing PDZ domain a K-box domain and a TPR region	Low abundance	3,3E-03
A0A1D6HZI0	RNA-binding protein CP31B chloroplastic	Low abundance	1,4E-02
A0A1D6IJ76	Glyceraldehyde -3-phosphate dehydrogenase A	Low abundance	5,3E-03
A0A1D6IJP9	Alanine aminotransferas e9	Low abundance	1,9E-04
A0A1D6JFP2	Bifunctional inhibitor/lipid-transfer protein/seed storage 2S albumin superfamily protein	Low abundance	2,1E-03
A0A1D6K7Q4	Uncharacterized protein	Low abundance	2,4E-03
A0A1D6KDA7	PsbP domain-containing protein 1 chloroplastic	Low abundance	1,3E-03

Protein	Annotation	Response to salt stress	ANOVA
A0A1D6KDZ0	Shikimate kinase family protein	Low abundance	2,1E-02
A0A1D6KKS1	Peptidylprolyl isomerase	Low abundance	2,8E-02
A0A1D6KTZ2	Chaperonin2	Low abundance	4,1E-03
A0A1D6KX29	Pyruvate dehydrogenase E1 component subunit beta-3 chloroplastic	Low abundance	4,6E-03
A0A1D6L5H8	Ferredoxin--NADP reductase leaf isozyme 1 chloroplastic	Low abundance	1,1E-02
A0A1D6L6A9	Malate dehydrogenase	Low abundance	2,9E-02
A0A1D6LI73	D-glycerate 3-kinase chloroplastic	Low abundance	2,3E-03
A0A1D6LIK1	Peptidyl-prolyl cis-trans isomerase	Low abundance	2,9E-02
A0A1D6LVU5	Glutathione S-transferase DHAR3 chloroplastic	Low abundance	6,6E-03
A0A1D6LZR2	Malic enzyme	Low abundance	1,1E-03

Protein	Annotation	Response to salt stress	ANOVA
A0A1D6M2W3	Heavy metal transport/detoxification superfamily protein	Low abundance	1,5E-03
A0A1D6N4R0	Uncharacterized protein	Low abundance	4,8E-02
A0A1D6NDJ3	Malic enzyme	Low abundance	1,2E-03
A0A1D6NFC1	ATP synthase subunit beta	Low abundance	1,1E-02
A0A1D6NHQ5	Carbonic anhydrase	Low abundance	9,1E-03
A0A1D6Q2W3	ATP synthase subunit beta chloroplastic	Low abundance	1,2E-02
A0A1D6Q7X7	Selenium-binding protein 3	Low abundance	6,4E-03
A0A1D6QRY7	Nucleoid-associated protein chloroplastic	Low abundance	2,2E-02
A0A1Q1AMW4	Ferredoxin	Low abundance	1,1E-02
A0A1X7YHE3	Uncharacterized protein	Low abundance	2,9E-03
B1PEY4	Superoxide dismutase [Cu-Zn]	Low abundance	5,9E-04

Protein	Annotation	Response to salt stress	ANOVA
B4F8P6	Malic enzyme	Low abundance	2,0E-03
B4F9N4	Cytochrome b6-f complex iron-sulfur subunit	Low abundance	3,1E-02
B4FB80	Thioredoxin F2 chloroplastic	Low abundance	8,2E-03
B4FBR9	Uncharacterized protein	Low abundance	1,9E-03
B4FL55	Chlorophyll a-b binding protein, chloroplastic	Low abundance	3,0E-02
B4FM07	2-Cys peroxiredoxin BAS1 chloroplastic	Low abundance	7,0E-04
B4FNQ8	Calmodulin	Low abundance	4,7E-02
B4FQ59	Phosphoribulokinase	Low abundance	1,7E-03
B4FQS5	36.4 kDa proline-rich protein	Low abundance	2,8E-03
B4FRJ4	Photosystem II 11 kD protein	Low abundance	4,5E-02
B4FRQ1	Ribulose-phosphate 3-epimerase	Low abundance	8,4E-03
B4FS10	Putative uncharacterized protein	Low abundance	2,9E-02

Protein	Annotation	Response to salt stress	ANOVA
B4FT19	Oxygen evolving enhancer protein 3 containing protein	Low abundance	8,0E-03
B4FT85	Isochorismate synthase 1	Low abundance	7,0E-03
B4FU15	Extensin-like protein	Low abundance	4,3E-02
B4FU98	Thylakoid lumenal 16.5 kDa protein chloroplastic	Low abundance	1,2E-03
B4FUM2	Ferredoxin--NADP reductase	Low abundance	2,1E-03
B4FVP6	Electron carrier/ electron transporter/ iron ion binding protein	Low abundance	8,9E-03
B4FX16	Macrophage migration inhibitory factor	Low abundance	6,1E-03
B4G095	Plastocyanin	Low abundance	1,1E-03
B6SLL8	Malate dehydrogenase	Low abundance	1,8E-03

Protein	Annotation	Response to salt stress	ANOVA
B6SPU1	Thioredoxin M-type	Low abundance	1,0E-02
B6T097	Photosystem I reaction center subunit IV A	Low abundance	1,3E-02
B6T2L2	Sedoheptulose-1,7-bisphosphatase	Low abundance	9,0E-03
B6T2W9	Thylakoid lumenal 19 kDa protein	Low abundance	6,8E-03
B6T3B2	Oxygen evolving complex 33kDa subunit	Low abundance	2,3E-02
B6T7Q7	Serine hydroxymethyltransferase	Low abundance	7,1E-04
B6T927	NAD(P)H-quinone oxidoreductase subunit S chloroplastic	Low abundance	1,7E-02
B6T9S0	Thioredoxin X	Low abundance	1,5E-02
B6T9S5	Ferredoxin--NADP reductase	Low abundance	1,9E-03

Protein	Annotation	Response to salt stress	ANOVA
B6TCE9	Peptidyl-prolyl cis-trans isomerase	Low abundance	2,2E-03
B6TEI9	Photosystem I reaction center subunit IV A	Low abundance	1,1E-02
B6TGS7	Cytochrome c	Low abundance	1,3E-02
B6TH55	Photosystem I reaction center subunit IV A	Low abundance	1,2E-02
B6TQG0	ATP synthase delta chain	Low abundance	1,7E-02
B6TW28	Ferredoxin-thioredoxin reductase, variable chain	Low abundance	5,6E-04
B6U3G5	Putative uncharacterized protein	Low abundance	2,0E-02
B6U5I1	Peptidyl-prolyl cis-trans isomerase	Low abundance	2,6E-02
C0HF32	ATP synthase subunit beta	Low abundance	1,4E-02
C0HFR9	Uncharacterized protein	Low abundance	2,8E-03
C0HH58	Uncharacterized protein	Low abundance	5,8E-05

Protein	Annotation	Response to salt stress	ANOVA
C0P3K2	Uncharacterized protein	Low abundance	2,4E-03
C0P5X6	Chloroplast ribulose bisphosphate carboxylase/oxygenase activase	Low abundance	4,7E-02
C0P6Z6	ATP synthase subunit delta chloroplastic	Low abundance	1,3E-02
C0P7G8	Photosystem II repair protein PSB27-H1 chloroplastic	Low abundance	1,2E-02
C0PAK8	Plastocyanin	Low abundance	1,9E-03
C0PEC4	30S ribosomal protein S5 chloroplastic	Low abundance	4,1E-02
C0PFW3	Malate dehydrogenase6	Low abundance	4,3E-02
C0PK04	Soluble inorganic pyrophosphatase 2	Low abundance	8,2E-04
C0PK47	Uncharacterized protein	Low abundance	4,0E-02
C4IYM7	Mitochondrial outer membrane protein porin 2	Low abundance	3,9E-03

Protein	Annotation	Response to salt stress	ANOVA
C4J9M7	2-Cys peroxiredoxin BAS1 chloroplastic	Low abundance	8,9E-04
C4J9R0	PLAT domain-containing protein 3	Low abundance	1,2E-02
E9NQE2	Malic enzyme	Low abundance	1,2E-03
F6MFD6	Malate dehydrogenase	Low abundance	3,8E-02
G0YVY7	Chloroplast thioredoxin M-type	Low abundance	5,3E-03
K7TXW7	Thioredoxin M-type, chloroplastic	Low abundance	1,1E-02
K7UGI3	Putative thioredoxin superfamily protein	Low abundance	1,3E-03
P29036	Ferritin-1, chloroplastic	Low abundance	3,3E-02
Q41746	Chlorophyll a-b binding protein, chloroplastic	Low abundance	1,8E-02
Q84PF5	Glucose-1-phosphate adenylyltransferase	Low abundance	2,3E-02

Protein	Annotation	Response to salt stress	ANOVA
Q947B9	Glucose-1-phosphate adenylyltransferase	Low abundance	2,0E-02
Q9SLP6	Ferredoxin	Low abundance	2,9E-02
Q9ST25	Cortical cell-delineating protein	Low abundance	3,4E-02
A0A059Q6M3	ATP synthase subunit alpha, chloroplastic		
A0A059Q6M9	Photosystem II reaction center protein H		
A0A059Q6N1	30S ribosomal protein S3, chloroplastic		
A0A059Q6P6	Cytochrome b6		
A0A059Q6R8	NAD(P)H-quinone oxidoreductase subunit J, chloroplastic		
A0A059Q6R9	Ribulose bisphosphate carboxylase large chain		

Protein	Annotation	Response to salt stress	ANOVA
A0A059Q6U3	Photosystem II CP47 reaction center protein		
A0A059Q6U7	30S ribosomal protein S8, chloroplastic		
A0A059Q6U9	30S ribosomal protein S19, chloroplastic		
A0A059Q6V4	Cytochrome b6-f complex subunit 4		
A0A059Q6W8	Photosystem I P700 chlorophyll a apoprotein A1		
A0A059Q6Y4	50S ribosomal protein L14, chloroplastic		
A0A059Q6Z3	NAD(P)H-quinone oxidoreductase subunit 1, chloroplastic		
A0A059Q7D4	Photosystem II D2 protein		
A0A059Q8E1	Photosystem II protein D1		

Protein	Annotation	Response to salt stress	ANOVA
A0A059Q8F8	ATP synthase subunit b, chloroplastic		
A0A059Q8J3	NAD(P)H-quinone oxidoreductase subunit H, chloroplastic		
A0A059Q8J9	30S ribosomal protein S4, chloroplastic		
A0A059Q8K1	Cytochrome f		
A0A060D6M0	OFP transcription factor (Fragment)		
A0A096PRE6	Fibrillin1		
A0A096R6Z8	Heat shock 70 kDa protein 6 chloroplastic		
A0A096RAV0	Photosystem I reaction center subunit III chloroplastic		
A0A096RYU5	40S ribosomal protein S14-3		
A0A096RZN2	Carbonic anhydrase1		

Protein	Annotation	Response to salt stress	ANOVA
A0A096S2Q4	ATP-dependent zinc metalloprotease FTSH 5 chloroplastic		
A0A097PLA8	Nitrilase/cyanide hydratase and apolipoprotein N-acyltransferase family protein (Fragment)		
A0A0A1P1P0	Cysteine proteinase inhibitor		
A0A0A7DIX5	Nucleoside diphosphate kinase		
A0A0B4J303	Eukaryotic initiation factor4a		
A0A1D6DUW9	26S proteasome non-ATPase regulatory subunit 7 homolog A		
A0A1D6DVH5	Lipoxygenase		
A0A1D6DVJ8	H(+)-ATPase 5		

Protein	Annotation	Response to salt stress	ANOVA
A0A1D6DW31	Insect resistance3		
A0A1D6DZA4	Germin-like protein subfamily 1 member 11		
A0A1D6DZK5	Adenosylmethionine aminotransferase1		
A0A1D6E3H6	Plasma membrane intrinsic protein1		
A0A1D6E4M0	Elongation factor G, chloroplastic		
A0A1D6E4W8	UPF0426 protein chloroplastic		
A0A1D6E4W9	UPF0426 protein chloroplastic		
A0A1D6E501	3-isopropylmalate dehydrogenase		
A0A1D6E8G3	Actin-7		

Protein	Annotation	Response to salt stress	ANOVA
A0A1D6E965	Glyceraldehyde -3-phosphate dehydrogenase		
A0A1D6ECC8	Dihydrolipoylly sine-residue succinyltransfer ase component of 2-oxoglutarate dehydrogenase complex		
A0A1D6EDK6	Acetyl-CoA carboxylase2		
A0A1D6EEB5	Transketolase-1 chloroplastic		
A0A1D6EEX6	CBS domain-containing protein CBSX1 chloroplastic		
A0A1D6EGN6	Adenosylhomoc ysteinase 1		
A0A1D6EHR6	Abscisic acid stress ripening2		
A0A1D6EHT1	Actin-7		
A0A1D6EIY3	Mannan endo-14-beta-mannosidase 6		
A0A1D6EKW2	Uncharacterized protein		

Protein	Annotation	Response to salt stress	ANOVA
A0A1D6ELX2	Aldo-keto reductase/ oxidoreductase		
A0A1D6EMG2	Aquaporin PIP2-2		
A0A1D6EPY8	Alpha/beta-Hydrolases superfamily protein		
A0A1D6EQY9	Sterile alpha motif (SAM) domain-containing protein		
A0A1D6ERU3	Carboxypeptidase		
A0A1D6ERU4	Carboxypeptidase		
A0A1D6ES19	Heat shock protein 90-2		
A0A1D6ES74	MLO-like protein		
A0A1D6ESJ9	L-ascorbate peroxidase 2 cytosolic		
A0A1D6ETY2	Triose phosphate isomerase2		
A0A1D6EUP8	UTP--glucose-1-phosphate		

Protein	Annotation	Response to salt stress	ANOVA
	uridylyltransferase 1		
A0A1D6EWS4	Adenosine 5'-phosphosulfate reductase-like2		
A0A1D6EXK9	Oxygen-evolving enhancer protein 3-1		
A0A1D6EZ36	Peptidyl-prolyl cis-trans isomerase CYP37 chloroplastic		
A0A1D6EZI1	Succinyl-CoA ligase alpha-chain 2		
A0A1D6F0E2	Eukaryotic translation initiation factor 5A		
A0A1D6F1Q8	Alanine aminotransferase10		
A0A1D6F3N8	Elongation factor Ts family protein		
A0A1D6F4C8	Peroxidase		

Protein	Annotation	Response to salt stress	ANOVA
A0A1D6F519	Ascorbate peroxidase2		
A0A1D6F5I7	Subtilisin-like serine endopeptidase family protein		
A0A1D6F5N8	Haloacid dehalogenase-like hydrolase domain-containing protein		
A0A1D6F5T1	Alpha-mannosidase		
A0A1D6F705	Subtilisin-like serine endopeptidase family protein		
A0A1D6F8J3	Eukaryotic aspartyl protease family protein		
A0A1D6F9C2	Oxygen-evolving enhancer protein 2-1 chloroplastic		
A0A1D6FCB3	Cysteine synthase		

Protein	Annotation	Response to salt stress	ANOVA
A0A1D6FD79	Fructose-bisphosphate aldolase		
A0A1D6FDV3	50S ribosomal protein L29 chloroplastic		
A0A1D6FH31	DUF4378 domain protein		
A0A1D6FH46	DUF4378 domain protein		
A0A1D6FKV6	Ketol-acid reductoisomerase		
A0A1D6FLN2	ATP-dependent zinc metalloprotease FTSH 4 mitochondrial		
A0A1D6FLR1	Spliceosome RNA helicase BAT1 isoform 1		
A0A1D6FPB9	Acidic ribosomal protein P2b (Rpp2b)		
A0A1D6FQ34	Guanosine nucleotide diphosphate dissociation inhibitor		

Protein	Annotation	Response to salt stress	ANOVA
A0A1D6FQ43	Guanosine nucleotide diphosphate dissociation inhibitor		
A0A1D6FQE4	Pyruvate, phosphate dikinase		
A0A1D6FRI4	ERBB-3 BINDING PROTEIN 1		
A0A1D6FSN1	Metacaspase type II		
A0A1D6FUX8	S-adenosylmethionine synthase		
A0A1D6FW13	Actin-7		
A0A1D6FZP3	Uroporphyrinogen decarboxylase		
A0A1D6G0U9	V-type proton ATPase subunit E3		
A0A1D6G0W4	Polynucleotidyl transferase ribonuclease H-like superfamily protein		
A0A1D6G0Z9	Ribokinase		

Protein	Annotation	Response to salt stress	ANOVA
A0A1D6G378	S-adenosyl-L-methionine-dependent methyltransferase superfamily protein		
A0A1D6G789	Membrane-associated protein VIPP1 chloroplastic		
A0A1D6G8L3	Triose phosphate isomerase5		
A0A1D6G8N5	Heat shock 70 kDa protein		
A0A1D6G927	RING-type E3 ubiquitin transferase		
A0A1D6GAX0	Chorismate mutase		
A0A1D6GB10	RHOMBOID-like protein 12 mitochondrial		
A0A1D6GCZ1	Outer envelope pore protein 24A chloroplastic		
A0A1D6GD77	Elongation factor Tu mitochondrial		

Protein	Annotation	Response to salt stress	ANOVA
A0A1D6GEK0	40S ribosomal protein S23-2		
A0A1D6GEX5	Short chain alcohol dehydrogenase1		
A0A1D6GF65	Photosystem I subunit d1		
A0A1D6GF76	Cytochrome b-c1 complex subunit 7		
A0A1D6GG23	Cullin-4		
A0A1D6GGM0	Retrovirus-related Pol polyprotein LINE-1		
A0A1D6GHW4	Histone H2A		
A0A1D6GJ73	Phosphoglucomutase2		
A0A1D6GK64	Heat shock 70 kDa protein 6 chloroplastic		
A0A1D6GKL8	Glycine-rich RNA-binding, abscisic acid-inducible protein		
A0A1D6GL75	5-methyltetrahydropteroyltrigluta		

Protein	Annotation	Response to salt stress	ANOVA
	mate--homocysteine methyltransferase 1		
A0A1D6GLV8	UDP-arabinopyranose mutase 3		
A0A1D6GM13	Uncharacterized protein		
A0A1D6GM23	Chloroplast post-illumination chlorophyll fluorescence increase protein		
A0A1D6GMN7	Heat shock 70 kDa protein		
A0A1D6GNG8	Nonspecific lipid-transfer protein		
A0A1D6GQ42	Cell division cycle protein 48		
A0A1D6GQ45	Cell division cycle protein 48		
A0A1D6GRI6	ATP sulfurylase 1 chloroplastic		
A0A1D6GRR2	Leucine aminopeptidase 2 chloroplastic		

Protein	Annotation	Response to salt stress	ANOVA
A0A1D6GU53	Oxygen-evolving enhancer protein 1-1 chloroplastic		
A0A1D6GUG0	Peroxidase		
A0A1D6GXQ6	Glycerate dehydrogenase HPR peroxisomal		
A0A1D6H1H6	Porphobilinogen deaminase chloroplastic		
A0A1D6H1J5	Glyceraldehyde-3-phosphate dehydrogenase		
A0A1D6H2L6	Chaperone protein ClpB4 mitochondrial		
A0A1D6H393	F-box/kelch-repeat protein OR23		
A0A1D6H4C4	Citrate synthase		
A0A1D6H4U6	Putative lactoylglutathione lyase chloroplastic		

Protein	Annotation	Response to salt stress	ANOVA
A0A1D6H539	UDP-glycosyltransferase 88A1		
A0A1D6H5B5	50S ribosomal protein L21 chloroplastic		
A0A1D6H5G3	Rhodanese-like domain-containing protein 4 chloroplastic		
A0A1D6H5I4	ATP synthase subunit 1		
A0A1D6H6Z1	Acetyltransferase component of pyruvate dehydrogenase complex		
A0A1D6H6Z3	Dihydrolipoamide acetyltransferase component of pyruvate dehydrogenase complex		
A0A1D6H8U7	Leucine aminopeptidase 2 chloroplastic		
A0A1D6HAE2	L-ascorbate peroxidase S		

Protein	Annotation	Response to salt stress	ANOVA
	chloroplastic/mitochondrial		
A0A1D6HAY8	RING/U-box superfamily protein		
A0A1D6HC33	Isocitrate dehydrogenase [NAD] regulatory subunit 3 mitochondrial		
A0A1D6HDG6	Succinate--CoA ligase [ADP-forming] subunit beta mitochondrial		
A0A1D6HE45	ATP-dependent Clp protease proteolytic subunit		
A0A1D6HIF7	Adenine nucleotide translocator1		
A0A1D6HJI6	Disease resistance protein RPM1		
A0A1D6HKA8	Arsenical pump-driving ATPase		

Protein	Annotation	Response to salt stress	ANOVA
A0A1D6HL75	Ferredoxin--nitrite reductase chloroplastic		
A0A1D6HN61	Leucine aminopeptidase 2 chloroplastic		
A0A1D6HNF6	Aspartate aminotransferase chloroplastic		
A0A1D6HP45	Glutathione reductase cytosolic		
A0A1D6HP47	Proteasome subunit beta type-1		
A0A1D6HPC4	NADH dehydrogenase [ubiquinone] 1 alpha subcomplex subunit 9 mitochondrial		
A0A1D6HPL2	3-ketoacyl-CoA thiolase 2 peroxisomal		
A0A1D6HR41	Pyridoxal 5'-phosphate synthase-like subunit PDX1.2		

Protein	Annotation	Response to salt stress	ANOVA
A0A1D6HR57	Pentatricopeptide repeat-containing protein ELI1 chloroplastic		
A0A1D6HR58	Pentatricopeptide repeat-containing protein ELI1 chloroplastic		
A0A1D6HRU2	Pathogenesis-related protein 1		
A0A1D6HS38	Oxygen-evolving enhancer protein 2-1 chloroplastic		
A0A1D6HSJ1	Glycolate oxidase1		
A0A1D6HTG4	Putative ribose-5-phosphate isomerase 3 chloroplastic		
A0A1D6HU99	Histone1a		
A0A1D6HWI7	Proteasome subunit beta type		
A0A1D6HWJ3	Glucose-1-phosphate		

Protein	Annotation	Response to salt stress	ANOVA
	adenylyltransferase		
A0A1D6HXK1	PGR5-like protein 1B chloroplastic		
A0A1D6HXP2	Starch synthase, chloroplastic/amyloplastic		
A0A1D6HXQ3	40S ribosomal protein S4-3		
A0A1D6HY75	Photosystem I reaction center subunit IV A		
A0A1D6I5Q9	Mitochondrial phosphate carrier protein 2 mitochondrial		
A0A1D6I6C2	Peroxidase 17		
A0A1D6I6H5	Heat shock protein 90-5 chloroplastic		
A0A1D6I6S9	Heat shock protein 90-2		
A0A1D6I8Y8	Inactive LRR receptor-like serine/threonine-protein kinase BIR2		

Protein	Annotation	Response to salt stress	ANOVA
A0A1D6I905	Inactive LRR receptor-like serine/threonine -protein kinase BIR2		
A0A1D6IAH3	Uncharacterized protein		
A0A1D6IAH8	Protein CURVATURE THYLAKOID 1B chloroplastic		
A0A1D6IAS7	UDP-glucose pyrophosphoryl ase2		
A0A1D6IAS8	UDP-glucose pyrophosphoryl ase2		
A0A1D6IAS9	UDP-glucose pyrophosphoryl ase2		
A0A1D6IF53	Protein THYLAKOID FORMATION 1 chloroplastic		
A0A1D6IFM3	SH3 domain-containing protein		
A0A1D6IJJ1	Elongation factor 1-beta		

Protein	Annotation	Response to salt stress	ANOVA
A0A1D6IKI2	RNA binding protein 1		
A0A1D6ILV6	NADPH-dependent thioredoxin reductase 3		
A0A1D6IMH7	Hydroxyproline-rich glycoprotein family protein		
A0A1D6IMZ9	Peroxidase		
A0A1D6INM6	Superoxide dismutase		
A0A1D6ISX4	Elongation factor P		
A0A1D6ISX9	Phospholipid transfer protein homolog1		
A0A1D6ITB4	Signal recognition particle 54 kDa protein chloroplastic		
A0A1D6IUW7	Glycine cleavage system H protein		
A0A1D6IW93	Binding		

Protein	Annotation	Response to salt stress	ANOVA
A0A1D6IXG3	Argininosuccinate synthase chloroplastic		
A0A1D6IYD1	Uncharacterized protein		
A0A1D6IYD6	Glyoxylase1		
A0A1D6IZQ8	Acyl-CoA-binding protein1		
A0A1D6IZR3	Rubredoxin family protein		
A0A1D6J0S0	Monodehydroascorbate reductase 5 mitochondrial		
A0A1D6J3B2	Phosphoenolpyruvate carboxylase 3		
A0A1D6J5C2	WPP domain-associated protein		
A0A1D6J8X7	Glucose-1-phosphate adenylyltransferase small subunit chloroplastic		
A0A1D6J965	Phosphoglycolate phosphatase 1A chloroplastic		

Protein	Annotation	Response to salt stress	ANOVA
A0A1D6JB86	NAD(P)H-quinone oxidoreductase subunit M chloroplastic		
A0A1D6JDH0	Uncharacterized protein		
A0A1D6JG12	Cysteine protease 1		
A0A1D6JG49	6,7-dimethyl-8-ribityllumazine synthase		
A0A1D6JGF2	Glutamine synthetase		
A0A1D6JGZ9	26S proteasome non-ATPase regulatory subunit 7 homolog A		
A0A1D6JH85	Putative plastid-lipid-associated protein 13 chloroplastic		
A0A1D6JKT7	Uncharacterized protein		
A0A1D6JKW8	Nonspecific lipid-transfer protein		
A0A1D6JMR5	Catalase		

Protein	Annotation	Response to salt stress	ANOVA
A0A1D6JMX7	Glutathione transferase11		
A0A1D6JMY2	Glutathione transferase10		
A0A1D6JMZ9	Aconitate hydratase		
A0A1D6JNT8	Proteasome subunit alpha type		
A0A1D6JPD5	1,2-dihydroxy-3-keto-5-methylthiopentene dioxygenase		
A0A1D6JPH3	Glutathione reductase chloroplastic		
A0A1D6JTN4	Glutamine synthetase		
A0A1D6JWL2	Chorismate synthase		
A0A1D6JXJ7	Fructose-1,6-bisphosphatase		
A0A1D6JYG6	Photosynthetic NDH subunit of lumenal location 1 chloroplastic		
A0A1D6JYM2	Glutathione S-transferase L2 chloroplastic		

Protein	Annotation	Response to salt stress	ANOVA
A0A1D6JYW6	Ascorbate peroxidase homolog3		
A0A1D6K0A0	Calvin cycle protein CP12-2 chloroplastic		
A0A1D6K1B9	Hydroxyproline -rich glycoprotein family protein		
A0A1D6K584	Pectinesterase		
A0A1D6K5Y7	Chaperone protein ClpB3 chloroplastic		
A0A1D6K6E6	Uncharacterized protein		
A0A1D6K7U3	Glutathione transferase14		
A0A1D6K8P1	Peptide methionine sulfoxide reductase		
A0A1D6KE29	Heat shock protein 70		
A0A1D6KEX3	Adenine phosphoribosylt ransferase 1 chloroplastic		

Protein	Annotation	Response to salt stress	ANOVA
A0A1D6KF74	BTB/POZ domain-containing protein		
A0A1D6KGM2	5-methyltetrahydropteroyltriglutamate--homocysteine methyltransferase 1		
A0A1D6KGP0	Cysteine synthase2		
A0A1D6KIE7	60S ribosomal protein L12-3		
A0A1D6KIH4	Serine--glyoxylate aminotransferase		
A0A1D6KJP4	Peptidylprolyl isomerase		
A0A1D6KKP0	Putative 14-3-3 protein		
A0A1D6KLS3	Glutaredoxin-C5 chloroplastic		
A0A1D6KMJ5	Thioredoxin family protein		
A0A1D6KMS3	Cytochrome c1 1 heme protein mitochondrial		

Protein	Annotation	Response to salt stress	ANOVA
A0A1D6KPH6	Aminoaldehyde dehydrogenase 1b		
A0A1D6KS88	Alpha-galactosidase		
A0A1D6KXU0	NAD(P)-linked oxidoreductase superfamily protein		
A0A1D6KZ65	5-methyltetrahydropteroyltriglutamate--homocysteine methyltransferase		
A0A1D6L0I4	Adenylosuccinate synthetase, chloroplastic		
A0A1D6L2J8	Uncharacterized protein		
A0A1D6L376	Glucose-1-phosphate adenylyltransferase		
A0A1D6L7H7	Glutamate dehydrogenase		
A0A1D6L7H8	Glutamate dehydrogenase		

Protein	Annotation	Response to salt stress	ANOVA
A0A1D6LBR7	Nucleic acid-binding proteins superfamily		
A0A1D6LC16	Pentatricopeptide repeat-containing protein mitochondrial		
A0A1D6LC68	Outer envelope pore protein 24A chloroplastic		
A0A1D6LC84	Plastid-specific 30S ribosomal protein 1		
A0A1D6LDB6	Acyl-CoA N-acyltransferase (NAT) superfamily protein		
A0A1D6LER3	Glyceraldehyde-3-phosphate dehydrogenase		
A0A1D6LHI5	Dehydroascorbate reductase like3		
A0A1D6LHI9	Beta-hexosaminidase		
A0A1D6LHK3	Soluble inorganic		

Protein	Annotation	Response to salt stress	ANOVA
	pyrophosphatase 4		
A0A1D6LHK7	Histone H2A		
A0A1D6LHK9	Histone H2A		
A0A1D6LIU5	DEAD-box ATP-dependent RNA helicase 7		
A0A1D6LJP0	6-phosphogluconate dehydrogenase, decarboxylating		
A0A1D6LJS9	Chaperonin 60 subunit beta 2 chloroplastic		
A0A1D6LJT6	ATOZI1		
A0A1D6LLE4	Phospholipase A1-Igamma1 chloroplastic		
A0A1D6LLW6	Photosystem II1		
A0A1D6LMS5	Chitinase2		
A0A1D6LNJ7	60S acidic ribosomal protein P3		
A0A1D6LP96	Blight-associated protein p12		

Protein	Annotation	Response to salt stress	ANOVA
A0A1D6LPC1	Calcineurin-like metallo-phosphoesterase superfamily protein		
A0A1D6LSP0	Elongation factor gamma1		
A0A1D6LYW3	Peroxidase		
A0A1D6LZ57	USP family protein		
A0A1D6M0B0	Threonine synthase 1 chloroplastic		
A0A1D6M0D9	Lactoylglutathione lyase		
A0A1D6M244	Malic enzyme		
A0A1D6M323	Ribosomal protein		
A0A1D6M3P0	Alpha/beta-Hydrolases superfamily protein		
A0A1D6M428	Pyruvate orthophosphate dikinase1		
A0A1D6M439	Pyruvate orthophosphate dikinase1		

Protein	Annotation	Response to salt stress	ANOVA
A0A1D6M7C2	Phosphoglycerate kinase		
A0A1D6M7L9	Sulfite reductase1		
A0A1D6M7R4	Calreticulin-3		
A0A1D6MB69	Putative aldehyde dehydrogenase MIS1		
A0A1D6MDI4	GTP-binding nuclear protein		
A0A1D6ME97	Hypersensitive induced reaction3		
A0A1D6MEM8	Nucleoside diphosphate kinase		
A0A1D6MEZ6	Plasma membrane-associated cation-binding protein 1		
A0A1D6MFZ9	RING-H2 finger protein ATL3		
A0A1D6MIA3	Phospholipase A1-Igamma1 chloroplastic		

Protein	Annotation	Response to salt stress	ANOVA
A0A1D6MJB1	MAR-binding filament-like protein 1		
A0A1D6MK12	NADH-cytochrome b5 reductase-like protein		
A0A1D6MK40	Alba DNA/RNA-binding protein		
A0A1D6MLF7	Triose phosphate isomerase4		
A0A1D6MLW3	Helicase protein MOM1		
A0A1D6MN18	Fructose-bisphosphate aldolase		
A0A1D6MRJ6	Uncharacterized protein		
A0A1D6MSC0	Peroxidase		
A0A1D6MSE3	Dihydrolipoyl dehydrogenase		
A0A1D6MUE6	Adenylate kinase 4		
A0A1D6MUE8	Heat shock 70 kDa protein 6 chloroplastic		

Protein	Annotation	Response to salt stress	ANOVA
A0A1D6MUE9	Heat shock 70 kDa protein 6 chloroplastic		
A0A1D6MVN6	Glycosyltransferase		
A0A1D6MWU8	Heat shock 70 kDa protein 3		
A0A1D6MY43	Beta-glucosidase 17		
A0A1D6N0K3	Peroxidase		
A0A1D6N0R5	Protein RETICULATA-RELATED 4 chloroplastic		
A0A1D6N2D5	RING finger protein		
A0A1D6N450	Structural maintenance of chromosomes protein		
A0A1D6N4X3	60S ribosomal protein L5-1 homolog a		
A0A1D6N4Z9	Membrane-associated protein VIPP1 chloroplastic		
A0A1D6N531	Lipoxygenase		

Protein	Annotation	Response to salt stress	ANOVA
A0A1D6N5A6	Diphosphocytidyl methyl erythritol synthase1		
A0A1D6N5N4	Mitotic spindle checkpoint protein MAD1		
A0A1D6N672	Photosystem II subunit PsbS1		
A0A1D6N6G5	Fructose-16-bisphosphatase cytosolic		
A0A1D6N6H1	Actin-7		
A0A1D6N760	Bowman-birk inhibitor1		
A0A1D6N764	Aldose reductase		
A0A1D6N932	Osmotin-like protein OSM34		
A0A1D6N9F5	Cytidine methyl kinase1		
A0A1D6N9H2	Phosphoglycerate kinase		
A0A1D6NC89	50S ribosomal protein L13 chloroplastic		
A0A1D6NCX2	Phosphotransferase		

Protein	Annotation	Response to salt stress	ANOVA
A0A1D6ND55	Glycosyltransferase		
A0A1D6NHQ1	Carbonic anhydrase		
A0A1D6NJK9	Phosphoglucomutase chloroplastic		
A0A1D6NNV9	Alpha/beta-Hydrolases superfamily protein		
A0A1D6NQF1	Alpha-L-arabinofuranosidase 1		
A0A1D6NQP9	Non-specific lipid-transfer protein		
A0A1D6NQQ1	Non-specific lipid-transfer protein		
A0A1D6NST8	Chloroplast RNA splicing4		
A0A1D6NSU5	Chloroplast RNA splicing4		
A0A1D6NUP6	Thiol protease SEN102		
A0A1D6NV83	Proteasome subunit beta type		

Protein	Annotation	Response to salt stress	ANOVA
A0A1D6NVA4	Profilin		
A0A1D6NVW6	Enolase 1		
A0A1D6NVZ7	Transketolase 1		
A0A1D6NWP6	Chaperonin 60 subunit beta 2 chloroplastic		
A0A1D6NX08	WAT1-related protein		
A0A1D6NYE8	Restorer of fertility2		
A0A1D6P248	Vacuolar proton pump2		
A0A1D6P2J7	Uncharacterized protein		
A0A1D6P2R8	Elongation factor 1-alpha9		
A0A1D6P305	Uncharacterized protein		
A0A1D6PBN3	30S ribosomal protein S1		
A0A1D6PD08	Ascorbate peroxidase-like protein		
A0A1D6PD09	Ascorbate peroxidase-like protein		
A0A1D6PDJ3	Heat shock 70 kDa protein 5		

Protein	Annotation	Response to salt stress	ANOVA
A0A1D6PEH7	Phosphoenolpyruvate carboxykinase homolog2		
A0A1D6PH49	ATP synthase subunit gamma mitochondrial		
A0A1D6PHF7	Beta-glucosidase 11		
A0A1D6PHI2	Peptidase beta subunit		
A0A1D6PHK8	40S ribosomal protein S23-2		
A0A1D6PI62	40S ribosomal protein S3a		
A0A1D6PID0	Chloroplast 30S ribosomal protein S10		
A0A1D6PJL0	Aconitate hydratase		
A0A1D6PKZ8	Histone H2B		
A0A1D6PUK8	Aconitate hydratase		
A0A1D6PX24	Ribosome-recycling factor chloroplastic		
A0A1D6PYB8	Nuclear transport factor1		

Protein	Annotation	Response to salt stress	ANOVA
A0A1D6PYI3	Protein PROTON GRADIENT REGULATION 5 chloroplastic		
A0A1D6PZ66	Enoyl-[acyl-carrier-protein] reductase [NADH] chloroplastic		
A0A1D6Q048	Adenylate kinase 5 chloroplastic		
A0A1D6Q1L8	Glyceraldehyde-3-phosphate deHaseN1		
A0A1D6Q4Q1	GrpE protein homolog		
A0A1D6Q567	Succinate--CoA ligase [ADP-forming] subunit beta, mitochondrial		
A0A1D6Q7Z8	Soluble inorganic pyrophosphatase 2		
A0A1D6QH21	Putative alpha-L-arabinofuranosi		

Protein	Annotation	Response to salt stress	ANOVA
	dase family protein		
A0A1D6QHJ6	Aluminum induced protein with YGL and LRDR motifs		
A0A1D6QK06	14-3-3-like protein A		
A0A1D6QKI4	HSP protein		
A0A1D6QQD8	Acetyltransferase component of pyruvate dehydrogenase complex		
A0A1D6QRG1	Lipoxygenase		
A0A1D6QS96	Uncharacterized protein		
A0A1D6QTM8	NAD(P)-linked oxidoreductase superfamily protein		
A0A1D8RGD7	Chloroplast ribulose bisphosphate carboxylase/oxygenase activase (Fragment)		
A0A1J0FBZ3	Ribulose bisphosphate		

Protein	Annotation	Response to salt stress	ANOVA
	carboxylase large chain (Fragment)		
A0A1P7ZDI1	Chitinase		
A0A1R3M158	Benzoxazinone synthesis9		
A0A1R3M7Z7	High mobility group family A 102		
A0A1R3MB28	Malate dehydrogenase		
A0A1R3MNR4	Actin-7 (Fragment)		
A0A1R3MNS1	Actin-7 (Fragment)		
A0A1R3P4Z6	Triose phosphate/phosphate translocator TPT chloroplastic		
A0A1R3QF47	Chloroplast stem-loop binding protein of 41 kDa a chloroplastic		
A0A1X7YDI6	Uncharacterized protein		

Protein	Annotation	Response to salt stress	ANOVA
A0A1X7YG26	Uncharacterized protein		
A0A1X7YHF8	Uncharacterized protein		
A0A1X7YIG0	Uncharacterized protein		
A5A5E7	Protein disulfide-isomerase		
A6YSM3	PL3K2		
B1P2H3	Filamentation temperature-sensitive H 2A		
B1P2H4	Filamentation temperature-sensitive H 2B		
B4F820	Uncharacterized protein		
B4F848	20 kDa chaperonin chloroplastic		
B4F871	Protein DJ-1 homolog D		
B4F874	Acclimation of photosynthesis to environment		
B4F8L7	Glyceraldehyde -3-phosphate dehydrogenase		

Protein	Annotation	Response to salt stress	ANOVA
B4F8V5	NADH dehydrogenase [ubiquinone] iron-sulfur protein 1 mitochondrial		
B4F925	Superoxide dismutase		
B4F9B5	Cysteine proteinase 2		
B4F9G0	60S ribosomal protein L4-1		
B4F9T3	Putative uncharacterized protein		
B4F9X0	Alpha-galactosidase		
B4F9Z6	Enzyme of the cupin superfamily		
B4FAC2	Photosystem I N subunit1		
B4FAC5	Rubredoxin-like superfamily protein		
B4FAD4	Isocitrate dehydrogenase [NAD] subunit, mitochondrial		

Protein	Annotation	Response to salt stress	ANOVA
B4FAR8	Proteasome subunit alpha type		
B4FAW3	Photosystem I reaction center subunit II		
B4FBC2	GDP-mannose 35-epimerase		
B4FBF4	Serine hydroxymethyltransferase		
B4FBF6	Mitochondrial dicarboxylate/tricarboxylate transporter DTC		
B4FBH1	Multiple organellar RNA editing factor 2 chloroplastic		
B4FBJ5	Uncharacterized protein		
B4FC21	Uncharacterized protein		
B4FD69	Uncharacterized protein		
B4FDG2	Acyl carrier protein		
B4FDH5	Histone H2B		

Protein	Annotation	Response to salt stress	ANOVA
B4FDI5	Bifunctional monothiol glutaredoxin-S16 chloroplastic		
B4FDT6	Eucaryotic initiation factor7		
B4FE18	Histone H2B		
B4FEH8	Uncharacterized protein		
B4FF62	Uncharacterized protein		
B4FFV3	Malate dehydrogenase		
B4FFZ2	Ketol-acid reductoisomerase		
B4FGN4	Uncharacterized protein		
B4FH16	30S ribosomal protein 3 chloroplastic		
B4FH62	NAD(P)-binding Rossmann-fold superfamily protein		

Protein	Annotation	Response to salt stress	ANOVA
B4FH69	Uncharacterized protein		
B4FHA0	Thylakoid lumenal 17.4 kDa protein chloroplastic		
B4FHE4	60S ribosomal protein L17-2		
B4FHH4	Uncharacterized protein		
B4FHK4	Natterin-4		
B4FHN3	L-ascorbate peroxidase S chloroplastic/mitochondrial		
B4FIA6	Histone H2A		
B4FIV0	Succinate--CoA ligase [ADP-forming] subunit alpha, mitochondrial		
B4FJG1	Chlorophyll a-b binding protein, chloroplastic		
B4FJP7	Photosynthetic NDH subunit of subcomplex B 2 chloroplastic		

Protein	Annotation	Response to salt stress	ANOVA
B4FK23	Peptidylprolyl isomerase		
B4FKB3	50S ribosomal protein L31		
B4FKR5	Uncharacterized protein		
B4FKV6	Peroxidase		
B4FL72	Uncharacterized protein		
B4FLG7	Triphosphate tunel metalloenzyme 3		
B4FLK3	Uncharacterized protein		
B4FLP0	Uncharacterized protein		
B4FLS7	Ribosome-recycling factor chloroplastic		
B4FLT7	Photosystem I H subunit1		
B4FN24	Peroxiredoxin-2B		
B4FNK1	Uncharacterized protein		
B4FP22	Glycosyltransferase		
B4FPB2	Lipoxygenase6		

Protein	Annotation	Response to salt stress	ANOVA
B4FPE4	V-type proton ATPase subunit G		
B4FPJ2	Sm-like protein LSM3B		
B4FQ80	Chlorophyll a-b binding protein, chloroplastic		
B4FQI8	Peptidylprolyl isomerase		
B4FR47	Fructose-bisphosphate aldolase		
B4FRC8	FAD/NAD(P)-binding oxidoreductase		
B4FRG1	14-3-3-like protein		
B4FRH5	Succinate--CoA ligase [ADP-forming] subunit beta, mitochondrial		
B4FRH8	Actin-7		
B4FRM3	Uncharacterized protein		
B4FRM5	Red chlorophyll catabolite		

Protein	Annotation	Response to salt stress	ANOVA
	reductase chloroplastic		
B4FRP8	Plastid-lipid-associated protein 2		
B4FRR1	Soluble inorganic pyrophosphatase 6 chloroplastic		
B4FS17	Thylakoid lumenal 29 kDa protein chloroplastic		
B4FS55	Peroxiredoxin Q chloroplastic		
B4FSD8	Cytochrome b6-f complex iron-sulfur subunit		
B4FSJ1	V-type proton ATPase subunit C		
B4FSJ3	Ribulose bisphosphate carboxylase small chain		
B4FSP6	Uncharacterized protein		
B4FSQ4	40S ribosomal protein SA		

Protein	Annotation	Response to salt stress	ANOVA
B4FST4	SKP1-like protein 1A		
B4FSV3	Uncharacterized protein		
B4FSX7	(+)-neomenthol dehydrogenase		
B4FSZ7	Putative mitochondrial-processing peptidase subunit alpha-2 chloroplastic/mitochondrial		
B4FT76	ABC transporter I family member 6 chloroplastic		
B4FTD1	Glutathione S-transferase III		
B4FTI5	Fructose-bisphosphate aldolase		
B4FTP2	Thioredoxin-like protein CDSP32 chloroplastic		
B4FU39	Uncharacterized protein		

Protein	Annotation	Response to salt stress	ANOVA
B4FUA1	Chlorophyll a-b binding protein, chloroplastic		
B4FUB4	60S acidic ribosomal protein P1		
B4FUC4	Plasma membrane-associated cation-binding protein 1		
B4FUR2	Cysteine-rich repeat secretory protein 55		
B4FV03	Glutathione transferase11		
B4FV91	Pathogenesis related protein5		
B4FV94	Chlorophyll a-b binding protein, chloroplastic		
B4FVP5	Pathogenesis related protein4		
B4FVT1	Peroxidase		
B4FW90	ER luminal binding protein		
B4FWD0	NAD(P)H dehydrogenase		

Protein	Annotation	Response to salt stress	ANOVA
	(Quinone) FQR1		
B4FWG2	Photosynthetic NDH subunit of subcomplex B 2 chloroplastic		
B4FWN1	NADPH:quinone oxidoreductase		
B4FWR7	60S ribosomal protein L13		
B4FXB0	Chlorophyll a-b binding protein, chloroplastic		
B4FXR6	Uncharacterized protein		
B4FY73	Germin-like protein subfamily 2 member 1		
B4FYU2	Glyceraldehyde-3-phosphate dehydrogenase A		
B4FZ14	Protein CHLORORESPIRATORY REDUCTION 6 chloroplastic		

Protein	Annotation	Response to salt stress	ANOVA
B4FZB4	50S ribosomal protein L17		
B4FZD8	Protein STRICTOSIDINE SYNTHASE-LIKE 6		
B4FZL4	Chlorophyll a-b binding protein, chloroplastic		
B4FZU8	Malate dehydrogenase		
B4FZZ2	Peptidyl-prolyl cis-trans isomerase		
B4G054	Photosynthetic NDH subunit of subcomplex B 5 chloroplastic		
B4G0K4	Phosphoglycerate kinase		
B4G143	Chlorophyll a-b binding protein, chloroplastic		
B4G177	Uncharacterized protein		
B4G1A1	Uncharacterized protein		
B4G1B0	Remorin		

Protein	Annotation	Response to salt stress	ANOVA
B4G1D2	CBS domain protein		
B4G1K9	Photosystem I reaction center subunit V		
B4G1P1	Glutamine synthetase		
B4G1Q5	50S ribosomal protein L10 chloroplastic		
B4G1S4	Peroxidase		
B4G1V7	Nodulin-related protein 1		
B4G243	Ribosomal protein L29		
B4G259	Oxygen evolving complex2		
B4G262	Carbonic anhydrase		
B5AK47	Dhurrinase-like B-glucosidase		
B6SGV9	Lactoylglutathione lyase		
B6SH12	Win1		
B6SH83	RuBisCO large subunit-binding protein subunit beta		

Protein	Annotation	Response to salt stress	ANOVA
B6SI53	Fructose-bisphosphate aldolase		
B6SIF0	Glycine-rich RNA-binding protein 2		
B6SJ21	Guanine nucleotide-binding protein beta subunit-like protein		
B6SJF9	Cortical cell-delineating protein		
B6SJL0	Putative uncharacterized protein		
B6SJZ5	Histone H2B		
B6SK03	Ubiquitin-conjugating enzyme E2 variant 1C		
B6SK54	Superoxide dismutase [Cu-Zn]		
B6SKA0	Glutathione S-transferase 1		
B6SLN4	Uncharacterized protein		

Protein	Annotation	Response to salt stress	ANOVA
B6SLQ7	60S ribosomal protein L23a		
B6SP61	Ferredoxin		
B6SP99	Photosynthetic NDH subunit of subcomplex B 1 chloroplastic		
B6SPR5	Fb14		
B6SQD9	Uncharacterized protein		
B6SQU8	Bowman-Birk type trypsin inhibitor		
B6SQV5	Photosystem II 10 kDa polypeptide		
B6SQZ7	16kDa membrane protein		
B6SRG3	Uncharacterized protein		
B6SRJ5	Bifunctional 3-phosphoadenosine 5-phosphosulfate synthetase 2		
B6SRY5	Glycosyltransferase		

Protein	Annotation	Response to salt stress	ANOVA
B6SRZ0	Putative uncharacterized protein		
B6SSE4	Glycosyltransferase		
B6SST7	50S ribosomal protein L5		
B6SST9	ATP synthase delta chain		
B6SSU6	Fructose-bisphosphate aldolase, cytoplasmic isozyme 1		
B6ST36	Chloroplast oxygen-evolving complex/thylakoid lumenal 25.6kDa protein		
B6STG2	Photosystem I reaction center subunit XI		
B6STP9	Photosystem I reaction center subunit XI		
B6STV6	Putative uncharacterized protein		

Protein	Annotation	Response to salt stress	ANOVA
B6SU38	Phosphoserine phosphatase		
B6SU63	Carbonic anhydrase		
B6SUC4	Chlorophyll a-b binding protein, chloroplastic		
B6SUC7	Putative uncharacterized protein		
B6SUH6	Non-cyanogenic beta-glucosidase		
B6SUH9	PsbP domain-containing protein 3 chloroplastic		
B6SVH7	Putative uncharacterized protein		
B6SX34	Photosystem I reaction center subunit psaK		
B6SXH1	Putative uncharacterized protein		
B6SXI1	CP12-1		
B6SXW8	RuBisCO large subunit-binding		

Protein	Annotation	Response to salt stress	ANOVA
	protein subunit alpha		
B6SZG7	Peptidylprolyl isomerase		
B6SZK3	NAD(P)H-dependent oxidoreductase		
B6SZP7	Phosphoribulokinase		
B6SZR1	Chlorophyll a-b binding protein, chloroplastic		
B6SZT9	Chlorophyll a-b binding protein, chloroplastic		
B6SZZ1	Cortical cell-delineating protein		
B6T026	Cortical cell-delineating protein		
B6T037	Chlorophyll a-b binding protein, chloroplastic		
B6T0G9	Histone H4		
B6T0X0	Histone H4		
B6T0Y2	ATP synthase epsilon chain, mitochondrial		

Protein	Annotation	Response to salt stress	ANOVA
B6T1G5	Histone H2B		
B6T1G9	Elongation factor 1-beta		
B6T275	Histone H4		
B6T2E7	ADP-ribosylation factor 1		
B6T2Y1	Peroxiredoxin-5		
B6T2Y9	Chlorophyll a-b binding protein, chloroplastic		
B6T3P5	Glutamine synthetase		
B6T5N8	Glycine-rich RNA-binding protein 2		
B6T5U0	F1F0-ATPase inhibitor protein		
B6T706	Aspartic proteinase oryzasin-1		
B6T7A4	Glyceraldehyde -3-phosphate dehydrogenase		
B6T7L9	14-3-3-like protein		

Protein	Annotation	Response to salt stress	ANOVA
B6T7W8	Cortical cell-delineating protein		
B6T892	Chlorophyll a-b binding protein, chloroplastic		
B6T8M1	50S ribosomal protein L19		
B6T9P0	UDP-glucose 6-dehydrogenase		
B6TBJ2	Uncharacterized protein		
B6TBK4	Ribonucleoprotein		
B6TBN6	Pyruvate kinase		
B6TCN7	Threonine endopeptidase		
B6TDN0	NADH-ubiquinone oxidoreductase 10.5 kDa subunit		
B6TE43	Glutamine synthetase		
B6TET7	Abscisic stress ripening protein 1		

Protein	Annotation	Response to salt stress	ANOVA
B6TEW2	Ferredoxin--NADP reductase		
B6TFY4	40S ribosomal protein S27		
B6TGD4	F1F0-ATPase inhibitor protein		
B6TGG2	2,3-bisphosphoglycerate-independent phosphoglycerate mutase		
B6THG1	Legumin-like protein		
B6THR9	3-isopropylmalate dehydrogenase		
B6THZ8	Threonine synthase		
B6TI65	Fructose-bisphosphate aldolase		
B6TIG6	Transaminase/ transferase, transferring nitrogenous groups		
B6TJ90	Multifunctional fusion protein		

Protein	Annotation	Response to salt stress	ANOVA
B6TJM1	Isocitrate dehydrogenase [NAD] subunit, mitochondrial		
B6TJM7	Translocon Tic40		
B6TLW2	Nucleoside diphosphate kinase		
B6TLX2	Fiber protein Fb15		
B6TM52	Hsp20/alpha crystallin family protein		
B6TN41	4-hydroxy-4-methyl-2-oxoglutarate aldolase		
B6TN48	3-hydroxyisobutyryl-CoA hydrolase-like protein 5		
B6TNP4	Histone H1		
B6TNR7	Ferredoxin-thioredoxin reductase, catalytic chain		

Protein	Annotation	Response to salt stress	ANOVA
B6TNX7	Proteasome subunit alpha type		
B6TP17	Enzyme of the cupin superfamily		
B6TP39	FHA domain containing protein		
B6TP44	Histone H4		
B6TPG0	Elongation factor Tu		
B6TPX4	Plastid-lipid-associated protein 2		
B6TQ06	Aminomethyltransferase		
B6TQI8	Dirigent protein		
B6TR69	Putative uncharacterized protein		
B6TRA8	Histone H1		
B6TS84	Transaldolase 2		
B6TT67	Glycosyltransferase		

Protein	Annotation	Response to salt stress	ANOVA
B6TTP1	Non-specific lipid-transfer protein		
B6TUA2	Acetyltransferase component of pyruvate dehydrogenase complex		
B6TUG5	Putative uncharacterized protein		
B6TUZ6	Macrophage migration inhibitory factor		
B6TVT9	Protein LHCP TRANSLOCATION DEFECT		
B6TXS5	Photosystem I reaction center subunit N		
B6TXY3	Quinone oxidoreductase-like protein		
B6TYM1	Phosphoribulokinase		
B6TYZ1	Putative uncharacterized protein		

Protein	Annotation	Response to salt stress	ANOVA
B6U016	Senescence-associated protein DIN1		
B6U284	14-3-3-like protein		
B6U2F2	2C-type protein phosphatase protein		
B6U463	Subtilisin-chymotrypsin inhibitor-2A		
B6U4G5	Beta-propeller domain of methanol dehydrogenase type		
B6U534	Photosystem I reaction center subunit V		
B6U5G4	Glutathione S-transferase GSTU6		
B6U5L3	UDP-glucose 6-dehydrogenase		
B6U6B2	Putative uncharacterized protein		
B6UAK0	6-phosphoglucono lactonase		

Protein	Annotation	Response to salt stress	ANOVA
B6UCK2	Zinc finger protein		
B6UCP6	Putative uncharacterized protein		
B6UDS5	Glutamine synthetase		
B6UE00	Soluble inorganic pyrophosphatase		
B6UE14	Bowman-Birk type bran trypsin inhibitor		
B6UE15	Soluble inorganic pyrophosphatase		
B6UFB3	Stromal 70 kDa heat shock-related protein		
B6UH55	Vacuolar ATP synthase catalytic subunit A		
B6UH77	Histone H3		
B6UHU1	Catalase		
B6UI46	RNA-binding protein Nova-1		

Protein	Annotation	Response to salt stress	ANOVA
B6UIC1	50S ribosomal protein L12-1		
B7ZYI0	14-3-3-like protein GF14-6		
B7ZYP0	Glycosyltransferase		
B7ZYP6	Uncharacterized protein		
B7ZYT6	Ribulose bisphosphate carboxylase small chain		
B7ZYU3	Uncharacterized protein		
B7ZYV4	Arginine decarboxylase		
B8A064	Phosphoribulokinase		
B8A068	S-adenosylmethionine synthase		
B8A270	Protease Do-like 2 chloroplastic		
B8A3S1	Uncharacterized protein		
B9TSW5	Glutamine synthetase		
C0HED8	Uncharacterized protein		

Protein	Annotation	Response to salt stress	ANOVA
C0HFB2	Uncharacterized protein		
C0HGV5	Enolase2		
C0HHC4	Nucleoside diphosphate kinase		
C0HHU2	23-bisphosphoglycerate-independent phosphoglycerate mutase 1		
C0HIC4	40S ribosomal protein S21		
C0HJ28	Glycosyltransferase		
C0LFT6	Phosphoenolpyruvate carboxylase (Fragment)		
C0P2S3	Cytokinin response regulator1		
C0P3R8	Glutathione peroxidase		
C0P3S5	Fumarylacetoacetate (FAA) hydrolase family		

Protein	Annotation	Response to salt stress	ANOVA
C0P3W9	Phosphoenolpyruvate carboxykinase1		
C0P441	Carbonic anhydrase		
C0P4Q3	Heat shock protein 90 kDa		
C0P4U8	Putative ATP synthase 24 kDa subunit mitochondrial		
C0P5I2	Uncharacterized protein		
C0P699	Elongation factor Tu		
C0P7R2	Albino or pale green mutant1		
C0P7X7	30S ribosomal protein S6 alpha chloroplastic		
C0P7Y2	Stress-induced protein1		
C0P821	Uncharacterized protein		
C0P937	Uncharacterized protein		
C0P948	Uncharacterized protein		

Protein	Annotation	Response to salt stress	ANOVA
C0P9F5	Chlorophyll a-b binding protein, chloroplastic		
C0P9Q2	Protein THYLAKOID FORMATION 1 chloroplastic		
C0PA83	Uncharacterized protein		
C0PAG2	Uncharacterized protein		
C0PAQ4	Chlorophyll a-b binding protein, chloroplastic		
C0PAT3	Uncharacterized protein		
C0PBL7	Uncharacterized protein		
C0PC75	Thioredoxin		
C0PCV2	40S ribosomal protein S8		
C0PCX9	Mg-protoporphyrin IX chelatase		
C0PDH2	Plasma membrane ATPase		
C0PE12	Protein plastid transcriptionally		

Protein	Annotation	Response to salt stress	ANOVA
	active 16 chloroplastic		
C0PE24	Uncharacterized protein		
C0PF34	Heme-binding-like protein chloroplastic		
C0PFK3	Proteasome subunit alpha type		
C0PFV4	Chaperone protein ClpC1 chloroplastic		
C0PGM1	Acyl-coenzyme A oxidase		
C0PGN4	Obg-like ATPase 1		
C0PHE3	Eucaryotic initiation factor4		
C0PHR4	Adenosylhomocysteinase		
C0PIR4	Uncharacterized protein		
C0PK55	Cytochrome c-2		
C0PKS1	Peroxidase		
C0PL72	Uncharacterized protein		

Protein	Annotation	Response to salt stress	ANOVA
C0PP19	Uncharacterized protein		
C0PP27	Inositol-1-monophosphatase		
C0PPF5	Calcium sensing receptor chloroplastic		
C4J6J5	40S ribosomal protein S6		
C4J9Y2	Aluminum-induced protein homolog1		
C4J9Z9	Uncharacterized protein		
C4JBF5	60S ribosomal protein L9-1		
C4JBS8	Glyceraldehyde-3-phosphate dehydrogenase		
C5IHC4	Pyruvate, phosphate dikinase		
C5IHC6	Pyruvate, phosphate dikinase		
C5IHD0	Pyruvate, phosphate dikinase		

Protein	Annotation	Response to salt stress	ANOVA
C5IHE4	Pyruvate, phosphate dikinase		
D1MN58	ABA-, stress- and fruit-ripening inducible-like protein		
D3K3U9	Pyruvate orthophosphate dikinase		
E1AFV5	Beta-1,3-glucanase		
G0YVY6	Beta-D-glucosidase		
I7EGH6	Glutamine synthetase		
K7TFI4	NAD(P)H-quinone oxidoreductase subunit U chloroplastic		
K7TGE1	Beta-glucosidase2		
K7TIN2	Glycine cleavage system P protein		
K7TL05	General regulatory factor2		

Protein	Annotation	Response to salt stress	ANOVA
K7TQM1	Heat shock 70 kDa protein 3		
K7U6M0	NAD(P)-binding Rossmann-fold superfamily protein		
K7UGM3	Catalase		
K7UGQ1	Omega-hydroxypalmitate O-feruloyl transferase		
K7UMB3	Signal recognition particle 54 kDa protein chloroplastic		
K7UXK5	Putative alcohol dehydrogenase superfamily protein		
K7V067	Isocitrate dehydrogenase [NADP]		
K7V321	ATP-dependent zinc metalloprotease FTSH 4 mitochondrial		

Protein	Annotation	Response to salt stress	ANOVA
K7V5G0	NAD(P)H-quinone oxidoreductase subunit O chloroplastic		
K7VAE7	HB transcription factor		
K7VD78	Putative chaperone clbp family protein		
K7VH58	Peroxidase		
K7VNE0	Phosphoenolpyruvate carboxykinase homolog2		
O23813	Sulfite reductase [ferredoxin], chloroplastic		
O24561	Chlorophyll a-b binding protein, chloroplastic		
O48950	Sec-independent protein translocase protein TATB, chloroplastic		

Protein	Annotation	Response to salt stress	ANOVA
P06671	Chlorophyll a-b binding protein, chloroplastic		
P0C1M0	ATP synthase subunit gamma, chloroplastic		
P11155	Pyruvate, phosphate dikinase 1, chloroplastic		
P27497	Chlorophyll a-b binding protein M9, chloroplastic		
P27787	Ferredoxin-1, chloroplastic		
P38563	Glutamine synthetase root isozyme 5		
P41978	Superoxide dismutase [Mn] 3.2, mitochondrial		
P43188	Adenylate kinase, chloroplastic		
P49237	Glucan endo-1,3-beta-glucosidase, acidic isoform		

Protein	Annotation	Response to salt stress	ANOVA
P93519	PRm 6b		
P93638	Actin (Fragment)		
P93639	Actin (Fragment)		
Q0GR44	ATP synthase subunit alpha		
Q2XXC2	Pathogenesis-related maize seed protein OS=Zea diploperennis GN=prms PE=3 SV=1		
Q38JE7	Temperature-induced lipocalin-1		
Q41728	Carbonic anhydrase		
Q41729	Carbonic anhydrase		
Q41741	Eukaryotic initiation factor 4A		
Q41806	Oxygen-evolving enhancer protein 3-2, chloroplastic		

Protein	Annotation	Response to salt stress	ANOVA
Q41823	Chlorophyll a-b binding protein, chloroplastic		
Q42420	Protease inhibitor		
Q43272	NADP-dependent glyceraldehyde-3-phosphate dehydrogenase		
Q4W1F7	Thioredoxin		
Q53WW9	Beta-D-glucosidase		
Q5NKN3	DNA-binding protein MNB1B		
Q5QJA2	Harpin binding protein 1		
Q6TM44	Germin-like protein		
Q84JX6	Phosphoglycerate kinase (Fragment)		
Q84KR7	Phosphoenolpyruvate carboxylase		
Q8LLS4	Phosphoglycerate kinase (Fragment)		

Protein	Annotation	Response to salt stress	ANOVA
Q8W522	Glycine cleavage system H protein (Fragment)		
Q94G64	T-cytoplasm male sterility restorer factor 2		
Q9FQC6	Glutathione S-transferase GST 13		
Q9FQD0	Glutathione S-transferase 6		
Q9FUZ6	Elongation factor Tu		
Q9M583	Hypersensitive induced response2		
S5TDC1	Chlorophyll a-b binding protein, chloroplastic (Fragment)		
V5JUG0	Heme oxygenase 1		

Supplementary Table S5.2 List of proteins found in roots of five maize genotypes at the seventh week after sowing (Chapter 5).

In addition, the relative abundance of proteins as a response to applied salt stress.

Protein	Annotation	Response to salt stress	ANOVA
A0A096Q8E7	Uncharacterized protein	Low Abundance	1,4E-02
A0A096QB84	Uncharacterized protein	Low Abundance	6,5E-04
A0A096QG19	Uncharacterized protein	Low Abundance	4,4E-02
A0A096QHR4	Uncharacterized protein	Low Abundance	3,6E-04
A0A096QKG4	Uncharacterized protein	Low Abundance	7,3E-03
A0A096QPK0	Uncharacterized protein	Low Abundance	2,2E-02
A0A096QPS8	Uncharacterized protein	Low Abundance	4,7E-03
A0A096R1Q6	Tubulin beta-6 chain	Low Abundance	1,8E-04
A0A096R5J8	Uncharacterized protein	Low Abundance	2,0E-02
A0A096RHV4	Uncharacterized protein	Low Abundance	2,7E-02
A0A096RK52	Uncharacterized protein	Low Abundance	7,1E-05
A0A096RMS8	Uncharacterized protein	Low Abundance	2,9E-02

Protein	Annotation	Response to salt stress	ANOVA
A0A096RNY4	Uncharacterized protein	Low Abundance	2,5E-02
A0A096RPU1	Uncharacterized protein	Low Abundance	5,9E-03
A0A096RSH2	Uncharacterized protein	Low Abundance	1,9E-02
A0A096RTH2	Uncharacterized protein	Low Abundance	2,2E-02
A0A096S518	Uncharacterized protein	Low Abundance	1,3E-04
A0A096SCE8	Uncharacterized protein	Low Abundance	3,6E-03
A0A096SIL2	Uncharacterized protein	Low Abundance	1,8E-02
A0A096STY1	Uncharacterized protein	Low Abundance	2,8E-03
A0A096T8H7	Uncharacterized protein	Low Abundance	5,7E-03
A0A096TME2	Uncharacterized protein	Low Abundance	3,7E-03
A0A096TRV6	Uncharacterized protein	Low Abundance	4,2E-02
A0A096TTJ9	Uncharacterized protein	Low Abundance	4,9E-04
A0A096TW96	Uncharacterized protein	Low Abundance	6,0E-06
A0A096UCQ5	Uncharacterized protein	Low Abundance	3,9E-04
B4F946	Uncharacterized protein	Low Abundance	2,8E-05

Protein	Annotation	Response to salt stress	ANOVA
B4F9B5	Uncharacterized protein	Low Abundance	3,1E-02
B4FAD1	S-adenosylmethionine synthase	Low Abundance	4,4E-03
B4FAG0	Uncharacterized protein	Low Abundance	2,0E-02
B4FBB9	Uncharacterized protein	Low Abundance	8,1E-03
B4FHJ8	Heterogeneous nuclear ribonucleoprotein A3 isoform 1	Low Abundance	9,4E-03
B4FHZ4	NADH ubiquinone oxidoreductase B14 subunit	Low Abundance	6,7E-03
B4FIE9	S-adenosylmethionine synthase	Low Abundance	1,3E-03
B4FQK5	Eukaryotic peptide chain release factor subunit 1-1	Low Abundance	5,1E-03
B4FRI1	Phosphoserine aminotransferase	Low Abundance	4,2E-02
B4FS90	Cysteine protease 1	Low Abundance	1,3E-02

Protein	Annotation	Response to salt stress	ANOVA
B4FUC4	Uncharacterized protein	Low Abundance	3,5E-02
B4FW68	Phenylalanine ammonia-lyase	Low Abundance	6,4E-03
B4FWD0	Minor allergen Alt a 7	Low Abundance	6,7E-03
B4G080	Caffeoyl-CoA O-methyltransferase 1	Low Abundance	1,2E-02
B4G1S4	Peroxidase	Low Abundance	3,9E-02
B4G1Z0	Alpha-L-fucosidase 2	Low Abundance	1,3E-04
B6SJL0	Putative uncharacterized protein	Low Abundance	4,9E-02
B6SJS7	Nascent polypeptide-associated complex subunit beta	Low Abundance	1,7E-02
B6SPX4	Tubulin alpha-3 chain	Low Abundance	7,1E-05
B6SQI1	Bundle sheath cell specific protein 1	Low Abundance	1,0E-02
B6SUK0	LOL3	Low Abundance	6,6E-04

Protein	Annotation	Response to salt stress	ANOVA
B6T173	Peroxidase	Low Abundance	2,9E-02
B6T7B1	Peroxidase	Low Abundance	1,8E-02
B6T7Z2	Cytochrome b5	Low Abundance	4,2E-02
B6TAL1	Vacuolar processing enzyme	Low Abundance	1,4E-02
B6TF38	Tubulin beta-8 chain	Low Abundance	3,3E-05
B6TFN1	Minor allergen Alt a 7	Low Abundance	1,7E-02
B6TGS7	Cytochrome c	Low Abundance	2,6E-02
B6TIG6	Transaminase/ transferase, transferring nitrogenous groups	Low Abundance	5,5E-03
B6TQ08	Actin-1	Low Abundance	2,9E-02
B6TRC0	Gibberellin receptor GID1L2	Low Abundance	1,5E-02
B6TYW3	Ribonuclease 1	Low Abundance	3,0E-03
B6U4D6	Phenylalanine ammonia-lyase	Low Abundance	2,0E-05

Protein	Annotation	Response to salt stress	ANOVA
B6U7D8	Cinnamyl alcohol dehydrogenase	Low Abundance	3,5E-02
B6U8D9	Bundle sheath cell specific protein 1	Low Abundance	9,2E-03
B6UD26	O-methyltransferase ZRP4	Low Abundance	4,6E-02
B6UF45	Caffeoyl-CoA O-methyltransferase 1	Low Abundance	2,5E-02
B8A046	Phenylalanine ammonia-lyase	Low Abundance	3,2E-05
B8A068	S-adenosylmethionine synthase	Low Abundance	1,5E-02
C0HDZ6	Uncharacterized protein	Low Abundance	3,4E-02
C0HE72	Uncharacterized protein	Low Abundance	4,8E-03
C0HFP5	Uncharacterized protein	Low Abundance	2,0E-04
C0HHR4	Uncharacterized protein	Low Abundance	2,3E-02
C0HIY6	Uncharacterized protein	Low Abundance	5,3E-03
C0P664	Uncharacterized protein	Low Abundance	2,1E-04

Protein	Annotation	Response to salt stress	ANOVA
C0P6I5	Uncharacterized protein	Low Abundance	9,8E-03
C0P6Q4	Transcribed sequence 1087 protein	Low Abundance	2,8E-03
C0P6Z0	Uncharacterized protein	Low Abundance	4,5E-04
C0P8R6	Uncharacterized protein	Low Abundance	2,1E-02
C0PA44	Uncharacterized protein	Low Abundance	1,4E-02
C0PA91	Uncharacterized protein	Low Abundance	4,8E-02
C0PF40	Uncharacterized protein	Low Abundance	4,7E-03
C0PH85	Uncharacterized protein	Low Abundance	1,6E-04
C0PKT5	Uncharacterized protein	Low Abundance	2,8E-03
C0PMJ0	Phenylalanine ammonia-lyase	Low Abundance	1,6E-02
C0PNP5	Uncharacterized protein	Low Abundance	1,9E-02
C4J639	Uncharacterized protein	Low Abundance	1,4E-02
C4JBJ2	Uncharacterized protein	Low Abundance	1,6E-02
C4JBL2	Uncharacterized protein	Low Abundance	4,1E-02

Protein	Annotation	Response to salt stress	ANOVA
K7TSW9	Acyl carrier protein	Low Abundance	2,8E-02
K7U159	Peroxidase	Low Abundance	2,9E-02
K7U9N2	Putative subtilase family protein	Low Abundance	2,9E-02
K7UNP2	Uncharacterized protein (Fragment)	Low Abundance	2,6E-04
K7USX8	Peroxidase	Low Abundance	3,8E-02
K7UX63	Phenylalanine ammonia-lyase	Low Abundance	9,0E-06
K7UZ21	Peroxidase	Low Abundance	3,6E-02
K7V3I5	Beta tubulin2	Low Abundance	3,4E-04
K7VA33	Uncharacterized protein	Low Abundance	3,3E-02
K7VC35	S-adenosylmethionine synthase	Low Abundance	1,3E-03
K7VEA6	Caffeoyl-CoA O-methyltransferase 2	Low Abundance	3,1E-02
K7VKH1	Uncharacterized protein	Low Abundance	2,0E-02

Protein	Annotation	Response to salt stress	ANOVA
K7VM46	Uncharacterized protein	Low Abundance	2,9E-02
Q41784	Tubulin beta-7 chain	Low Abundance	3,6E-04
Q5GLJ6	O-methyltransferase	Low Abundance	6,3E-03
Q5GLK6	Caffeoyl-CoA 3-O-methyltransferase 1	Low Abundance	2,9E-02
Q6RFK0	Peroxidase (Fragment)	Low Abundance	7,7E-03
Q6RFK3	Peroxidase (Fragment)	Low Abundance	1,0E-02
Q6VWE6	O-methyltransferase	Low Abundance	5,8E-03
Q6VWF1	O-methyltransferase (Fragment)	Low Abundance	6,8E-03
Q6VWF2	O-methyltransferase (Fragment)	Low Abundance	4,1E-03
Q6VWG5	O-methyltransferase	Low Abundance	2,9E-03
Q8S531	Cytosolic aldehyde	Low Abundance	1,1E-02

Protein	Annotation	Response to salt stress	ANOVA
	dehydrogenase RF2C		
Q9FER6	Putative legumain	Low Abundance	9,8E-04
Q9FRX0	Bundle sheath cell specific protein 1	Low Abundance	2,7E-02
A0A096PHD9	Uncharacterized protein (Fragment)	High Abundance	3,2E-02
A0A096PJN2	Uncharacterized protein	High Abundance	5,9E-03
A0A096PJN3	Uncharacterized protein	High Abundance	3,3E-02
A0A096PLW5	Uncharacterized protein	High Abundance	1,3E-03
A0A096PQ28	Uncharacterized protein	High Abundance	1,5E-02
A0A096PRG4	Uncharacterized protein	High Abundance	1,8E-04
A0A096PT43	Uncharacterized protein	High Abundance	8,7E-03
A0A096PV29	Uncharacterized protein	High Abundance	3,4E-02
A0A096PVU1	Uncharacterized protein	High Abundance	5,1E-04
A0A096PVU9	Uncharacterized protein	High Abundance	7,9E-03
A0A096PXW1	Uncharacterized protein	High Abundance	2,3E-02

Protein	Annotation	Response to salt stress	ANOVA
A0A096PZV4	Uncharacterized protein	High Abundance	1,2E-02
A0A096PZY0	Uncharacterized protein	High Abundance	1,4E-03
A0A096Q026	Uncharacterized protein	High Abundance	1,6E-02
A0A096Q2J6	Uncharacterized protein	High Abundance	3,0E-02
A0A096Q9I4	Uncharacterized protein	High Abundance	9,9E-04
A0A096QA70	Uncharacterized protein	High Abundance	2,7E-02
A0A096QCN9	Uncharacterized protein	High Abundance	1,9E-02
A0A096QGB9	Uncharacterized protein	High Abundance	1,5E-02
A0A096QGV4	Uncharacterized protein	High Abundance	2,7E-02
A0A096QHZ1	Uncharacterized protein	High Abundance	7,7E-03
A0A096QHZ4	Uncharacterized protein	High Abundance	1,1E-02
A0A096QRB1	Uncharacterized protein	High Abundance	1,6E-03
A0A096QU58	Uncharacterized protein	High Abundance	4,3E-02
A0A096QVG7	Uncharacterized protein	High Abundance	4,8E-02
A0A096QXB7	Uncharacterized protein	High Abundance	1,4E-04

Protein	Annotation	Response to salt stress	ANOVA
A0A096QYG0	Uncharacterized protein	High Abundance	1,5E-02
A0A096R1R9	Uncharacterized protein	High Abundance	3,7E-02
A0A096R2D3	Uncharacterized protein	High Abundance	1,7E-02
A0A096R2F4	Uncharacterized protein	High Abundance	7,0E-03
A0A096R557	Uncharacterized protein	High Abundance	2,4E-02
A0A096R718	Uncharacterized protein	High Abundance	1,4E-02
A0A096R8B3	Uncharacterized protein	High Abundance	1,6E-02
A0A096R8Z3	Uncharacterized protein	High Abundance	4,4E-03
A0A096RBC4	Uncharacterized protein	High Abundance	4,1E-03
A0A096RBX6	Uncharacterized protein	High Abundance	3,4E-02
A0A096RCF3	Uncharacterized protein	High Abundance	4,8E-02
A0A096RDT2	Uncharacterized protein	High Abundance	2,7E-02
A0A096RFZ7	Uncharacterized protein	High Abundance	1,4E-03
A0A096RM05	Uncharacterized protein	High Abundance	4,7E-02
A0A096RN78	Uncharacterized protein	High Abundance	2,9E-02

Protein	Annotation	Response to salt stress	ANOVA
A0A096RU40	Uncharacterized protein	High Abundance	2,5E-02
A0A096RUZ6	Uncharacterized protein	High Abundance	1,8E-02
A0A096RW01	Uncharacterized protein	High Abundance	3,3E-02
A0A096RX02	Uncharacterized protein	High Abundance	3,3E-02
A0A096RY70	Uncharacterized protein	High Abundance	3,9E-02
A0A096S0A2	Uncharacterized protein	High Abundance	3,8E-04
A0A096S105	Uncharacterized protein	High Abundance	1,3E-02
A0A096S1N9	Uncharacterized protein	High Abundance	4,4E-04
A0A096S4P4	Uncharacterized protein	High Abundance	1,4E-02
A0A096S5K1	Uncharacterized protein	High Abundance	7,6E-03
A0A096S7C2	Uncharacterized protein	High Abundance	1,4E-02
A0A096S842	Uncharacterized protein	High Abundance	3,3E-02
A0A096S9W1	Uncharacterized protein	High Abundance	2,6E-02
A0A096S9Y5	Uncharacterized protein	High Abundance	4,5E-03
A0A096SA71	Uncharacterized protein	High Abundance	3,1E-02

Protein	Annotation	Response to salt stress	ANOVA
A0A096SCH4	Uncharacterized protein	High Abundance	2,6E-02
A0A096SF47	Uncharacterized protein	High Abundance	8,9E-03
A0A096SHX1	Uncharacterized protein	High Abundance	1,6E-02
A0A096SI68	Uncharacterized protein	High Abundance	1,1E-04
A0A096SIT0	Uncharacterized protein	High Abundance	7,6E-04
A0A096SMR9	Uncharacterized protein	High Abundance	2,8E-03
A0A096SMS0	Uncharacterized protein	High Abundance	9,3E-04
A0A096ST25	Uncharacterized protein	High Abundance	2,3E-02
A0A096ST53	Uncharacterized protein	High Abundance	6,5E-03
A0A096SW39	Uncharacterized protein	High Abundance	5,7E-04
A0A096SWH3	Uncharacterized protein	High Abundance	8,1E-04
A0A096SXH3	Uncharacterized protein	High Abundance	3,9E-02
A0A096SXT9	Uncharacterized protein	High Abundance	4,0E-03
A0A096SXV5	Uncharacterized protein	High Abundance	2,1E-02
A0A096T094	Uncharacterized protein	High Abundance	1,2E-02

Protein	Annotation	Response to salt stress	ANOVA
A0A096T241	Uncharacterized protein	High Abundance	1,1E-02
A0A096T366	Glyceraldehyde -3-phosphate dehydrogenase 2, cytosolic	High Abundance	3,6E-03
A0A096T3E1	Uncharacterized protein	High Abundance	1,2E-02
A0A096T433	Uncharacterized protein	High Abundance	4,1E-03
A0A096T4D8	Uncharacterized protein	High Abundance	4,7E-03
A0A096T4N9	Uncharacterized protein	High Abundance	5,8E-03
A0A096T4U7	Uncharacterized protein	High Abundance	3,2E-02
A0A096T6C4	Uncharacterized protein	High Abundance	1,6E-02
A0A096T6L8	Uncharacterized protein	High Abundance	3,1E-02
A0A096T8M4	Uncharacterized protein	High Abundance	2,5E-03
A0A096T901	Uncharacterized protein	High Abundance	6,0E-03
A0A096T9R1	Histone H4	High Abundance	3,4E-02
A0A096TBT6	Uncharacterized protein	High Abundance	1,6E-02

Protein	Annotation	Response to salt stress	ANOVA
A0A096TEB2	Uncharacterized protein (Fragment)	High Abundance	4,9E-02
A0A096TEK8	Uncharacterized protein	High Abundance	1,1E-02
A0A096TIB6	Uncharacterized protein	High Abundance	5,5E-03
A0A096TP32	Uncharacterized protein	High Abundance	5,2E-03
A0A096TP60	Uncharacterized protein	High Abundance	1,5E-02
A0A096TQ81	Uncharacterized protein	High Abundance	1,3E-02
A0A096TRU3	Uncharacterized protein	High Abundance	1,0E-02
A0A096TS52	Uncharacterized protein	High Abundance	1,9E-02
A0A096TSJ8	Uncharacterized protein	High Abundance	9,0E-03
A0A096TUG3	Uncharacterized protein	High Abundance	4,8E-03
A0A096TUS3	Uncharacterized protein	High Abundance	8,6E-03
A0A096U2E6	Uncharacterized protein	High Abundance	4,0E-02
A0A096U669	Uncharacterized protein	High Abundance	1,0E-03
A0A096U7P6	Uncharacterized protein	High Abundance	8,4E-03

Protein	Annotation	Response to salt stress	ANOVA
A0A096U7Y9	Uncharacterized protein	High Abundance	3,5E-02
A0A096UCN0	Uncharacterized protein	High Abundance	8,1E-04
A0A096UDH7	Uncharacterized protein	High Abundance	2,3E-03
A0A096UDS3	Uncharacterized protein	High Abundance	3,2E-02
A0A096UE42	Uncharacterized protein	High Abundance	3,0E-02
A0A096UFY0	Uncharacterized protein	High Abundance	3,8E-03
A0A096UGP5	Uncharacterized protein	High Abundance	2,8E-02
A0A096UI88	Uncharacterized protein	High Abundance	2,1E-02
A1XCI0	Lipoxygenase	High Abundance	1,9E-02
A3FMB9	Proteasome subunit alpha type	High Abundance	2,3E-02
A5A5E7	Protein disulfide-isomerase	High Abundance	6,8E-04
B1PEY4	Superoxide dismutase [Cu-Zn]	High Abundance	1,5E-02
B3GQB5	Hexokinase	High Abundance	2,5E-02

Protein	Annotation	Response to salt stress	ANOVA
B4F840	Uncharacterized protein	High Abundance	2,8E-02
B4F8V9	T-complex protein 1 subunit delta	High Abundance	1,2E-02
B4F957	Uncharacterized protein	High Abundance	3,0E-03
B4F9G0	Uncharacterized protein	High Abundance	1,6E-03
B4F9G1	Aspartate aminotransferase	High Abundance	7,0E-03
B4F9G6	60S ribosomal protein L6	High Abundance	8,5E-04
B4F9M6	Uncharacterized protein	High Abundance	2,6E-02
B4F9S7	Uncharacterized protein	High Abundance	4,4E-02
B4F9X0	Alpha-galactosidase	High Abundance	7,0E-03
B4FA06	APx4-Peroxisomal Ascorbate Peroxidase	High Abundance	4,8E-03
B4FA27	Alpha-galactosidase	High Abundance	1,6E-02
B4FA76	Dolichyl-diphosphooligosaccharide--protein	High Abundance	4,0E-02

Protein	Annotation	Response to salt stress	ANOVA
	glycosyltransferase 48 kDa subunit		
B4FAE5	Uncharacterized protein	High Abundance	1,7E-02
B4FAE6	Pyrophosphate-fructose 6-phosphate 1-phosphotransferase subunit alpha	High Abundance	7,3E-03
B4FAF8	Uncharacterized protein	High Abundance	3,6E-02
B4FAL9	Fructose-bisphosphate aldolase	High Abundance	4,2E-02
B4FAM6	Uncharacterized protein	High Abundance	3,4E-03
B4FAR8	Proteasome subunit alpha type	High Abundance	1,6E-02
B4FAV3	40S ribosomal protein S3a	High Abundance	5,5E-03
B4FBM9	Uncharacterized protein	High Abundance	3,6E-03
B4FBV8	Eukaryotic translation initiation factor 3 subunit G	High Abundance	2,1E-02

Protein	Annotation	Response to salt stress	ANOVA
B4FBY6	Uncharacterized protein	High Abundance	2,8E-02
B4FCG9	60S ribosomal protein L11-1	High Abundance	7,5E-03
B4FD74	Uncharacterized protein	High Abundance	2,1E-02
B4FD90	40S ribosomal protein S19	High Abundance	2,6E-02
B4FDT0	40S ribosomal protein S20	High Abundance	4,6E-02
B4FEF4	Uncharacterized protein	High Abundance	5,8E-03
B4FFA7	Enoyl-[acyl-carrier-protein] reductase isoform 1	High Abundance	3,1E-02
B4FFZ3	Uncharacterized protein	High Abundance	2,1E-03
B4FFZ7	Uncharacterized protein	High Abundance	4,1E-02
B4FGL4	60S ribosomal protein L23	High Abundance	1,7E-03
B4FGL9	60S ribosomal protein L11-1	High Abundance	7,3E-03
B4FHH2	Uncharacterized protein	High Abundance	1,3E-02
B4FHH4	Triosephosphate isomerase	High Abundance	3,2E-02
B4FHT1	Annexin	High Abundance	2,8E-03

Protein	Annotation	Response to salt stress	ANOVA
B4FI86	Proteasome subunit beta type	High Abundance	8,0E-03
B4FJ27	40S ribosomal protein S24	High Abundance	3,3E-02
B4FK84	Uncharacterized protein	High Abundance	1,4E-03
B4FL28	Uncharacterized protein	High Abundance	2,7E-03
B4FLB0	Uncharacterized protein	High Abundance	1,1E-03
B4FLJ3	Isocitrate dehydrogenase [NADP]	High Abundance	2,4E-02
B4FMI5	40S ribosomal protein S4	High Abundance	5,7E-03
B4FMS7	Mitochondrial prohibitin complex protein 2	High Abundance	2,6E-02
B4FN17	USP family protein	High Abundance	5,9E-03
B4FN19	Uncharacterized protein	High Abundance	1,8E-02
B4FN24	Peroxiredoxin-5	High Abundance	3,1E-02
B4FNN9	Uncharacterized protein	High Abundance	3,6E-02
B4FPB7	60S ribosomal protein L7a	High Abundance	3,0E-02

Protein	Annotation	Response to salt stress	ANOVA
B4FQC2	Uncharacterized protein	High Abundance	2,8E-02
B4FQI3	NADH-ubiquinone oxidoreductase B16.6 subunit	High Abundance	3,3E-02
B4FQK0	Uncharacterized protein	High Abundance	3,2E-03
B4FQY1	Pathogeneis protein1	High Abundance	1,6E-02
B4FQZ2	Uncharacterized protein	High Abundance	1,1E-02
B4FRC6	Uncharacterized protein	High Abundance	5,6E-03
B4FRC9	Transaldolase 2	High Abundance	3,0E-03
B4FRF0	Glutathione peroxidase	High Abundance	8,0E-03
B4FRG1	14-3-3-like protein	High Abundance	4,3E-02
B4FRM7	60S ribosomal protein L12	High Abundance	2,5E-02
B4FSV6	6-phosphogluconate dehydrogenase, decarboxylating	High Abundance	1,3E-02
B4FT85	Isochorismate synthase 1	High Abundance	2,5E-02

Protein	Annotation	Response to salt stress	ANOVA
B4FTS6	Uncharacterized protein	High Abundance	3,5E-02
B4FU56	Uncharacterized protein	High Abundance	2,1E-03
B4FUR2	Uncharacterized protein	High Abundance	9,8E-03
B4FUS2	40S ribosomal protein S18	High Abundance	7,9E-04
B4FUT3	Germin-like protein subfamily 1 member 17	High Abundance	1,3E-03
B4FVB2	Elongation factor Tu	High Abundance	4,1E-02
B4FVP5	Uncharacterized protein	High Abundance	1,3E-02
B4FWN1	NADPH quinone oxidoreductase 2	High Abundance	4,6E-02
B4FWP0	Fructose-bisphosphate aldolase	High Abundance	2,1E-02
B4FY16	Elongation factor 1-alpha	High Abundance	3,2E-03
B4FY74	Retrotransposon protein Ty1-copia subclass	High Abundance	2,0E-02
B4G019	Uncharacterized protein	High Abundance	1,9E-04

Protein	Annotation	Response to salt stress	ANOVA
B4G043	Uncharacterized protein	High Abundance	2,8E-04
B4G082	Rab GDP dissociation inhibitor alpha	High Abundance	2,1E-02
B4G087	Uncharacterized protein	High Abundance	3,7E-04
B4G0F3	Probable bifunctional methylthioribulose-1-phosphate dehydratase/enolase-phosphatase E1	High Abundance	1,0E-03
B4G0K5	Uncharacterized protein	High Abundance	3,1E-04
B4G0S0	Uncharacterized protein	High Abundance	3,2E-02
B4G1C2	Uncharacterized protein	High Abundance	1,1E-04
B4G1D2	CBS domain protein	High Abundance	2,3E-03
B4G1T3	Uncharacterized protein	High Abundance	1,6E-02
B4G1Y5	Uncharacterized protein	High Abundance	4,6E-02
B4G233	Disease resistance response protein 206	High Abundance	1,3E-03

Protein	Annotation	Response to salt stress	ANOVA
B4G286	40S ribosomal protein S18	High Abundance	1,0E-03
B6SH12	Uncharacterized protein	High Abundance	1,2E-02
B6SHW0	60S ribosomal protein L6	High Abundance	1,1E-04
B6SHX8	Putative uncharacterized protein	High Abundance	9,0E-03
B6SIG5	Triosephosphate isomerase	High Abundance	1,0E-02
B6SII4	40S ribosomal protein S15	High Abundance	2,2E-02
B6SII7	40S ribosomal protein S15	High Abundance	4,1E-02
B6SIL5	40S ribosomal protein S11	High Abundance	9,5E-03
B6SIP4	40S ribosomal protein S26	High Abundance	5,6E-03
B6SJ08	60S ribosomal protein L18	High Abundance	1,6E-02
B6SJC1	RALF	High Abundance	7,4E-03
B6SK79	60S ribosomal protein L4	High Abundance	3,0E-03
B6SKA7	Elongation factor 1-alpha	High Abundance	3,6E-03
B6SKN3	1,2-dihydroxy-3-keto-5-	High Abundance	1,1E-02

Protein	Annotation	Response to salt stress	ANOVA
	methylthiopentene dioxygenase		
B6SMQ5	Triosephosphate isomerase	High Abundance	8,6E-03
B6SPI9	60S ribosomal protein L38	High Abundance	3,9E-02
B6SPZ2	Glyceraldehyde-3-phosphate dehydrogenase	High Abundance	1,3E-02
B6SQE5	BRASSINOSTEROID INSENSITIVE 1-associated receptor kinase 1	High Abundance	1,1E-03
B6SS21	Dehydrin COR410	High Abundance	1,6E-02
B6SWN1	2-isopropylmalate synthase B	High Abundance	6,8E-03
B6SWX0	Ribosomal protein L15	High Abundance	3,2E-02
B6SZD1	Mitochondrial import receptor subunit TOM20	High Abundance	3,1E-02
B6T188	40S ribosomal protein S26	High Abundance	2,6E-02
B6T267	Ribosomal protein L15	High Abundance	2,3E-02

Protein	Annotation	Response to salt stress	ANOVA
B6T281	40S ribosomal protein S14	High Abundance	6,5E-03
B6T2A5	40S ribosomal protein S11	High Abundance	6,3E-03
B6T2S0	26S protease regulatory subunit 4	High Abundance	2,6E-03
B6T2Y1	Peroxiredoxin-5	High Abundance	8,4E-03
B6T315	Jasmonate-induced protein	High Abundance	4,2E-02
B6T3G4	40S ribosomal protein S19	High Abundance	1,6E-02
B6T3P5	Glutamine synthetase	High Abundance	8,3E-03
B6T4Q5	Pro-resilin	High Abundance	1,7E-03
B6T5I0	Replication factor C subunit 5	High Abundance	1,1E-02
B6T5R1	Ran-binding protein 1	High Abundance	1,6E-02
B6T6G1	60S ribosomal protein L12	High Abundance	2,5E-02
B6T6W2	40S ribosomal protein S15	High Abundance	2,4E-02
B6T7A4	Glyceraldehyde -3-phosphate dehydrogenase	High Abundance	3,1E-03

Protein	Annotation	Response to salt stress	ANOVA
B6T7G7	Elongation factor 1-gamma 3	High Abundance	1,6E-03
B6T7L9	14-3-3-like protein	High Abundance	4,7E-02
B6T831	60S ribosomal protein L37a	High Abundance	3,7E-02
B6T872	60S ribosomal protein L32	High Abundance	4,0E-02
B6T8M9	Mitochondrial prohibitin complex protein 2	High Abundance	2,2E-02
B6T8R5	60S ribosomal protein L34	High Abundance	1,3E-03
B6T969	Proteasome subunit alpha type	High Abundance	3,6E-02
B6T9W1	Wound/stress protein	High Abundance	9,4E-04
B6TD69	40S ribosomal protein S17-4	High Abundance	1,0E-02
B6TDT6	Methylthioribose kinase	High Abundance	3,7E-03
B6TE40	60S ribosomal protein L22-2	High Abundance	1,5E-02
B6TG61	40S ribosomal protein S16	High Abundance	1,2E-03
B6TGG7	3-oxoacyl-[acyl-carrier-	High Abundance	1,3E-02

Protein	Annotation	Response to salt stress	ANOVA
	protein] synthase		
B6TH42	60S ribosomal protein L9	High Abundance	7,8E-03
B6THZ8	Threonine synthase	High Abundance	2,2E-02
B6TKY3	Putative TCP-1/cpn60 chaperonin family protein	High Abundance	4,7E-02
B6TLX2	Fiber protein Fb15	High Abundance	2,6E-02
B6TM55	APx1-Cytosolic Ascorbate Peroxidase	High Abundance	3,9E-02
B6TMP6	60 ribosomal protein L14	High Abundance	8,5E-03
B6TN41	4-hydroxy-4-methyl-2-oxoglutarate aldolase	High Abundance	8,6E-03
B6TRR5	Formate dehydrogenase 1	High Abundance	6,3E-05
B6TS84	Transaldolase 2	High Abundance	5,7E-03
B6TT93	Annexin A4	High Abundance	5,0E-02
B6TV55	Stem 28 kDa glycoprotein	High Abundance	1,3E-02

Protein	Annotation	Response to salt stress	ANOVA
B6TWH9	Rhicadhesin receptor	High Abundance	4,1E-02
B6TWN7	Elongation factor 1-alpha	High Abundance	1,3E-02
B6TX10	6-phosphogluconate dehydrogenase, decarboxylating	High Abundance	9,4E-04
B6TY76	Elongation factor 1-gamma 2	High Abundance	1,3E-02
B6U0S1	Elongation factor 2	High Abundance	2,7E-02
B6U297	Lipoxygenase	High Abundance	9,4E-04
B6U4D9	Protein ROOT HAIR DEFECTIVE 3 homolog	High Abundance	1,4E-02
B6U6S4	Heat shock protein STI	High Abundance	4,6E-02
B6U6W0	Peroxidase	High Abundance	1,6E-03
B6U7P4	Nonspecific lipid-transfer protein AKCS9	High Abundance	2,8E-02
B6UB73	APx1-Cytosolic Ascorbate Peroxidase	High Abundance	3,6E-02

Protein	Annotation	Response to salt stress	ANOVA
B6UE01	40S ribosomal protein S29	High Abundance	1,4E-02
B6UE23	60S ribosomal protein L18a	High Abundance	1,6E-02
B6UE29	60S ribosomal protein L18a	High Abundance	4,5E-03
B6UFY5	60S ribosomal protein L9	High Abundance	9,2E-03
B6UGQ9	Rhicadhesin receptor	High Abundance	2,6E-02
B6UGR9	60S ribosomal protein L10-3	High Abundance	2,7E-02
B6UH57	40S ribosomal protein S17-4	High Abundance	3,0E-02
B6UHJ4	Elongation factor 1-alpha	High Abundance	3,0E-03
B8A095	Uncharacterized protein	High Abundance	4,8E-02
B8A193	Uncharacterized protein	High Abundance	1,3E-02
B8A377	Cysteine synthase	High Abundance	9,5E-03
C0HE15	Uncharacterized protein	High Abundance	3,0E-02
C0HFM4	Uncharacterized protein	High Abundance	5,3E-03
C0HFU7	Phospholipase D	High Abundance	7,2E-04

Protein	Annotation	Response to salt stress	ANOVA
C0HGT5	T-complex protein 1 subunit delta	High Abundance	2,6E-02
C0HHC4	Nucleoside diphosphate kinase	High Abundance	4,9E-04
C0P2K9	Uncharacterized protein	High Abundance	8,4E-04
C0P3Q1	Uncharacterized protein	High Abundance	2,0E-02
C0P455	Uncharacterized protein	High Abundance	9,7E-04
C0P7L2	Eukaryotic translation initiation factor 3 subunit E	High Abundance	3,2E-02
C0P840	Lipoxygenase	High Abundance	3,4E-04
C0P8I4	2-isopropylmalate synthase B	High Abundance	7,3E-03
C0P9J6	Aminoaldehyde dehydrogenase 1	High Abundance	3,1E-02
C0PBH7	Ribose-5-phosphate isomerase	High Abundance	1,6E-02
C0PBY7	Nucleoside diphosphate kinase	High Abundance	7,5E-03

Protein	Annotation	Response to salt stress	ANOVA
C0PC61	Transaldolase 2	High Abundance	1,0E-02
C0PC62	Uncharacterized protein	High Abundance	3,7E-02
C0PCV2	40S ribosomal protein S8	High Abundance	3,4E-03
C0PEP6	Peroxidase	High Abundance	1,6E-04
C0PGM6	Uncharacterized protein	High Abundance	1,2E-02
C0PHB0	2-oxoglutarate dehydrogenase E1 component	High Abundance	9,5E-03
C0PHV6	Uncharacterized protein	High Abundance	2,8E-02
C0PI00	Uncharacterized protein	High Abundance	5,6E-03
C0PK59	Uncharacterized protein	High Abundance	1,0E-02
C0PLF0	Protein disulfide-isomerase	High Abundance	1,9E-02
C0PMC5	Uncharacterized protein	High Abundance	1,8E-04
C0PNM8	Cytochrome b-c1 complex subunit 7	High Abundance	1,5E-02
C0RWW9	Ameiotic 1	High Abundance	3,2E-02

Protein	Annotation	Response to salt stress	ANOVA
C4IYM8	Uncharacterized protein	High Abundance	2,3E-02
C4J3S6	Uncharacterized protein	High Abundance	5,7E-03
C4J5Y0	Protein binding protein	High Abundance	0,0E+00
C4J6K9	Rab GDP dissociation inhibitor alpha	High Abundance	1,8E-02
C4J9Y2	Uncharacterized protein	High Abundance	2,8E-05
C4JA47	Elongation factor 1-alpha	High Abundance	3,0E-03
C4JBF5	60S ribosomal protein L9, mRNA	High Abundance	5,0E-03
C4JBS8	Glyceraldehyde -3-phosphate dehydrogenase	High Abundance	1,2E-02
D9IZY9	Pathogenesis-related protein 5	High Abundance	3,0E-02
F2YHN5	Glyceraldehyde -3-phosphate dehydrogenase	High Abundance	1,4E-02
K7TGW6	Putative polyphenol oxidase family protein	High Abundance	7,6E-03
K7TNK3	Uncharacterized protein	High Abundance	2,4E-02

Protein	Annotation	Response to salt stress	ANOVA
K7TSQ4	Carboxypeptidase	High Abundance	1,9E-03
K7TT73	40S ribosomal protein S3	High Abundance	4,8E-03
K7TVZ1	6-phosphogluconate dehydrogenase, decarboxylating	High Abundance	7,9E-04
K7TYG5	40S ribosomal protein S8	High Abundance	1,7E-02
K7U473	Uncharacterized protein	High Abundance	1,3E-02
K7U5W7	Uncharacterized protein	High Abundance	1,0E-03
K7UB20	Uncharacterized protein	High Abundance	1,2E-02
K7UCZ5	Stromal heat shock protein	High Abundance	1,7E-02
K7UEU8	Uncharacterized protein	High Abundance	4,4E-02
K7UH13	Uncharacterized protein	High Abundance	4,7E-02
K7UJJ8	Uncharacterized protein	High Abundance	2,4E-02
K7UQT7	Elongation factor 1-gamma 2	High Abundance	1,0E-02
K7UT72	Catalase	High Abundance	1,1E-05

Protein	Annotation	Response to salt stress	ANOVA
K7UXK5	Putative alcohol dehydrogenase superfamily protein	High Abundance	2,1E-03
K7UY19	Fructose-bisphosphate aldolase	High Abundance	4,8E-02
K7UY44	Nucleoside diphosphate kinase	High Abundance	3,8E-02
K7UZN5	Putative oxidoreductase, aldo/keto reductase family protein	High Abundance	8,4E-03
K7V067	Isocitrate dehydrogenase [NADP]	High Abundance	2,1E-02
K7V0F3	Uncharacterized protein	High Abundance	2,1E-02
K7V0N8	Putative ribosomal protein S4 (RPS4A) family protein	High Abundance	9,5E-03
K7V106	Phosphoglycerate kinase	High Abundance	1,8E-02
K7V1I3	Uncharacterized protein	High Abundance	1,1E-02

Protein	Annotation	Response to salt stress	ANOVA
K7V228	Uncharacterized protein	High Abundance	3,4E-03
K7V2Q5	Uncharacterized protein (Fragment)	High Abundance	1,1E-02
K7V5H4	Phosphoenolpyruvate carboxylase isoform 1	High Abundance	2,9E-03
K7VDI6	Peroxidase	High Abundance	1,7E-02
K7VDR8	Shrunken1 isoform 1	High Abundance	6,0E-03
K7VE57	Putative peptidase C48 domain family protein	High Abundance	1,3E-02
K7VG47	Uncharacterized protein	High Abundance	2,3E-02
K7VG53	Uncharacterized protein	High Abundance	2,3E-02
K7VH58	Peroxidase	High Abundance	1,4E-02
K7VIK9	Uncharacterized protein	High Abundance	1,5E-02
K7VJC3	Uncharacterized protein	High Abundance	2,3E-02
K7VQ65	Putative translation elongation	High Abundance	2,0E-02

Protein	Annotation	Response to salt stress	ANOVA
	factor family protein		
K7VQG5	Phospholipase D	High Abundance	2,3E-03
K7VVT1	Putative translation elongation factor Tu family protein isoform 1	High Abundance	2,5E-04
K7VZH5	Uncharacterized protein	High Abundance	8,4E-04
M1H246	Lipoxygenase (Fragment)	High Abundance	1,4E-02
M1H272	Lipoxygenase (Fragment)	High Abundance	1,3E-02
M1H6T5	Lipoxygenase (Fragment)	High Abundance	2,6E-03
O22453	40S ribosomal protein S4	High Abundance	3,7E-03
O50018	Elongation factor 1-alpha	High Abundance	2,7E-03
O81217	Bowman-Birk type bran trypsin inhibitor	High Abundance	5,6E-03
O82086	Pathogenesis related protein-1	High Abundance	1,3E-02
P12365	Catalase isozyme 2	High Abundance	3,3E-04

Protein	Annotation	Response to salt stress	ANOVA
P29185	Chaperonin CPN60-1, mitochondrial	High Abundance	4,8E-03
Q0PCF2	Deoxymugineic acid synthase1	High Abundance	1,8E-02
Q3S3T0	Hemoglobin 2	High Abundance	2,1E-03
Q42420	Proteinase inhibitor	High Abundance	1,2E-02
Q43298	Chaperonin CPN60-2, mitochondrial	High Abundance	8,2E-03
Q4W1F7	Thioredoxin	High Abundance	4,5E-02
Q5EUE1	Protein disulfide-isomerase	High Abundance	7,5E-04
Q6JAH6	Glutathione peroxidase	High Abundance	1,5E-03
Q7FS88	Glutathione peroxidase	High Abundance	8,9E-03
Q84TL6	Legumin-like protein	High Abundance	3,0E-04
Q8L5G8	Hexokinase	High Abundance	1,4E-02
Q8W0V2	Lipoxygenase	High Abundance	6,2E-03
Q9FYS5	High mobility group I/Y-2	High Abundance	2,5E-03

Protein	Annotation	Response to salt stress	ANOVA
Q9M7E0	Elongation factor 1-alpha	High Abundance	2,7E-03
Q9M7E1	Elongation factor 1-alpha	High Abundance	1,2E-02
Q9M7E2	Elongation factor 1-alpha	High Abundance	9,1E-05
Q9M7E3	Elongation factor 1-alpha	High Abundance	1,6E-02
Q9M7E5	Elongation factor 1-alpha	High Abundance	2,7E-03
Q9SAZ6	Phosphoenolpyruvate carboxylase	High Abundance	2,8E-03
Q9SM20	Glutathione transferase III(B)	High Abundance	6,6E-04
Q9ZTT0	6-phosphogluconate dehydrogenase isoenzyme B (Fragment)	High Abundance	4,4E-02
A0A060D6M0	OFP transcription factor (Fragment)		
A0A068EY47	Wound-induced serine protease inhibitor-1		

Protein	Annotation	Response to salt stress	ANOVA
A0A075T3E7	Pyrabactin resistance-like protein		
A0A096PGC6	Uncharacterized protein		
A0A096PHN7	Uncharacterized protein		
A0A096PI14	Uncharacterized protein		
A0A096PII0	Uncharacterized protein		
A0A096PIX9	Uncharacterized protein		
A0A096PJC5	Uncharacterized protein		
A0A096PJG1	Uncharacterized protein		
A0A096PKY4	Uncharacterized protein		
A0A096PL51	Uncharacterized protein		
A0A096PLJ0	Uncharacterized protein		
A0A096PLU3	Uncharacterized protein		
A0A096PMM2	Uncharacterized protein		
A0A096PN03	Uncharacterized protein		

Protein	Annotation	Response to salt stress	ANOVA
A0A096PNR5	Uncharacterized protein		
A0A096PNV5	Uncharacterized protein		
A0A096PPA4	Uncharacterized protein		
A0A096PPW5	Uncharacterized protein		
A0A096PPZ7	Uncharacterized protein		
A0A096PQS4	Uncharacterized protein		
A0A096PQX5	Uncharacterized protein		
A0A096PQY2	Uncharacterized protein		
A0A096PR13	Uncharacterized protein		
A0A096PRE7	Uncharacterized protein		
A0A096PRZ1	Uncharacterized protein		
A0A096PSR5	Uncharacterized protein		
A0A096PTJ4	Uncharacterized protein		
A0A096PTL0	Uncharacterized protein		

Protein	Annotation	Response to salt stress	ANOVA
A0A1D6NQF3	α-L-arabinofuranosidase 1		
A0A096PTM0	Uncharacterized protein		
A0A096PTR6	Uncharacterized protein		
A0A096PU41	Uncharacterized protein		
A0A096PU61	Uncharacterized protein		
A0A096PUN1	Uncharacterized protein		
A0A096PUR6	Uncharacterized protein		
A0A096PUW8	Uncharacterized protein		
A0A096PUW9	Uncharacterized protein		
A0A096PVP6	Uncharacterized protein (Fragment)		
A0A096PVU4	Uncharacterized protein		
A0A096PW86	Uncharacterized protein		
A0A096PWY3	Uncharacterized protein		
A0A096PX16	Uncharacterized protein		

Protein	Annotation	Response to salt stress	ANOVA
A0A096PYB0	Uncharacterized protein		
A0A096PYB4	Uncharacterized protein		
A0A096PYL3	Uncharacterized protein		
A0A096PYV1	Uncharacterized protein		
A0A096PZ49	Uncharacterized protein		
A0A096PZ84	Uncharacterized protein		
A0A096PZA7	Uncharacterized protein		
A0A096PZT8	Uncharacterized protein		
A0A096Q0G2	Uncharacterized protein		
A0A096Q0H4	Uncharacterized protein		
A0A096Q0T1	Uncharacterized protein		
A0A096Q0T5	Uncharacterized protein		
A0A096Q0U1	Uncharacterized protein		
A0A096Q155	Uncharacterized protein		
A0A096Q1E4	Uncharacterized protein		

Protein	Annotation	Response to salt stress	ANOVA
A0A096Q1Q2	Uncharacterized protein		
A0A096Q1S0	Uncharacterized protein		
A0A096Q1Z5	Uncharacterized protein		
A0A096Q277	Uncharacterized protein		
A0A096Q2C3	Uncharacterized protein		
A0A096Q2E3	Uncharacterized protein		
A0A096Q2Y1	Uncharacterized protein		
A0A096Q3J8	Uncharacterized protein		
A0A096Q3L3	Uncharacterized protein		
A0A096Q4Q2	Uncharacterized protein		
A0A096Q560	Uncharacterized protein		
A0A096Q5Z9	Uncharacterized protein		
A0A096Q7L4	Uncharacterized protein		
A0A096Q7P7	Uncharacterized protein		
A0A096Q7T7	Uncharacterized protein		

Protein	Annotation	Response to salt stress	ANOVA
A0A096Q7U7	Uncharacterized protein		
A0A096Q7W9	Uncharacterized protein		
A0A096Q7Z0	Uncharacterized protein		
A0A096Q886	Eukaryotic translation initiation factor 3 subunit I		
A0A096Q8J4	Uncharacterized protein		
A0A096Q8N1	Uncharacterized protein		
A0A096Q8R5	Uncharacterized protein		
A0A096Q8S3	Uncharacterized protein		
A0A096Q8V2	Uncharacterized protein		
A0A096Q911	Uncharacterized protein		
A0A096Q9E6	Uncharacterized protein		
A0A096Q9I5	Uncharacterized protein		
A0A096QA09	Uncharacterized protein		
A0A096QA11	Uncharacterized protein		

Protein	Annotation	Response to salt stress	ANOVA
A0A096QA17	Uncharacterized protein		
A0A096QAJ4	Uncharacterized protein		
A0A096QAP5	Uncharacterized protein		
A0A096QB18	Uncharacterized protein		
A0A096QB80	Uncharacterized protein		
A0A096QB86	Uncharacterized protein		
A0A096QBL2	Uncharacterized protein		
A0A096QBQ1	Uncharacterized protein		
A0A096QCL2	Uncharacterized protein		
A0A096QCP1	Uncharacterized protein		
A0A096QCP6	Uncharacterized protein		
A0A096QCT4	Uncharacterized protein		
A0A096QCW0	Uncharacterized protein		
A0A096QD90	Uncharacterized protein		
A0A096QDJ2	Uncharacterized protein		

Protein	Annotation	Response to salt stress	ANOVA
A0A096QE21	Uncharacterized protein		
A0A096QE36	Uncharacterized protein		
A0A096QEM9	Uncharacterized protein		
A0A096QEP1	Uncharacterized protein		
A0A096QEY4	Uncharacterized protein		
A0A096QEZ3	Uncharacterized protein		
A0A096QF11	Uncharacterized protein		
A0A096QFD4	Uncharacterized protein		
A0A096QFM0	Uncharacterized protein		
A0A096QG41	Uncharacterized protein		
A0A096QGN4	Uncharacterized protein		
A0A096QGZ5	Uncharacterized protein		
A0A096QHC2	Uncharacterized protein		
A0A096QHE8	Uncharacterized protein		
A0A096QHG8	Uncharacterized protein		

Protein	Annotation	Response to salt stress	ANOVA
A0A096QHH6	Uncharacterized protein		
A0A096QIC5	Uncharacterized protein		
A0A096QID4	Uncharacterized protein		
A0A096QIN9	Uncharacterized protein		
A0A096QIX5	Uncharacterized protein		
A0A096QJN8	Uncharacterized protein		
A0A096QJW6	Uncharacterized protein		
A0A096QK58	Uncharacterized protein		
A0A096QK67	Uncharacterized protein		
A0A096QM72	Uncharacterized protein		
A0A096QMF4	Uncharacterized protein		
A0A096QMX5	Uncharacterized protein		
A0A096QN00	Uncharacterized protein		
A0A096QN84	Uncharacterized protein		
A0A096QNL6	Uncharacterized protein		

Protein	Annotation	Response to salt stress	ANOVA
A0A096QP96	Uncharacterized protein		
A0A096QQ79	Uncharacterized protein		
A0A096QQB3	Uncharacterized protein		
A0A096QQE3	Uncharacterized protein		
A0A096QRB6	Uncharacterized protein		
A0A096QRH2	Uncharacterized protein		
A0A096QRL3	Uncharacterized protein		
A0A096QRU9	Uncharacterized protein		
A0A096QRX1	Uncharacterized protein (Fragment)		
A0A096QS54	Uncharacterized protein		
A0A096QS88	Uncharacterized protein		
A0A096QSH9	Uncharacterized protein		
A0A096QSW5	Uncharacterized protein		
A0A096QSZ4	Uncharacterized protein		

Protein	Annotation	Response to salt stress	ANOVA
A0A096QTG7	Uncharacterized protein		
A0A096QTK8	Uncharacterized protein		
A0A096QU37	Uncharacterized protein		
A0A096QUH4	Uncharacterized protein		
A0A096QUK2	Uncharacterized protein		
A0A096QV19	Uncharacterized protein		
A0A096QV77	Uncharacterized protein		
A0A096QVH3	Uncharacterized protein		
A0A096QVU7	Uncharacterized protein		
A0A096QW50	Uncharacterized protein		
A0A096QWG0	Uncharacterized protein		
A0A096QXN0	Uncharacterized protein		
A0A096QY04	Uncharacterized protein		
A0A096QY45	Uncharacterized protein		

Protein	Annotation	Response to salt stress	ANOVA
A0A096QY80	60S acidic ribosomal protein P0		
A0A096QYR1	Uncharacterized protein		
A0A096QYW3	Uncharacterized protein		
A0A096QZC1	Uncharacterized protein		
A0A096QZM3	Uncharacterized protein		
A0A096R049	Uncharacterized protein		
A0A096R091	Uncharacterized protein		
A0A096R0C8	Uncharacterized protein		
A0A096R0R6	Uncharacterized protein		
A0A096R0U2	Uncharacterized protein		
A0A096R0Z5	Uncharacterized protein		
A0A096R286	Uncharacterized protein		
A0A096R2K8	Uncharacterized protein		
A0A096R2T3	Uncharacterized protein		

Protein	Annotation	Response to salt stress	ANOVA
A0A096R3F8	Uncharacterized protein		
A0A096R3P4	Uncharacterized protein		
A0A096R3R9	Uncharacterized protein		
A0A096R4G6	Uncharacterized protein		
A0A096R4T9	Uncharacterized protein		
A0A096R4Z4	Uncharacterized protein		
A0A096R584	Uncharacterized protein		
A0A096R5Q2	Uncharacterized protein		
A0A096R5Q4	Uncharacterized protein		
A0A096R5S6	Uncharacterized protein		
A0A096R5Y3	Uncharacterized protein		
A0A096R6A1	Uncharacterized protein		
A0A096R6P3	Uncharacterized protein		
A0A096R6Z8	Uncharacterized protein		
A0A096R737	Uncharacterized protein		

Protein	Annotation	Response to salt stress	ANOVA
A0A096R8F6	Uncharacterized protein		
A0A096R8K8	Uncharacterized protein		
A0A096R8S9	Uncharacterized protein		
A0A096R949	Uncharacterized protein		
A0A096R999	Uncharacterized protein		
A0A096R9A2	Uncharacterized protein		
A0A096R9Y2	Uncharacterized protein		
A0A096R9Y9	Uncharacterized protein		
A0A096RA51	Uncharacterized protein		
A0A096RAD6	Uncharacterized protein		
A0A096RAH6	Uncharacterized protein		
A0A096RAK1	Uncharacterized protein		
A0A096RAP0	Uncharacterized protein		
A0A096RBP1	Uncharacterized protein		
A0A096RBS9	Uncharacterized protein		

Protein	Annotation	Response to salt stress	ANOVA
A0A096RCQ8	Uncharacterized protein		
A0A096RD23	Uncharacterized protein		
A0A096RD67	Uncharacterized protein		
A0A096RDN9	Uncharacterized protein		
A0A096RDV2	Uncharacterized protein		
A0A096RDV7	Uncharacterized protein		
A0A096RE30	Uncharacterized protein		
A0A096REA7	Uncharacterized protein		
A0A096RF31	Uncharacterized protein		
A0A096RF87	Uncharacterized protein		
A0A096RG34	Uncharacterized protein		
A0A096RG76	Uncharacterized protein		
A0A096RGH5	Uncharacterized protein		
A0A096RGH6	Uncharacterized protein		
A0A096RGK0	Uncharacterized protein		

Protein	Annotation	Response to salt stress	ANOVA
A0A096RGR3	Uncharacterized protein		
A0A096RH42	Uncharacterized protein (Fragment)		
A0A096RH49	Uncharacterized protein		
A0A096RH70	Uncharacterized protein		
A0A096RH94	Uncharacterized protein		
A0A096RH95	Elongation factor Ts, mitochondrial		
A0A096RHA4	Uncharacterized protein		
A0A096RHR4	Uncharacterized protein		
A0A096RHZ5	Uncharacterized protein		
A0A096RHZ7	Uncharacterized protein		
A0A096RI70	Uncharacterized protein		
A0A096RIA9	Uncharacterized protein		
A0A096RIC1	Uncharacterized protein		

Protein	Annotation	Response to salt stress	ANOVA
A0A096RIM2	Uncharacterized protein (Fragment)		
A0A096RJ27	Uncharacterized protein		
A0A096RJY3	Uncharacterized protein		
A0A096RLA7	Uncharacterized protein		
A0A096RLJ6	Uncharacterized protein		
A0A096RLJ7	Uncharacterized protein		
A0A096RLR4	Uncharacterized protein		
A0A096RLS0	Uncharacterized protein		
A0A096RLT4	Uncharacterized protein		
A0A096RM44	Uncharacterized protein		
A0A096RME9	Uncharacterized protein		
A0A096RN19	Uncharacterized protein		
A0A096RN21	Uncharacterized protein		
A0A096RN43	Uncharacterized protein		

Protein	Annotation	Response to salt stress	ANOVA
A0A096RNV3	Uncharacterized protein		
A0A096RP46	Uncharacterized protein		
A0A096RQ32	Uncharacterized protein		
A0A096RQ47	Uncharacterized protein		
A0A096RQ70	Uncharacterized protein		
A0A096RQE2	Uncharacterized protein		
A0A096RQS3	Uncharacterized protein		
A0A096RQT3	Uncharacterized protein		
A0A096RQW0	Translationally-controlled tumor protein homolog		
A0A096RR57	Uncharacterized protein		
A0A096RRJ2	Uncharacterized protein		
A0A096RRN7	Uncharacterized protein		
A0A096RS36	Uncharacterized protein		
A0A096RSF2	Uncharacterized protein		

Protein	Annotation	Response to salt stress	ANOVA
A0A096RSI2	Uncharacterized protein		
A0A096RSM5	Uncharacterized protein		
A0A096RT08	Uncharacterized protein		
A0A096RT35	Uncharacterized protein		
A0A096RTH6	Uncharacterized protein		
A0A096RTN1	Uncharacterized protein		
A0A096RU09	Uncharacterized protein		
A0A096RU64	Uncharacterized protein		
A0A096RUJ4	Uncharacterized protein		
A0A096RW35	Uncharacterized protein		
A0A096RW64	Uncharacterized protein		
A0A096RX71	Uncharacterized protein		
A0A096RX88	Uncharacterized protein		
A0A096RXC7	Uncharacterized protein		
A0A096RXE7	Uncharacterized protein		

Protein	Annotation	Response to salt stress	ANOVA
A0A096RXU4	Uncharacterized protein		
A0A096RY69	Uncharacterized protein		
A0A096RY98	Uncharacterized protein		
A0A096RYC9	Uncharacterized protein		
A0A096RYL4	Uncharacterized protein		
A0A096RYM0	Uncharacterized protein		
A0A096RYZ1	Uncharacterized protein		
A0A096RZA0	Uncharacterized protein		
A0A096RZA2	Uncharacterized protein		
A0A096RZC6	Uncharacterized protein		
A0A096RZC8	Uncharacterized protein		
A0A096RZZ1	Uncharacterized protein		
A0A096S029	Uncharacterized protein		
A0A096S0A7	Uncharacterized protein		
A0A096S0N9	Uncharacterized protein		

Protein	Annotation	Response to salt stress	ANOVA
A0A096S0Y5	Uncharacterized protein		
A0A096S130	Uncharacterized protein		
A0A096S1A7	Uncharacterized protein		
A0A096S1G2	Uncharacterized protein		
A0A096S1J5	Uncharacterized protein		
A0A096S1K7	Uncharacterized protein		
A0A096S1L3	Uncharacterized protein		
A0A096S1M8	Uncharacterized protein		
A0A096S1W4	Uncharacterized protein		
A0A096S334	Uncharacterized protein		
A0A096S360	Uncharacterized protein		
A0A096S3G3	Uncharacterized protein		
A0A096S3P5	Uncharacterized protein		
A0A096S3X0	Uncharacterized protein		
A0A096S3Y4	Uncharacterized protein		

Protein	Annotation	Response to salt stress	ANOVA
A0A096S499	Uncharacterized protein		
A0A096S4A0	Uncharacterized protein		
A0A096S4A1	Uncharacterized protein		
A0A096S4I9	Uncharacterized protein		
A0A096S4K7	Uncharacterized protein		
A0A096S532	Uncharacterized protein		
A0A096S5A7	Uncharacterized protein		
A0A096S627	Uncharacterized protein		
A0A096S6C6	Uncharacterized protein		
A0A096S6G1	Uncharacterized protein		
A0A096S6I9	Uncharacterized protein		
A0A096S6Q1	Uncharacterized protein		
A0A096S6T1	Uncharacterized protein		
A0A096S6X8	Uncharacterized protein		
A0A096S7C9	Peroxidase 66		

Protein	Annotation	Response to salt stress	ANOVA
A0A096S7I9	Uncharacterized protein		
A0A096S7T9	Uncharacterized protein		
A0A096S818	Uncharacterized protein		
A0A096S8H0	Uncharacterized protein		
A0A096S8H2	Uncharacterized protein		
A0A096S954	Uncharacterized protein		
A0A096S9A0	Uncharacterized protein		
A0A096S9C5	Uncharacterized protein		
A0A096SA13	Uncharacterized protein		
A0A096SAK5	Uncharacterized protein		
A0A096SAM6	Uncharacterized protein		
A0A096SAP4	Uncharacterized protein		
A0A096SBR4	Uncharacterized protein		
A0A096SBV9	Uncharacterized protein		
A0A096SC26	Uncharacterized protein		

Protein	Annotation	Response to salt stress	ANOVA
A0A096SCG9	Uncharacterized protein		
A0A096SCS4	Uncharacterized protein		
A0A096SD14	Uncharacterized protein		
A0A096SD27	Uncharacterized protein		
A0A096SDT4	Uncharacterized protein		
A0A096SFM6	Uncharacterized protein		
A0A096SFU6	Uncharacterized protein		
A0A096SFW3	Uncharacterized protein		
A0A096SGI5	Uncharacterized protein		
A0A096SGY5	Uncharacterized protein		
A0A096SGZ3	Uncharacterized protein		
A0A096SHX7	Uncharacterized protein		
A0A096SIN0	Uncharacterized protein		
A0A096SIZ0	Uncharacterized protein		
A0A096SJ15	Uncharacterized protein		

Protein	Annotation	Response to salt stress	ANOVA
A0A096SJI7	Uncharacterized protein		
A0A096SK21	Uncharacterized protein		
A0A096SK94	Uncharacterized protein		
A0A096SKV8	Uncharacterized protein		
A0A096SM43	Uncharacterized protein		
A0A096SMD1	Uncharacterized protein		
A0A096SMM7	Uncharacterized protein		
A0A096SN13	Uncharacterized protein		
A0A096SN39	Uncharacterized protein		
A0A096SNB4	Uncharacterized protein		
A0A096SNE7	Uncharacterized protein		
A0A096SNK0	Uncharacterized protein		
A0A096SP77	Uncharacterized protein		
A0A096SP79	Uncharacterized protein		
A0A096SPK3	Uncharacterized protein		

Protein	Annotation	Response to salt stress	ANOVA
A0A096SPM8	Uncharacterized protein		
A0A096SPP2	Uncharacterized protein		
A0A096SQG6	Uncharacterized protein		
A0A096SQH2	Uncharacterized protein		
A0A096SRE7	Uncharacterized protein		
A0A096SRL9	Uncharacterized protein		
A0A096SS08	Uncharacterized protein		
A0A096SS60	Uncharacterized protein		
A0A096SSA0	Uncharacterized protein		
A0A096SSH2	Uncharacterized protein		
A0A096SSR2	Uncharacterized protein		
A0A096ST65	Uncharacterized protein		
A0A096STN8	Uncharacterized protein		
A0A096SUU7	Uncharacterized protein		
A0A096SVF5	Uncharacterized protein		

Protein	Annotation	Response to salt stress	ANOVA
A0A096SVP6	Uncharacterized protein		
A0A096SVV9	Uncharacterized protein		
A0A096SVZ5	Uncharacterized protein		
A0A096SWY6	Uncharacterized protein		
A0A096SXU4	Uncharacterized protein		
A0A096SYA9	Uncharacterized protein		
A0A096SZ92	Uncharacterized protein		
A0A096SZM5	Uncharacterized protein		
A0A096T0B5	Uncharacterized protein		
A0A096T0B7	Uncharacterized protein		
A0A096T0Z6	Uncharacterized protein		
A0A096T161	Uncharacterized protein		
A0A096T1A5	Uncharacterized protein		
A0A096T1S3	Uncharacterized protein		
A0A096T1S5	Uncharacterized protein		

Protein	Annotation	Response to salt stress	ANOVA
A0A096T1T5	Uncharacterized protein		
A0A096T2B2	Uncharacterized protein		
A0A096T340	Uncharacterized protein		
A0A096T3A1	Uncharacterized protein		
A0A096T3C5	Uncharacterized protein		
A0A096T3V8	Uncharacterized protein		
A0A096T4D3	Uncharacterized protein		
A0A096T4L2	Uncharacterized protein		
A0A096T4L3	Uncharacterized protein		
A0A096T4T2	Uncharacterized protein		
A0A096T503	Uncharacterized protein		
A0A096T536	Uncharacterized protein		
A0A096T569	Uncharacterized protein		
A0A096T5C2	Uncharacterized protein		
A0A096T5Y3	Uncharacterized protein		

Protein	Annotation	Response to salt stress	ANOVA
A0A096T686	Uncharacterized protein		
A0A096T6H4	Uncharacterized protein		
A0A096T792	Uncharacterized protein		
A0A096T7J3	Uncharacterized protein		
A0A096T7R4	Uncharacterized protein		
A0A096T8H1	Uncharacterized protein		
A0A096T8L8	Uncharacterized protein		
A0A096T8W7	Uncharacterized protein		
A0A096T909	Uncharacterized protein		
A0A096T927	Uncharacterized protein		
A0A096T9C7	Uncharacterized protein		
A0A096T9F6	Uncharacterized protein		
A0A096T9Y8	Uncharacterized protein		
A0A096T9Z6	Uncharacterized protein		
A0A096TA36	Uncharacterized protein		

Protein	Annotation	Response to salt stress	ANOVA
A0A096TA80	Uncharacterized protein		
A0A096TA97	Uncharacterized protein		
A0A096TAC4	Uncharacterized protein		
A0A096TAE2	Uncharacterized protein		
A0A096TAG1	Uncharacterized protein		
A0A096TAI4	Uncharacterized protein		
A0A096TAP2	Uncharacterized protein		
A0A096TB53	Uncharacterized protein		
A0A096TB83	Uncharacterized protein		
A0A096TBV3	Uncharacterized protein		
A0A096TCF9	Uncharacterized protein		
A0A096TCZ7	Uncharacterized protein		
A0A096TD23	Uncharacterized protein		
A0A096TDC4	Uncharacterized protein		
A0A096TDT6	Uncharacterized protein		

Protein	Annotation	Response to salt stress	ANOVA
A0A096TDT7	Uncharacterized protein		
A0A096TE88	Uncharacterized protein		
A0A096TEG5	Uncharacterized protein		
A0A096TEI0	Uncharacterized protein		
A0A096TEZ0	Uncharacterized protein		
A0A096TFA9	Uncharacterized protein		
A0A096TFZ6	Uncharacterized protein		
A0A096TG21	Uncharacterized protein		
A0A096TG88	Uncharacterized protein		
A0A096THE6	Uncharacterized protein		
A0A096THK1	Uncharacterized protein		
A0A096THR9	Uncharacterized protein		
A0A096TI40	Uncharacterized protein		
A0A096TI68	Uncharacterized protein		
A0A096TIE6	Uncharacterized protein		

Protein	Annotation	Response to salt stress	ANOVA
A0A096TIX1	Uncharacterized protein		
A0A096TIX9	Uncharacterized protein		
A0A096TJ64	Uncharacterized protein		
A0A096TK39	Uncharacterized protein		
A0A096TK78	Uncharacterized protein		
A0A096TKT9	Uncharacterized protein		
A0A096TL34	Uncharacterized protein		
A0A096TL51	Uncharacterized protein		
A0A096TL90	Uncharacterized protein		
A0A096TL93	Uncharacterized protein		
A0A096TLG3	Uncharacterized protein		
A0A096TLG5	Uncharacterized protein		
A0A096TLY3	Uncharacterized protein		
A0A096TM60	Uncharacterized protein		
A0A096TM90	Uncharacterized protein		

Protein	Annotation	Response to salt stress	ANOVA
A0A096TMX7	Uncharacterized protein		
A0A096TMZ5	Uncharacterized protein		
A0A096TP50	Uncharacterized protein		
A0A096TP55	Uncharacterized protein		
A0A096TPX1	Uncharacterized protein		
A0A096TPX2	Uncharacterized protein		
A0A096TQ96	Uncharacterized protein		
A0A096TQE7	Uncharacterized protein		
A0A096TQV9	Uncharacterized protein		
A0A096TQZ6	Uncharacterized protein		
A0A096TRA5	Uncharacterized protein		
A0A096TRN6	Uncharacterized protein		
A0A096TS58	Uncharacterized protein		
A0A096TSH6	Uncharacterized protein		
A0A096TSJ1	Uncharacterized protein		

Protein	Annotation	Response to salt stress	ANOVA
A0A096TSW5	Uncharacterized protein		
A0A096TSW6	Uncharacterized protein		
A0A096TT47	Uncharacterized protein		
A0A096TTB4	Uncharacterized protein		
A0A096TTG2	Uncharacterized protein		
A0A096TTS5	Uncharacterized protein		
A0A096TU86	Uncharacterized protein		
A0A096TUD0	Uncharacterized protein		
A0A096TUS0	Histone H3.2		
A0A096TUV6	Uncharacterized protein		
A0A096TVE9	Uncharacterized protein		
A0A096TVF7	Uncharacterized protein (Fragment)		
A0A096TWE5	Uncharacterized protein		
A0A096TX06	Uncharacterized protein		

Protein	Annotation	Response to salt stress	ANOVA
A0A096TXA8	Uncharacterized protein		
A0A096TY27	Uncharacterized protein		
A0A096TY67	Uncharacterized protein		
A0A096TYA3	Uncharacterized protein		
A0A096TYG8	Uncharacterized protein		
A0A096TYI0	Uncharacterized protein		
A0A096TYW4	Uncharacterized protein		
A0A096TZT8	Uncharacterized protein		
A0A096TZV2	Uncharacterized protein		
A0A096U063	Uncharacterized protein		
A0A096U0A2	Uncharacterized protein		
A0A096U194	Uncharacterized protein		
A0A096U3B2	Uncharacterized protein		
A0A096U487	Uncharacterized protein		
A0A096U554	Uncharacterized protein		

Protein	Annotation	Response to salt stress	ANOVA
A0A096U5P7	Uncharacterized protein		
A0A096U6N8	Uncharacterized protein		
A0A096U6T7	Uncharacterized protein		
A0A096U7H4	Uncharacterized protein		
A0A096U7R9	Uncharacterized protein		
A0A096U8U9	Uncharacterized protein		
A0A096U8Z4	Uncharacterized protein		
A0A096UA28	Uncharacterized protein		
A0A096UA85	Uncharacterized protein		
A0A096UAA6	Uncharacterized protein		
A0A096UAH9	Uncharacterized protein		
A0A096UAK8	Uncharacterized protein		
A0A096UAM5	Uncharacterized protein		
A0A096UC48	Uncharacterized protein		
A0A096UC79	Uncharacterized protein		

Protein	Annotation	Response to salt stress	ANOVA
A0A096UCG5	Uncharacterized protein		
A0A096UCP7	Uncharacterized protein		
A0A096UCV3	Uncharacterized protein		
A0A096UD12	Uncharacterized protein		
A0A096UD55	Uncharacterized protein		
A0A096UDB7	Uncharacterized protein		
A0A096UDH0	Uncharacterized protein		
A0A096UE25	Uncharacterized protein (Fragment)		
A0A096UE98	Uncharacterized protein		
A0A096UEL0	Uncharacterized protein		
A0A096UEP2	Uncharacterized protein		
A0A096UEQ1	Uncharacterized protein		
A0A096UFY3	Uncharacterized protein		
A0A096UGN2	Uncharacterized protein		

Protein	Annotation	Response to salt stress	ANOVA
A0A096UGV2	Uncharacterized protein		
A0A096UJ35	Uncharacterized protein		
A0A096UJ49	Uncharacterized protein		
A0A096UJ90	Uncharacterized protein		
A0A096UJE5	Uncharacterized protein		
A0A097C0X0	Sus1		
A0A097PKB3	Homoserine kinase (Fragment)		
A0A097PLA8	Nitrilase/cyanide hydratase and apolipoprotein N-acyltransferase family protein (Fragment)		
A0A097PSD6	ARM repeat superfamily protein (Fragment)		
A0A0A0Z0N3	MAPK1		
A0SMH9	Carotenoid cleavage dioxyganase 1		

Protein	Annotation	Response to salt stress	ANOVA
A2T1W7	Aldose reductase		
A3FMA3	Putative serine type endopeptidase inhibitor		
A3FMA4	Bowman-Birk type trypsin inhibitor		
A3KLI1	RAB17 protein		
A5H452	Peroxidase 70		
A5H8G4	Peroxidase 1		
A6YSM3	PL3K2		
A8IK79	Asr protein		
B1A9R4	Peroxidase		
B1P123	TRIBOA-glucoside O-methyltransferase BX7		
B4F7S3	Plasma membrane intrinsic protein1		
B4F7T1	Uncharacterized protein		

Protein	Annotation	Response to salt stress	ANOVA
B4F7U0	Proteasome subunit alpha type		
B4F7V1	2-dehydro-3-deoxyphosphooctonate aldolase		
B4F7V3	Orphans transcription factor		
B4F7Z5	Arginine/serine-rich splicing factor RSZ28I		
B4F817	Dehydroascorbate reductase		
B4F820	Triosephosphate isomerase		
B4F839	Uncharacterized protein		
B4F848	Chaperonin		
B4F871	Uncharacterized protein		
B4F8B4	Oxidoreductase		
B4F8B9	Uncharacterized protein		
B4F8D7	Peroxidase		
B4F8J8	Pyruvate kinase		

Protein	Annotation	Response to salt stress	ANOVA
B4F8L9	Uncharacterized protein		
B4F8Q8	Uncharacterized protein		
B4F8T3	Uncharacterized protein		
B4F8U2	Uncharacterized protein		
B4F8V5	Uncharacterized protein		
B4F8Z8	Uncharacterized protein		
B4F917	Putative RAN GTPase activating family protein		
B4F925	Superoxide dismutase		
B4F932	Uncharacterized protein		
B4F935	Uncharacterized protein		
B4F939	Uncharacterized protein		
B4F972	Glutamate decarboxylase		
B4F993	Uncharacterized protein		
B4F9B1	Reticulon-like protein		

Protein	Annotation	Response to salt stress	ANOVA
B4F9D6	Uncharacterized protein		
B4F9G8	Pyruvate kinase		
B4F9H1	Uncharacterized protein		
B4F9I5	ATP synthase delta chain		
B4F9J5	Glutamate dehydrogenase		
B4F9K0	Uncharacterized protein		
B4F9K2	Uncharacterized protein		
B4F9L6	Purple acid phosphatase		
B4F9M9	Isocitrate dehydrogenase [NADP]		
B4F9T3	Uncharacterized protein		
B4F9U8	Uncharacterized protein		
B4F9U9	Uncharacterized protein		
B4FA21	Purple acid phosphatase		
B4FA59	Uncharacterized protein		

Protein	Annotation	Response to salt stress	ANOVA
B4FAB0	Uncharacterized protein		
B4FAC0	Uncharacterized protein		
B4FAD4	Isocitrate dehydrogenase [NAD] subunit, mitochondrial		
B4FAD9	Uncharacterized protein		
B4FAE1	Ras protein RIC1		
B4FAJ4	2-hydroxyphytanoyl-CoA lyase		
B4FAK9	Glyceraldehyde-3-phosphate dehydrogenase		
B4FAQ5	Uncharacterized protein		
B4FAS3	Uncharacterized protein		
B4FAV5	Germin-like protein 1		
B4FAX6	Uncharacterized protein		
B4FAY8	Negatively light-regulated protein		

Protein	Annotation	Response to salt stress	ANOVA
B4FB55	Ras-related protein ARA-3		
B4FB81	Uncharacterized protein		
B4FBC2	Uncharacterized protein		
B4FBC9	Uncharacterized protein		
B4FBD6	Ribonuclease 3		
B4FBF2	Carboxypeptidase		
B4FBF4	Serine hydroxymethyltransferase		
B4FBF6	Uncharacterized protein		
B4FBJ5	Uncharacterized protein		
B4FBP0	Putative TCP-1/cpn60 chaperonin family protein isoform 1		
B4FBW5	Mannitol dehydrogenase		
B4FBY5	40S ribosomal protein S23		
B4FC14	Cytochrome b-c1 complex		

Protein	Annotation	Response to salt stress	ANOVA
	subunit Rieske, mitochondrial		
B4FC49	Uncharacterized protein		
B4FC92	Nuclear transport factor 2		
B4FCB4	Carboxypeptidase		
B4FCF8	Uncharacterized protein		
B4FCM3	Uncharacterized protein		
B4FCM8	Histone H2B		
B4FCR7	Soluble inorganic pyrophosphatase		
B4FCU1	Uncharacterized protein		
B4FCX3	Proteasome subunit beta type		
B4FCY9	26S proteasome non-ATPase regulatory subunit 8		
B4FD03	Uncharacterized protein		

Protein	Annotation	Response to salt stress	ANOVA
B4FDH5	Histone H2B		
B4FDN9	Uncharacterized protein		
B4FE17	Uncharacterized protein		
B4FE18	Histone H2B		
B4FE20	Uncharacterized protein		
B4FEJ6	Actin-depolymerizing factor 3		
B4FEP4	Ras-related protein ARA-4		
B4FEQ4	Uncharacterized protein		
B4FER1	Uncharacterized protein		
B4FER8	Acyl-CoA-binding protein		
B4FES7	Uncharacterized protein		
B4FF02	60S ribosomal protein L23a		
B4FF24	UDP-glucuronic acid decarboxylase 1 isoform 1		
B4FF31	Uncharacterized protein		

Protein	Annotation	Response to salt stress	ANOVA
B4FF57	Uncharacterized protein		
B4FFE7	Acyl carrier protein		
B4FFF1	Uncharacterized protein		
B4FFG8	Uncharacterized protein		
B4FFH8	Adenosine kinase 2		
B4FFI2	Nitrilase-associated protein		
B4FFJ0	Asparagine synthetase		
B4FFJ9	Uncharacterized protein		
B4FFL1	Ubiquitin-like protein 5		
B4FFP2	Glutamate dehydrogenase		
B4FFV3	Malate dehydrogenase		
B4FFZ2	Ketol-acid reductoisomerase		
B4FG11	Uncharacterized protein		
B4FG39	Peroxidase		

Protein	Annotation	Response to salt stress	ANOVA
B4FG53	Malate dehydrogenase		
B4FGC8	40S ribosomal protein S12		
B4FGK8	Eukaryotic translation initiation factor 2 alpha subunit		
B4FGL3	Uncharacterized protein		
B4FGQ3	Uncharacterized protein		
B4FH43	Uncharacterized protein		
B4FH44	Thioredoxin		
B4FH55	Histone H2A		
B4FH61	Protein transporter		
B4FH68	Peroxidase		
B4FH69	Uncharacterized protein		
B4FH98	Uncharacterized protein		
B4FHA8	Histone deacetylase HDT2		
B4FHM1	Uncharacterized protein		

Protein	Annotation	Response to salt stress	ANOVA
B4FHN3	Uncharacterized protein		
B4FHS0	Uncharacterized protein		
B4FI05	Ferredoxin--NADP reductase		
B4FI22	Uncharacterized protein		
B4FIA6	Histone H2A		
B4FIB2	Ras-related protein RIC2		
B4FIC7	Superoxide dismutase [Cu-Zn]		
B4FIE5	Nascent polypeptide-associated complex subunit beta		
B4FIJ9	Uncharacterized protein		
B4FIT6	Uncharacterized protein		
B4FIT7	CHY1		
B4FIZ5	Uncharacterized protein		
B4FJ16	Succinate dehydrogenase		

Protein	Annotation	Response to salt stress	ANOVA
	[ubiquinone] iron-sulfur subunit, mitochondrial		
B4FJB2	Ras protein Rab11D		
B4FJD7	Uncharacterized protein		
B4FJR7	Uncharacterized protein		
B4FJT7	Uncharacterized protein		
B4FJY1	Uncharacterized protein		
B4FJY5	Proteasome subunit beta type		
B4FK69	Acyl carrier protein		
B4FKD5	Eukaryotic translation initiation factor 6		
B4FKE8	Pi starvation-induced protein		
B4FKG6	Uncharacterized protein		
B4FKH7	Cytochrome b5		

Protein	Annotation	Response to salt stress	ANOVA
B4FKM1	Guanine nucleotide-binding protein beta subunit-like protein		
B4FKW0	Uncharacterized protein		
B4FL77	Rickettsia 17 kDa surface antigen family protein		
B4FLA1	Uncharacterized protein		
B4FLA2	Chorismate synthase		
B4FLD1	SNARE domain containing protein		
B4FLN7	PUR ALPHA-1		
B4FLQ8	26S proteasome non-ATPase regulatory subunit 14		
B4FMB6	Induced stolen tip protein TUB8		
B4FMJ0	ADP-ribosylation factor 1		

Protein	Annotation	Response to salt stress	ANOVA
B4FML8	40S ribosomal protein S13		
B4FML9	Pyruvate dehydrogenase E1 component subunit alpha		
B4FMR9	Uncharacterized protein		
B4FMS0	NHP2-like protein 1		
B4FN21	Proteasome subunit beta type		
B4FN22	Uncharacterized protein		
B4FN97	Isocitrate dehydrogenase [NADP]		
B4FNA7	Uncharacterized protein		
B4FNC9	Small ubiquitin-related modifier		
B4FNF8	Uncharacterized protein		
B4FNK1	Uncharacterized protein		
B4FNK8	Uncharacterized protein		
B4FNL7	MAP3K-like protein kinase		

Protein	Annotation	Response to salt stress	ANOVA
B4FNT0	Uncharacterized protein		
B4FNU6	Uncharacterized protein		
B4FNW7	Activator of 90 kDa heat shock protein ATPase		
B4FNZ2	Tubulin-specific chaperone A		
B4FP96	Uncharacterized protein		
B4FPA0	Uncharacterized protein		
B4FPA4	Uncharacterized protein		
B4FPD1	Membrane steroid-binding protein 1		
B4FPE4	Uncharacterized protein		
B4FPG2	Actin1 isoform 1		
B4FPJ2	U6 snRNA-associated Sm-like protein LSm3		
B4FPK8	Cytochrome b5		
B4FPL1	Bowman-Birk type wound-		

Protein	Annotation	Response to salt stress	ANOVA
	induced proteinase inhibitor WIP1		
B4FPT6	GTP-binding protein SAR1A		
B4FPT7	Polyubiquitin 2		
B4FPZ7	GrpE protein homolog		
B4FQ03	60S ribosomal protein L7-2		
B4FQ13	Thioredoxin reductase		
B4FQ61	40S ribosomal protein S15a		
B4FQC6	Glucose-6-phosphate isomerase		
B4FQE6	Uncharacterized protein		
B4FQH2	Uncharacterized protein		
B4FQJ6	Uncharacterized protein		
B4FQM2	Pyrophosphate--fructose 6-phosphate 1-phosphotransferase beta subunit		

Protein	Annotation	Response to salt stress	ANOVA
B4FQM3	Uncharacterized protein		
B4FQP4	Uncharacterized protein		
B4FQQ1	Uncharacterized protein		
B4FQQ2	Uncharacterized protein		
B4FQS1	4,5-DOPA dioxygenase extradiol		
B4FQS5	36.4 kDa proline-rich protein		
B4FQS9	Putative cytochrome P450 superfamily protein		
B4FQV3	Uncharacterized protein		
B4FQW0	Stem-specific protein TSJT1		
B4FQW8	Aquaporin PIP1.1		
B4FQX1	Uncharacterized protein		
B4FR02	Uncharacterized protein		

Protein	Annotation	Response to salt stress	ANOVA
B4FR03	OB-fold nucleic acid binding domain containing protein		
B4FR38	Uncharacterized protein		
B4FR72	Purple acid phosphatase		
B4FR89	Phosphomanno mutase		
B4FR97	Uncharacterized protein		
B4FR99	Uncharacterized protein		
B4FRC2	Uncharacterized protein		
B4FRD6	Peroxidase		
B4FRH5	Succinyl-CoA ligase subunit beta		
B4FRK0	Uncharacterized protein		
B4FRL9	Uncharacterized protein		
B4FRR1	Uncharacterized protein		
B4FRR4	Uncharacterized protein		

Protein	Annotation	Response to salt stress	ANOVA
B4FRS8	Uncharacterized protein		
B4FS65	Uncharacterized protein		
B4FS99	ATP synthase D chain, mitochondrial		
B4FSA7	ADP,ATP carrier protein		
B4FSC8	Uncharacterized protein		
B4FSE9	Histone H2B		
B4FSF1	Uncharacterized protein		
B4FSG3	60S ribosomal protein L7-1		
B4FSG4	Jasmonate-induced protein		
B4FSJ1	Uncharacterized protein		
B4FSN1	Uncharacterized protein		
B4FSP6	Uncharacterized protein		
B4FST4	SKP1-like protein 1A		
B4FSV5	Uncharacterized protein		

Protein	Annotation	Response to salt stress	ANOVA
B4FSX7	Carbonyl reductase 1		
B4FSZ7	Uncharacterized protein		
B4FT23	14-3-3-like protein		
B4FT31	Dehydroascorbate reductase		
B4FT61	Uncharacterized protein		
B4FT62	Uncharacterized protein		
B4FT65	Uncharacterized protein		
B4FT96	Uncharacterized protein		
B4FTC0	Uncharacterized protein		
B4FTF8	Glutathione S-transferase		
B4FTG6	Mitogen-activated protein kinase		
B4FTJ4	Uncharacterized protein		
B4FTJ6	Uncharacterized protein		
B4FTK9	1,4-beta-D-glucanase		

Protein	Annotation	Response to salt stress	ANOVA
B4FTM9	Uncharacterized protein		
B4FTV5	Uncharacterized protein		
B4FTX3	Uncharacterized protein		
B4FTY8	Harpin inducing protein		
B4FU88	Peroxidase		
B4FUA7	Aldehyde dehydrogenase		
B4FUE0	Obg-like ATPase 1		
B4FUH2	Aspartate aminotransferase		
B4FUK2	Peptidyl-prolyl cis-trans isomerase		
B4FUK7	Uncharacterized protein		
B4FUK9	COP9 signalosome complex subunit 5b		
B4FUR6	Uncharacterized protein		
B4FUS5	ATP-dependent Clp protease		

Protein	Annotation	Response to salt stress	ANOVA
	proteolytic subunit		
B4FV44	Uncharacterized protein		
B4FV46	Rapid alkalinization factor 1		
B4FV82	Uncharacterized protein		
B4FV91	Uncharacterized protein		
B4FVB1	Uncharacterized protein		
B4FVD5	Uncharacterized protein		
B4FVD6	Uncharacterized protein		
B4FVE1	NADPH quinone oxidoreductase 1		
B4FVE4	Uncharacterized protein		
B4FVH1	Malate dehydrogenase		
B4FVI0	Aspartic proteinase nepenthesin-2		
B4FVM0	Thaumatin-like protein		

Protein	Annotation	Response to salt stress	ANOVA
B4FVT1	Peroxidase		
B4FVY2	Uncharacterized protein		
B4FVZ2	Uncharacterized protein		
B4FW42	Uncharacterized protein		
B4FW57	Uncharacterized protein		
B4FW90	ER luminal binding protein		
B4FWI4	Uncharacterized protein		
B4FWJ8	Luminal-binding protein 3		
B4FWN5	Uncharacterized protein		
B4FWU6	Uncharacterized protein		
B4FWY4	Uncharacterized protein		
B4FX16	Macrophage migration inhibitory factor		
B4FX25	Uncharacterized protein		
B4FX40	Uncharacterized protein		

Protein	Annotation	Response to salt stress	ANOVA
B4FXA3	Histone H2B		
B4FXU0	Uncharacterized protein		
B4FXW5	Uncharacterized protein		
B4FXZ3	Grx_C2.2-glutaredoxin subgroup I		
B4FY83	Peroxidase		
B4FYD8	Peroxidase		
B4FYG9	NADH-ubiquinone oxidoreductase 13 kDa-B subunit		
B4FYN0	Mitochondrial import inner membrane translocase subunit Tim13		
B4FYV4	Saposin-like type B, region 1 family protein		
B4FYX5	Uncharacterized protein		
B4FYZ0	Histone H2B		

Protein	Annotation	Response to salt stress	ANOVA
B4FZ29	Argininosuccinate synthase		
B4FZ84	40S ribosomal protein SA		
B4FZ86	Histone H2A		
B4FZM3	Uncharacterized protein		
B4FZN6	40S ribosomal protein S7		
B4FZT5	Uncharacterized protein		
B4FZU8	Malate dehydrogenase		
B4FZU9	Uncharacterized protein		
B4FZW5	Malate dehydrogenase		
B4FZY5	Uncharacterized protein		
B4FZZ2	Peptidyl-prolyl cis-trans isomerase		
B4G029	3-N-debenzoyl-2-deoxytaxol N-benzoyltransferase		
B4G031	Uncharacterized protein		

Protein	Annotation	Response to salt stress	ANOVA
B4G039	Uncharacterized protein		
B4G058	Uncharacterized protein		
B4G066	Uncharacterized protein		
B4G072	DIMBOA UDP-glucosyltransferase BX9		
B4G0N0	Glucose-6-phosphate isomerase		
B4G0Q9	Abscisic stress ripening protein 2		
B4G0U0	Uncharacterized protein		
B4G0V3	Adenosylhomocysteinase		
B4G0V4	Coatomer subunit delta		
B4G0V7	Carbonic anhydrase		
B4G0V9	Lipase/lipooxygenase, PLAT/LH2		
B4G126	Carboxypeptidase		
B4G137	Uncharacterized protein		

Protein	Annotation	Response to salt stress	ANOVA
B4G177	Uncharacterized protein		
B4G194	40S ribosomal protein SA		
B4G195	Aspartate aminotransferase		
B4G1B0	Remorin		
B4G1E1	Uncharacterized protein		
B4G1G0	Uncharacterized protein		
B4G1L5	Uncharacterized protein		
B4G1P1	Glutamine synthetase		
B4G1P9	3-N-debenzoyl-2-deoxytaxol N-benzoyltransferase		
B4G1Q4	Uncharacterized protein		
B4G262	Carbonic anhydrase		
B6SGB6	Pyrophosphate--fructose 6-phosphate 1-phosphotransfer		

Protein	Annotation	Response to salt stress	ANOVA
	ase alpha subunit		
B6SGJ5	Ectonucleotide pyrophosphatase/phosphodiesterase 1		
B6SGM5	Putative oxidoreductase, aldo/keto reductase family protein		
B6SGP2	Ras-related protein RGP1		
B6SGY0	Subtilisin-chymotrypsin inhibitor CI-1B		
B6SHF6	Mitochondrial-processing peptidase alpha subunit		
B6SHT0	OB-fold nucleic acid binding domain containing protein		
B6SHT6	PVR3-like protein		
B6SHU4	Histone H2B		
B6SHX9	Histone H2A		

Protein	Annotation	Response to salt stress	ANOVA
B6SHY0	ATOZI1		
B6SHZ1	40S ribosomal protein S5		
B6SIA2	40S ribosomal protein S26		
B6SIA9	Peroxidase		
B6SID3	Putative uncharacterized protein		
B6SIF0	Glycine-rich RNA-binding protein 2		
B6SIL7	Eukaryotic translation initiation factor 5A		
B6SIM9	60S ribosomal protein L17		
B6SIP0	NHP2-like protein 1		
B6SIR7	Uncharacterized protein		
B6SIR9	1-aminocyclopropane-1-carboxylate oxidase		
B6SIU4	Peroxidase		

Protein	Annotation	Response to salt stress	ANOVA
B6SIU9	Glycine-rich RNA-binding protein 2		
B6SJ21	Guanine nucleotide-binding protein beta subunit-like protein		
B6SJI7	Splicing factor, arginine/serine-rich 7		
B6SJJ1	60S ribosomal protein L31		
B6SJP0	Putative uncharacterized protein		
B6SJP9	Putative uncharacterized protein		
B6SJQ5	Histone H3		
B6SJQ6	Histone H2A		
B6SJU5	Polyubiquitin containing 7 ubiquitin monomers		
B6SJZ5	Histone H2B		

Protein	Annotation	Response to salt stress	ANOVA
B6SK03	Ubiquitin-conjugating enzyme spm2		
B6SK54	Superoxide dismutase [Cu-Zn]		
B6SKA0	Glutathione S-transferase GSTF2		
B6SKU4	Kinesin light chain		
B6SKW5	Inosine-5'-monophosphate dehydrogenase		
B6SLE7	Legumin-like protein		
B6SLH5	Putative uncharacterized protein		
B6SLI1	40S ribosomal protein S30		
B6SLK4	Elongation factor 1-beta		
B6SLL8	Malate dehydrogenase		
B6SLX1	Chaperonin		
B6SM71	Uncharacterized protein		
B6SMC1	Thioredoxin		

Protein	Annotation	Response to salt stress	ANOVA
B6SMR2	Peroxidase		
B6SMZ7	Remorin		
B6SNM4	Protein transport protein Sec61 beta subunit		
B6SP06	Glycine-rich protein 2b		
B6SP74	Glycine-rich RNA-binding protein 2		
B6SPB2	Flavoprotein wrbA		
B6SPL7	Copper chaperone		
B6SPP9	Bowman-Birk type wound-induced proteinase inhibitor WIP1		
B6SPR5	Fb14		
B6SQM6	Pathogeneis protein 10		
B6SR40	Putative uncharacterized protein		

Protein	Annotation	Response to salt stress	ANOVA
B6SRE7	Peptidyl-prolyl cis-trans isomerase		
B6SRI4	14-3-3-like protein		
B6SRL2	Aconitate hydratase		
B6SS31	Putative uncharacterized protein		
B6SSB3	Anthocyanidin 5,3-O-glucosyltransferase		
B6SST9	ATP synthase delta chain		
B6ST04	Beta-hexosaminidase		
B6STA5	Glycine-rich RNA-binding protein 2		
B6STH7	Ferredoxin-3		
B6SUD1	Alcohol dehydrogenase 2		
B6SUV6	Hypersensitive-induced response protein		

Protein	Annotation	Response to salt stress	ANOVA
B6SV64	Heat shock 70 kDa protein 4		
B6SVE1	Carboxypeptidase		
B6SVE6	Putative uncharacterized protein		
B6SVK5	ACS-like protein		
B6SVK8	Serine/threonine-protein kinase NAK		
B6SVV9	ATP synthase subunit beta		
B6SX67	60S ribosomal protein L32		
B6SXB4	Putative uncharacterized protein		
B6SXF5	Pathogenesis-related protein 1		
B6SXV2	RNA-binding protein AKIP1		
B6SXV4	Peroxisomal fatty acid beta-oxidation multifunctional protein		
B6SXW8	RuBisCO large subunit-binding		

Protein	Annotation	Response to salt stress	ANOVA
	protein subunit alpha		
B6SYD0	60S ribosomal protein L22-2		
B6SYF5	Peptidyl-prolyl cis-trans isomerase		
B6SZ69	Heat shock cognate 70 kDa protein 2		
B6SZ83	Actin-7		
B6SZB9	14-3-3-like protein		
B6SZK9	Coatomer subunit epsilon		
B6SZW3	Hydroquinone glucosyltransferase		
B6SZZ9	Soluble inorganic pyrophosphatase		
B6T033	Glutathione S-transferase GSTU6		
B6T056	Superoxide dismutase [Cu-Zn]		
B6T0A2	Calmodulin		

Protein	Annotation	Response to salt stress	ANOVA
B6T0Q2	Histone H2A		
B6T0W1	Histone H2B		
B6T0X0	Histone H4		
B6T0Y1	Ras-related protein RIC2		
B6T0Y2	ATP synthase epsilon chain, mitochondrial		
B6T1G5	Histone H2B		
B6T1H0	40S ribosomal protein S6		
B6T1H9	Uncharacterized protein		
B6T1R0	60S ribosomal protein L22-2		
B6T1T4	Histone H4		
B6T207	Ras-related protein Rab7		
B6T275	Histone H4		
B6T291	Actin-depolymerizing factor 3		
B6T2C6	Peptide methionine sulfoxide reductase msrB		

Protein	Annotation	Response to salt stress	ANOVA
B6T2P8	Chloroplastic quinone-oxidoreductase		
B6T2T6	60S ribosomal protein L21		
B6T2Y5	Esterase D		
B6T329	Nuclease PA3		
B6T3E9	Histone H2A		
B6T3J3	Histone H2A		
B6T3V1	Peroxidase		
B6T428	Succinyl-CoA ligase alpha-chain 2		
B6T451	Importin subunit alpha		
B6T4B7	Histone H1		
B6T4M4	Histone H1		
B6T4R2	Flavoprotein wrbA		
B6T4R3	UTP--glucose-1-phosphate uridylyltransferase		

Protein	Annotation	Response to salt stress	ANOVA
B6T4U2	Vegetative storage protein PNI288		
B6T4U8	Calmodulin		
B6T504	Proteasome subunit alpha type		
B6T533	Ribosomal protein		
B6T5F2	60S ribosomal protein L13		
B6T5U0	Uncharacterized protein		
B6T5Z1	L-lactate dehydrogenase		
B6T5Z7	Alpha-expansin 1		
B6T6B3	Eukaryotic translation initiation factor 3 subunit M		
B6T6D2	Disease resistance response protein 206		
B6T6U2	Nucleic acid binding protein		
B6T6Y2	S-glutathione dehydrogenase/		

Protein	Annotation	Response to salt stress	ANOVA
	class III alcohol dehydrogenase		
B6T706	Aspartic proteinase oryzasin-1		
B6T711	DNA repair protein RAD23		
B6T727	Putative uncharacterized protein		
B6T766	60S ribosomal protein L21		
B6T7B6	Glutathione S-transferase, C-terminal-like		
B6T7E7	Histone H2A		
B6T7H0	Glutathione S-transferase 6		
B6T7J7	Serine hydroxymethyltransferase		
B6T7Q7	Serine hydroxymethyltransferase		
B6T828	Grx_C4-glutaredoxin subgroup I		

Protein	Annotation	Response to salt stress	ANOVA
B6T836	Cortical cell-delineating protein		
B6T8F4	Ran-binding protein 1		
B6T8I3	Disease resistance response protein 206		
B6T8U5	ER6 protein		
B6T904	UMP-CMP kinase		
B6T914	Pop3 peptide		
B6T9C0	Uncharacterized protein		
B6T9G3	Alpha-1,4-glucan-protein synthase 1		
B6T9P0	UDP-glucose 6-dehydrogenase		
B6T9S6	Retrotransposon protein SINE subclass		
B6T9T0	O-methyltransferase ZRP4		
B6TAA7	Chaperonin		

Protein	Annotation	Response to salt stress	ANOVA
B6TAJ3	Proteasome subunit alpha type		
B6TAL4	12-oxophytodienoate reductase 3		
B6TB21	Anamorsin homolog		
B6TB29	Fructokinase-2		
B6TB58	Putative uncharacterized protein		
B6TB84	Soluble inorganic pyrophosphatase		
B6TBA8	Aspartic proteinase nepenthesin-2		
B6TBE1	NHP2-like protein 1		
B6TBM1	Alpha-soluble NSF attachment protein		
B6TBN6	Pyruvate kinase		
B6TBW2	ATP synthase delta chain		

Protein	Annotation	Response to salt stress	ANOVA
B6TBW4	Proliferation-associated protein 2G4		
B6TBY8	UDP-glucose 6-dehydrogenase		
B6TC95	Histone H1		
B6TCB2	Dehydrin 13		
B6TCE9	Peptidyl-prolyl cis-trans isomerase		
B6TCI3	ADP,ATP carrier protein		
B6TCI5	Ras protein RHN1		
B6TCK3	NADH-cytochrome b5 reductase		
B6TD22	Stromal cell-derived factor 2		
B6TD89	WD-40 repeat protein MSI4		
B6TDA9	2-cys peroxiredoxin BAS1		
B6TDH1	DAG protein		
B6TDH5	Ubiquitin-conjugating		

Protein	Annotation	Response to salt stress	ANOVA
	enzyme E2-17 kDa		
B6TDH6	H/ACA ribonucleoprotein complex subunit 3-like protein		
B6TDW7	Secretory protein		
B6TE08	ATP binding protein		
B6TE13	Spliceosome RNA helicase BAT1		
B6TE43	Glutamine synthetase		
B6TET7	Abscisic stress ripening protein 1		
B6TF12	Glycine-rich RNA-binding protein 8		
B6TFE4	Ribokinase		
B6TFF1	Putative thioredoxin superfamily protein		
B6TFS9	14-3-3-like protein A		

Protein	Annotation	Response to salt stress	ANOVA
B6TFY4	40S ribosomal protein S27		
B6TG58	GTP-binding protein SAR1A		
B6TG70	Mitochondrial-processing peptidase beta subunit		
B6TG98	Copper ion binding protein		
B6TGD4	Uncharacterized protein		
B6TGF0	Proteasome subunit alpha type		
B6TGF1	Malate dehydrogenase		
B6TGG2	2,3-bisphosphoglycerate-independent phosphoglycerate mutase		
B6TGJ7	Ras-related protein Rab-18		
B6TGL5	Reticulon-like protein		
B6TH57	Succinyl-CoA ligase alpha-chain 2		

Protein	Annotation	Response to salt stress	ANOVA
B6TH67	MFP1 attachment factor 1		
B6THH3	Chalcone-flavonone isomerase family protein		
B6THN2	RuBisCO large subunit-binding protein subunit beta		
B6THR4	Thioredoxin-like 4		
B6THT0	Peroxiredoxin-5		
B6THT6	3-oxoacyl-reductase		
B6THU5	Elongation factor 1-delta 1		
B6THU9	Peroxidase		
B6TI56	Ribose-5-phosphate isomerase		
B6TI78	Peptidyl-prolyl isomerase		
B6TIL4	GDP-mannose 3,5-epimerase 2		
B6TIM2	Deoxyribodipyrimidine photolyase		

Protein	Annotation	Response to salt stress	ANOVA
B6TIQ8	ATP/GTP binding protein		
B6TJ22	Glutathione S-transferase parA		
B6TJ40	Lipid transfer protein		
B6TJ78	3-N-debenzoyl-2-deoxytaxol N-benzoyltransferase		
B6TJ90	Histone H4		
B6TJ93	40S ribosomal protein S15a		
B6TJB6	Proteasome subunit alpha type		
B6TJM1	Isocitrate dehydrogenase [NAD] subunit, mitochondrial		
B6TJT2	Auxin-induced protein PCNT115		
B6TK17	DREPP2 protein		
B6TKG5	Quercetin 3-O-methyltransferase 1		

Protein	Annotation	Response to salt stress	ANOVA
B6TKI9	Rae1-like protein		
B6TKU7	Sex determination protein tasselseed-2		
B6TKZ3	Hydrolase, carbon-nitrogen family		
B6TL20	Glutathione S-transferase GSTU6		
B6TL22	Protein P21		
B6TL91	Hsc70-interacting protein		
B6TLC8	Uncharacterized protein		
B6TLL8	Argininosuccinate synthase		
B6TLM5	Glutathione S-transferase GSTU6		
B6TLN7	Vacuolar sorting protein 4b		
B6TLT1	Serine/threonine -protein phosphatase 2A		

Protein	Annotation	Response to salt stress	ANOVA
	65 kDa regulatory subunit Abeta isoform		
B6TLT4	Ribosomal protein L37		
B6TLU5	Lipid binding protein		
B6TLX0	NADH-ubiquinone oxidoreductase 10.5 kDa subunit		
B6TLY8	Mitochondrial ATP synthase		
B6TMA0	Dehydrin 13		
B6TMF3	Wound/stress protein		
B6TMW7	Transaminase/ transferase isoform 1		
B6TN48	3-hydroxyisobutyryl-CoA hydrolase/ catalytic		
B6TNF1	Calnexin		
B6TNI6	DREPP4 protein		

Protein	Annotation	Response to salt stress	ANOVA
B6TNQ7	Ninja-family protein 6		
B6TNR8	40S ribosomal protein S2		
B6TNT5	Peptide methionine sulfoxide reductase		
B6TP19	Thioredoxin-like protein 5		
B6TP36	Prohibitin		
B6TP58	Histone H3		
B6TPA4	Carnitine racemase/ catalytic		
B6TPG0	Elongation factor Tu		
B6TPJ8	Fructokinase-2		
B6TQ25	RNA-binding protein-like		
B6TQ36	Pyruvate dehydrogenase E1 component subunit beta		
B6TQC0	3-N-debenzoyl-2-deoxytaxol N-benzoyltransferase		

Protein	Annotation	Response to salt stress	ANOVA
B6TQL4	Jasmonate-induced protein		
B6TQW0	Carboxypeptidase		
B6TR38	Basic endochitinase A		
B6TRA8	Histone H1		
B6TRF2	Transferase, transferring glycosyl groups		
B6TRL2	Brain acid soluble protein 1		
B6TRM9	Mitochondrial-processing peptidase alpha subunit		
B6TRQ7	Pre-mRNA-splicing factor 19		
B6TRW8	Dihydrolipoyllysine-residue succinyltransferase component of 2-oxoglutarate dehydrogenase complex		

Protein	Annotation	Response to salt stress	ANOVA
B6TS21	Succinyl-CoA ligase subunit beta		
B6TS22	O-methyltransferase ZRP4		
B6TS83	Aquaporin PIP2.1		
B6TSB3	Glucose-6-phosphate 1-dehydrogenase		
B6TSH6	60S ribosomal protein L21		
B6TSQ9	Aspartic proteinase oryzasin-1		
B6TSR7	Hsp20/alpha crystallin family protein		
B6TT27	Glutamate decarboxylase		
B6TT67	Putative uncharacterized protein		
B6TTP0	Histone H3		
B6TTP1	Non-specific lipid-transfer protein		

Protein	Annotation	Response to salt stress	ANOVA
B6TU33	Rapid alkalinization factor 1		
B6TUA2	Acetyltransferase component of pyruvate dehydrogenase complex		
B6TUB8	Phospho-2-dehydro-3-deoxyheptonate aldolase 1		
B6TUE7	Uncharacterized protein		
B6TVE3	Patellin-1		
B6TVG1	Malic enzyme		
B6TVN6	Protein translation factor SUI1		
B6TVT8	18.3 kDa class I heat shock protein		
B6TVU6	Uncharacterized protein		
B6TW62	Disease resistance response protein 206		

Protein	Annotation	Response to salt stress	ANOVA
B6TWE1	USP family protein		
B6TWL4	26S proteasome non-ATPase regulatory subunit 11		
B6TWW1	Aspartate-semialdehyde dehydrogenase		
B6TXH5	Transaminase/ transferase, transferring nitrogenous groups		
B6TXM6	10-deacetylbaccatin III 10-O-acetyltransferase		
B6TXS9	ATP synthase subunit gamma		
B6TYS6	Glutathione S-transferase zeta class		
B6TYT3	Cysteine protease 1		
B6TZ71	Glycerol kinase		

Protein	Annotation	Response to salt stress	ANOVA
B6TZD1	Methylthioribose-1-phosphate isomerase		
B6TZS3	Uncharacterized protein		
B6TZY4	60S ribosomal protein L28		
B6U0V6	Endoplasmin		
B6U0X3	Cytokinin-O-glucosyltransferase 1		
B6U118	T-complex protein 1 subunit zeta		
B6U1C5	Uncharacterized protein		
B6U219	Alpha-1,4-glucan-protein synthase		
B6U242	Uncharacterized protein		
B6U284	14-3-3-like protein		
B6U2C3	Leucine aminopeptidase 3		
B6U346	DSBA-like thioredoxin domain		

Protein	Annotation	Response to salt stress	ANOVA
	containing protein		
B6U3H8	Lipid transfer protein		
B6U4A3	Heat shock 70 kDa protein		
B6U4M0	Polyadenylate-binding protein 2		
B6U4Q7	Sterol 3-beta-glucosyltransferase		
B6U543	Versicolorin reductase		
B6U579	Thaumatin-like protein		
B6U5F8	Putative uncharacterized protein		
B6U5W6	Mitochondrial import inner membrane translocase subunit Tim9		
B6U656	ATP binding protein		
B6U6T7	Putative uncharacterized protein		

Protein	Annotation	Response to salt stress	ANOVA
B6U6U2	Hexose transporter		
B6U724	Flavoprotein wrbA		
B6U7X7	Serine/threonine -protein kinase CTR1		
B6U7Y1	Activator of 90 kDa heat shock protein ATPase		
B6U857	Purple acid phosphatase		
B6U8P6	ABA-responsive protein		
B6U9B0	Histone H2B.2		
B6UA90	36.4 kDa proline-rich protein		
B6UB82	Protein kinase APK1B		
B6UC34	Glutaminyl-tRNA synthetase		
B6UCK2	Zinc finger protein		
B6UCR8	Proteasome subunit alpha type		

Protein	Annotation	Response to salt stress	ANOVA
B6UCV5	Shikimate biosynthesis protein aroDE		
B6UDS5	Glutamine synthetase		
B6UE22	Translationally-controlled tumor protein		
B6UEB0	Lipid binding protein		
B6UEL1	Germin-like protein subfamily 1 member 11		
B6UEM6	Protein transport protein Sec61 beta subunit		
B6UES0	Charged multivesicular body protein 4b		
B6UF11	Ribosomal protein L37		
B6UF55	5-methyltetrahydropteroyltriglutamate--homocysteine methyltransferase		

Protein	Annotation	Response to salt stress	ANOVA
B6UFY2	Putative uncharacterized protein		
B6UG30	Triosephosphate isomerase		
B6UG51	Cytochrome b5		
B6UG81	Cortical cell-delineating protein		
B6UGA2	Cortical cell-delineating protein		
B6UGJ0	Globulin-1 S allele		
B6UGK8	3-isopropylmalate dehydratase small subunit 2		
B6UGL1	Mitochondrial NADH ubiquinone oxidoreductase 13kD-like subunit		
B6UGM5	60S ribosomal protein L21		
B6UGS3	Oleosin		
B6UH77	Histone H3		

Protein	Annotation	Response to salt stress	ANOVA
B6UHB6	Histone H1		
B6UHQ8	Blue copper protein		
B6UHS0	Uncharacterized protein		
B6UHU1	Catalase		
B6UIQ8	Receptor-like protein kinase RK20-1		
B7ZWY9	Citrate synthase		
B7ZXQ8	Peroxidase		
B7ZY15	Uncharacterized protein		
B7ZY29	Uncharacterized protein		
B7ZYI1	Uncharacterized protein		
B7ZYP0	Uncharacterized protein		
B7ZYX8	UDP-glucose 6-dehydrogenase		
B7ZZ04	Uncharacterized protein		
B7ZZ42	Uncharacterized protein		
B7ZZ56	Anthocyanidin 5,3-O-		

Protein	Annotation	Response to salt stress	ANOVA
	glucosyltransferase		
B7ZZJ0	3-oxoacyl-[acyl-carrier-protein] synthase		
B7ZZN9	Uncharacterized protein		
B7ZZR2	Uncharacterized protein		
B8A0Q3	Carboxypeptidase		
B8A0S8	Uncharacterized protein		
B8A0V6	Uncharacterized protein		
B8A1C0	Proliferating cell nuclear antigen		
B8A2I0	Uncharacterized protein		
B8A324	Uncharacterized protein		
B8A390	Uncharacterized protein		
C0HE58	Uncharacterized protein		
C0HE84	Uncharacterized protein		

Protein	Annotation	Response to salt stress	ANOVA
C0HEE6	Peroxidase		
C0HER4	Aconitate hydratase		
C0HEX8	Uncharacterized protein		
C0HF27	Uncharacterized protein		
C0HF32	ATP synthase subunit beta		
C0HF51	Uncharacterized protein		
C0HF92	Uncharacterized protein		
C0HFB2	Uncharacterized protein		
C0HFG9	Uncharacterized protein		
C0HGE1	Uncharacterized protein		
C0HGE9	Uncharacterized protein		
C0HGH8	Peroxidase		
C0HGS3	Uncharacterized protein		
C0HGV5	Uncharacterized protein		
C0HH28	Uncharacterized protein		

Protein	Annotation	Response to salt stress	ANOVA
C0HH87	Uncharacterized protein		
C0HHA6	Peroxidase		
C0HHU2	Uncharacterized protein		
C0HHY2	Purple acid phosphatase		
C0HI97	Uncharacterized protein		
C0HIS1	Uncharacterized protein		
C0HIT1	Peroxidase		
C0HJ49	Uncharacterized protein		
C0HJ53	Uncharacterized protein		
C0P2F3	Uncharacterized protein		
C0P3B4	Uncharacterized protein		
C0P3K6	Uncharacterized protein		
C0P3T3	Peroxidase		
C0P3W9	Uncharacterized protein		
C0P3Z8	Uncharacterized protein		

Protein	Annotation	Response to salt stress	ANOVA
C0P406	Uncharacterized protein		
C0P429	Uncharacterized protein		
C0P464	Uncharacterized protein		
C0P484	Uncharacterized protein		
C0P4G2	Putative cytochrome P450 superfamily protein		
C0P4K4	Uncharacterized protein		
C0P4M0	Uncharacterized protein		
C0P4P3	Uncharacterized protein		
C0P4Q3	Putative heat shock protein 90 family protein		
C0P4S1	Peroxidase		
C0P4T2	Uncharacterized protein		
C0P4T5	Uncharacterized protein		
C0P4U8	ATP synthase		

Protein	Annotation	Response to salt stress	ANOVA
C0P516	Uncharacterized protein		
C0P530	Putative TCP-1/cpn60 chaperonin family protein isoform 1		
C0P558	Uncharacterized protein		
C0P567	Uncharacterized protein		
C0P576	Uncharacterized protein		
C0P594	Uncharacterized protein		
C0P5B0	Asparaginyl-tRNA synthetase, cytoplasmic 3		
C0P5C0	Importin subunit alpha		
C0P5C9	Uncharacterized protein		
C0P5U8	Glutathione S-transferase 4		
C0P6C5	Uncharacterized protein		
C0P6K2	Uncharacterized protein		

Protein	Annotation	Response to salt stress	ANOVA
C0P758	Malic enzyme		
C0P790	Eukaryotic translation initiation factor 3 subunit B		
C0P7J4	Uncharacterized protein		
C0P7Q1	Uncharacterized protein		
C0P7X2	Aldehyde dehydrogenase		
C0P7Y7	Putative AMP-dependent synthetase and ligase superfamily protein		
C0P869	Uncharacterized protein		
C0P8K3	Uncharacterized protein		
C0P8V8	Uncharacterized protein		
C0P9G2	Propionyl-CoA carboxylase beta chain		
C0P9S2	Uncharacterized protein		

Protein	Annotation	Response to salt stress	ANOVA
C0P9T1	Uncharacterized protein		
C0P9Y5	Uncharacterized protein		
C0PA04	Uncharacterized protein		
C0PA34	Uncharacterized protein		
C0PA71	Uncharacterized protein		
C0PA83	Uncharacterized protein		
C0PAS6	Uncharacterized protein		
C0PAU7	Glucose-6-phosphate isomerase		
C0PBL7	Uncharacterized protein		
C0PBX3	Uncharacterized protein		
C0PCM5	Xyloglucan endotransglucosylase/hydrolase		
C0PCR1	Uncharacterized protein		
C0PD04	3-isopropylmalate dehydrogenase		

Protein	Annotation	Response to salt stress	ANOVA
C0PD71	Uncharacterized protein		
C0PD90	Uncharacterized protein		
C0PDA6	Uncharacterized protein		
C0PDG2	Uncharacterized protein		
C0PDG3	Uncharacterized protein		
C0PDH2	Uncharacterized protein		
C0PDJ1	Lipoxygenase		
C0PDM1	Uncharacterized protein		
C0PE62	Uncharacterized protein		
C0PEC6	Uncharacterized protein		
C0PF28	Uncharacterized protein		
C0PF45	Peroxidase		
C0PF88	Uncharacterized protein		
C0PFA1	Adenylosuccinate synthetase, chloroplastic		

Protein	Annotation	Response to salt stress	ANOVA
C0PFK3	Proteasome subunit alpha type		
C0PFL1	Uncharacterized protein		
C0PFM8	Uncharacterized protein		
C0PFN9	Uncharacterized protein		
C0PFV1	Uncharacterized protein		
C0PFV4	Cytokinin inducible protease1		
C0PFX0	Glucose-6-phosphate 1-dehydrogenase		
C0PFY0	ATP-dependent Clp protease proteolytic subunit		
C0PG78	Uncharacterized protein		
C0PGG5	Pyruvate kinase		
C0PGM1	Acyl-coenzyme A oxidase		
C0PGU8	Uncharacterized protein		

Protein	Annotation	Response to salt stress	ANOVA
C0PH19	Putative cytochrome P450 superfamily protein		
C0PH20	Uncharacterized protein		
C0PH28	Uncharacterized protein		
C0PHC0	Putative ATPase, V1 complex, subunit A protein		
C0PHH5	Dihydrolipoyl dehydrogenase		
C0PHR4	Adenosylhomocysteinase		
C0PHV9	Uncharacterized protein		
C0PI30	Uncharacterized protein		
C0PIH1	Uncharacterized protein		
C0PIR4	N-acetyl-gamma-glutamyl-phosphate reductase		

Protein	Annotation	Response to salt stress	ANOVA
C0PIU9	Uncharacterized protein		
C0PJG8	Uncharacterized protein		
C0PK04	Uncharacterized protein		
C0PK05	Lactoylglutathione lyase		
C0PK55	Uncharacterized protein		
C0PKN9	Uncharacterized protein		
C0PKQ4	Uncharacterized protein		
C0PKR0	Uncharacterized protein		
C0PLI2	Uncharacterized protein		
C0PLU8	Uncharacterized protein		
C0PLX5	Uncharacterized protein		
C0PM03	Uncharacterized protein		
C0PM74	Uncharacterized protein		
C0PMH6	Glucose-6-phosphate/phosphate translocator		

Protein	Annotation	Response to salt stress	ANOVA
	2Glucose-6-phosphate/phosphate-translocator		
C0PMU3	Uncharacterized protein		
C0PN00	Uncharacterized protein		
C0PN25	Uncharacterized protein		
C0PN30	Uncharacterized protein		
C0PN38	Uncharacterized protein		
C0PN92	Uncharacterized protein		
C0PPB6	Peroxidase		
C1K9J1	Heat shock protein 90		
C3UZ63	HSP protein		
C3VQ48	Ascorbate peroxidase		
C4IYM7	Uncharacterized protein		
C4IZC7	Carboxypeptidase		
C4IZW9	Malate dehydrogenase		

Protein	Annotation	Response to salt stress	ANOVA
C4J159	Putative glycine-rich protein		
C4J2K0	Uncharacterized protein		
C4J306	Inosine-5'-monophosphate dehydrogenase		
C4J3E2	Uncharacterized protein		
C4J410	Heat shock protein1		
C4J477	Dehydrin		
C4J4E4	Uncharacterized protein		
C4J4M8	Histone H2B		
C4J4W3	Uncharacterized protein		
C4J6M5	Uncharacterized protein		
C4J6Q3	Citrate synthase		
C4J6R6	Uncharacterized protein		
C4J748	Uncharacterized protein		
C4J757	Uncharacterized protein		

Protein	Annotation	Response to salt stress	ANOVA
C4J8D4	Coatomer subunit zeta-1		
C4J929	Ribosomal protein		
C4J950	Uncharacterized protein		
C4J9A9	Superoxide dismutase [Cu-Zn]		
C4J9H8	Uncharacterized protein		
C4J9K0	APx3-Peroxisomal Ascorbate Peroxidase, mRNA		
C4J9R0	Uncharacterized protein		
C4J9U1	Uncharacterized protein		
C4JAB2	Uncharacterized protein		
C4JBB8	Uncharacterized protein		
C4JBJ3	Uncharacterized protein		
C4JBL9	Glycine cleavage system H protein 1		

Protein	Annotation	Response to salt stress	ANOVA
C4JBW5	Uncharacterized protein		
D1ME28	Uncharacterized protein		
D1MN58	ABA-, stress- and fruit-ripening inducible-like protein		
D2JSP9	ATP synthase subunit 4		
D7NLB3	Peroxidase		
E7DDW6	Putative uncharacterized protein		
E9NQE2	Malic enzyme		
G9I6E1	Acyl activating enzyme		
H7BRM0	Pyrophosphate-dependent fructose-6-phosphate 1-phosphotransferase alpha subunit short variant		
K7TFB0	Uncharacterized protein		

Protein	Annotation	Response to salt stress	ANOVA
K7TGE1	Beta-glucosidase2		
K7TI14	Clathrin heavy chain		
K7TI47	Calcium-transporting ATPase		
K7TIN2	Glycine cleavage complex P-protein		
K7TJV6	Uncharacterized protein		
K7TL05	14-3-3-like protein GF14-12		
K7TM76	Uncharacterized protein		
K7TMY3	Uncharacterized protein		
K7TNB3	Uncharacterized protein		
K7TP64	Non-cyanogenic beta-glucosidase		
K7TP73	6,7-dimethyl-8-ribityllumazine synthase		
K7TPR9	Pyruvate kinase		

Protein	Annotation	Response to salt stress	ANOVA
K7TQJ7	Uncharacterized protein		
K7TQQ6	Benzoxazinone synthesis8		
K7TR72	Uncharacterized protein		
K7TSU4	Putative O-Glycosyl hydrolase superfamily protein		
K7TSU8	Putative aminotransferase class III superfamily protein		
K7TSX2	Uncharacterized protein		
K7TT00	Uncharacterized protein		
K7TT54	Uncharacterized protein		
K7TTP9	Uncharacterized protein		
K7TW58	CASP-like protein		
K7TWH6	Putative apyrase family protein		

Protein	Annotation	Response to salt stress	ANOVA
K7TWT4	Uncharacterized protein (Fragment)		
K7TWV7	Peptidyl-prolyl cis-trans isomerase		
K7TX67	Plasma membrane H+-transporting ATPase-like protein		
K7TY03	Alanine--tRNA ligase		
K7TY22	Uncharacterized protein		
K7TYB0	Uncharacterized protein		
K7U0X0	Uncharacterized protein		
K7U1I2	Succinate dehydrogenase [ubiquinone] iron-sulfur subunit, mitochondrial		
K7U1M0	Uncharacterized protein		
K7U2L3	Ferritin		

Protein	Annotation	Response to salt stress	ANOVA
K7U3J5	Histone-lysine N-methyltransferase		
K7U4L2	Uncharacterized protein		
K7U545	Uncharacterized protein		
K7U658	Uncharacterized protein		
K7U6L5	Uncharacterized protein		
K7U735	Uncharacterized protein		
K7U7Q6	Uncharacterized protein		
K7U845	Calcium-transporting ATPase		
K7U850	ADP,ATP carrier protein 2, mitochondrial		
K7U891	Uncharacterized protein		
K7U8E4	Acyl-coenzyme A oxidase		
K7U9T3	Uncharacterized protein		

Protein	Annotation	Response to salt stress	ANOVA
K7UB12	Calcium-transporting ATPase		
K7UC74	Putative oxidoreductase, aldo/keto reductase family protein		
K7UC80	Putative TCP-1/cpn60 chaperonin family protein		
K7UCH1	Putative TCP-1/cpn60 chaperonin family protein		
K7UDS1	Putative ribosomal protein S4 (RPS4A) family protein		
K7UEH3	Uncharacterized protein		
K7UEU9	Uncharacterized protein		
K7UFI7	Sulfurtransferase		
K7UFV4	Uncharacterized protein		

Protein	Annotation	Response to salt stress	ANOVA
K7UGU4	Putative WD40-like beta propeller repeat family protein		
K7UJ05	FUSICOCCIN receptor proteins		
K7UJD9	Uncharacterized protein		
K7UK34	Uncharacterized protein		
K7UKI6	Uncharacterized protein (Fragment)		
K7ULE9	Uncharacterized protein		
K7ULX0	Uncharacterized protein		
K7UNV8	Uncharacterized protein		
K7UP24	Benzoxazinone synthesis8		
K7UPD0	Putative TCP-1/cpn60 chaperonin family protein		
K7UQ89	Putative DEAD-box ATP-dependent RNA		

Protein	Annotation	Response to salt stress	ANOVA
	helicase family protein		
K7UR24	Multi-protein bridging factor-like protein		
K7URD0	Uncharacterized protein		
K7URE0	Aconitate hydratase		
K7US09	Uncharacterized protein		
K7US39	Dihydrolipoyl dehydrogenase		
K7US41	Uncharacterized protein		
K7USC0	Calmodulin		
K7USN8	Uncharacterized protein		
K7UTA2	Uncharacterized protein		
K7UTL5	Uncharacterized protein		
K7UU30	Uncharacterized protein		
K7UU41	Uncharacterized protein		
K7UU80	Triosephosphate isomerase		

Protein	Annotation	Response to salt stress	ANOVA
K7UUB5	Uncharacterized protein		
K7UUV6	Putative ribosomal protein L11 family protein		
K7UV49	Peroxidase (Fragment)		
K7UVC8	ATP synthase beta subunit-like protein		
K7UVD7	Uncharacterized protein		
K7UVP7	Uncharacterized protein		
K7UW74	Uncharacterized protein		
K7UXH2	Uncharacterized protein		
K7UXM0	Uncharacterized protein		
K7UXM3	Putative thioredoxin superfamily protein		
K7UXY9	Putative leucine-rich repeat receptor-like protein		

Protein	Annotation	Response to salt stress	ANOVA
	kinase family protein		
K7UY17	Uncharacterized protein		
K7UYM2	Putative XH domain family protein		
K7UYX2	Uncharacterized protein		
K7UZS8	Ribosomal protein		
K7UZU9	Uncharacterized protein		
K7V0S5	Uncharacterized protein		
K7V1V1	Calcium-transporting ATPase		
K7V1X8	Uncharacterized protein		
K7V2D8	Uncharacterized protein		
K7V2X9	Uncharacterized protein		
K7V2Z8	Uncharacterized protein		
K7V3B1	Putative patellin family protein		
K7V3S0	Malic enzyme (Fragment)		

Protein	Annotation	Response to salt stress	ANOVA
K7V679	Ras protein Rab11C		
K7V6F3	Ubiquitin carboxyl-terminal hydrolase		
K7V6H1	Uncharacterized protein		
K7V6L0	Uncharacterized protein		
K7V6R3	Uncharacterized protein		
K7V6X2	Sulfurtransferase		
K7V6Z1	Putative patellin family protein		
K7V763	Uncharacterized protein		
K7V794	Enolase1		
K7V9K5	Uncharacterized protein		
K7VAV1	Uncharacterized protein		
K7VB29	Uncharacterized protein		
K7VB79	Uncharacterized protein		
K7VBG5	Histone H3		

Protein	Annotation	Response to salt stress	ANOVA
K7VBJ0	Putative cytochrome P450 superfamily protein		
K7VBT8	Putative AMP-dependent synthetase and ligase superfamily protein		
K7VC91	Uncharacterized protein		
K7VCJ9	Uncharacterized protein		
K7VCN5	Peroxidase		
K7VCP7	Putative homeodomain-like transcription factor superfamily protein		
K7VD78	Putative chaperone clbp family protein		
K7VDT6	Uncharacterized protein		

Protein	Annotation	Response to salt stress	ANOVA
K7VE21	Cytochrome c oxidase subunit 2		
K7VEB9	Importin subunit alpha		
K7VEJ7	Uncharacterized protein		
K7VF24	Uncharacterized protein		
K7VGD2	Uncharacterized protein		
K7VHA0	Uncharacterized protein		
K7VI04	Uncharacterized protein		
K7VIL3	Methionine S-methyltransferase		
K7VIM1	Fructose-bisphosphate aldolase		
K7VKX8	Uncharacterized protein		
K7VLK5	Uncharacterized protein		
K7VLZ9	Uncharacterized protein		
K7VNV5	Peroxidase		

Protein	Annotation	Response to salt stress	ANOVA
K7VP16	Uncharacterized protein		
K7VPE1	Uncharacterized protein		
K7VQA7	Uncharacterized protein		
K7VQR1	Uncharacterized protein		
K7VRG8	Uncharacterized protein		
K7VRI2	Uncharacterized protein		
K7VUB7	Serine hydroxymethyltransferase		
K7VV75	Uncharacterized protein		
K7VVC4	Uncharacterized protein		
K7VVS6	Serine-threonine kinase receptor-associated protein		
K7VW90	Uncharacterized protein		
K7VXP0	Uncharacterized protein		
K7VZN8	60S ribosomal protein L22-2		

Protein	Annotation	Response to salt stress	ANOVA
K7W2H4	Uncharacterized protein		
K7W2V5	Putative vesicle-associated membrane protein family protein		
K7W3D2	Uncharacterized protein		
K7W3R6	Glutathione S-transferase GST 25		
K7W5L7	Sesquiterpene cyclase1		
K7W5Y5	Uncharacterized protein		
K7W888	Peroxidase		
K7W8D2	Uncharacterized protein		
K7WAJ9	Uncharacterized protein		
K7WBY4	Pyrabactin resistance-like protein		
K7WDG3	Uncharacterized protein		
K7WE51	Uncharacterized protein		

Protein	Annotation	Response to salt stress	ANOVA
K7WFP0	Non-symbiotic hemoglobin (Fragment)		
L7WLJ8	Clathrin heavy chain		
M1H6E9	Lipoxygenase (Fragment)		
O23888	Indole-3-acetaldehyde oxidase		
O24449	Translational initiation factor eIF-4A		
O24595	Glutathione transferase		
O49010	Herbicide safener binding protein		
O76014	Keratin, type I cuticular Ha7 OS=Homo sapiens GN=KRT37 PE=2 SV=3		
P00761	Trypsin OS=Sus scrofa PE=1 SV=1		
P04264	Keratin, type II cytoskeletal 1 OS=Homo		

Protein	Annotation	Response to salt stress	ANOVA
	sapiens GN=KRT1 PE=1 SV=6		
P05022	ATP synthase subunit alpha, chloroplastic		
P13867	Alpha-amylase/trypsin inhibitor		
P16243	NADP-dependent malic enzyme, chloroplastic		
P19013	Keratin, type II cytoskeletal 4 OS=Homo sapiens GN=KRT4 PE=1 SV=4		
P23444	Histone H1		
P29023	Endochitinase B (Fragment)		
P35527	Keratin, type I cytoskeletal 9 OS=Homo sapiens GN=KRT9 PE=1 SV=3		

Protein	Annotation	Response to salt stress	ANOVA
P35908	Keratin, type II cytoskeletal 2 epidermal OS=Homo sapiens GN=KRT2 PE=1 SV=2		
P38559	Glutamine synthetase root isozyme 1		
P38562	Glutamine synthetase root isozyme 4		
P38563	Glutamine synthetase root isozyme 5		
P51059	Phosphoenolpyruvate carboxylase 2		
P80627	Unknown protein from spot 443 of 2D-PAGE of etiolated coleoptile (Fragment)		
P93634	Actin (Fragment)		
P93638	Actin (Fragment)		

Protein	Annotation	Response to salt stress	ANOVA
P93639	Actin (Fragment)		
P94044	Ferredoxin-6, chloroplastic		
Q01546	Keratin, type II cytoskeletal 2 oral OS=Homo sapiens GN=KRT76 PE=1 SV=2		
Q10724	Peptidyl-prolyl cis-trans isomerase, microsomal (Fragment)		
Q14532	Keratin, type I cuticular Ha2 OS=Homo sapiens GN=KRT32 PE=1 SV=3		
Q15323	Keratin, type I cuticular Ha1 OS=Homo sapiens GN=KRT31 PE=2 SV=3		
Q208U9	CFM6		

Protein	Annotation	Response to salt stress	ANOVA
Q2MJJ9	Putative RH2 protein		
Q3MST8	Putative uncharacterized protein pk8-b (Fragment)		
Q41741	Eukaryotic initiation factor 4A		
Q41798	Calnexin (Fragment)		
Q41811	Histone H4.3		
Q41830	Mgp1 GTP-binding protein		
Q43242	Plasma-membrane H+ ATPase (Fragment)		
Q43243	H(+)-transporting ATPase		
Q43260	Glutamate dehydrogenase		
Q43261	Histone H2B.3		
Q43271	H(+)-transporting ATPase		

Protein	Annotation	Response to salt stress	ANOVA
Q49HD8	12-oxo-phytodienoic acid reductase		
Q49HD9	12-oxo-phytodienoic acid reductase		
Q49HE1	12-oxo-phytodienoic acid reductase		
Q4A1J8	Putative cystatin (Fragment)		
Q4FZ47	Putative cystatin		
Q4W1F6	Thioredoxin		
Q52R09	Cytochrome c oxidase subunit 2		
Q53WW9	Beta-D-glucosidase		
Q5EBY7	Heat shock protein 70 (Fragment)		
Q5EUD5	Protein disulfide isomerase		
Q5EUD6	Protein disulfide isomerase		
Q5G1U0	Malic enzyme		

Protein	Annotation	Response to salt stress	ANOVA
Q5GAQ3	Putative alanine aminotransferase		
Q5GAR6	Putative uncharacterized protein		
Q5I204	Brain acid soluble protein 1		
Q5IBC6	DANA2		
Q5K097	NADH dehydrogenase, subunit 9		
Q5XLD9	Putative 60S ribosomal protein L31		
Q5XPI0	Putative 14-3-3 protein		
Q6B7Q9	RuBisCo subunit binding-protein beta subunit (Fragment)		
Q6PLR9	14-3-3-like protein		
Q6R979	NADH-ubiquinone oxidoreductase chain 6		

Protein	Annotation	Response to salt stress	ANOVA
Q6R985	Cytochrome c oxidase subunit 2		
Q6R987	ATP synthase subunit alpha		
Q6R9A4	Ribosomal protein S7		
Q6R9G1	NADH dehydrogenase subunit 7		
Q6RW09	Allene oxide cyclase		
Q6VWG2	O-methyltransferase (Fragment)		
Q6XZ78	Fructokinase-2		
Q7SIC9	Transketolase, chloroplastic		
Q7Z794	Keratin, type II cytoskeletal 1b OS=Homo sapiens GN=KRT77 PE=2 SV=3		
Q84JX6	Phosphoglycerate kinase (Fragment)		
Q84TL7	Legumin-like protein		

Protein	Annotation	Response to salt stress	ANOVA
Q84UE6	Isoamylase-type starch debranching enzyme ISO2		
Q8RVD0	Hydroxymethyltransferase-like protein (Fragment)		
Q8S2U8	Plasma membrane H+-transporting ATPase-like protein (Fragment)		
Q8S2X6	Glycine-rich RNA binding protein (Fragment)		
Q8S4C4	Uncharacterized protein		
Q8S4W8	Pyruvate decarboxylase		
Q8S529	Cytosolic aldehyde dehydrogenase RF2D		
Q8W0Q2	Putative aldehyde dehydrogenase MIS1		

Protein	Annotation	Response to salt stress	ANOVA
Q8W2K4	NADH-cytochrome b5 reductase		
Q92764	Keratin, type I cuticular Ha5 OS=Homo sapiens GN=KRT35 PE=2 SV=5		
Q93XG1	Kinesin-like protein (Fragment)		
Q94G64	T-cytoplasm male sterility restorer factor 2		
Q94IQ8	Putative methyl-binding domain protein MBD106		
Q9ATM4	Aquaporin PIP2-7		
Q9C075	Keratin, type I cytoskeletal 23 OS=Homo sapiens GN=KRT23 PE=1 SV=2		
Q9FQC1	Glutathione S-transferase		

Protein	Annotation	Response to salt stress	ANOVA
Q9FQC4	Glutathione S-transferase GST 15		
Q9FQC5	Glutathione S-transferase GST 14		
Q9FQC6	Glutathione S-transferase GST 13		
Q9FQD0	Glutathione S-transferase 6		
Q9LKY1	WD-repeat protein RBAP2 (Fragment)		
Q9M585	Stomatin-like protein		
Q9S7Z7	HMGI/Y protein		
Q9SE94	Methylenetetrahydrofolate reductase 1		
Q9SPD7	Outer mitochondrial membrane protein porin		
Q9SWR9	Acetyltransferase component of pyruvate dehydrogenase complex		

Protein	Annotation	Response to salt stress	ANOVA
Q9T0N7	Phytase		
Q9XF58	Aquaporin PIP2-5		
Q9ZPN0	NADH-cytochrome b5 reductase		
Q9ZTS7	Peroxidase		
Q9ZTS9	Peroxidase J (Fragment)		
U3PB48	CCT protein		